An Open-Loop Photovoltaic-Solar-Thermal Evacuated Tube Energy System for Health Clinics in Nigeria.

Zwalnan Selfa Johnson

[B.Eng., MEng]

A Thesis Submitted for the Degree of

Doctor of Philosophy in Mechanical Engineering

University of Nottingham

September 2022

Abstract

The closed loop system photovoltaic solar thermal collector (PVT) is primarily conceived to cool the solar module for higher power production. One inherent problem with the closed loop configuration is the gradual loss of module efficiency with repeated circulation of the cooling water in a closed loop. This study, therefore, proposes a new hybridisation of the PVT collector with an evacuated tube based on an open-loop cooling strategy. The aim is to boost energy output and improve energy utilisation leading to reduce costs and improve economic viability. Therefore, a numerical model of the new system is formulated using TRNSYS 18 software. To assess the benefit of the proposed system, a numerical model of the conventional hybrid PVT closed-loop energy system is equally developed as benchmark, and the simulated performances of these systems are assessed and compared. A comparison of the new system's performance to the conventional system reveals that the solar fraction, is 0.74 and 0.80 for the basic and proposed systems, respectively. Similarly, the basic and proposed systems total collector efficiency was found to be 53% and 66% respectively. According to an economic analysis, the basic and new systems have Return on Investment (ROIs) of 33% and 14%, respectively. Even though the above results show that the proposed system outperformed the basic system based on the matrices used, it is also clear that the proposed system configuration and cooling strategy have met the goal of increasing net energy production and utilisation while minimising CO_2 emissions in the energy mix far above the minimum acceptable technical standard of 30% solar fraction by National Renewable Energy Laboratory (NREL) for good profitability and environmental protection. This result is significant, exposing to individuals and investors, the business outlook of the new system. It equally a good roadmap for government to increase access to power in communities with poor grid access. The findings of this study are promising; however, this study could be expanded by using the parallel arrangement of the PVT.

Declaration

I hereby declare that the work presented in this thesis has not been submitted for any other degree or professional qualification and that it is the result of my independent work.

Zwalnan Selfa Johnson

Full Name

Signature Date

.

List of publications

1. Z. S. Johnson, N. N. Caleb, M. M. Mangai, and N. Y. Sanda, “Comparative analysis of the thermal performance of a solar water heating system based on the serpentine and risers-head configurations,” *Journal of Renewable Energy Environent.*, vol. 8, no. 2, pp. 21–30, 2021, https://doi.org/10.30501/JREE.2020.251190.1150.

2. Z. S. Johnson, G. A. Duvuna, Y. A. Abakr, and T. Banda, “Design and performance evaluation of a multi-temperature flat plate solar collector,” *International Journal of Renewable Energy Development*, vol.10, no.3, pp. 537–549, 2021, https://doi.org/10.14710/ijred.2021.33213.

3. Z. S. Johnson, A. Y. Abdalla, S. Anandan, and ..., “A Numerical Evaluation of the Effect of Building Thermal Load on the Overall Performance Characteristic of a Grid-Coupled PV/T Energy System,” *Journal of Advanced Reasearch in Numerical Heat Transfer. ...*, vol 4,no.1, pp.32–43,2021, [Online]. Available: https://akademiabaru.com/submit/index.php/arnht/article/view/3798.

4. Z. S. Johnson, Y. A. Abakr, A. Shanmungam, and D. I. Mustapha, “Global energy transition: A review of status and future challenges,” In *18th International Conference on Sustainable Energy Technologies*, 2019, pp. 462-471

5. Z. S. Johnson, A. Y. Abdalla, S. Anandan, and A. Chan “A multi-objective decision framework for the selection of feasible hybrid energy system for energy-constrained communities”: *International of Renewable energy Technology; Accepted for publication*

Acknowledgements

First, I wish to acknowledge with sincere gratitude my supervisors, Prof. Yousif Abdalla Abakr and Mr S. Anandan Shanmugam, and Dr Su Yuehong, for their unconditional support, constructive input, and criticism of my research work. Without them, this journey would not be possible. Specifically, I would like to thank them for providing a conducive learning environment, especially their willingness and for always opening their doors whenever I need their help. I will forever cherish what I have learned from your style of supervision. I would also like to express my gratitude to all Faculty of Engineering, especially Galoh Munawwarah Osman (Ms Muna) and Siti Zaharatul Asyiqin (Ms Shikin), for their dedication to duty in making sure all PhD students get the proper support and enjoy their study. Indeed, you are all passionate and dedicated to your work. I cannot forget my fellow PhD friends' emotional and otherwise support, like Tiyamike Banda and Mustapha Danladi. Words cannot thank you all enough. I pray we will all graduate and enjoy the fruit of our labour. Finally, I would like to thank my wife and two kids. They are the pillar that supports me. Without them, I cannot finish this work. My parents, you are the blessings that have taken me this far. I cannot be grateful enough to you. To God, Almighty be all the glory.

Table of contents

Declaration ..... **ii**

List of publications ..... **iii**

Acknowledgements ..... **iv**

Table of contents ..... **v**

List of Figures ..... **viii**

List of Tables ..... **xii**

Abbreviations ..... **xiv**

Nomenclatures ..... **xv**

Chapter 1: Introduction **1**

1.1 Background of the study 1

1.2 Problem statement 9

1.3 Research questions 12

1.4 Aim and objectives 13

1.5 Contribution and significance of the research 13

1.6 Scope and assumptions of the study 15

1.7 Research methodology 17

1.8 Thesis structure 18

1.9 Chapter summary 19

Chapter 2: Literature review **20**

2.1 Introduction 20

2.2 Overview of the studies conducted on the PVT hybrid collector 20

2.3 A review of solar photovoltaic systems cooling methods 26

2.4 Hybrid PVT integration and operational control strategies 41

2.5 Economic analysis 54

2.6 Identifying the gap and contribution of this study 57

2.7 Chapter summary 62

Chapter 3: Research Method 64

3.1 Introduction 64

3.2 Description of the case study area health clinic energy demand 66

3.3 Description of the proposed energy system 73

3.4 Estimating the building cooling and heating load 77

3.5 Power and thermal energy demand estimation 85

3.6 Modelling of proposed OPVETC System 89

3.7 Energy management and the dispatch strategy 98

3.8 Modelling of the cooling water flow control 103

3.9 OPVETC parametric analysis and components sizing 107

3.10 Performance assessment and analysis 108

3.11 The reference and the baseline systems 112

3.12 Modelling of the basic PVT hybrid system (The baseline) 113

3.13 Validation and verification of simulation model 116

3.14 Methodology for the project economic assessment 123

3.15 Chapter Summary 130

Chapter 4: Results and Discussion 133

4.1 Introduction 133

4.2 Thermal characteristics of building zones 133

4.3 Estimating the total power and DHW demand 139

4.4 System response to energy management and flow control strategies 145

4.5 Optimal system sizing and parameters determination 163

4.6 Comparison of the basic PVT and the OPVETC hybrid energy system 168

4.7 Monthly average daily system performance analysis 186

4.8 Comparison of system performance indicators 196

4.9 Model validation 204
4.10 Results and discussion of economic assessment 217
4.11 Economic sensitivity analysis of proposed system 231
4.12 Geographic mapping of economic system viability 242
4.13 Chapter summary 247

Chapter 5: Conclusions and future work 249
5.1 Introduction 249
5.2 Summary of key findings 249
5.3 Novelty and contributions 251
5.4 Limitations of study 252
5.5 Future work and recommendation 253

REFERENCE 255
APPENDIX 293
A1: SARA equipment inventory numbering survey form 294
A1: SARA health clinic electrical power profile form 295
Appendix B: TRNSYS model of the OPVETC 297
Appendix C: TRNSYS model of the Basic hybrid PVT 298
Appendix D: Building's measured indoor temperature for zone 2. 299
E1: MATLAB code OPVTEC economics 306
E2: MATLAB code basic hybrid economics 311
F1: The basic hybrid system economic analysis result 315
F2: The proposed OPVETC hybrid system economic analysis result 316
G. Data sheet of the commercial TEZEUS PVT collector 317
H. Data sheet of the commercial AP evacuated tube collector 318

List of Figures

Figure 1.1: Urban grid reliability for some selected countries [11].....2

Figure 1.2 Estimates of household countries' electricity reliability [11].....3

Figure 1.3: Expected CO_2 mitigation by renewables and energy efficiency [21].....7

Figure 1.4: Flow chart of methodology and summary of the study.....18

Figure 2.2: A parabolic reflective surface PVT collector.....23

Figure 2.3: Nanofluid cooled PVT collector.....23

Figure 2.4: Cross-sectional of (a) glazed (b) unglazed collector.....26

Figure 2.5: Solar panel cooled by the water spray method [87].....28

Figure 2.7: Temperature variation between nodes in a water tank [163].....59

Figure 3.1. Flow chart of the research methodology.....65

Figure 3.2. Monthly average temperature and precipitation pattern in Jos [170].....66

Figure 3.3. Monthly average daily solar irradiation and sunshine hours [170].....68

Figure 3.4. Map of Nigeria showing the case study location.....70

Figure 3.5. Wind speed distribution and direction of Jos [170].....71

Figure 3.6. Front and side view of the case study health centre in Jos, Nigeria.....72

Figure 3.7: System schematic diagram of the OPVETC grid-coupled system.....76

Figure 3.8: Proof of concept and case study application of the OPVETC.....77

Figure 3.9.Case study building floor plan and dimensions.....79

Figure 3.11. The occupancy period for HVAC heating and cooling control.....81

Figure 3.12: Operation and control of the HVAC device.....83

Figure 3.13: Schematic of the 3D building model developed in TRNSYS.....84

Figure 3.14. Equipment electric power profile of the case study health centre.....85

Figure 3.15 Daily hot water demand for the three applications.....87

Figure 3.16. Process flow diagram of the proposed OPVETC TRNSYS model.....93
Figure 3.17. The detailed control logic and the modelled energy management strategy 101
Figure 3.18. Flow chart model of grid power dispatch.....102
Figure 3.19. Cooling pump control flow and algorithm. 105
Figure 3.20: The reheated hot water flow network.....107
Figure 3.21. Summary of modelling approach 113
Figure 3.22: The basic PVT: Equivalent of the proposed OPVETC 115
Figure 3.23. Verification and validation flow chart in model development.....118
Figure 3.24. System's power model energy balance 121
Figure 3.25. System's thermal model energy balance 122
Figure 4.2:Zones uncontrolled temperature on typical sunny days 28/4/21 to 30/4/21.....136
Figure 4.3. Zones controlled temperature on typical sunny days in April.....137
Figure 4.4 Zones HVAC power demand on typical sunny days.....137
Figure 4.5: Zones HVAC power demand on typical cloudy days 138
Figure 4.6. The health clinic equipment power demand profile 140
Figure 4.7: Monthly average daily hot water demand 141
Figure 4.8:Total monthly average daily hot water demand 142
Figure 4.9: Building annual hourly cooling and heating rate 143
Figure 4.10. Solar radiation of typical sunny, cloudy, and overcast day 146
Figure 4.11 Dynamic performance of the system on an overcast day 148
Figure 4.12 Dynamic performance of the system on a cloudy day 149
Figure 4.13. Dynamic performance of the system on a sunny day.....150
Figure 4.14. Dynamic flow characteristics based on the proposed strategy.....152
Figure 4.15 Effect of pump flow rate on the net PV power produced.....154
Figure 4.16. Effect of collector outlet temperature on net power of the PV module.....155
Figure 4.17. Temperature variation of sterilising and laundry hot water 156

Figure 4.18. Temperature variation of the DHW delivered for postnatal.....157
Figure 4.19. Monthly average mains water temperature variation 159
Figure 4.20. Variation of PV module temperature 162
Figure 4.21: Effect of flow rate on the system thermal solar fraction 164
Figure 4.22:Effect of the number PVT on TLCC and solar fraction 166
Figure 4.23. Effect of tank volume on tank delivered useful energy.....167
Figure 4.24: Solar irradiation for a typically sunny and cloudy day in April and August.....169
Figure 4.25: Comparison of the PV module power output.....172
Figure 4.26: Comparison of the pump power consumption 173
Figure 4.27:Monthly averaged daily PV array power production 175
Figure 4.28: Comparison of the PV module surface temperature 178
Figure 4.29 Monthly averaged daily module temperature from 11 am to 4 pm.....179
Figure 4.30: Load delivered hot water temperature for postnatal services.....182
Figure 4.31:Load delivered hot water temperature for laundry services 184
Figure 4.32:Load delivered hot water temperature for sterilisation services.....185
Figure 4.33. Comparison of monthly average daily delivered thermal energy 187
Figure 4.34. Comparison of monthly average daily useful thermal energy.....189
Figure 4.35.Comparison of monthly average daily PV array power output.....193
Figure 4.36. Comparison of systems solar fraction 197
Figure 4.37. Comparison of PVT solar energy conversion efficiency 198
Figure 4.38. Comparison of annual system self-reliability.....201
Figure 4.39. Comparison of TRNSYS and Pantic et al.'s PVT power model.....205
Figure 4.40. Statistical analysis of TRNSYS and Pantic et al.'s PVT model.....206
Figure 4.42 Comparison of the temperature of the case study building on 10th/01/ 2020....208
Figure 4.43. Comparison of the temperature of the case study building on 11th/01/ 2020...209
Figure 4.44. Analysis of simulated and measured building temperature.....210

Figure 4.47. Dynamic cooling water flow characteristic on a day with good irradiance 214
Figure 4.48.Dynamic cooling water flow characteristic on days with low irradiance 215
Figure 4.49. Comparison of system components cost 220
Figure 4.51. Comparison of operating costs between the OPVETC and basic PVT.....223
Figure 4.52. Comparison of the basic PVT and OPVETC cash flow.....225
Figure 4.53. Comparison of the basic PVT and OPVETC cumulative cash flow.....226
Figure 4.54. The net worth of the project based on different periods of analysis 227
Figure 4.55. Comparison of ROI between the basic and OPVETC.....229
Figure 4.56. Comparison of the OPVETC, Grid and diesel generator LCOE.....230
Figure 4.57. Sensitivity of project ROI and NPV to the inflation rate change.....234
Figure 4.58. Effect of change in inflation rate on the NPV 235
Figure 4.59. Effect of change in inflation rate on the LCOE.....236
Figure 4.60 Effect of hot water demand volume on ROI, CO_2 emission and SSF 237
Figure 4.61. Effect of change in the size of the hot water demand volume.....238
Figure 4.63. Geographical locations for the energy project mapping.....242
Figure 4.65. Mapping of project NPV by location 245
Figure 4.66. Mapping of energy project LCOE by location.....246

List of Tables

Table 2.1: Efficiency and temperature of some available PV modules [84] 25

Table 2.2: Summary of studies on water-cooled PVT with their findings 36

Table 3.1 Thermal properties of building materials.....80

Table 3.2 U-values of building surfaces 80

Table 3.3:Geometric and thermal properties of temperature zones. 82

Table 3.5: Technical parameter of the TESZEUS flat plate PVT collector.....96

Table 3.6 Other system components' design parameters for the proposed system.....97

Table 3.7: ETC technical and design parameters.....98

Table 3.8: Flow control and its action on the pump 106

Table 3.9: The Basic PVT and the OPVETC components size.....116

Table 4.1: Monthly averaged daily maximum cooling and heating demand.....138

Table 4.2:Monthly average power and hot water demand of the building 144

Table 4.3. Hot water load and temperature difference between demand and supply 158

Table 4.4 Hot water auxiliary energy demand based on the weather condition 161

Table 4.5: Comparison of power production of OPVETC and basic PVT.....176

Table 4.6. Comparison of monthly average auxiliary energy demand 190

Table 4.7. Comparison of monthly average daily thermal energy utilisation.....191

Table 4.8. Comparison of monthly average daily fossil fuel energy utilisation 192

Table 4.9. Comparison of monthly average daily power generation and utilisation 195

Table 4.10: Comparison of LOLP between the basic PVT and the OPVETC 200

Table 4.11. Comparison of systems CO_2 emission and the computed ACO_2 Ratio.....203

Table 4.13. Analysis of the formulated model thermal energy balance 217

Table 4.14:System components and the current market prices of system components.....219

Table 4.15: Parameters for system economics and CO_2 impact 220

Table 4.16 Economic performance mapping of the OPVETC in different locations.....244

Abbreviations

AC	Alternating current
BIPVT	Building-integrated photovoltaic-solar thermal
C	Controller
CFD	computational fluid dynamics
CPVT	Concentrating photovoltaic solar thermal
DC	Direct current
DHW	Domestic hot water
EMCS	Energy management control strategy
ETC	Evacuated tube collector
HRES	Hybrid renewable energy system
HVAC	Heating Ventilation and Air Conditioning
MPP	Maximum power point
NREL	National Renewable Energy Laboratory
OPVETC	Open-loop photovoltaic evacuated tube collector
P	Pump
PHES	Pumped hydroelectric energy storage
PM	Particulate matter
PV	Photovoltaic
PVT	Photovoltaic solar thermal
SAM	System adviser model
SDG	Sustainable development goal
SDHW	Solar domestic hot water systems
TIC	Total Initial Cost
TMY	Typical Meteorological Year
TRNSYS	Transient systems simulation

Nomenclatures

(Q_{PVT})	PVT collector useful thermal energy	[kWh]
(η_T)	Collector thermal efficiency	[-]
(T_exit)	Collector water exit temperature	[^oC]
(Ac_{PVT})	PVT total array area	[m^2]
(Air_{ACH})	Air exchange per hour	[1/hr]
$\dot{m}_{sl}^{`}$	Water flow rate for sterilisation and laundry services	[kg/hr]
$\dot{m}_{req}$	Estimated cooling water flow rate	[kg/hr]
$C_{p_{air}}$	Heat capacity of air	[J/ kg.K]
C_p	Water specific heat	[J/kg.K]
E_{ma}	Similarity evaluation matrix	[-]
T_{mains}	Main water temperature	[^oC]
$Tset_{heat}$	Setpoint temperature for heating	[^oC]
$Tset_{cool}$	Setpoint temperature for cooling	[^oC]
T_{zone}	The temperature of the building zone.	[^oC]
V_{zone}	Zone volume	[m^3]
m_{load}	Hot water demand rate	[kg/hr]
x_i	Ideal carbon dioxide emission	[kg]
x_n	None-ideal carbon dioxide emission	[kg]
y_i	Ideal d return on investment	[%]
y_n	None-ideal return on investment	[%]
z_i	Ideal initial investment cost	[$]
z_n	None-ideal initial investment cost	[$]
y_{pump}	Pump control signal	[-]
ρ_{air}	Density of air	[kg/m^3]
ACD	Avoidable carbon dioxide	[kg]
BSOC	Battery state of charge	[%]
FSOC	Fractional state of charge	[-]
IRR	Internal rate of return	[%]
L	Length	[m]
LCOE	Levelised cost of energy	[$/kWh]
LOLP	Loss of load probability	[%]
NPV	Net present value	[$]
NSE	Nash Sutcliffe model efficiency	[-]

PBP	Payback period	[yrs]
Qaux	Auxiliary energy demand	[kWh]
$Q_{cooling}$	Quantity of heat required to cool the zone	[kWh]
$Q_{heating}$	Quantity of heat required to heat the zone	[kWh]
ROI	Return on investment	[%]
ROI	Return on Investment	[%]
TIC	Total Initial Cost	[$]
TLCC	Total life cycle cost	[$]
EDi	Euler distance of optimal indicator from the ideal	[m]
EDn	Euler distance of optimal indicator from the non-ideal	[m]
C_{batt}	The unit cost of the battery	[-]
C_c	Components cost	[$]
C_{cont}	The unit cost of the controller	[-]
C_{instal}	Installation cost	[$]
C_{inv}	The unit cost of the inverter	[-]
C_{opvetc}	The unit cost of PVT	[-]
C_{pump}	The unit cost of the pump	[-]
C_{tank}	The unit cost of the tank	[-]
E_s	Energy savings	[kWh]
F_n	Assumed or expected cash flow	[$]
N_{batt}	Number of Batteries	[-]
N_{coll}	Number of PVT collectors	[-]
N_{cont}	Number of controllers	[-]
N_{pump}	Number of pumps	[-]
N_{tk}	Number of tanks	[-]
V_p	Present value	[$]
N	Analysis period/project life	[-]
$Cash_{inflow}$	Cash inflow	[$]
$Cash_{outflow}$	Cash outflow	[$]
FC_T	Total fuel costs	[$]
FC	Fuel costs	[$]
IC	Installation costs	[$]
LCS	Life cycle savings	[$]
OMC_T	Total operating and maintenance costs	[$]
OMC	Operating and maintenance costs	[$]

PSV_T	Total residual values	[$]
PSV	Residual values	[$]
$PVIF_n$	Present value interest factor	[-]
RC_T	Total replacement costs	[$]
RC	Replacement costs	[$]
d	Annual discount rate	[%]
i	Annual inflation rate	[%]
n	Base year of analysis after year zero	[-]
δ	Degradation factor	[-]

Chapter 1: Introduction

1.1 Background of the study

Sustainable Development Goal 7 (SDG 7) was one of 17 goals established by the United Nations General Assembly in 2015 to ensure that every country has access to clean and affordable energy by 2030 [1]. However, a recent assessment shows that global access to electricity continues to be characterised by uneven progress toward this goal [2]. Electricity, for example, is available in more than 98% of most developed countries, particularly in Latin America and Eastern and Southern Asia. In stark contrast, only 46% of Sub-Saharan Africa's population has access to reliable power, making this region the world's region with an enormous power access gap [2]. For example, in Nigeria and the Democratic Republic of the Congo, 90 million and 70 million people are still without electricity in 2019 [1]. According to the 2019 SDG 7 Tracking Report, only 28% of health facilities in Sub-Saharan Africa have access to reliable electricity[3]. Adequate power for health centres is critical for providing quality health care. Taking Nigeria as a case study, many studies [4]–[6] , for example, have reported the adequacy of Nigeria's solar and wind capacity for viable wind and solar power projects.

Nevertheless, it still has a low install capacity of solar and wind energy systems even amidst a persistent power crisis [4]. Nigeria's energy sector generates slightly more than 7000MW of power for a population of over 200 million people. A modern-day energy requirement of 1500MWh per 1000 persons/km^2 is considered adequate in most developed countries [7], [8]. Most developing countries' power is grossly inadequate, going by their population [9]. Moreover, frequent and unpredictable outages are the dominant characteristic of grid power in most developing countries, as reported by the recent report released by the International

Finance and Cooperation (IFC) [10], [11], a member of the world bank group in 2018 through its Lighting Global Programme. As seen in Figure 1.1 and Figure 1.2, the report reveals that grid power is randomly unavailable over 80% of the time in most developing countries, including Nigeria [5].

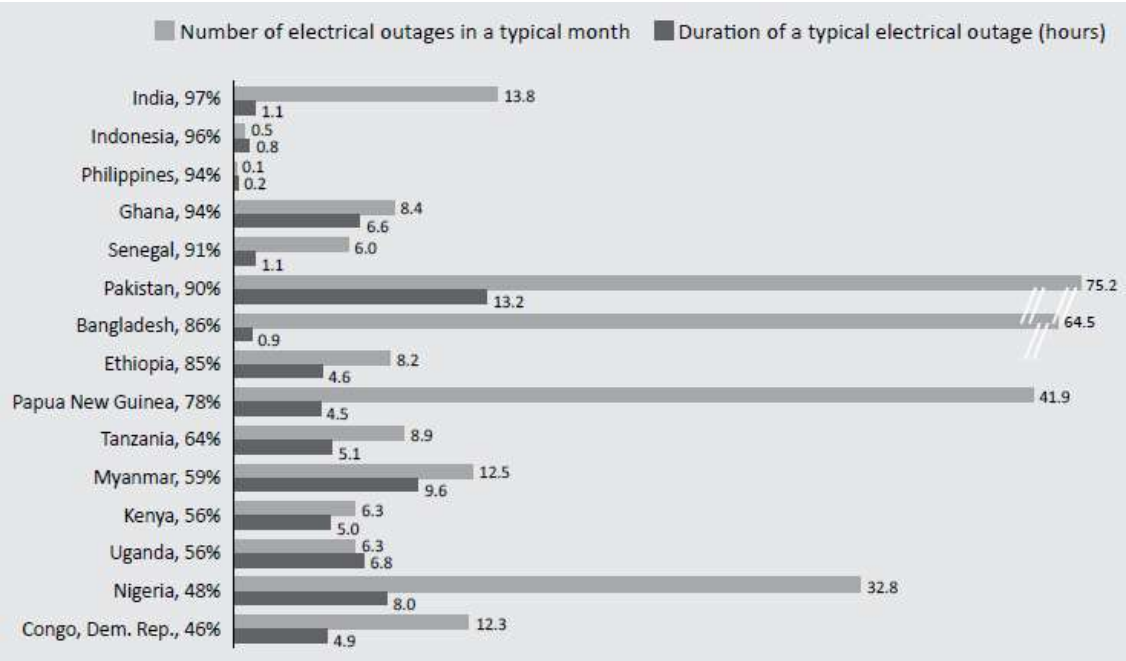


Figure 1.1: Urban grid reliability for some selected countries [11]

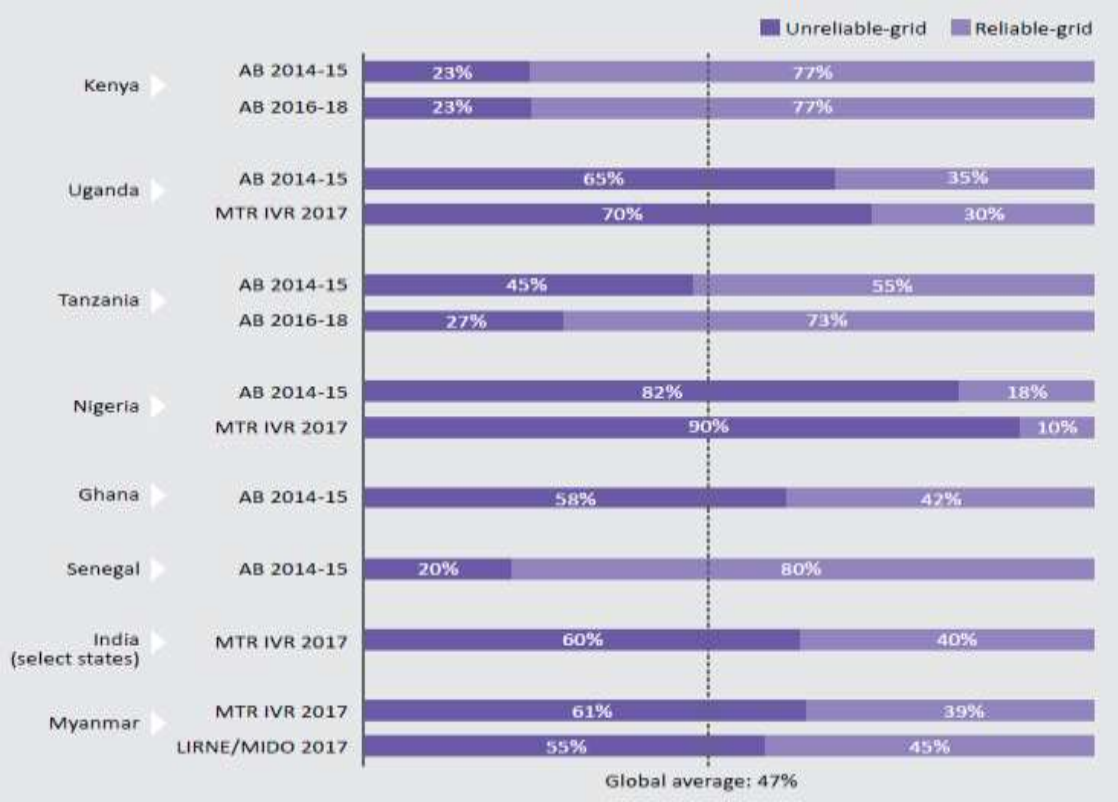


Figure 1.2 Estimates of household countries' electricity reliability [11]

Nigeria has an average monthly power outage of 33 times per month, lasting between 5 - 8 hours per day[5][9]. Figure 1.2 revealed an increase in the grid unreliability from 82% in 2015 to 90% in 2017. High unreliability of about 90% means that facilities connected to the grid can only be less than 10% confident of the availability of power from the grid. Therefore with the recent coronavirus outbreak, most developing countries are not adequately positioned to content the crisis, partly because of poor access to energy due to the weak framework that monitors the Sustainable Development Goal7 (SDG7) of clean energy for all in developing countries [12]. With the current burden created on every country by the pandemic, the support for developing countries may likely slow or stop in the nearest future. Hence, it is critical to find economical, innovative energy solutions that match each country's peculiarity despite advancing world technology [12].

Renewable energy systems, especially solar and wind, are good alternatives for energy-constraints communities. For communities without grid power, renewable energy solutions are a viable alternative to fossil fuels, a way to increase access to power and reduce fossil fuel-based CO_2 [13]. Again, renewable energy resources like wind and solar radiation are intermittent and random. The fluctuating nature of these resources creates the need to integrate multiple renewable energy sources and storage systems to meet the challenge of mismatch between power generated and the load. Furthermore, for an equivalent amount of conventional energy, renewable energy technologies require more installation areas than the traditional energy source, making solar and wind less competitive with the conventional source of energy in terms of cost. Undoubtedly, for now, fossil fuel power production will continue to dominate the global energy mix because of its lower price compared to renewables. As expected, conventional energy sources will continue to be cheaper than renewables until they fully develop the technological infrastructure required to support the full development of renewable technologies. Nevertheless, the resulting consequence of the continued usage of fossil-based energy is an increase in the net carbon dioxide, leading to an irreversible and unbearable increase in global temperature [14].

In the meantime, the hybrid energy system, which combines conventional and renewable energy systems, is unarguably the option that offers the best compromise between the economic and environmental protection for communities with low access to grid power [15]. Interestingly, the hybrid energy system equally addresses the intermittent fluctuations of the unhybridised renewable energy system and provide suitable energy alternative in communities with unstable grid power.

Power is essential for delivering high-quality health services in critical sectors like health facilities. Dabaro [16], in the study of factors affecting tuberculosis case detection in Kersa District, South West Ethiopia, for example, argued that equipment failure and malfunctioning are a consequence of frequent power outages. Related to equipment failure, even test results that are supposed to be provided in fewer days take weeks [16]. In most cases, patients referred to a health facility far away and without means ended up staying back and infecting others in the community. Hybrid photovoltaic-solar thermal energy systems are suitable for hospital applications since they deliver power and thermal energy, the predominant energy demand in most rural health centres. The modular nature of these alternative power systems is an advantage that makes them easy to be installed and move to any remote area. For example, in Nigeria, it took the Rural Electrification Agency only two weeks during this coronavirus crisis to equip four hospitals designated for treating COVID-19 patients with photovoltaic mini-grid power systems [17]. With the abundance of solar and wind energy, renewable energy systems are adjudged and forecast as low-cost energy solutions for most rural health centres in sub-Saharan Africa [18]. Fortunately, both Government and world organisations like the USAID are now offering many opportunities to support alternative energy development in providing reliable alternative power in remote sub-Saharan African health clinics [19]. Therefore, now is the time to increase energy access to communities with poor access to electric power.

Moreover, with the outburst of COVID-19 and the new norm of working from home [20], addressing buildings, especially health centres and residential energy demands, is critical in reducing the environmental impact of a high rise in energy demand. In recent times, the building energy demand has significantly increased, accounting for about 40 to 50% of the total energy consumption of most developed countries. As a result, the building share of energy

accounts for about 28% of the global energy-link carbon dioxide emission. More so, over 65% of the carbon dioxide in the building sector is related to power consumption [21].

With the safety objectives, energy systems are gradually evolving from a comprehensive passive system generated over a long distance to independent and small smart grid systems closer to consumers[22]. Moreover, according to the independent statistics and analysis by the U.S Energy Information Agency (EIA) report in 2021, the distribution and transmission of power from the centralised production constitute about 44% of the total cost of production [23], making the decentralisation of energy systems like hybrid renewable intelligent energy systems an option to be considered. The adverse effect of climate change is an additional force that drives the need to evolve from fossil fuel-based technologies [24]–[26]. Besides, recent indications have also shown a global awareness created by the apparent effect of climate change, resulting in huge losses arising from flooding in almost all major cities worldwide. The sudden realisation of the finite nature of even the fossil fuel reserve is also a significant factor in shaping the transition to alternative energy sources [15], [27]. Therefore, the replacement or integration of buildings with renewable energy technologies will reduce carbon emissions in the global effort to produce cleaner, affordable energy for all in the future. In recent times, the use of the micro and intelligent grid for power use in different facilities is increasingly examined [28], [29]. The use of sustainable and environmentally friendly technologies, especially renewables and energy efficiencies, is expected in the transition roadmap to unleash a massive decline of about 500 million tons per year of energy-related emissions from the building sector between now and 2050 [21]. For example, the photovoltaic -solar thermal energy system is a technology that simultaneously produces both power and thermal energy suitable for application in the building section since its energy demand is predominantly power and thermal energy. Even though the great potential of the hybrid PVT energy system is a good

match for residential applications, its wide adoption in many locations is still a challenge. The slow acceptance is unrelated to the high cost due to poor infrastructure to support the mass production of this technology. To promote the adoption of renewable energy technologies, at present, in most developing countries, substantial research and development programmes have been dedicated to the applications of solar energy technologies to meet domestic energy demands like water pumping for irrigation, hot water, and drying of agricultural products, particularly in remote areas with poor access to grid power[30]. Figure 1.3 below reflects the expected decrease in CO_2 emissions from the building sector if renewables and energy efficiency are implemented under the ReMap scenario [21].

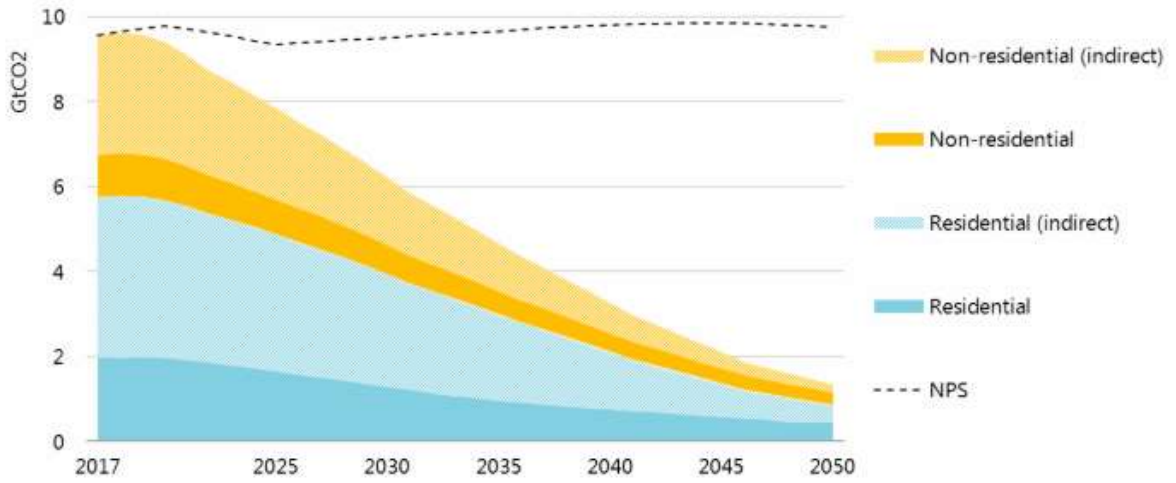


Figure 1.3: Expected CO_2 mitigation by renewables and energy efficiency [21].

As seen in Figure 1.3, the residential sector is expected to play a crucial role in the global effort to decarbonise the energy mix. Therefore, meeting residential energy demand with renewable energy technologies is one roadmap to reducing emissions from the building sector. Even though hybrid photovoltaic-solar thermal energy systems are an excellent match for building applications since the demand for power and hot water are the predominant load, there are still obstacles to their extensive deployment to replace fossil-based energy technologies [31]. The

low installed capacity of renewable power systems in most countries despite reported good potential [32]–[34] and persistent energy crisis is evidence of these obstacles. Over the past decade, enormous efforts and work have been geared toward using hybrid energy systems to meet building energy requirements with different objectives. Interestingly, solar thermal and photovoltaic energy systems use are gaining commendable attention among researchers to design building-integrated hybrid renewable energy systems in recent times.

In conclusion, electricity from the grid is the cheapest energy source to satisfy energy demand. However, grid power is exceptionally unreliable and unsustainable in most developing countries, including Nigeria. In most cases, the high unreliability is mainly due to inadequate power generation coupled with dilapidated infrastructure to transmit and distribute the generated power to the final consumers [35]. Regrettably, critical facilities, particularly health facilities, require a reliable and affordable energy source to deliver quality health services. Photovoltaic-Solar thermal hybrid energy systems are an excellent alternative for rural health centres. However, the low energy harvesting efficiency and high cost have made PVT hybrid a low appealing option.

Undoubtedly, extensive research has been carried out to enhance the thermal and electrical output of the conventional hybrid PVT for residential building applications. One challenge of the conventional hybrid PVT is that the cooling water is typically circulated in a closed loop. As a result, the cooling effect of the circulated water diminishes over time with multiple recirculation. Moreover, if the cooling water is targeted to meet hot water demand, the surface temperature of the PV module is usually more than that of the uncooled PV module. Hence, for the standard hybrid PVT energy system, which meets both electricity and hot water needs, the electricity production is lower than the power output of the uncool PV module [36]. This observation means that if the demand for hot water is adequately supplied, the electrical power

of a traditional hybrid PVT energy system is impaired, and vice versa. Furthermore, a wide range of literature has reported studies on hybrid PVT energy systems integrated with reliable or grid with scheduled outages for domestic application. Therefore, to meet power and hot water demand reliably and economically in rural health centres clinics, the PVT energy hybrid configuration can be reconfigured to enhance its power production while still meeting the demand for hot water with no consequential loss in power production efficiency as in most conventional hybrid PVT energy systems.

1.2 Problem statement

Energy is essential for the growth and development of every nation. However, the evidences and revelation in generality of most published work [35], [37]–[39] on the current status and access to grid power source in developing countries especially Nigeria, supports the general conclusion that grid electricity supply in most developing countries is grossly inadequate and randomly unreliable[2], [40], [41] . Hence residential building and critical facility like the health clinics are prompt to grid failure lasting average of 8 hours per day [42]. Consequently, critical sectors, mainly health centres, cannot fully operate to deliver quality services to their total capacity with an unreliable and unsustainable power source. The consequences of poor health service, among others, are a high infant mortality rate and lower life expectancy

Furthermore, the global target of limiting temperature increase to below $+2^{o}C$ compared to the pre-industrial level [43] requires that the energy systems transit to a low carbon technology before the end of 2050 especially for countries with high population like Nigeria. Consequently, targeting the building sector is a good roadmap because it is responsible for about 19% of global greenhouse emissions [30] and in Nigeria, building energy represent about 77% of total demand for energy [44].

Renewable energy systems are an excellent roadmap for lowering greenhouse emissions in the building sector since they are carbon dioxide free[43], [45], [46]. The photovoltaic solar thermal hybrid energy system (hybrid PVT) is a good match for residential building application since its energy production is both electric power and thermal energy, as adopted in wide range of studies[47]–[49] . However, its low power conversion efficiency and low energy utilisation is due to its inherent closed-loop cooling configuration. In a closed-loop PVT hybrid system, the cooling fluid is recirculated in a closed loop pattern to the PV module with the primary aim of cooling the PV for better power production[50], [51] and thermal efficiency and utility is seldom a simultaneous target[32], [51] . The implication of a recent study by [52] indicates that the power yield of the module is better improved if the collector inlet cooling fluid is maintained as low as possible. In building applications, cooling water is required for a secondary application to meet the hot water demand in the building and therefore the system architecture is typically closed loop. In the closed loop hybrid PVT system configuration, the requirement to cool the PV effectively to improve its power production negates the goal of adequately meeting the thermal production of the PVT hybrid energy for hot water applications especially if hot water is required at elevated temperature say 80 or 90^{o}C [53]–[55]

Again, it is practically impossible to keep cooling the PV without increasing the cooling fluid temperature in a closed loop. Thus, it then implies that if the conventional PVT hybrid energy system is utilised to meet hot water demand at elevated temperatures, an improvement in the thermal solar fraction of the conventional closed-loop hybrid PVT energy system would come with a consequential trade-off in the power fraction of the system and vice-visa [53]–[55]. On the contrary, cooling the PV module near its operating temperature will lower thermal performance. Undoubtedly, even though the PVT has higher overall energy than the stand-alone PV module, in reality, the actual power output of the couped PV module is potentially

reduced due to the increased surface temperature from the recirculated cooling water [36][50]. One major problem of the traditional closed loop system configuration cooling method is the drop in power efficiency of PV modules with continuous recirculation, especially if the volume of water is not adequate to effectively cool the module. The low energy conversion and utilisation of the conventional hybrid PVT energy system is the major reason for the poor energy savings resulting to extended payback period with lower economic net worth of this technology making the adoption unattractive.

Therefore, improving the thermal production of the PVT hybrid collector with the simultaneous increase in electrical power in order to improve on the system economic performance by increasing the total energy harvesting for domestic applications especially for high temperature application like in health clinics craves innovative ideas.

Nonetheless, from the literature reviewed in this study, majority of the studies are focused on the closed-loop cooling[56]–[58] and the concept of the open-loop cooling are seldomly considered as approach to improve the performance of PVT hybrid systems to adequately meet thermal and electrical demand based on an open-loop hybrid system architecture integrated with the evacuated tube collector coupled to a randomly unavailable grid power system for building application.

Overall, there is a need to increase the thermal performance of the conventional hybrid PVT energy system. This research, therefore, fills this gap by proposing a novel open-loop photovoltaic solar thermal evacuated tube (OPVETC) hybrid energy system operated based on open-loop flow control and an energy management strategy that coordinates the operation of the hybrid system tied to a grid with random outages. The goal is to reduce the loss of power when thermal efficiency is improved and vis-vasa as with the conventional closed-loop water-

cooled PVT hybrid energy system. Hence the overall energy production of the proposed system will be higher with a higher solar fraction leading to better energy savings, unveiling the potential applicability of the water-cooled PVT in reducing the energy burden in rural health centres with poor access to power.

1.3 Research questions

The aim of this study is to improve the economic and environmental benefits of the conventional PVT hybrid energy system in order to lower the barrier that prevents the fast adoption of this system. To fulfil the aim and objectives in this research, this study is focused and organised to look into and respond to the following research questions:

1. How can the traditional hybrid PVT energy system configuration and cooling approach be modified to simultaneously improve electric power and domestic hot water at elevated temperature?
2. How can any proposed solution be comprehended, evaluated, and compared to the current conventional hybrid PVT closed-loop energy system?
3. How can an energy management and control strategies be formulated to manage and coordinate the system with a randomly unavailable grid to meet load reliably, in the most economically and with maximum environmental benefit?
4. How can the economic and environmental benefits of the proposed solution be measured in different geographical locations?

1.4 Aim and objectives

The aim of this study is to assess the cooling, energetic, economic, and environmental impact of the novel integration of the conventional hybrid photovoltaic solar thermal with the evacuated tube collector coupled to a grid power source characterised by random and unpredictable outages based on the unique open-loop cooling control strategy. The following specific research objectives would facilitate the achievement of this aim.

1. To formulate a numerical model for the annual performance simulation of the conventional hybrid photovoltaic solar thermal with the evacuated tube collector coupled to a grid power characterised by random and unpredictable.
2. To develop an Energy Management Strategy and Control (EMSC) to coordinate and manage the operation of the formulated model of the energy system to improve renewable energy utilisation for maximum economic and environmental benefits.
3. To assess the thermal and energetic behaviour of the open-loop photovoltaic evacuated tube relative to the simple conventional grid-connected photovoltaic hybrid energy system to measure the improvement.
4. To evaluate and map the economic benefit of the proposed energy system in different geographical regions of the study country to serve as information for potential investors and governments for policymaking.

1.5 Contribution and significance of the research

This research, proposes, and evaluates a novel open-loop photovoltaic evacuated tube solar thermal collector hybrid energy system (OPVETC) coupled to a grid characterised by random power failure. A novel energy management strategy for the proposed reconfiguration of the basic hybrid PVT to the open-loop system was developed for a randomly unreliable grid power source for energy-constrained communities. Moreover, previous work sets the fluid flow at a

constant flow rate based on the availability of solar energy[59]. In this study, a new flow control strategy ensures that the PV module temperature is lower while adequately meeting thermal and electrical demand is further developed to enhance system performance. The proposed flow control attempts to find the required flow rate to extract adequate thermal energy to meet hot water demand while keeping the PV module temperature at the minimum possible temperature.

Furthermore, a unique load-sharing technique of the domestic hot water load separating into three applications to enhance higher solar fraction is also developed. Finally, geographic mapping of the techno-economic and environmental potential of the proposed energy system in the study's country was conducted to be the basis for policymaking and information for potential investors.

The significance of hybrid renewable open-loop photovoltaic evacuated tube solar thermal collector hybrid energy system (OPVETC) integrated with the conventional backup energy system is the provision of an energy mix that provides the best compromise between profitability and environmental protection. For this study compared to conventional grid power electrification, which requires a longer time to complete, this research, provides quick, clean, and affordable energy alternative to providing access to power in countries with relatively inadequate and unpredictable grid power source. Particularly, a new prospect in applying hybrid PVT for health centres applications revealing the significant increase in profitability with good environmental impact is revealed for investors in health sector. Besides, it provides an enhanced means to meet domestic buildings and health centres power and hot water demand in a more efficient and cost-effective approach resulting to significant increase in the economic net worth of system from the energy savings because of improve efficiency.

The major barrier to the wide deployment of the PVT hybrid technology for domestic and commercial applications in most residential buildings particularly in health facilities is the high cost of initial investment, with poor energy savings leading to extended payback time. The approach in this study, significantly improved the energy harvesting resulting in huge energy savings. The significant energy savings from the new configuration and cooling approach has the benefit of reducing the cost of investment and payback period in this technology thereby reducing the risk and the uncertainty of potential investors, lifting the barrier to the adoption of this technology.

The findings of this study equally reveal the proposed system's business outlook exposing the profitability of the proposed hybrid photovoltaic energy system in the health centres in different geographical locations of the study country.

At the local level, the study is a means to reduce Nigerian over-dependence on the conventional electric power source and provide a cheaper, cleaner, and more reliable energy alternative for domestic buildings in countries with inadequate grid power characterised with random outages. At the global level, the research is an excellent roadmap contributing to the worldwide effort of reducing the carbon dioxide content of the energy mix of the building sector to achieve the Paris Agreement (PA) of reducing global warming to below 2^{o}C relative to the pre-industrial level [60]–[62].

1.6 Scope and assumptions of the study

The following approach is adopted to achieve the expected outcome of this research. The implementation of the method will be limited to, Modelling the proposed energy system using TRNSYS software. The power requirement needed for the system's design will be obtained based on the data acquired using a survey form in the study area. The study case health facility's

electrical cooling and heating power requirements would also be predicted using the 3D building model. Domestic hot water (DHW) demand profiles for health facilities would be generated based on a standard load profile for three separate hot water applications in the health facility, confined to only laundry, sterilising, and postnatal application services. Likewise, the power demand profile would be developed based on the power requirement of the appliances acquired using the survey form and the Heating, Ventilation, and Air Conditioning (HVAC) power demand obtained from the 3D building model for the simulation system performance. Furthermore, the study will develop energy management and cooling flow control strategy to coordinate the various energy sources.

The performance evaluations of the system will be limited to energetic, economic, and environmental performance indicators within the project lifetime of 25 years. An economic assessment of the proposed energy system will also be conducted, in different geographical locations of Nigeria. Finally, a case study to demonstrate the research findings will be adopted.

For ease of modelling and performance evaluation some assumptions for the wide applicability of the system are made. The study and model formulated is based on the following assumption and limitation, viz: The weather condition parameters which are inputs for the performance simulation remains the same during the entire project lifetime of 25 years. With this assumption, the annual energy performance of the energy system in the first year of operation is taken as subsequent year performance but reduce based on a depreciation factor. For simplifying the economic analysis, replacement of any system component due to failure before the replacement is neglected. Another limitation in this study is the assumption that the power and hot water demand do not change during the project's lifetime. In addition, for simplifying the evaluation, the grid random power outage for the first year is assumed to be the same throughout the analysis period. The change in the economic indices for the study location is

kept constant throughout the analysis period. Finally, the performance of the energy system in all geographical locations are evaluated under identical power demand, hot water demand size and building configuration

1.7 Research methodology

The hybrid photovoltaic solar thermal energy system integrates different power sources, both renewable and conventional, with the PVT collector to provide an energy solution for various load conditions. The combination can either be two or more renewable energy systems or various renewable and non-renewable energy systems. In most situations, renewable-based hybrid energy systems are created to form energy systems that complement one other to maximise a location's renewable energy potential. [63]. Renewable energy sources vary randomly and are unpredictable to a large extent. Consequently, a single renewable energy system cannot reliably meet energy demand. Therefore, a combination of two or more renewable (RE) systems with a conventional energy source offers options that reduce or even eliminate the intermittent nature of the power output of individual RE systems. The hybrid energy system has more savings over its life span than the conventional power system [10].

For this study, the data required to estimate the actual power demand of the case study health facility selected to demonstrate the method is acquired using the data acquisition sheet. Since the HVAC power demand depends highly on the weather condition and occupancy period, a numerical 3D dynamic model of the building envelope was developed to estimate the HVAC power demand. Consequently, the proposal OPVETC is modelled and simulated based on the developed multi-objective EMSC that meets total building power and hot water demand in the most reliably, economical, and environmentally friendly manner. Lastly, an equivalent basic PVT hybrid energy system is modelled, and the performance of the proposed OPVETC is

benchmarked against the basic PVT hybrid system to evaluate the benefit of the new system relative to what is currently adopted. Figure 1.4 is a mind map and a summary of this research.

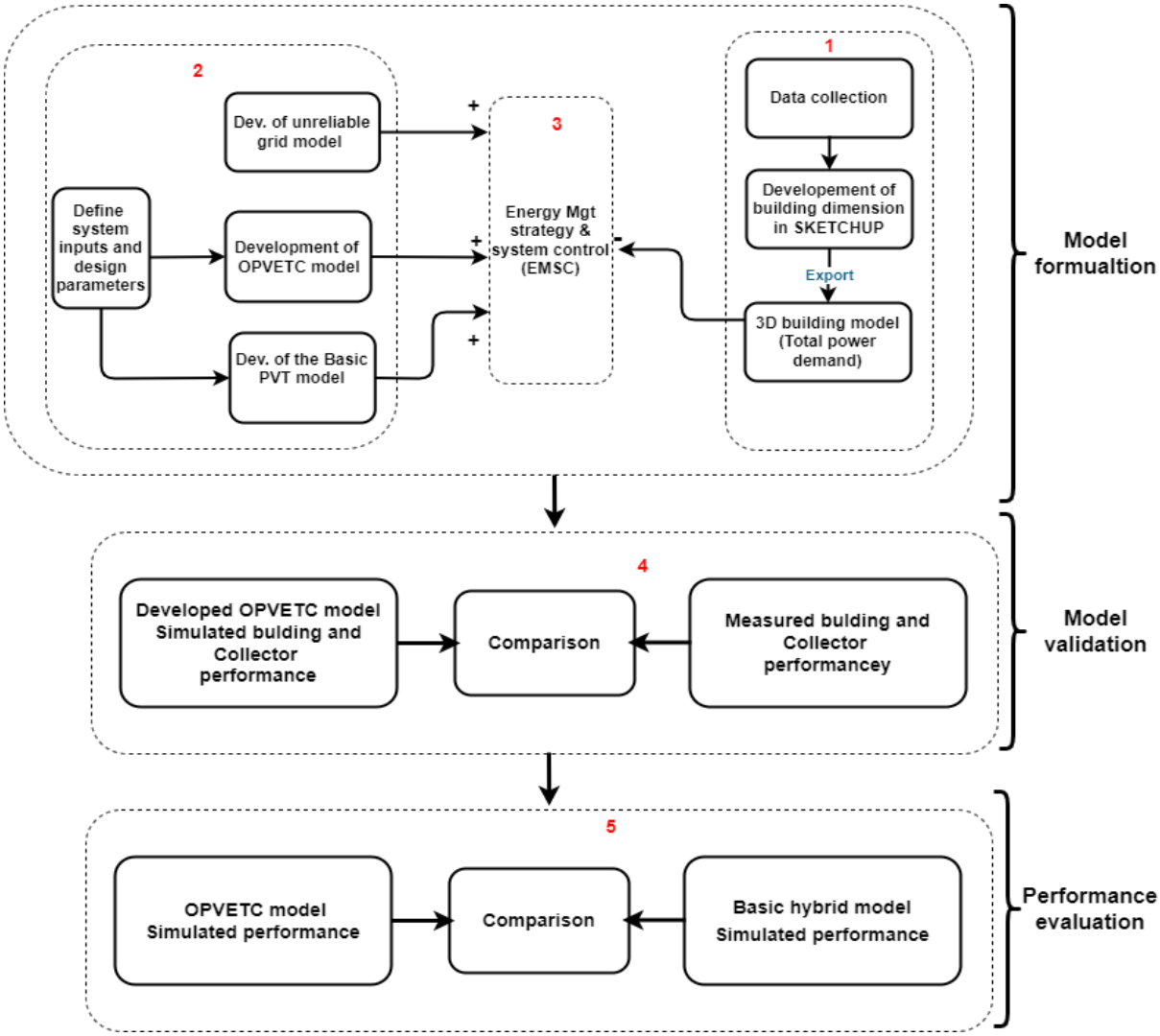


Figure 1.4: Flow chart of methodology and summary of the study

1.8 Thesis structure

The remainder of the thesis is organised as follows: Chapter 2 provides an overview of the literature review on hybrid photovoltaic energy systems, considering the various structural modifications and cooling strategies. Chapter 3 discusses the approaches used to attain the objectives indicated in chapter 1, while chapter 4 discusses the study's findings and implications. This chapter also evaluates the economics of the proposed hybrid energy system

and the techno-economics in six geographical locations of the study country to serve as a basis for policymakers and investors. Chapter 5 is the conclusion and recommendations for future research.

1.9 Chapter summary

Grid power, the primary energy source, is randomly unreliable and inadequate to meet the growing demand for energy in most developing countries, including Nigeria. Most worrisome is that grid power outages can occur 33 times, lasting a minimum of 8 hours in a month in the case of Nigeria. Sadly, critical sectors like the health centres solely rely on reliable power systems to operate to their total capacity. Renewable energy systems are suitable for remote areas and even areas with unreliable grid power sources. The photovoltaic solar thermal hybrid energy system is most appropriate for building applications, especially health centres, since its energy demand is primarily power and thermal. Since the basic photovoltaic solar thermal hybrid system is conceived principally to cool the module to enhance its power production, an enhanced cooling method and system reconfiguration may improve the system's total power output better than the existing basic system configuration and cooling method. The gap here is finding a better cooling approach and system reconfiguration that would be beneficial in improving the system total energy production targeted at better system economics. This study, therefore, is directed at filling this gap incredibly, revealing the business outlook of the proposed contribution.

Chapter 2: Literature review

2.1 Introduction

This chapter provides a detailed overview of previous studies conducted in the field of conventional water-cooled PVT hybrid energy system, which is currently the subject of extensive research to identify the gaps and the methodology needed to fill these gaps. The focus is on the system configuration and hybridization, energy management and cooling strategy, and methods to evaluate the techno-economic performance of the PVT hybrid energy system connected to a randomly unstable grid power source for electric and hot water applications. The last part of this section is a summary of the results of the literature review and a description of the research gaps identified in the comprehensive literature review.

2.2 Overview of the studies conducted on the PVT hybrid collector

Four decades after the first PVT collector was developed in 1978 [64] the commercialisation of this technology is still slow and limited. To some extent, the slow acceptance of this technology is related to the inability to produce a cost-effective collector and its intrinsic low energy conversion efficiency, like with other renewable energy technologies.

Therefore, so much attention and research studies have attempted different methods that progressively increase the efficiency in recovering the total available energy in the PVT collector. To this effect, various modifications of the PVT collector based on the top covering led to classification based on configuration as an unglazed and glazed collector. The study by Hissouf et al [65] concluded that the glazed hybrid PVT collector has 21.49% higher thermal efficiency relative to the unglazed hybrid PVT collector while the unglazed is 11.78% more

effective for power production than the glazed collector. Other classifications based on configuration include flat plate PVT collector, Concentrator PVT (CPVT) and building integrated. Based on the cooling fluid, the collector is classified as PVT-water [66] or PVT-air [67]. Others are PVT-nanofluid[68]. Figure 2.1 is a schematic representation of the classification of PVT collectors.

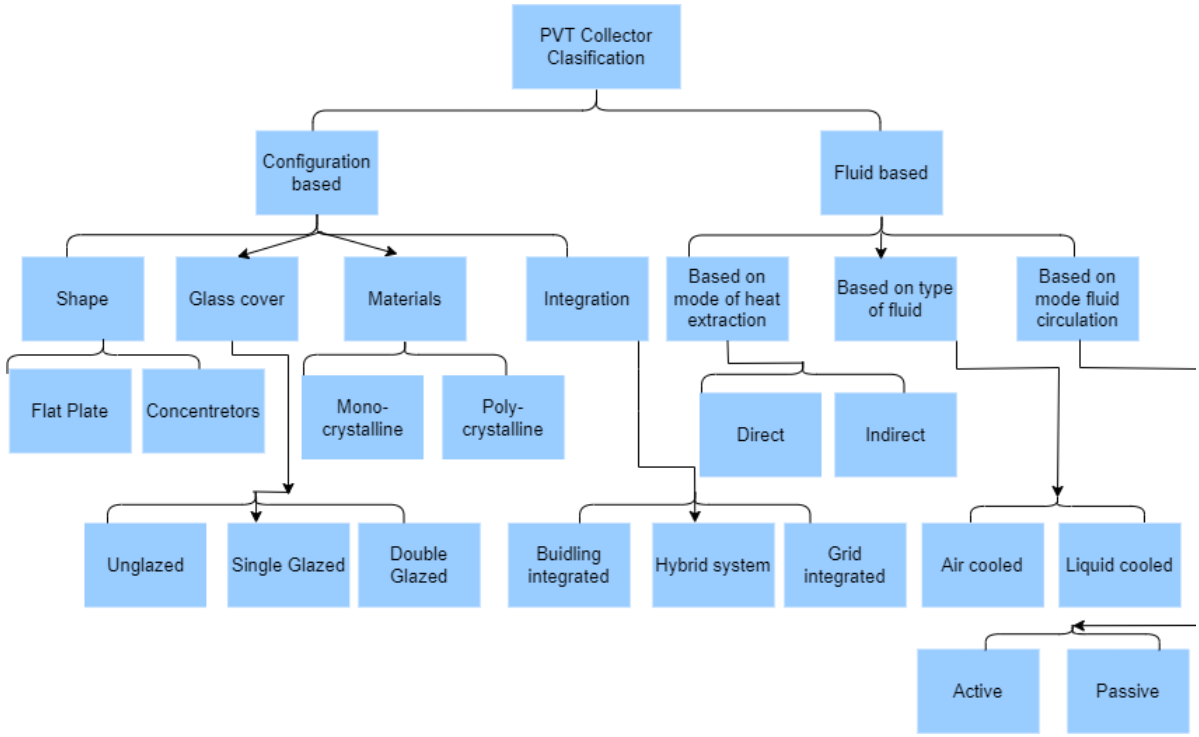


Figure 2.1: Major classification of the hybrid PVT collector

The flat plate is the most widely adopted due to its simplicity in design [69]. It is most suitable for application in residential buildings and Health centres since hot water is required at low-grade temperatures in these facilities. For large-scale applications where many collectors are necessary, the system employs a pump to circulate the cooling water through the collector [70]. The typical configuration of the sheet and tube flat plate is shown in Figure 2.4.

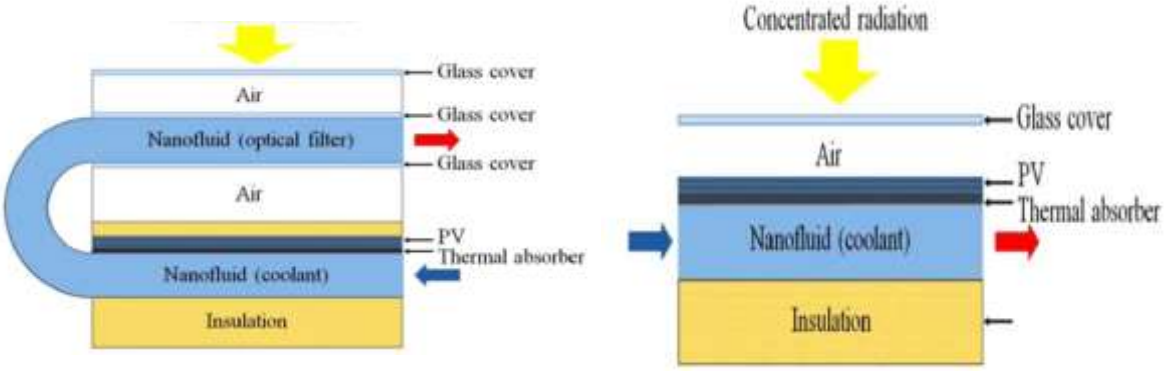
As seen in Figure 2.2, [71] the concentrating PVT collectors use reflecting surfaces to concentrate the rays to the PV module, and they typically have higher fluid outlet temperatures in the range of 100 to 500◦C [72]. Additionally, the flexibility in adjusting the temperature level makes it more desirable [73]. The complexity in design and high cost of the concentrating PVT collectors is a hindrance to its wide adoption for small scale applications. A significant advantage of the flat plate PVT over the concentrating PVT is its ability to utilise both beam and diffuse components of the global radiation. Hence, making the flat plate PVT collector adaptable in a wide range of weather conditions.

In contrast, the concentrating PVT collector functions best only with the global solar radiation beam component. Moreover, CPVT requires tracking while operating; consequently, some system energy goes into tracking. Different studies have shown that the fluid type and the surface cover also influence the thermal and electrical characteristics of the PVT collector. Water, for example, has a higher thermal capacity; therefore, when used to cool the PVT, the thermal and electrical output is higher than the air-cooled PVT collector [74]. As seen in Figure 2.3 [89], the use of nanoparticles in liquid in the indirect cooling configuration has significantly increased the liquid-type collector's thermal and electrical output [75]. The recirculated fluid in the indirect cooling method, usually liquid refrigerants, will have to be cooled through a heat exchanger before returning to the PVT collector. The demand for a cooling unit in the indirect PVT collector cooling configuration has a higher cost and additional demand for power to operate the cooling unit [76]. In naturally cooled liquid type PVT collector, fluid movement is through the natural force of buoyancy created by the fluid density (passive system). While for force circulation, fluid motion is through a fan for air-type or pump as the case may be. While the passive approach is relatively less expensive and requires no pump for water circulation,

the active system is flexible for building integration and easily controlled to achieve the desired temperature for different applications than the passive system.



Figure 2.2: A parabolic reflective surface PVT collector [71]



(a) (b)

Figure 2.3: Nanofluid cooled PVT collector [89]

Most commercially available PV modules now have a solar conversion efficiency of 5 to 25%, and the remaining radiation is trapped and converted to heat in the PV panel [77]–[80]. Since most commercially available modules have negative temperature dependence efficiency, the resultant effect of an elevated temperature in the collector is a corresponding decrease in the

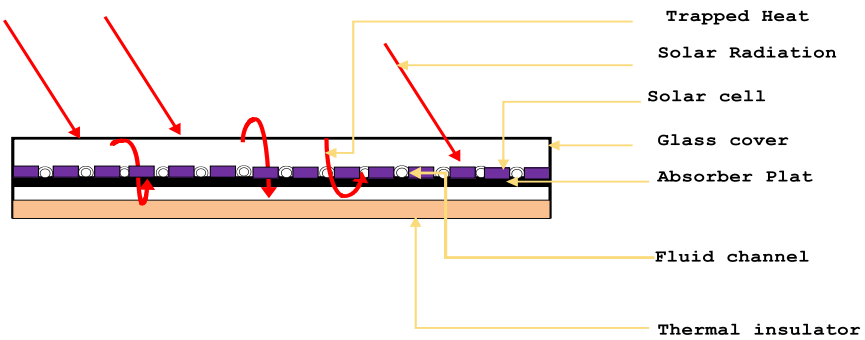
electrical performance. For a constant value of solar radiation, Moharram et al. [81] demonstrated that the power output of the PV dramatically decreases with an increase in PV cell temperature. An increase in the solar cell temperature brings about a decrease in the voltage, which leads to a significant drop in the power output of the PV panel. Moreover, the trapped heat and the one absorbed by the solar cell may cause permanent deformation to the cells when left untapped for long hours[82]. Table 2.1 shows the power loss coefficient range of efficiency and value of some standard commercially available PV modules [83]. The table shows that the power production of the PV modules with higher efficiency highly depends on the PV collector temperature. Conversely, their power output decreases faster with increasing temperature than lower efficiency modules. As observed in Table 2.1, the power output of mono-crystalline (c-si) and poly-crystalline (pc-si) silicon modules is more sensitive, decreasing at 0.45% per degree rise in temperature [83].

In contrast, the amorphous silicon module is less responsive to increased PV module temperature, with a power loss of 0.25% per degree increase [84]. The type of PV module used in developing a PVT collector can have profound power implications. Because higher efficiency PV modules have a higher temperature dependence, using this type for a PVT collector will result in more power if an appropriate cooling approach is used. On the other hand, a poor cooling strategy will result in a significant loss of power. The cooling method may not significantly impact power output in the case of low efficiency and temperature-dependent modules as it does in the case of high-temperature dependent modules. Choosing between the high and low-temperature dependent modules comes with a trade-off.

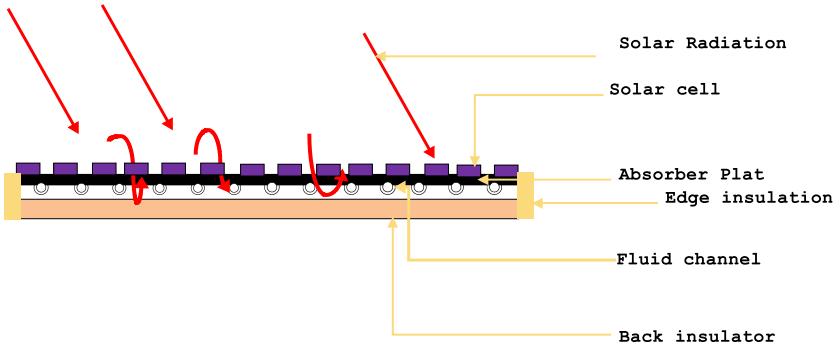
Table 2.1: Efficiency and temperature of some available PV modules [84]

S/N	Type of collector	Efficiency (%)	Temperature coefficient (%)
1	Mono c-si	15-20	-0.446
2	Poly-Si	10-14	-0.387
3	a-si	5-9	-0.234
4	CdTe	7	-0.172

In some PVT collectors, the top surface is covered (Glazed collector) with a transparent material, usually glass, as in Figure 2.4a. For an unglazed collector Figure 2.4b, the laminated solar cells on the absorber plate are directly exposed to the sun. The advantage of the unglazed over the glazed is increased electricity production. On the other hand, the glazed PVT collector has a higher thermal output than the unglazed collector. The choice of glazed or unglazed collector is solely determined by the intended use of the generated energy. The glazed collector is a good choice for applications where thermal energy is prioritised. If the power is of more importance, the unglazed PVT collector will be more appropriate.



(a)



(b)

Figure 2.4: Cross-sectional of (a) glazed (b) unglazed collector

The unglazed flat plate PVT collector and the active direct cooling method are the best fit for this study because the collector is easy to integrate with other systems and can be easily controlled to achieve the desired goal of higher electrical production. The cooling method chosen is water-based, and the fluid passage is made up of sheet and tube geometry channels (Figure 2.4a). Despite its higher level of complexity, the liquid-based exchanger was chosen because it has a higher heat transfer capacity than air-based systems [85]. Furthermore, because water heating is one of the applications in this project, the liquid systems can be used directly for preheating domestic hot water (DHW).

2.3 A review of solar photovoltaic systems cooling methods

Many studies have attempted to reduce the loss of electrical efficiency due to increased temperature associated with an increase in solar irradiance. Considerable studies have reported improving system efficiency based on several configurations and cooling methods. For

example, in fin and sink cooling, the heat content of the solar cells is conducted away by a fin or a heat sink having excellent thermal conductivity properties. The collector fin or the heat sink is attached to the PV module surface either at the back or sides. Usually, the collector fins made from metals with good thermal conductivity are channels through which heat is conducted from the solar cells. As a result, the convective heat loss coefficient of the absorber plate surface is enhanced by the fin or heat sink [86].

Their findings revealed that the heat sink lowered the solar cell's temperature and improved its power output. In conclusion, the authors reported that the heat sink cools the solar cell better in force convection mode when the movement of air over the surface of the heat sink is aided through a blower. The result improved the power output by about 8% and 16% over the uncooled solar cell for natural and forced convection.

Another study conducted by Egab [86] using ANSYS-fluent software showed that the geometry and the number of fins on the heat sink are essential factors to consider. In their analysis, the heat reduction increases as the number of fins increases. However, in their findings, no mention of how the rise in the number of fins has a positive benefit on the heat reduction affects the cost.

For the water spray technique, the PV module temperature is lowered by sprinkling water or water-based nanofluid via the sprinkler to lower the PV module temperature to setpoint temperature, as seen in Figure 2.5 and Figure 2.6. The operation starts with a solar pump pushing water from a storage tank into a pipe located at the edge of the module. Subsequently, the water or water-based nanofluid is sprayed through the nozzles from the tank via a suction pipe.

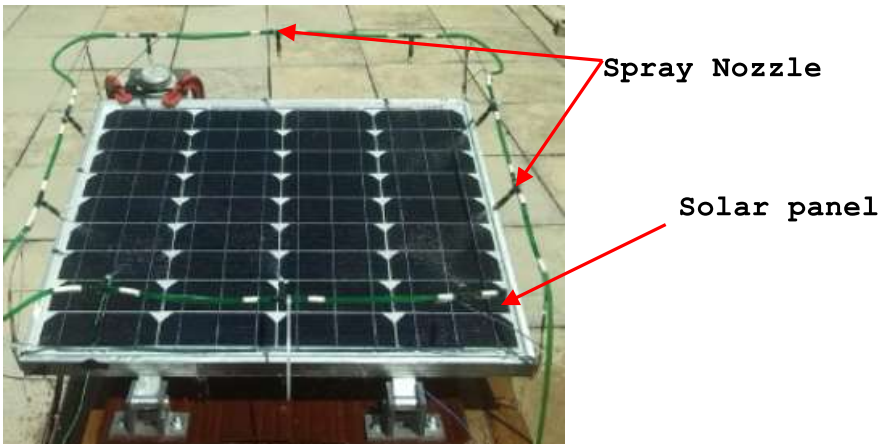


Figure 2.5: Solar panel cooled by the water spray method [87]

Wai Zhe [52] used computational fluid dynamics (CFD) to simulate the effectiveness of the water spraying technique used in cooling the PV module. In that study, a range of cooling water inlet temperatures starting from 20 °C to 45 ° was sprayed over the front surface of the PV module C at a fixed volume flow rate of 350 L/h. The result showed that the average PV module temperature was reduced by about 15.63^{o}C when the module surface was cooled by water at 20.0^{o}C. The outcome showed that the lower the inlet water temperature, the more effectively removed the PV module's heat. This study suggests that it is almost impossible to keep the cooling inlet water temperature at 20^{o}C in practical systems designed to meet both thermal and electrical energy. Hence, further study can include a novel cooling unit other than the widely used heat exchanger unit and further investigation to justify the additional unit cost and energy savings. In a similar study, Hasan and Sopian investigated the effects of jet impingement on the electrical and thermal PVT efficiencies based on the sprayed and heat exchanger cooling methods using various types of nanofluids (nanoparticles). Figure 2.6 depicts the experimental setup used to assess system performance [68]. The findings revealed that the maximum power of the PVT collector improved by about 62.5% relative to the conventional PV module.

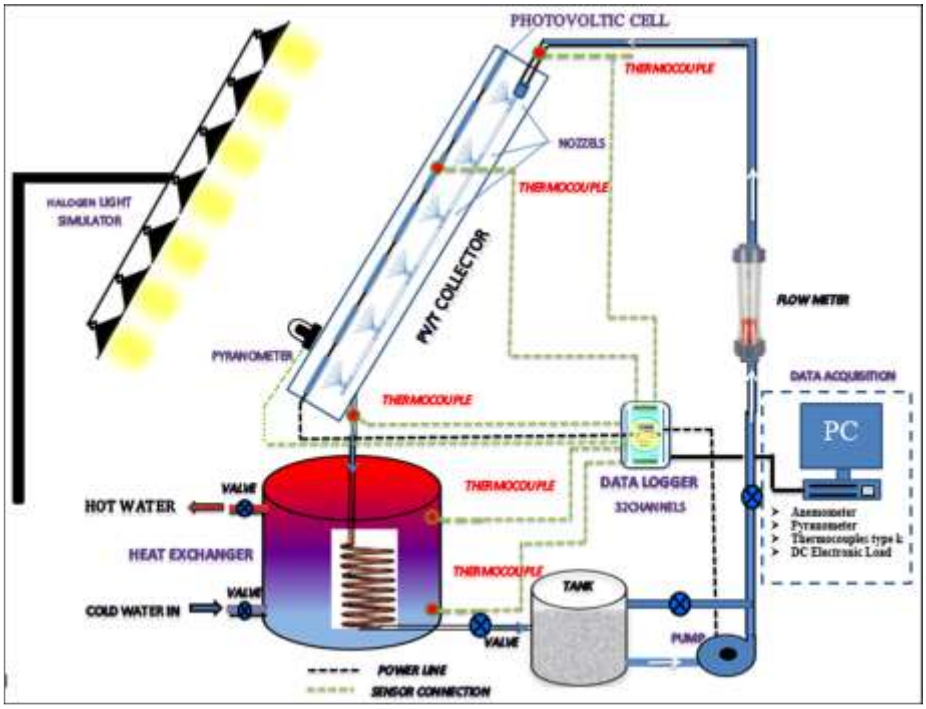


Figure 2.6: Combined jet impingement & heat exchanger cooling method [68]

Yang [88], in an experimental investigation, compared the performance of the PV module operated under three conditions. Firstly, the performance was evaluated without the cooling of the PV module. Secondly, water in the spray cooling circuit was sprayed over the surface to cool the PV module. Lastly, the cooling water in the cooling loop was passed through a shallow u-shape heat exchanger installed in an existing well to be cooled before returning for another round of cooling. The results show that the U-tube heat exchanger kept the recirculated cooling water at a maximum temperature of 29 °C, so the PV efficiency was 4.29% higher than when the sprayed water temperature was not reduced. When solar radiation is high, the benefit of cooled sprayed water on the efficiency is significant. As a result, it is more beneficial in areas with high solar irradiance.

In similar research, Ibrahim et al. [89] modified the solar absorber fluid passages of the basic PVT attached beneath the PV module to several spiral patterns using a hollow rectangular channel. The goal is to enhance circulated water's cooling efficiency and improve the hybrid PVT thermal and electrical potential in meeting power and hot water for household applications in Malaysia. Additionally, the prototype of the novel PVT collector was produced and connected to a water storage tank in a closed loop to set up the experimental rig required to test the performance of the novel PVT collector. The formulated test rig was tested under an outdoor condition based on 0.027kg/s of the circulating water flowrate. From the findings, the maximum collector outlet temperature of the cooling water was 49^{o}C. The collector combined thermal and power efficiency was between 73% to 81% in December 2010. The combined efficiency of the new system is comparatively higher than the combined efficiency of 65% and 49.78% of similar work conducted by Zhang et al. [90]and He et al. [91], respectively. However, no mention of PV nameplate efficiency and how it was influenced by the cooling flow control and the hot water demand profile.

The use of active cooling has also been shown to lower module temperatures. The natural heat transfer has a minor cooling effect [92]. The demerit of supporting the heat transfer effectiveness of the cooling by employing a pump or fan is that it uses more power than natural convection. However, with proper control, active heat transfer can be justified. In light of this assertion, Moharram [81] developed a mathematical model that controls the water pump to spray water on the PV module operated in the desert area in Egypt only when the temperature of the PV module reaches the maximum allowable. The cooling water's spraying stopped when the PV module's temperature dropped the operating temperature of 35^{o}C—the method aimed at conserving the available water and minimising the amount of power required for pumping. Based on the prevailing condition, the model predicted a cooling rate of 2^{o}C/min. The

experimental cooling curve had good agreement with the expected result. Several recent research works have proposed unique design approaches to increase the available energy within the water-cooled BIPVT. Ibrahim et al.[89] proposed a water-cooled BIPVT energy system that employs a stainless rectangular steel tube constructed in a spiral pattern as the heat absorber through which water is circulated beneath the surface of the PV cells. The spiral design of the absorber tube used as the water passage placed beneath the PV cells enables the water to move forward and reverse within the collector, allowing the water to stay longer under the PV cell, hence absorbing more heat before exiting the collector. The result of the experimental testing under outdoor conditions showed that the novel cooling method limited the maximum rise in PV temperature to about 54 ^{o}C. In comparison, the cooling water exited the collector at a temperature of about 49 ^{o}C. Maximum thermal efficiency and the system's electrical efficiency of 51% and 11.3%, respectively, were recorded.

Gagliano etal., [93] reported that the annual simulated performance of hybrid PVT energy system by Kalogirou [94] designed for building energy application in Cyprus could potentially approximately 49% of the hot water demand. However, the total annual system solar fraction for both power and thermal energy demand was only approximately 31.7%. This result indicates the electrical power demand for poorly met resulting to low overall solar fraction

Akbarzadeh and Wadowski [95] found that the power efficiency of a solar trough concentrator PVT collector was increased by about 50% when water based on a thermosyphon method of circulation was used to maintain the PVT collector keeping the collector temperature below 46^{o}C for about 4 hours. Long et al. [96] studied a novel cooling technique for a building integrated PVT collector using the water-cooled copper heat pipes. In their study, the evaporation section of the heat pipe configuration is welded under the solar panel absorber plate. The heat pipe's condenser section, where the heat removed from the PV panel by the

evaporator is discharged, is linked to an external closed-loop water circuit. The external water circuit consists of a water storage tank, and a pump connected through a pipe to the condenser side of the heat pipe serves as a means where the heat removed by the heat pipe is conducted away from the heat pipe. The experimental results conducted to validate the predicted performance of the studied system under the climate of Guangdong province of China showed that the system had an average annual thermal and electrical efficiency of 34.7% and 9.8%, respectively. After comparison, the authors concluded that the system is similar in performance to a direct water-cooled BiPVT energy system.

Chow et al. [97] conducted an experimental study on a water-cooled photovoltaic solar thermal energy system vertically integrated on the southwest-facing wall of the experimental building thermal zone constructed at the University of Hong Kong for empirical research. The experimental building thermal zone was insulated to avoid thermal losses, and the internal temperature of the zone was maintained at 22^{o}C. The study investigates the electrical and thermal characteristics of a water-type building-integrated hybrid PVT energy system under the storage tank's water draw and no-water draw conditions. The electrical and thermal performance of BIPVT were obtained under two cooling modes. First, the hybrid system was cooled by the natural thermosyphon effect aided by gravity. This method was possible since the water storage tank was placed on top of the constructed building thermal zone and water circulation was by the force of buoyancy. Second, a pump recorded system performance under an active cooling water circulation. The second mode of water circulation was possible because the connecting pipes are designed to operate using a bypass that diverts water from the thermosyphon closed-loop to the pump close-loop. The panel's temperature was measured and recorded for each operating mode (thermosyphon or active).

Additionally, the effect of water draws and no water during the system's operation was also studied. The water drawn from the storage tank was automated per the domestic hourly daily hot water load profile. The analysis of the experiment results showed that under a no water draw and based on the passive mode cooling, the thermal efficiency was 38.9% and electrical efficiency of 8.58%. However, the electrical efficiency was lower than the PV's rated efficiency of 14.5%. The result also showed no significant difference in the thermal and electrical performance of the PVT's natural and active operation mode under a water draw condition. However, the annual average electrical performance of the active water circulation mode was 8.7%, a performance considered slightly better than the 8.5% of the PVT collector under the same condition operated under the passive mode.

Chow et al. [98] adopted an experimental approach to study the significant role of box-structure absorber design on the overall performance of a hybrid PVT energy system operated based on the natural circulation of the cooling fluid (water). In their approach, a PVT collector with the rectangular water channels placed below the PV cells was used as the test rig. First, a numerical model based on the finite element method of the system was developed and used to predict the electrical and thermal performance of the system. Second, the measured system performance obtained from the experiment was used to validate the modelled system performance. The results show that the simulated water temperature variation in the storage tank and the electrical efficiency of the box-structure absorber PVT collector utilising water in a close-loop thermosiphon vary in agreement with the experimental result. Based on the close agreement of the experimental result with the model performance, the authors concluded that predicted annual thermal and electrical performance of 57.4 % and 12.3%, respectively, for box-type PVT is a quite promising and desirable alternative in meeting thermal and electrical load.

Bahaidarah et al. [99] investigated the effect of back cooling of a PV module under the weather of Dhanhan, Saudi Arabia, using a heat box-type heat exchanger fitted at the back of the module. The authors developed a numerical model to predict the system's thermal and electrical characteristics to understand the effect of back cooling using water as a cooling fluid in the heat exchanger. Measure system performance obtained during the experiment to validate the simulated performance. The experimental setup consists of a hybrid PVT made from a monocrystalline module with a rated power of 230 watts and electrical conversion efficiency of 18% integrated with the thermal heat collector unit. Water from an isolated tank is circulated through the hybrid system to take away the heat of the PV cells through a pump. The results also revealed that with active cooling, the operating temperature of the hybrid system decreased by about 20% compared to a system with no cooling. The authors concluded that an increase in electrical efficiency of about 9% was achievable due to the cooling of the hybrid PVT system. Hernando et al. [50] developed a numerical model to assess the viability of a water-cooled PVT hybrid energy system for domestic application in UK residential buildings. The aim was to use the model developed to predict the thermal and electrical behaviour to assess its viability for building application under the weather condition of the UK. Parametric studies were also conducted to determine the performance's sensitivity to cooling water flow rate variation and the PV surface coverage. A water-type hybrid PVT energy system was proposed and modelled to achieve the set goal. The cooling circuit for the proposed water-type hybrid PVT energy system consists of a parallel copper pipes riser network embedded under the PV module used as a water channel to pass water under the PV module. The inlet and outlet of the copper pipe network are connected via PVC pipes to the heat exchanger unit located inside a water storage tank. The heat absorbed by the water from the collector is then transferred to water in the tank through the heat exchanger full of water at a lower temperature. For this reason, the water returns to the collector at a lower temperature.

Where the collector exit temperature is lower than the water temperature in the storage tank, a control system is activated to transfer the water to be reheated by the solar collector before it is eventually directed to the storage tank. Hence with this type of control, the water in the cooling circuitry only heats the water in the storage tank. Their findings showed that a PVT collector fully covered with PV module and cooled at a low flow rate of 20L/hr gives the most benefit of the PVT as about 51% and 36% of the electrical and hot water demand, respectively met using the system. The results also reveal that the system's performance is significantly sensitive to variation in cooling water flow. Interestingly, the system's electrical output improved substantially with an increase in flow rate up to 120l/hr.

In comparison, the thermal output increased with an increase in flow rate up to 20l/hr and started decreasing after 20l/hr. The authors concluded that saving from using PVT in a residential building can result in massive mitigation of carbon dioxide of about 16 tonnes over its estimated life span of 20 years. Similarly, a hybrid PVT energy modelled using the advanced tool for simulation (TRNSYS) under the environmental condition of Nicosia in Cyprus revealed that the system could meet 50% of the domestic hot water requirement [100].

Kalogirou and Tripanagnostopoulos [54] presented a technical and economic evaluation of a prototype hybrid energy that coupled a heat extraction unit to a PV module. The aim was to assess the system performance for domestic application under the climatic condition of Nicosia, Athens, and Madison. Consequently, two prototype configurations were considered and modelled; a minor double glaze system operated under the natural circulation of water and a more extensive double glaze operated under the forced water circulation were developed using TRNSYS software. Two scenarios were studied for the two configurations (more minor and more comprehensive); a PVT hybrid system collector with a poly-silicon PV module and a PVT collector with an amorphous-silicon module was assessed. The effect of the water flow

rate on the technical performance of the systems was also studied. The results showed that the a-si hybrid PVT had lower annual electrical energy production than the pc-si hybrid PVT system in thermosyphon and forced circulation operated systems for three locations. A similar trend of better thermal and overall performance is observed for the a-si PVT in all three areas.

Contrary to most results, the analysis of the electrical output for all the modelled configurations with a typical PV module under the same climate conditions showed that the traditional PV system outperforms the PVT collector by more than 50%. The lower electrical performance of the hybrid PVT was due to the recirculation of water to cool the PV component at a higher temperature than the operating temperature of the PV module. The economic analysis showed that the a-si PVT configuration, which is less efficient for power production than the pc-si PVT collector, has a better economy due to the module's lower cost. A summary of the work reviewed is presented in Table 2.2

Table 2.2: Summary of studies on water-cooled PVT with their findings

Ref.	**Cooling Configuration**	**Primary focus**	**Results**	**Remark/Conclusion**
[89]	Direct Water-cooled closed-loop circulation utilising a solar pump	To improve the cooling effect of water on the PVT collector based on a proposed novel spiral absorber tube	Electrical power output improvement varied between 10.4–11.3% Thermal efficiency also varied due to varying solar conditions from 45–51%	The authors concluded that the proposed cooling method has more improvement in days with higher solar radiation
[54]	Direct Water-cooled closed-loop circulation utilising a solar pump	Cooling of the PV collector while using the cooling water to meet hot water demand	Electrical efficiency was improved by 4.8%	PVT hybrid system potentially offset about 49% of the

				hot water demand
[95]	indirect cooling using water in a closed-loop circulation based on thermosyphon	Cooling primarily focused on cooling the collector to improve electrical efficiency	power output increased by about 50% compared to the power output PVT without cooling	Even though the proposed cooling method has improved power production, there remains the need to reduce the considerable cost involved.
[55]	Direct cooling using river water circulated over the surface of the PV panel	Primarily targeted for only cooling PV panel	Power output increased by 12.8% No utilisation of the thermal energy of water	Heat is not made available for reuse
[101]	Cooling using the water-copper heat pipe technique	To improve electrical performance	Power efficiency was found to be 9.8% The average annual thermal efficiency was about 34.7%	Thermal and electrical efficiencies like that of the Bi-PVT/w system
[97]	Direct water cooling of vertically installed PVT collector	A study to understand the thermal and electrical behaviour of a vertically installed PVT on the wall of the building	Electrical efficiency in the range of 6.8% to 8.7% is even lower than the rated electrical efficiency of the panel by about 4% In natural cooling mode, thermal efficiency was 38.9%. However, the efficiency dropped to about 28% when cooled	For the natural and active operation mode of the PVT under a water draw condition, there is no significant difference in the thermal and electrical performance of the vertically installed PVT collector Only one-third of the thermal heat demand for

			in the active mode.	domestic hot water is covered
[98]	Close-loop water circulation based on thermosyphon	Enhancing the overall efficiency of the PVT collector through the use of a box-structured absorber as a water channel	The achieved thermal efficiency varied between 37-45%, depending on the year's season.	The thermal effect of high collector temperature resulted in a loss in electrical efficiency of about 3%
[50]	Water was used as the refrigerant in a closed-loop system operated with a pump to cool a PV module and same time, deposit the extracted heat in a water storage tank	Focused on achieving an optimum electrical and thermal output from the PVT system	The simulated performance indicated that the electrical reference efficiency of the PV is achievable with a flow rate of 20L/hr as against 104l/hr as specified in the reference manual The system could cover only 36% of the total domestic hot water requirement	Electrical and thermal efficiency can be improved with the right flow rate based on the thermal and electrical profile characteristics
[54]	Water was used as the refrigerant in a closed-loop system operated with a pump to cool a PV module, and the same			When thermal heat is prioritised, the a-si PVT collector has better thermal and overall performance than the pc-si PVT operated under any mode.
[102]	Grid-connected hybrid PVT Closed-loop using a heat exchanger	Building heating and cooling	For a 10m^2 PVT, the initial (IC) cost is € 19682 with a	System profitability of identical systems in different locations

			payback period (PBP) of 7.3yrs in Moscow. For similar PVT IC=€39,894 PBP=5yrs in Dubai	depends on the local economic variable
[103]	PVT coupled with a Closed borehole loop employing water and borehole	The focus was on cooling	4.7% higher power compared to conventional PV module	Lower collector inlet water temperature is essential for increased cooling and higher power production
[32]	Stand-alone flat-box Hybrid PVT Closed-loop utilising heat exchanger in the cooling storage tank	Building domestic hot water, heating and power demand	The project has a PBP of 15.6 yrs. in Athens, a PBT of 11.6 yrs. in Zaragoza, 3% higher solar fraction than an equivalent sheet and tube. 65% of annual power demand & (60%), 45% 30% of the thermal demand in Athens, Zaragoza and London, respectively	System performance and economic parameters depend on the weather and economic variable of the location
[104] [47]	Grid-connected Stand-alone flat-plate Hybrid PVT Indirect closed loop utilising heat	Space heating, swimming pool and DHW heating for building application	82.3% and 51.3% of the power and thermal demands met	Integration of system with grid improves system economic indices.

	exchanger cooling loop		PBP of 13.7 years LCOE of 0.109 €/kWh	An equivalent PV system is more profitable than PVT, with an LCOE of 0.089 €/kWh
[66]	Hybrid PVT-water Direct closed-loop cooling circuit	Analysis of the thermal characteristic of different PVT collector configurations	The winning configuration reduces investment cost (by about 21% of the collector compared to conventional PVT	
[105]	BIPVT collectors coupled with micro-wind turbines Direct closed-loop cooling circuit	Comparison of BIPV and BIPVT in meeting building thermal and electrical load	9% increase in power relative to conventional 81% of total thermal and electrical load PBP of 7.61 years	
[106]	PVT-PCM	PVT-PCM and a traditional PV are compared. Effect of the PCM	The efficiency of the hybrid PVT-PCM increased a 7.43% with respect to the traditional PV module.	
[107]	Grid integrated PVT hybrid with battery storage Indirect closed-loop cooling circuit utilising an HX with phase change liquid as refrigerant	Supply the heating and cooling load of a residential building in the city of	53% of the total energy demand is supplied	

2.4 Hybrid PVT integration and operational control strategies

For successful hybridisation of renewable energy resources with grid power, selecting an energy management strategy that ensures optimal and dependable operation is necessary to deliver on the desired objective. It is technically and economically conceivable to have a well-managed energy system that can meet demand while also extending the life of the components, lowering operating costs, and enhancing overall system performance. Understanding the most important performance criteria, such as system reliability, solar fraction, and profitability indices of return on investment and net present worth among others depending on the desired objective, is the only way to arrive at the best technical and financial solution [108]. This is the only way to develop a management plan that ensures optimal system performance. For example, the ideal technological consideration for a hybrid system with battery storage is to keep the battery's operational status at 20% to 30% depth of discharge (DOD) and replaces the battery when its capacity falls to 80% of its nameplate capacity[109]. For example, a control strategy based on fuzzy logic in studying hybrid energy systems consisting of a photovoltaic panel, wind turbine, and fuel cell coupled to the grid power, the control algorithm is desired to reduce costs and increase the power elements' lifetimes [110].

There are several studies on the operational control of hybrid renewable energy systems whose main desire target is to satisfy load demand. For this purpose, the control algorithm is designed to ensure power balance and maintain a proper state of battery charge for battery-based systems. The main advantage of this strategy is the simplicity in design and control, governed mainly by algorithms based on simple flow chart diagrams. If the grid-connected topologies [111]–[113] are used in a hybrid renewable energy configuration, grid power serves as both a passive and active power source, absorbing excess renewable energy and replenishing the system's power deficit when renewables fall short of meeting demand. These topologies enable

greater strategic flexibility while also ensuring demand in any energy environment. Several studies have included the economic matrix in control and balancing demand to ensure system reliability. In most cases, the economic parameters are factors in the strategy to find the optimal energy configuration based on cost.

Energy management strategies used in integrated renewable energy systems to achieve various optimisation goals are based on a variety of technical and economic criteria. These strategies are designed to define the energy flows that occur during normal system operation and to determine which equipment must operate and its power reference. For example, in one study, to ensure that load demand is met satisfactorily with optimal economic value, a Genetic Algorithm (GA) is used for the coordination and operation of a hybrid PV/FC/battery system. [114].

An energy management strategy (EMS) that maximises the solar and wind resources and operates the photovoltaic and wind turbine hybrid energy system at maximum power point was proposed. The goal is to minimise the total life cycle cost while ensuring demand is met. A demonstration of the concept shows a reduction of overall system costs by about 15% compared to the conventional battery state of charge control strategy [115].

A concept of load shifting mechanism was employed by [116] to improve energy management to coordinate the utilisation of energy storage from a hybrid photovoltaic and wind with battery storage integrated with a grid power system. The result analysis found that the ideal load shifting in the control strategy resulted in a 25.66 % decrease in energy cost and a 91.72 % decrease in battery degradation cost compared to the simple basic control without load shifting when discharging the battery [116].

In an attempt to increase distributed energy system stability and reliability, a new control mechanism incorporating day-head demand response energy for the management of rural standalone energy systems was formulated [117]. Based on the objective of balancing power supply with the load demand[118] proposed based on a rule-based energy management algorithm, a smart energy management system for a grid coupled hybrid solar/wind/biomass. A flexible multi-winding magnetic link operating in both grid-connected and off-grid modes is proposed to synchronise the energy operation from PV panels and fuel cells with a battery bank storage. The goal was to have a real-time rule-based controller that controls the power flow in the system optimally based on the desired objective. The analysis of the results revealed a reduction in total energy costs for grid utilisation from 2.13 $/day to 0.315 $/day.[119]

The sizing methodology of a hybrid renewable energy system that utilises the economic predictive model energy management approach was investigated for a standalone hybrid wind/PV system with hydrogen and battery storage. [120]. In another study, a cost-effective algorithm for optimising the operation of a hybrid renewable smart grid distribution system was proposed. The proposed algorithm is focused on maximising the use of renewable energy sources while simultaneously minimising the overall cost of meeting the load demand. Furthermore, the batteries are also controlled by an intelligent energy technique that forecasts and discharges the battery only when there is no significant load expected in the near future [121].

The numerous uncertainties associated with a grid-connected hydrogen refuelling station may result in higher operating expenses during normal operations. It is proposed that a hybrid stochastic/distributional resilient optimisation strategy be utilised to cope with the many uncertainties involved with the energy management issue to achieve the best possible result. The results demonstrate that the proposed method is more cost-effective than the hybrid

stochastic/robust optimisation method in addressing solution conservatism when a high level of confidence is used in the analysis[122]. An evaluation of a hybrid energy system consisting of photovoltaic panels, hydrokinetic, wind turbine, battery storage and diesel generation for power generation under Persian Gulf Islands weather conditions was carried out by [123]. The study compared the optimal performance of the studied hybrid system based on the cycle charging (CC) and load following (LF) control algorithms. From the result, although the capital cost under LF is higher than the CC, the LF-based options allow higher renewable energy resources.

Hybrid renewable energy systems (HRESs), which combine solar and wind energy technologies with traditional energy technologies, are an excellent way to combat the unpredictability of renewable energy sources while ensuring system reliability and reducing CO_2 emissions, hence offering promising economic benefits. When one of the generation sources experiences intermittent operation, HRESs can ensure that electricity is available[13]. In attempts to solve the reliability and boost hybrid renewable energy systems to meet economically and environmentally friendly loads, many studies have combined photovoltaic solar thermal-based hybrid energy systems with different energy technologies. A sensitivity analysis of the influence of the number of components on the economic performance matrix shows that despite the reported good solar potential of the study location, the combined system is more viable with a lower number of CPVT collectors and a higher number of biomass heaters. Despite compromising the feasibility of the performance, further study could be carried out integrating the proposed system to a grid power source to explore the possibility of increasing the system's viability. A comprehensive literature review by [124] shows that different studies have been reported on combined heat and power systems, and few have considered the hybridisation of the PVT collector with geothermal energy. In this respect, the

author proposed a decentralised energy system comprised of PVT collector arrays, heat pumps, chillers, turbines, and flash chambers to meet a small urban settlement's power, cooling, and heating demand. The proposed system model was developed using TRNSYS software to predict and assess the system's performance under the weather of the Chinese location. Again, the controller and diverter were employed to achieve desired system operation as a response to the load and weather conditions. The result revealed that for a geothermal coupled hybrid PVT energy system with feedback to a reliable grid, the system could meet demand with excess energy fed to the grid. The LCOE of the project was found to be varied from $8.38/GJ to $32.8/GJ for months with good solar and poor levels of solar energy, respectively. However, the extreme assumption of ideal heat loss and rejection suggests that the economic analysis is overestimated.

A similar study was done for a secondary school in a hot climate using a flat plate PVT collector and an absorption chiller incorporated into the grid. MATLAB software was used to create the dynamic model that predicts the load on the building and simulates the system's performance. Economics were applied to evaluate the most cost-effective system components, including the purchase and sale of unmet and excess power to the grid. The study's findings reduced the micro-gas turbine's gas consumption was reduced by 30% from the study's findings. In addition, the cost of power per kilowatt-hour (kWh) decreased to $12.27/GJ [48].

Similarly, the economic analysis based on the dynamic system model of a PVT collector based energy system to supply power and thermal energy for building applications was studied by Beh zadi et al. [125] using TRNSYS software. A comparative analysis of the LCOE for the studied system with the grid revealed that the studied system has a 16.7 €/MWh lower energy cost than the conventional grid power system. The combination of the internal combustion engine, absorption heat pumps heat storage tank integrated with solar thermal based modules

resulted in an 11.3% saving in the quantity of natural gas burned when compared to the conventional power system, as reported by a study conducted by [126], [127]. A dynamic simulation using TRNSYS software by Gholamian et al. [128] of a system consisting of PVT panels integrated with a micro-GT and an absorption chiller to meet urban building load shows a cost of energy per unit megawatts-hour of 8.39€/MWh. Nami et al. [145] demonstrated the steady-state simulation of a hybrid solar and municipal waste-fired CCHP system for DG purposes for the Danish energy market. According to the thermodynamic and environmental analyses, this system's exergy efficiency was 28.58%, with a CO_2 emission reduction of 445.935 kg-CO_2/GJ. The bulk of research on the implementation of CCHP and hybrid renewable energy, for example, uses the dynamic load modelling approach to precisely estimate the load based on scenarios. Accordingly, the software package TRNSYS software was used to dynamically analyse the predicted performance of an integrated PVT collector energy integrated with a boiler and heat storage system for a hotel in cold weather by Farrokhi et al. [129]. The system's behaviour is evaluated using objective functions of energy, cost, and pollution. This study found that the system requires 34 kW of cooling and 47 kW of heating.

A review of the literature shows that the application of the combination of the ground source heat pump (GSHP) with the photovoltaic/thermal (PVT) technologies is one area that has received wide attention. For example, [130] conducted the operation optimisation of the GSHP integrated with the hybrid PVT energy system. [131] performance a sensitivity analysis on the [132] conducted a study that enhances the performance of GSHP. A general conclusion by You et al. [103] from the comprehensive hybrid PVT-Ground Source Heat Pump (PVT-GSHP) is evident when the PVT-GSHP system is utilised for preheating application; the PV efficiency is higher than the PV efficiency of the PVT-GSHP when it is employed for full heating. However, for full heating, the thermal efficiency is higher. It is again implying that the closed-

loop cooling of the PVT collector, an improvement in the thermal efficiency, is always traded-off with a consequential loss of electrical efficiency of the hybrid PVT energy system.

The intermittent nature of renewable energy sources (RES) poses significant operational challenges to the reliability of renewable energy systems. Energy storage can aid in addressing the issues of intermittency renewable power and improve the utilisation and efficiency of hybrid renewable systems. The integration of hybrid renewable energy systems into national utility distribution networks (Grid) is a general practice to increase system reliability and reduce the cost of hybrid renewable energy systems. One key factor necessary for effective performance is the energy management and control of the hybrid energy system.

An investigation by [133] revealed that the adoptive model control strategy used to control the GSHP-PVT hybrid system increased electricity production by 4.4% and 6.2% during cooling and heating, respectively.

Since renewable energy resources are highly random and unpredictable, system operation and reliability are significant challenges that many studies have attempted to address. Different studies have adopted energy storage to store excess power generation and make it available in the period of poor power from renewable sources. This approach certainly helps with concerns of renewable energy intermittency and boosts the usage and efficiency of hybrid renewable systems. The rapid decline in the battery cost is a supporting factor for energy storage employing large battery storage [134]. Sanjel and Baral [152] compare the grid power option with a photovoltaic hydro with diesel and battery storage as backup for power supply in rural communities of Nepal. The authors concluded that the grid power source is favourable with reduced cost of fossil-based power generation, whereas for islanded communities with low power demand, photovoltaic energy systems with battery and diesel generator provides reliable

and affordable power alternative. A similar evaluation of flat-box PVT collectors with a battery sub-storage system shows that the payback period in Anthem is 15.6 years, in contrast to the 11.6 years predicted for Zaragoza [135]. An optimal energy management solution for PV-battery energy systems to handle their energy more efficiently was conducted by [136]. According to their findings, longer battery life can be achieved by carefully choosing the discharge and charge limiting voltages for each battery type.

Similarly, energy management for a micro-grid system with a wind/PV/Battery system based on battery state of charge (SOC) was designed and assessed by Liu et al. [29]. The authors concluded that an intelligent decentralised energy system with wind /PV/battery meets the designed load with good reliability and provides a quick, smooth, and steady state of the switchover of the system. An examination of the benefit of combining the load following control (LF) with the cycle charging (CC) approach on a (PV)/diesel/battery hybrid energy system by [137] was assessed. The result reveals that the integrated use of the load following control with the cycle charging control method lowered the net present cost by 20.6% compared to the energy management approach employing separate LF and CC. A comparative analysis of an off-grid of a PV/diesel/battery hybrid with the diesel alone energy system for household application in Urumqi and China based on one-axis and two-axis tracking was conducted by Li and Yu [138]. This study found that a PV/diesel/battery power system configuration for a family in Urumqi is more economically sustainable than a diesel power system. Additionally, tracking-enabled off-grid PV/diesel/battery hybrid systems lower GHG emissions by 1.1tCO2/year than the untracked PV/diesel/battery hybrid.

Integration of hybrid renewable energy systems into national utility distribution networks (Grid) is a common strategy for improving system dependability and lowering hybrid renewable energy system costs. The energy management and control of the hybrid energy

system is a critical component for optimal functioning. According to [125], the adoptive model control method employed to control the GSHP-PVT hybrid system resulted in a 4.4% and 6.2% increase in power generation during cooling and heating. [139] investigated a grid-connected hybrid renewable energy system controlled based on the improved particle swarm optimization technique. Allouhi et al. [140] assessed the energetic performance of a grid integrated hybrid PVT energy system for building utilisation using TRNSYS software and an energy management control consisting of PVT/Wind/storage tank integrated with reliable grid power. The control strategy was based on the simple load balance ensuring system reliability. The economic performance indicator revealed a Solar fraction of 64.8%, a self-sufficient ratio (SSR) of 90.25% and a self-consumption ratio (SCR) of 43.08%. The lower SCR means about 57% of the power produced by the renewable energy system is sold back to the grid. However, whether the system has a positive Net Present Value (NPV) is unclear. No mention of temperature characteristics of the PV module.

Jazz and Sopian [141] analysed the hybrid compound parabolic concentrator (CPC) integrated with a hot water storage tank. The cooling circuit is closed loop in design for this hybrid system, employing a heat exchanger configuration to reduce the cooling water temperature before re-imping on the PV module's back. Direct water jet impingement enhances the power production of a compound parabolic photovoltaic solar thermal collector. This concept eliminates the need for fluid passages as in sheet and tube, PV power production increased by 31% and collector thermal efficiency was evaluated as 81%. No economic analysis was performed; even though the steady-state performance is promising, with over 80% thermal efficiency and a 7% improvement in electrical efficiency, the system performance could still be evaluated based on the actual thermal and electrical load scenario of a specific case study to assess its techno-economic performance.

The distributed hybrid renewable energy system consists of AC/DC microgrids operated on the bases of a Non-linear robust control technique using Particle Swarm Optimization to effectively coordinate the grid generation with various renewable sources to ensure a continuous supply of power to load, Improved dynamic response of the hybrid system was studied by [139]. The authors concluded that the IPSO control architecture is capable of controlling the dynamic performance to achieve power-sharing in a grid integrated renewable energy system under different modes of operation.

Another study [5] evaluated the techno economics of a hybrid energy system consisting of a diesel generator, stand-alone and hybrid PV/wind energy system controlled employing the HOMER control and optimisation technique. The study also examined and compared the economic viability of standalone and hybrid wind and solar energy systems in six geographical locations in Nigeria., The focus was the economic performance, and the lowest LCOE of $0.104/kWh is reported under the weather data of Jos based on the diesel generation LCOE of $0.226/kWh. Elkadeem [142] conducted a study on a solar-wind-diesel-battery-converter hybrid system controlled based on HOMER control, and an optimisation technique was employed; five grid-isolated PV/wind/diesel hybrid renewable energy systems for agricultural power use in Sudan have been analysed, and compared using a new methodology., The focus was the economic performance indicator, and a solar-wind-diesel-battery-converter hybrid system is comparatively the most economical option with NPC of 24.1M$ and LCOE of 0.387 $/kWh, and Return on investment (ROI) of 39.94%, even though, the system has a higher LCOE than the LCOE of diesel power generation in some cases, the hybrid system has a promising business outlook with 39.94% ROI.

The modified particle swarm based on four power dispatch scenarios was the basis for optimising the Photovoltaic–wind-turbine–fuel cell–solar-thermal collector. The control

algorithms aim to optimise the operation for a minimum cost of energy production based on different scenarios. Based on the four strategies relative to the baseline scenario, the findings showed a cost reduction of 5.01%, 25.59%, 19.42%, and 22.19% [143]. The authors concluded that a modified particle swarm optimization technique yields better results than the genetic algorithm. Belfedhal [144] designed and evaluated a control strategy for a Wind turbine /Flywheel /Battery/ Super-capacitor operated based on the flow chart that regulates power and loads considering the battery state of charge as well as local weather conditions to meet demand efficiently. This control strategy prioritised renewable energy resources to allow minimal dependence on grid power. Jose [145] proposed a new sizing method for a grid-tied wind/hydrogen hybrid energy system to eliminate the high variability. The grid-tied wind/hydrogen hybrid system was simulated based on the wind turbine power curve. Similarly, Hohne et al. [146] used the ON/OFF control strategy to regulate the running cost of a grid-connected solar water heater. The study aims to determine whether a time-based pricing system could be profitable in maintaining the desired quality of hot water temperature of a solar water heater. From the findings, the proposed control resulted in a 44.4% lower life cycle cost (LCC) compared to the baseline operation of a water heater with a solar collector.

Table 2.3 Summary of PVT integration and control strategies

Reference	Hybrid Architecture/	control strategy	Remarks
[140]	PVT/Wind/storage tank integrated with reliable grid power.	Control was the simple load balance ensuring system reliability	It is unclear whether the system has a positive Net Present Value (NPV). No mention of temperature characteristics of the PV module.
[139]	distributed hybrid renewable energy system consisting of AC/DC microgrids	A Non-linear robust control technique using Particle Swarm Optimisation to effectively coordinate the grid generation with various renewable sources to ensure a continuous supply of power to load	The IPSO is capable of controlling the dynamic performance to achieve power-sharing in grid integrated renewable energy systems under different modes of operation.
[142]	solar-wind-diesel-battery-converter hybrid system.	controlled based on HOMER control and optimisation technique was employed	Though higher than even the LCOE of diesel power generation in some cases, the hybrid system has a promising business outlook with a 39.94% ROI
[143]	Photovoltaic–wind turbine–fuel cell–solar-thermal	Collectors coordinated using the modified particle swarm optimization based on these different power dispatch scenarios. The control algorithms are aimed at optimizing the operation for a minimum cost of energy production based on different scenarios	A modified particle swarm optimization technique yields better results than the genetic algorithm.
[144]	Wind turbine /Flywheel /Battery/ Super-capacitor coupled to grid power	Managed using a flow chart that adjusts power and load based on battery state of charge and local weather conditions to satisfy demand while maximising renewable energy resources and reducing grid dependency.	The proposed system can work well for both islanded and/or grid-connected operation modes
[145]	Grid-tied wind/hydrogen hybrid system	Simulated operation is based on the wind turbine power curve to eliminate the high variability	The energy management was based on feedback since the grid in this study is stable and reliable

[146]	A solar water heater that is connected to the power grid.	The ON/OFF control strategy was used to control the operating costs of a grid-connected solar water heater.	The LCC comparison of the proposed system to the baseline system revealed a cost-saving of R48 609.79 over the project's lifetime.
[147], [148]	Grid-connected water heaters	Using a time-based control system, peak load shifting approaches are used in demand-side management (DSM) strategies to shift peak load demand.	Flexible load shifting strategy was concluded to have the benefit of increase in system performance, reduction in system size and increase efficiency for small air handling unit by about 40%
[104]	Grid-connected Stand-alone flat-plate Hybrid PVT	A thermal-load-following operational strategy is used to match the transient profile of thermal demand with the operational plan.	The energy management was based on feedback since the grid in this study is stable and reliable
[149]	CCHP-GSHP-PV-ST	Managed based on the followed total thermal demand and compared with the followed total electric demand	The focus of this study was to compare the follow total thermal and follow total electric demand control strategy on the techno economic of the hybrid system

2.5 Economic analysis

Even though renewable energy systems are profitable and environmentally friendly, their high initial cost per unit impedes their expansion and widespread acceptance [150]. Most renewable energy projects have the primary purpose of reducing greenhouse gas emissions while also ensuring that the project is advantageous to the country's economic growth and development. Furthermore, because the cost of renewable technologies is rapidly falling, the business outlook for renewables is being elevated to the top of the priority list. [134]. The cost of photovoltaic technologies is projected to further decline by about 59% of its cost in 2015 before 2025 [151]. For this reason, photovoltaic energy technologies are a targeted roadmap for the global transition from fossil-based energy systems to low-carbon emission systems. To achieve the global decarbonisation target, the economics of renewable energy technology must be viable to encourage investment and promote fast transition, especially now that the residential sector energy demand has drastically increased and consumes a major portion of electrical power [152] due to the ban on movement in most countries as a result of the recent outbreak of COVID 19 [153].

To assess the economics of renewable energy projects, some commonly agreed engineering indicators that are adapted are the Net Present Value (NPV), the Levelized Cost of Energy (LCOE), the Avoidable Carbon dioxide (ACD), and the Internal Rate of Return (IRR). Others include the Payback Period (PBP), Total Life cycle cost (TLCC), and the Return on Investment (ROI). Several studies reported the assessment of the viability of renewable energy projects based on the renewable potentials and the local economic variables of many locations [154].

For example, Rumman et al. [155] used the Total Life cycle cost and the NPV indicators to show that the novel integration of the photovoltaic solar thermal collector and the ground source heat pump (PV/T-GSHP) for electrical power production for application in building in

Jordan consequently reduced the TLCC by 3.8% and increased the NPV by 13.2% compared to PVT and GSHP used as separate energy systems. Similarly, another study investigated the benefit of coupling the linear Fresnel reflector to the tri-generation system to produce fresh water, chilled water, and electricity over the traditional tri-generation system [156]. This study revealed that the trigeneration system integrated with the linear Fresnel reflector could reduce CO_2 emissions. This study revealed that the trigeneration system integrated with the linear Fresnel reflector could reduce CO_2 emissions. The Levelised Cost of Energy (LCOE) produced by the system integrated with the linear Fresnel reflector was estimated at 6.37USD/kWh. In conclusion, the linear Fresnel reflector integrated hybrid energy system was considered a more viable option than the traditional trigeneration system. A similar integration of the trigeneration gas turbine plant with the parabolic trough [235] reduced the Levelised Cost of power to 5.75USD/kWh with an avoidable annual CO_2 emission of 114k-tone. Based on the desertic weather conditions, an economic analysis of a 1.4kW rooftop grid integrated photovoltaic energy system was designed, tested, and evaluated using Oman as the case study location. According to the techno-economic studies, the grid-connected PV system's levelised cost of energy is $0.045/kWh. Accordingly, the grid-connected PV system is promising since the price of energy generated by PV systems in Oman is lower than the subsidised price of energy generated by fossil fuels [157]

Hernando et al. [158] proposed a technical and economic assessment method of a polycarbonate flat-box structure PVT hybrid energy system designed to simultaneously meet energy demand for space heating, hot water, and power for domestic application in reference building used as the case study. The benefit of the investigated hybrid system was assessed using a reference house load in Athens, Zaragosa, and London weather conditions. The payback time and the avoided amount of CO_2 were used as matrices to compare the system's

performance at these sites. In Athens, the system has a payback period of 15.6 years. In contrast, a lower payback time for Zaragosa of 11.6 years was observed. The results also show that the system can displace 3.87, 1.65, and 1.54 tCO_2/year in Athens, London, and Zaragoza, respectively, if used as a replacement for the traditional household means of power supply. Furthermore, a comparison of the proposed system with the basic configuration of the PVT hybrid system as a benchmark revealed that the studied system has a 3% higher solar fraction and 9-11 % lower payback period in all three locations.

Wang et al. [104] assessed and compared the environmental and economic potential of the photovoltaic solar thermal (PV/T) energy system, the combined photovoltaic and evacuated tube (PV-ETC) energy system, the PV only and the ETC alone energy systems as solar combined heat and power (S-CHP) system to power the sports complex of the University of Bari, Italy. Each system is integrated such that its total area is 4000m^2 and simulated for the same load. The basic CHP system driven by an internal combustion engine was the benchmark for comparison. The result shows that the PV/T-S-CHP system has the highest total energy (both thermal and electrical) production, with an electrical and thermal solar fraction of 82.3% and 51%, respectively. On the other hand, the PV-ETC-S-CHP proved to be the most economically viable option with the least payback period of 9.4 years and LCOE of 0.089€/kWh. Even though the PV/T-S-CHP hybrid system has the most expensive initial investment, with a payback period of 13.7 years, it was shown that its high annual saving and high amount of CO_2 mitigation benefits make it a more sustainable and environmentally friendly option.

An economic assessment of a proposed hybrid PVT collector based on spectral-splitting parabolic-trough to produce hot water, steam, and electricity for a dairy farm in Bari (Italy), shows that the system is viable if the cost of the parabolic-trough hybrid photovoltaic-thermal

collector is reduced by about 70% of it cost then [159]. In a study, Calise et al. [169] concluded that the photovoltaic hybrid energy system is more profitable than the photovoltaic solar thermal (PV/T) hybrid energy system. In contrast, a side-by-side techno-economic evaluation of the PVT and the PV energy system by [160] revealed that despite the high initial investment of the PVT hybrid energy system, its energy performance is higher than the PV energy system when integrated with battery storage. Consequently, the LCOE of the PVT hybrid energy system was lower (0.33USD/kWh) than that of the PV hybrid energy system (0.45USD/kWh) when operated under the weather data northmost regions of Ghana.

Despite the substantial amount of research work in literature reviewed in this study on the integration of the PVT hybrid energy system with different energy technologies to explore the possibility of technical and economic improvement, majority of research are focused on the closed loop cooling configuration. There seem to be less attention on the open-loop photovoltaic evacuated tube hybrid system configuration (OPVETC) coupled to a randomly unavailable grid power source for energy-constrained communities. Therefore, this section conducts the economic and environmental assessment of the proposed OPVETC. For the first time, the economic potential and environmental benefits of the proposed OPVETC hybrid energy system will be evaluated and mapped using a case study health centre located in each of Nigeria's seven geographical areas. The consolidated basic PVT hybrid system architecture is the benchmark for comparing the proposed hybrid system architecture.

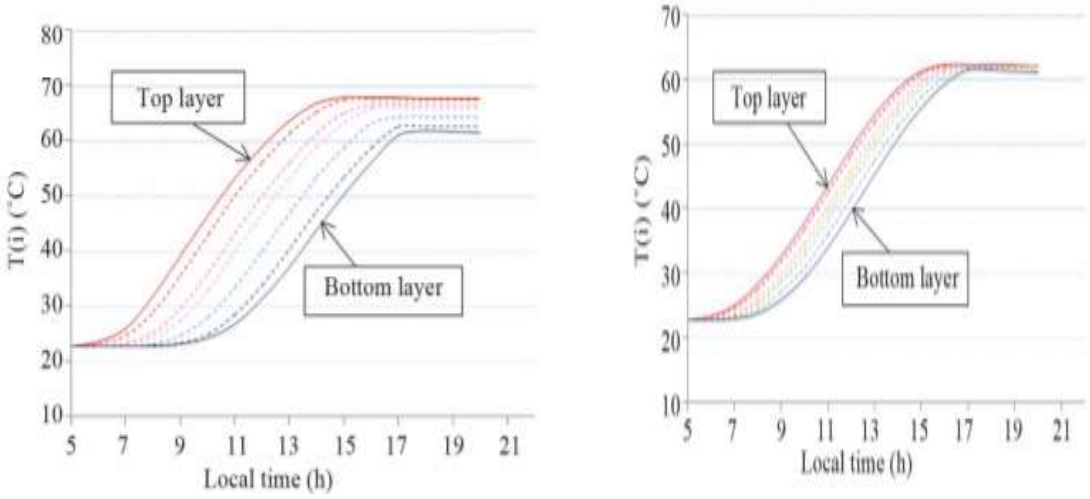
2.6 Identifying the gap and contribution of this study

Several studies have integrated the hybrid PVT system with other renewable energy sources or conventional energy sources to boost reliability and increase the energy efficiency of the entire system [57], [58], [96]. The choice of the system architecture and size is guided primarily by the intended application of the hybrid energy system. In most cases, the focus is to improve

electrical output, and therefore the system architecture adopted should be developed to primarily keep the temperature of the cooling fluid as low as possible to enhance heat transfer between the cooling liquid and the PV cells [50], [84], [161]. Even though the PVT collector is primarily conceived to increase the power efficiency of the PV module, it is evident in many studies, as reviewed in the preceding section, that the closed-loop PVT system configuration is equally tailored to serve the dual purpose of cooling and meeting hot water requirements for low-grade applications in residential buildings [162]. Even though the total energy of the closed-loop system, as reported in many studies, is higher than the uncooled PV module [71], [74], [83], a critical examination shows that the power output of the PV module is lower compared to the uncooled PV module, especially if the intention was to meet hot water at elevated temperature equally [36][50]. This observation implies that using the PVT collector based on the closed-loop configuration for the dual purpose of power supply and hot water services required at high temperatures, say 80^{o}C, reduces the energy conversion and harvesting potential of the PVT collector. Again, it is crucial to note that design considerations desired to increase the thermal output are detrimental to improving power efficiency. For example, flow controls focused on extracting the heat of the collector to improve the power output may negate the target of enhancing the valuable energy of the system. The drawback of the lower power of the closed-loop PVT collector is due to the cooling water entering the collector at a higher temperature due to recirculation and poor flow control resulting from several recirculation.

Consequently, the capacity for heat removal by the cooling water is potentially impaired. For instance, a poorly controlled water flow rate could quickly destroy temperature stratification in the storage tank, leading to uniformity in the tank inlet and exit temperature[53]–[55]. This assertion is supported by the study conducted by [163], as seen in Figure 2.7. It is evident from the graph that a higher flow rate significantly altered the temperature stratification in the

storage tank, making the tank water almost thoroughly mixed. A well-stratified storage tank is beneficial to the PVT collector as water at a low temperature at the bottom of the tank is recirculated to the PVT collector to cool it further. Therefore, an altered storage tank stratification between the top and bottom nodes consequently has an adverse effect on power production in the closed-loop PVT collector.



(a) Highly stratified tank (b) Partially mixed tank

Figure 2.7: Temperature variation between nodes in a water tank [163]

Interestingly, in an experimental study, Karami and Rahimi [164] proved that a higher flow rate of the cooling fluid increases the cooling effect of the cooling water. Their approach conducted an indoor experiment using water-based boehmite nanofluid passed through micro-channels to cool the solar panel. The aim was to investigate the cooling effect of the water-based boehmite nanofluid circulated in a closed-loop at varying flowrate. As shown in Figure 2.8, the results show that the panel temperature dropped from 65 ° C to 33ºC when flow rates were increased from 1ml /min to 300ml /min, leading to an increase in power production by about 27.15% [164][165].

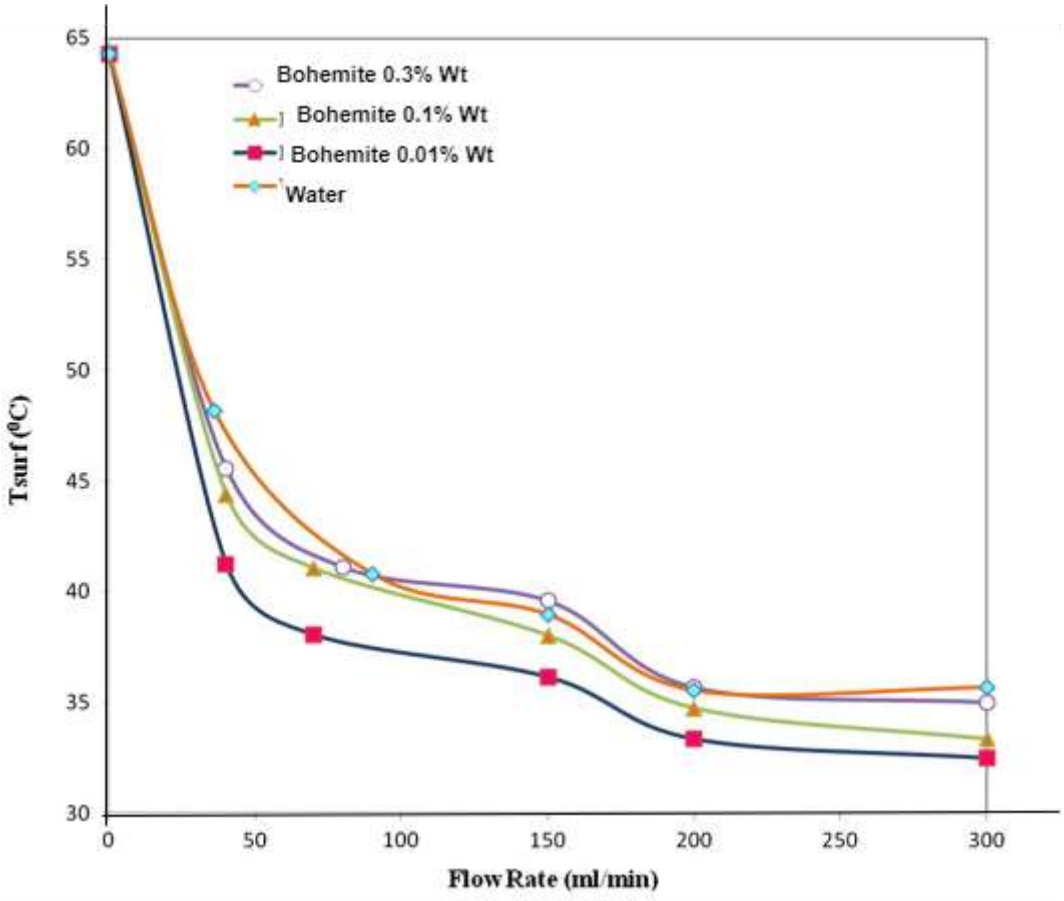


Figure 2.8. Effect of flow rate on the PV module surface temperature [164]

However, this sharp decrease in temperature due to an increased flow rate soon diminishes; as the storage tank becomes thoroughly mixed due to the high flow rate and several recirculation for an extended period.

In the case of the hybrid PVT collector, the simultaneous production of power and thermal energy from a single collector is one inherent characteristic that makes it difficult to size the collector to meet both thermal energy and power demands adequately if the total daily requirement for both is significantly different. For example, if the demand for power and thermal energy is about the same, sizing the collector to meet the power demand will certainly lead to an oversize collector for the hot water demand. Similarly, sizing to meet the hot water

energy demand will almost certainly result in an insufficient power supply since the electrical efficiency of 9.11 -12 % in most cases is far lower than the thermal efficiency of 56-63%, as reported in Refs. [141][166]. It follows that meeting both power and hot water demand will be difficult without a compromise. This compromise is the main reason for the PVT collector hybrid energy system's poor economic viability, resulting in high capital investment with a long payback time and a high LCOE, making the business outlook for investment in PVT technologies less appealing.

Furthermore, in a similar study, Kalogirou et al. [36] summited that in PV/T system applications where electricity production is the main priority, it is more effective to keep the PV modules at a low temperature to keep PV cell electrical efficiency at a sufficient level. It was further stated that in the case of using PV modules without glazing, satisfactory electrical output is obtained compared to PVT with single or double glazing. Again, where the power is improved, the thermal efficiency is reduced due to the increased thermal losses from the PV module surface. The addition of glazing increases the thermal efficiency significantly for a broader range of operating temperatures, but the additional optical losses from the glazing reduce the electrical output of the PV/T system [36]. This observation implies that meeting thermal demand will reduce the fraction of power demand met.

As a result, an innovative hybrid PVT energy system configuration is required to meet the demand for power and hot water in residential buildings. The design of a hybrid PVT energy system with the bi-objective of enhancing PV component performance while ensuring that the system meets the entire thermal load of the building is more complicated and craves innovative ideas and research. To that end, a novel hybrid PVT energy system that ensures good thermal output while still producing high power with minimal compromise to improve overall system

net energy is limited. In addition, from the literature reviewed, many studies have focused on integrating hybrid PVT with the grid with reliable power and feedback policy and tariff.

Furthermore, few studies have thoroughly evaluated the PVT/ETC integrated with a grid power characterised by random power outages based on an open-loop cooling configuration from multiple perspectives. This study aims to fill this knowledge gap by comprehensively assessing the energy, economic, and environmental potentials of a new grid-connected open-loop PVT/ETC hybrid energy system operated on unreliable grid-OPVETC system architecture. The proposed approach is compared explicitly to conventional hybrid PVT. The parameters and details of the methods and transient models of the aforementioned energy systems are introduced first, followed by a description of the methodologies used for the economic and environmental assessments. The Plateau State Polytechnic clinic Jos Nigeria's health clinic power and thermal energy demand is the case study to demonstrate the approach and benefit of the new hybrid PVT energy system configuration and cooling method compared to the conventional and widely adopted basic PVT hybrid energy system.

2.7 Chapter summary

The preceding section reviewed and analysed several studies conducted on the photovoltaic-solar thermal hybrid energy system. These conclusions can be drawn from the different results of these studies; In most studies, the water-cooling technique is predominantly based on the closed-loop cooling system architecture. In most of these studies, the common conclusion is that the total energy production of the PVT hybrid energy system is higher than side-by-side photovoltaic (PV) and solar domestic hot water systems (SDHW) operated as separate units. However, one inherent drawback in this basic PVT configuration and system architecture reviewed is the lower electrical efficiency of the PV module when cooling water is not adequate for effective cooling [97]. This lower power efficiency results from the closed-loop cooling of

the PV module. Since the circulated water is main to remove heat from the PV module, continuous recirculation results in heating the PV module again. Therefore, it implies that the perceived improvement in the total energy output of the PVT collector is mainly due to the increased thermal production. Sadly, the improvement of the thermal energy is the main reason for the compromise of the PV module power efficiency. Again, in most studies, the goal is to increase the electrical output of the BIPVT, and as such, the thermal output is seldom a target.

Moreover, most of these studies integrate the hybrid PVT energy system with a stable grid or scheduled power outage. No studies have been conducted on the open-loop hybrid PVT energy system combined with an evacuated tube for communities with a randomly unreliable grid power source. This novel innovation aims to cool the PV module better to produce higher electrical power and meet the thermal demand effectively with the minimal trade-off in power output as seen in the established PVT hybrid energy system.

Chapter 3: Research Method

3.1 Introduction

This chapter presents and discusses the tools and research method to assess the energetic and economic performance of a new direct water-cooled open-loop photovoltaic evacuated tube hybrid energy system operated based on the unreliable grid control strategy with application in energy-constraint rural health centres clinics to fill the mentioned gap. The energy demand characteristics of the case study health clinic and the weather and climatic conditions of the proposed study area will be used to evaluate the system's actual performance under real load and weather influence. The method to estimate the dynamic cooling and heating power requirement of the case study building using the 3D building modelling approach is described. The methodology to estimate the power demand for the building electrical and medical equipment employing the Service Availability and Readiness Assessment (SARA) survey method as recommended by World Health Organisation (WHO) is described in this section. The choice of TRNSYS as the modelling tool and the detailed steps in the modelling of the OPVETC is presented. The method for sizing the different system components using the parametric analysis approach based on a cost objective function is equally presented. The system's energy management and operating strategy are crucial to ensuring optimal energy production and high penetration and utilisation of renewable energy in meeting load. Therefore, this chapter presents the formulation of the energy management and control strategy to coordinate renewable energy sources with unreliable grid. The proposed cooling technique required to keep the module temperature at a temperature that improves the power conversion efficiency of the module while ensuring that the thermal output of the collector is not compromised is also presented in this chapter. The approach employed to measure the new system's technical, economic performance, and environmental impact based on the developed system model under the real weather and load scenario is

explained. A similar standard PVT hybrid energy system is also modelled as a benchmark to understand the improvement better. The methodology section also discusses the method for assessing the system's lifetime technical and economic performance. The economic viability of the new system configuration, as suggested in this study based on different geographical locations of Nigeria, is evaluated in six geographical regions to benefit policymakers and potential investors. The logical flow of the methodology is illustrated in the Figure 3.1below.

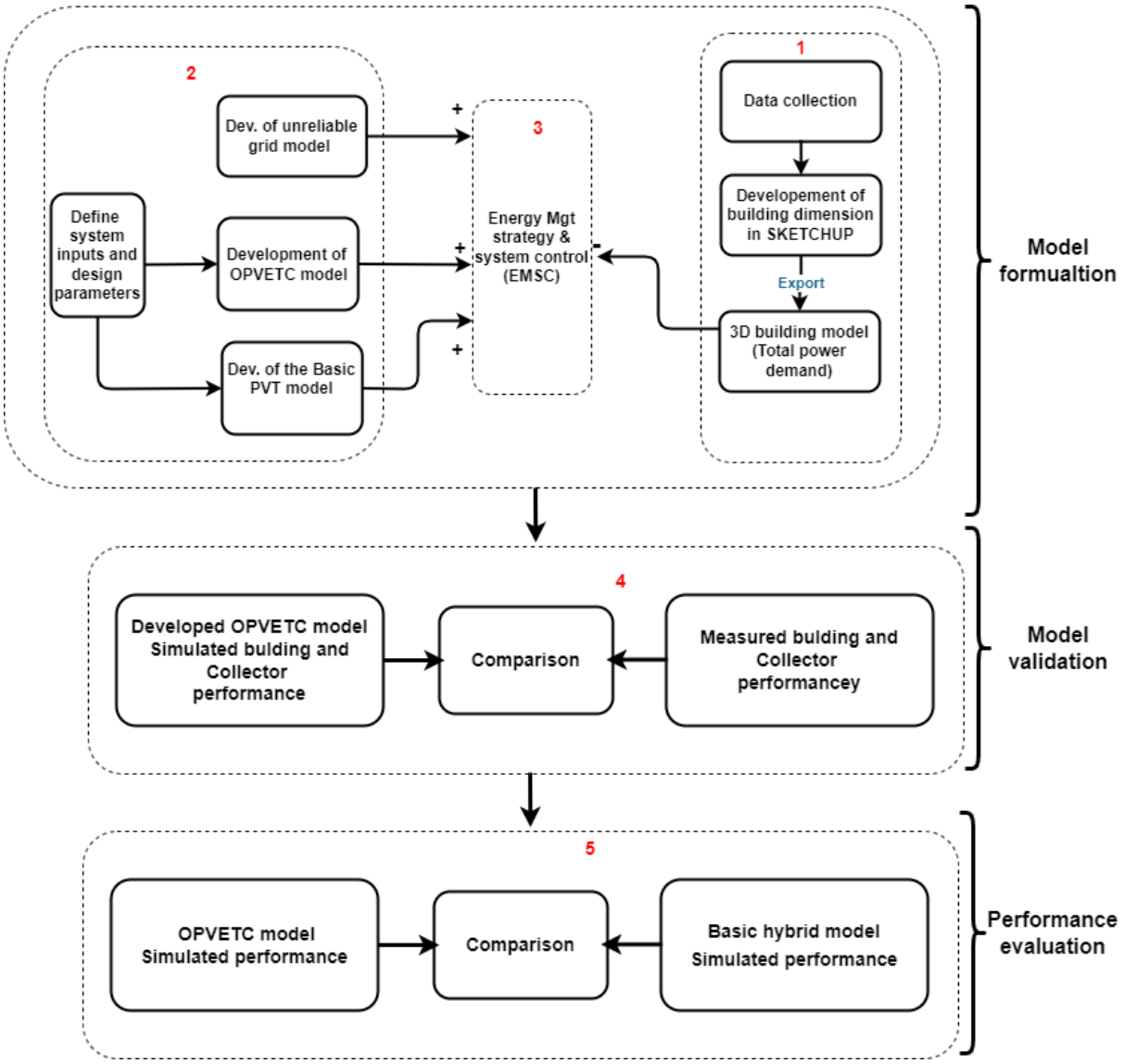


Figure 3.1. Flow chart of the research methodology

3.2 Description of the case study area health clinic energy demand

Weather data which are driving functions for solar photovoltaic and thermal energy systems vary with time and location; as a result, solar energy system performance is typically evaluated based on the climatic conditions of specific locations [167]–[169]. In this study, the actual energy demand of a health centre in Jos, Nigeria, is selected to assess the proposed system's overall technical and economic benefit.

The selected country and health centre represents typical health clinic in Sub–Saharan Africa connected to grid power source with highly unreliable grid power with random power failure. This case study is a good scenario to demonstrate the methodology and approach used in this study since its grid power is inadequate and randomly unavailable. As shown in Figure 4.64, Jos, Nigeria, is a moderate temperature region with an annual average daily solar irradiation of 5.6KWh/m^2 [9].

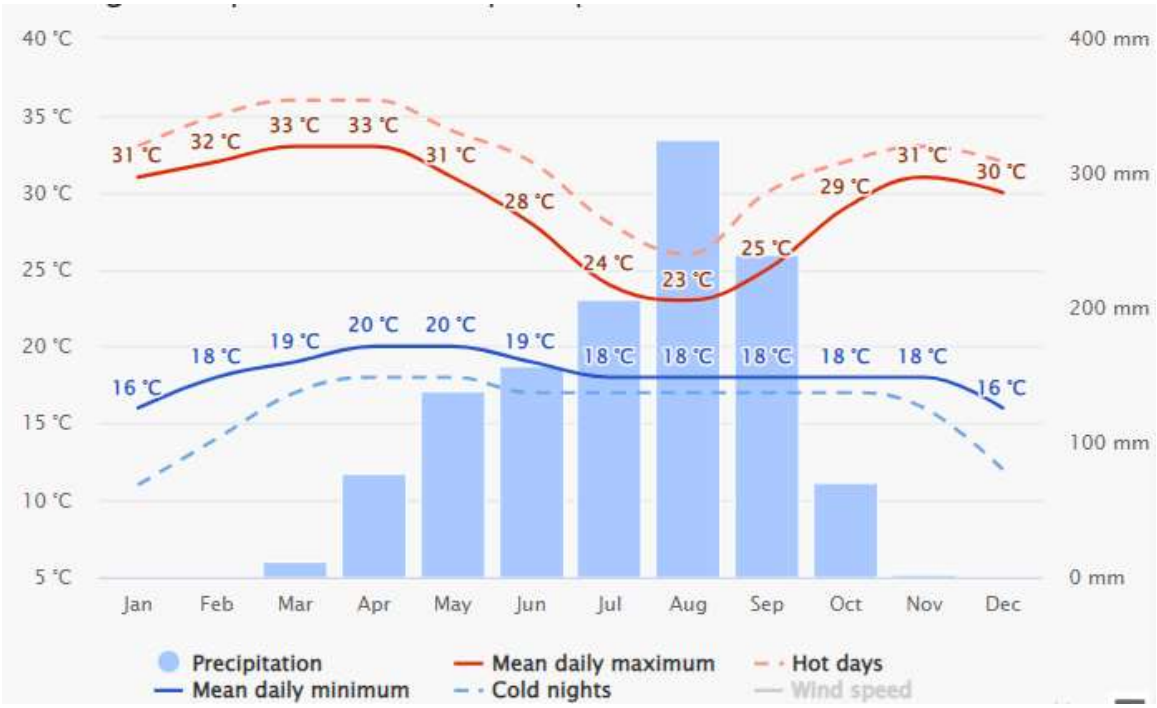
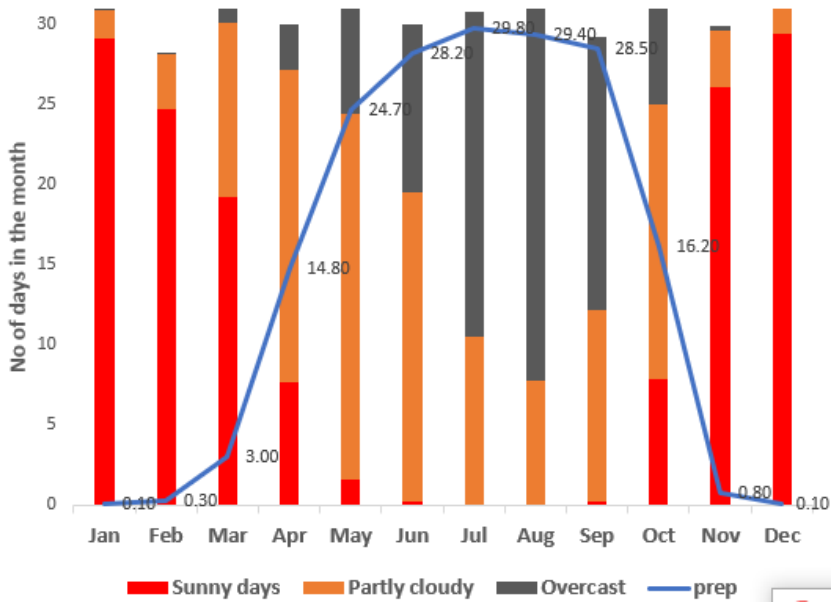
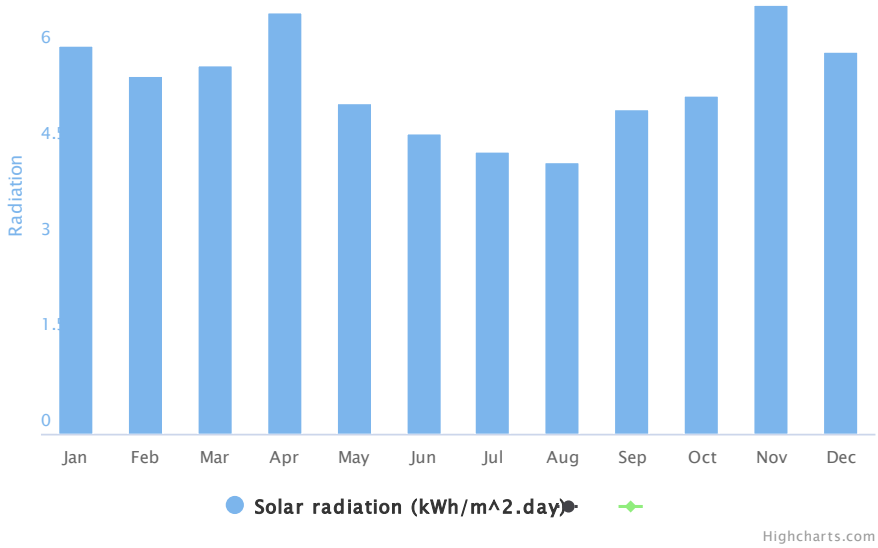


Figure 3.2. Monthly average temperature and precipitation pattern in Jos [170]

It is situated at latitude 9.93N and longitude 8.7 E, at 1200m above sea level. Jos has a tropical climate with a moderate average daily ambient temperature located almost at the centre of Nigeria, as seen in Figure 3.4. In the coolest months, average temperatures could drop as low as 11.5 °C to 18.5 °C, while in the hottest months, temperatures could rise from 23 °C to 35 °C, as seen in Figure 3.2 [170]. Extreme high and low temperatures of above 34^{o}C and below 16^{o}C respectively are experienced in April and January, respectively. In most cases, 67% (224 days) of the time of year, the maximum ambient temperature could rise as high as above 33^{o}C, while on the remaining days, the maximum temperature is below 30^{o}C. This observation has implications for cooling energy demand. It also means that heating energy demand is considered negligible for this location as less than 0.5% of the year's temperature falls below 20^{o}C. On the other hand, the demand for cooling is required throughout the year, with higher energy demand from February to May and October to December, considering that the mean average ambient temperature, as seen in Figure 3.2 for these months, is far above the comfort temperature range of 23^{o}C -25^{o}C.



(a)Monthly daily sunny, partly cloudy, and overcast days in Jos



(b) Monthly average daily irradiation on the horizontal surface of Jos

Figure 3.3. Monthly average daily solar irradiation and sunshine hours [170]

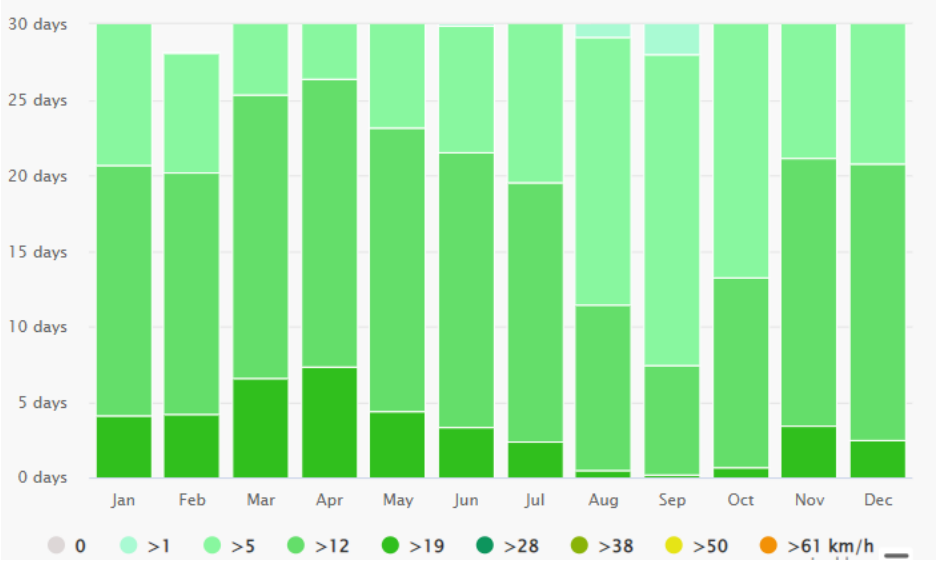
Precipitation usually starts in March and reaches its peak in August. The rainy season usually lasts until the end of October, with some light precipitation of less than 20 mm expected in November. During months of heavy rainfall, the sky is overcast, resulting in low penetration of solar energy radiation, as seen in Figure 3.3 [170]. Notably, the overcast is experienced in just a few days (83days), and for a significant part of the year about (281 days), the sky is clear

and receives an average of 5.6kWh/m^2 of irradiation per day. The implication of about 281 days (70%) of the days in the year with irradiance levels as high as 5.6kWh/m^2 portray good potential for solar energy projects.

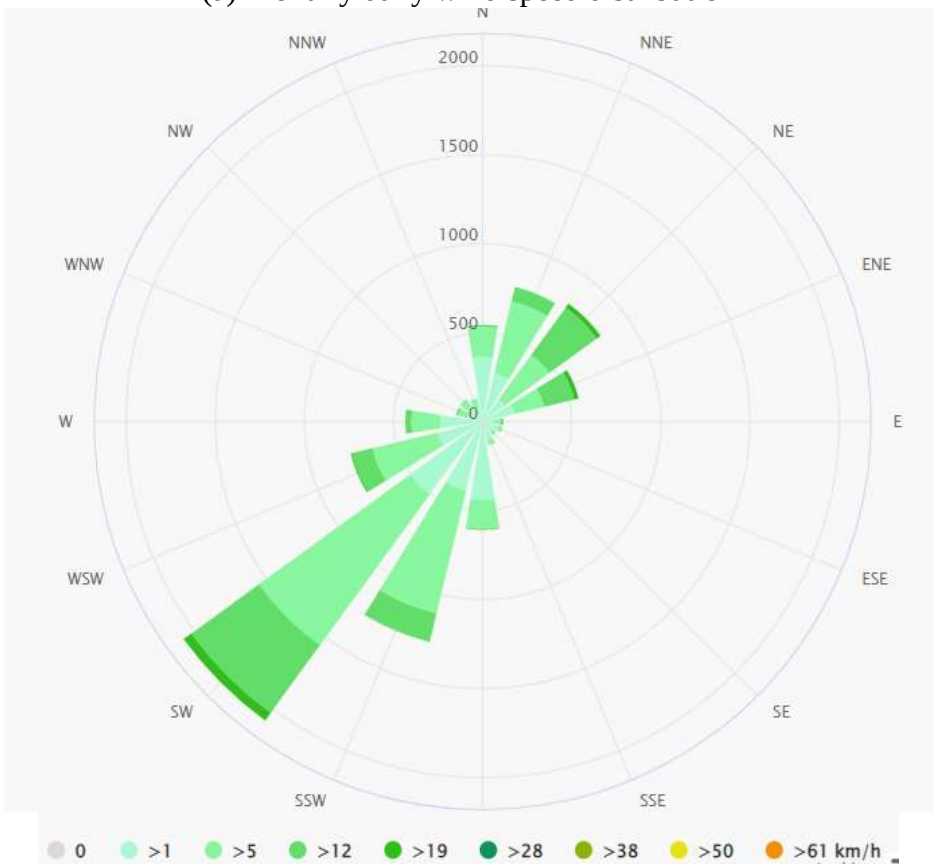
On the other hand, wind speed in Jos is below 10m/s, and about 87% of the time during the year, the wind speed is between 1.3 -5.3m/s and predominantly in the North-East South-West direction, as seen in Figure 3.5. For wind turbine energy systems, the potential for good power generation is within the wind limit of 3.3-5.3m/s. Unfortunately, as seen from Figure 3.5 [170], months with poor levels of solar energy equally have a low wind speed of below 3.3m/s. Implying that wind/solar energy hybrid systems in this location may not highly play a complementary role. Apart from the wind speed, an essential factor for consideration is the direction in which the wind blows. For Jos, the wind direction is South-West to North-East (NE), as seen in Figure 3.5 [170].



Figure 3.4. Map of Nigeria showing the case study location



(a) Monthly daily wind speed distribution



b). Wind speed direction

Figure 3.5. Wind speed distribution and direction of Jos [170]

The demand for power and thermal energy of a typical health clinic in Jos, Nigeria, is used to assess the applicability of this study and demonstrate the proof of concept. The health clinic is a ten-bed admitting ward with 7 rooms used as reception, laboratories, admission wards, and

stored rooms. Particularly two rooms and one room are used as admission wards and reception rooms respectively. The Figure 3.6 is the front and side view of the health centre building.



Figure 3.6. Front and side view of the case study health centre in Jos, Nigeria

The clinic provides simple outpatient health care services for simple case admission. The power demand for basic amenities such as lighting, computers, printers, and televisions, and medical equipment such as UV water purifiers, refrigerators for polio, measle, obstetric, and newborn babies vaccines, is included in the energy demand for power. In addition to power demand for all the equipment as detailed in the Serve Availability and Readiness Assessment (SARA) for as in the appendix A, there is equally a domestic hot water demand (DHW) for cooking, water heating of about 1000 litres per day. The hot water demand comprises of domestic hot water

demand of 2503L, 320L and 427L for sterilisation of medical equipment at temperature of 80^{o}C, laundry at temperature of 60^{o}C and post-natal at temperature of 45^{o}C services respectively.

This clinic is connected to the power grid and uses grid power as its primary energy source. Power failures or outages are a problem during peak demand, even in grid-connected cities and regions. Because of the unpredictability of the power outage, most clinics had to rely on costly backup generators or go without power. Stand-alone diesel-powered generators are the default energy scenario with no grid access in some areas.

Currently, the electric power from the grid is characterised by random and frequent outages, with an average of about 33 power outages per month lasting a minimum of about eight hours [5]. The standby generator meets the health facility's energy requirements during prolonged outages.

3.3 Description of the proposed energy system

The proposed OPVETC hybrid energy system consists of two renewable power components: the sheet-and-tube PVT collector array and the evacuated tube collector (ETC). In addition, it also includes two hot water storage tanks and battery storage as the system's main components. A small diesel generator set is added as a backup for instances where power from renewable sources, including the battery stored energy, cannot meet the building load. Other auxiliary components include the water diverters, pump controllers, and intelligent microcontrollers.

The PV module cooling system consists of (see Figure 3.7) connecting pipes conveying cold water (blue line) from the mains water reservoir to the PVT collector fluid inlet to cool the PV module. For this system architecture, cool water from the mains is conveyed through the array of PVT collectors arranged in series utilising a variable speed pump (P2). The cooling water

exiting the array of PVT collector's outlet is split into two; one portion equal and proportional to the hot water demand profile of the health centre for services at a temperature lower than 50^{o}C (e.g., bathing, dishwashing, etc.), and the remaining portion is further moved to the second diverter. At the second diverter, a portion of the warm water equal to the total hot water demand profile for sterilisation and laundry is again diverted to be reheated in the ETC heating configuration. One unique attribute of the cooling technique is the proportionate control of the cooling water flow rate to follow the available useful thermal energy of the PVT collector. In this case, controller C2 estimates the instantaneous useful energy of the collector based on the level of solar energy it received and the manufacturer's test characteristics of the collector. Based on the estimated useful energy, the flow rate required to keep the collector inlet and exit water temperature at a difference of 50^{o}C is estimated. Since the pump is a variable speed pump, the speed is adjusted to deliver the estimated flowrate from the control signal received from controller C2. The choice of 50^{o}C is based on the minimum hot water temperature necessary for low-temperature services in health centres. This control aims to ensure that the temperature rise of the PV module is prevented from rising as the solar radiation increases while harvesting significant thermal energy for application. Equally, with this type of control, the pump is only operated at rated capacity when the solar radiation is high, and the collector temperature rises, reducing the pump's energy consumption. Since the hot water temperature requirement for sterilisation and laundry are needed at a temperature above 60^{o}C, the preheated water (light red line) exiting the PVT collector array is directed to be reheated by the evacuated tube collector (ETC). In the ETC water heating circuit, the controller C2 is also programmed to control the operation of the pump2 to operate at a constant flow rate of 170kg/hr/m^{2} only when the solar radiation is more than zero. This way, the pump is run only between sunrise and sunset.

The cooling water from the PVT collector is again reheated in the ETC heating circuit. The heated water is conveyed and stored in a properly insulated tank situated in the health centre building. For instances where the hot water temperature stored in the two hot water tanks is below 45 ^{o}C and 90^{o}C for bathing and sterilisation services, the tanks are designed with an electric heating element to heat the water to the desired temperatures. Interestingly, the required auxiliary energy (Qaux) needed to increase the hot water temperature to the desired temperatures is provided first by the PV power and supplemented by the grid power, for instance, where the PVT does not meet all auxiliary energy demands. The PV power system also provides the energy requirement of the heating, ventilation, air conditioning system, and the power to run the pump. In every instance, the auxiliary energy for hot water and pump power consumption are added to the heating, ventilation, and air conditioning (HVAC) load to demand instantaneous power.

The instantaneous power produced from renewable energy sources, the power of the grid, and the total power demand are inputs to the intelligent micro-controller. The smart controller now manages and coordinates the various power sources with the power from the unreliable grid to intelligently meet total power demand reliably in the most economical and environmentally friendly manner. The control algorithm is based on the Followed-Electric-Load (FEL) strategy, where the power demand is first met with renewable energy, including that from the battery storage before the grid power is utilised to meet any deficit. In addition, the inverter component of the power system is added to convert the direct current (DC) power of the PV array to alternating current (AC). Figure 3.7 is a schematic of the hybrid energy system, demonstrating the coordination between the electrical power and thermal energy systems.

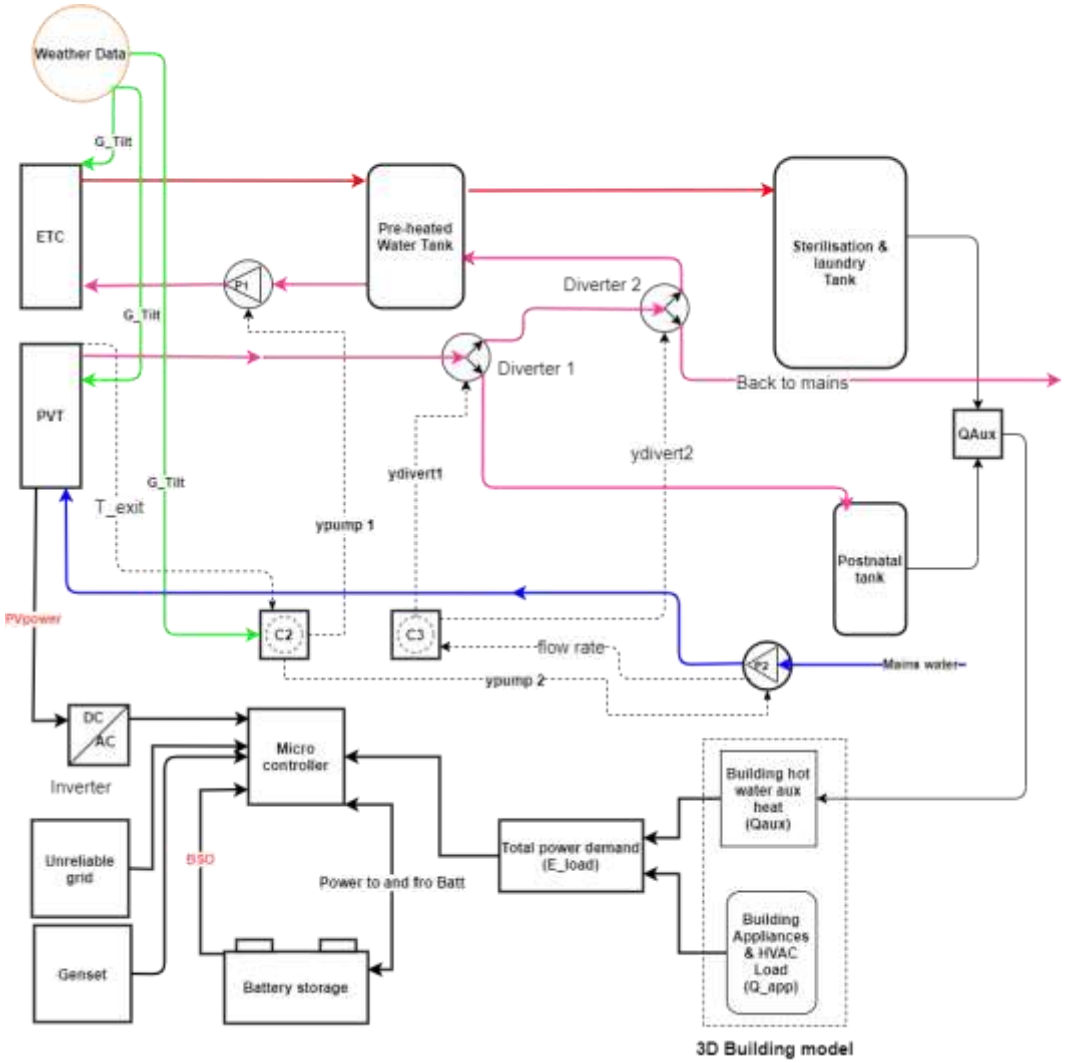


Figure 3.7: System schematic diagram of the OPVETC grid-coupled system

Figure 3.8 is a simple schematic diagram illustrating the applicability of the proposed OPVETC hybrid energy system for health centres' utilisation. The various components of the system are connected, as shown by the direction of the lines. The broken thick lines carry the control signals to components. All power components are connected to an intelligent energy management system (EMS). The aggregated load from the building is also input to the EMS control system. The innovative EMS now coordinates the energy sources to match the load, ensuring that the system is reliable and economical with the lowest possible negative environmental impact.

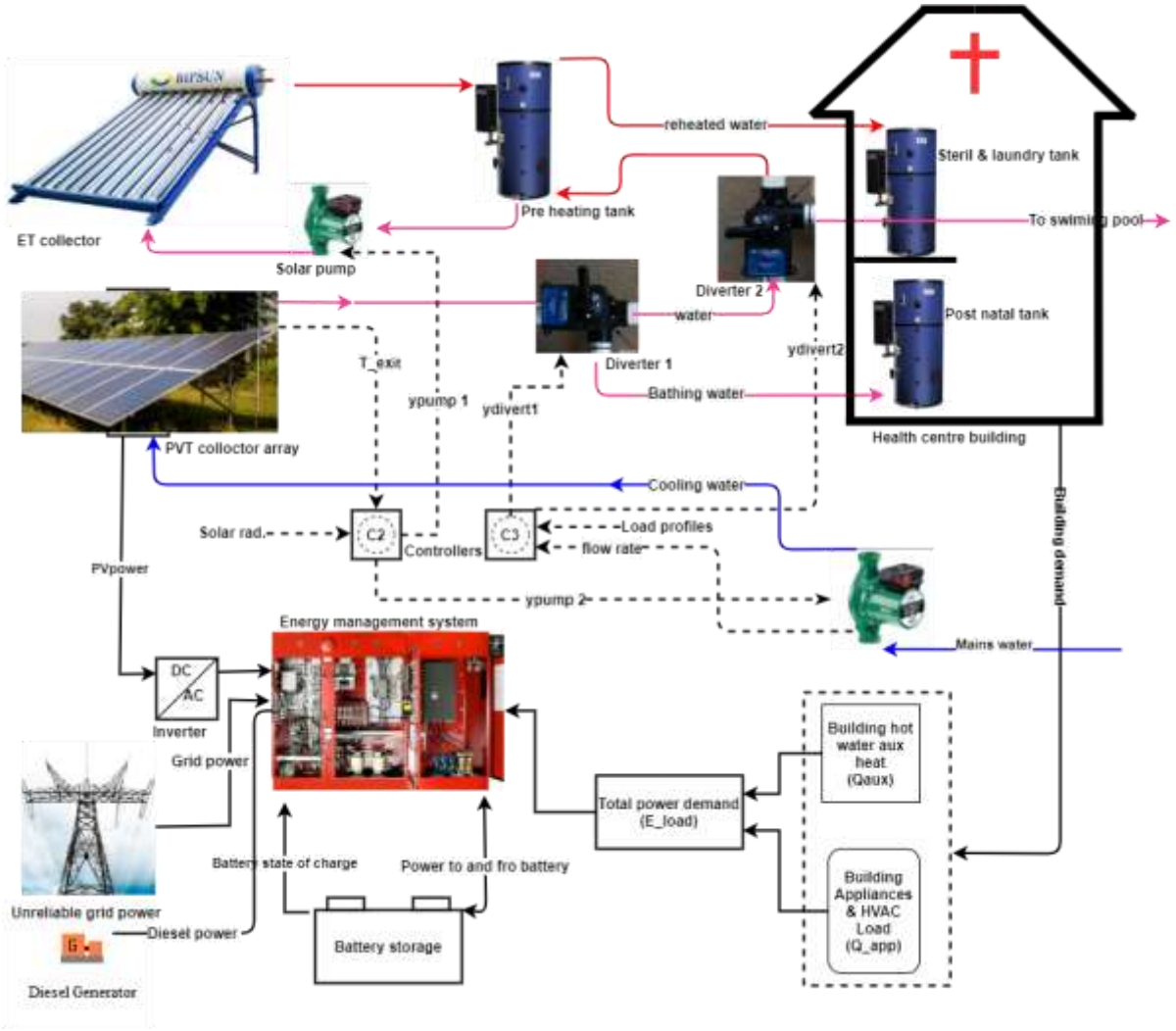


Figure 3.8: Proof of concept and case study application of the OPVETC

3.4 Estimating the building cooling and heating load

Energy systems are primarily designed to supply power reliably and economically for a specific amount of power demand. To accurately evaluate renewable energy systems' operational performance and reliability, it is crucial to forecast the time-dependent dynamics characteristics of the load, almost a close-to-accurate approximation [171]. Unfortunately, the energy demand profile of any building is challenging to estimate as it depends heavily on so many power-related activities carried out in the building. The occupancy and the available electrical appliances and their associated usage in the building may differ. For heating or cooling, the control of the HVAC equipment is mainly based on the occupancy period. In the past, several

studies were conducted which have tried to recommend approximate profiles in certain countries in Europe or the UK [41],[143]– [145]. However, the comfort temperature is subjective and varies based on the climatic zone. In one study, the comfort temperature for different countries was between 22 to 27^{o}C, with a relative humidity of 47.3 to 66% [172]. Even in some studies, it was argued that long-term exposure to temperatures below 22^{o}C increases the likelihood of illness, whereas temperatures above 25^{o}C are said to cause heat sensations in various parts of the body [172].

Since the adaptable comfort temperature is subjective and varies for different geographical zones, this study employs the 3D building modelling approach using TRNBUILD software to estimate the HVAC of the case study building. The dynamic characteristic of the heating and cooling load can be more accurately evaluated as a function of weather and period of operation using the 3D modelling approach as against the intuitive approach that may lead to under or overestimation of the HVAC demand. By this approach, the building HVAC power requirements are estimated by first transforming the geometric characteristics of the building, as seen in Figure 3.9, into an equivalent thermal zone (Figure 3.10) using the 3D TRNSYS 18 plugins in Sketch-Up.

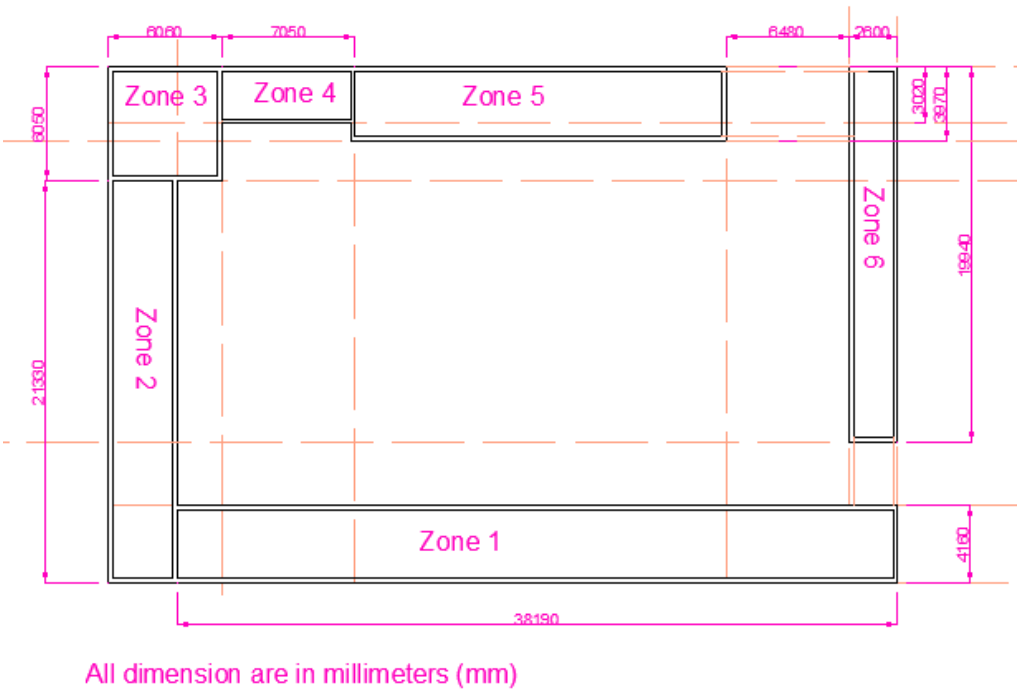


Figure 3.9.Case study building floor plan and dimensions

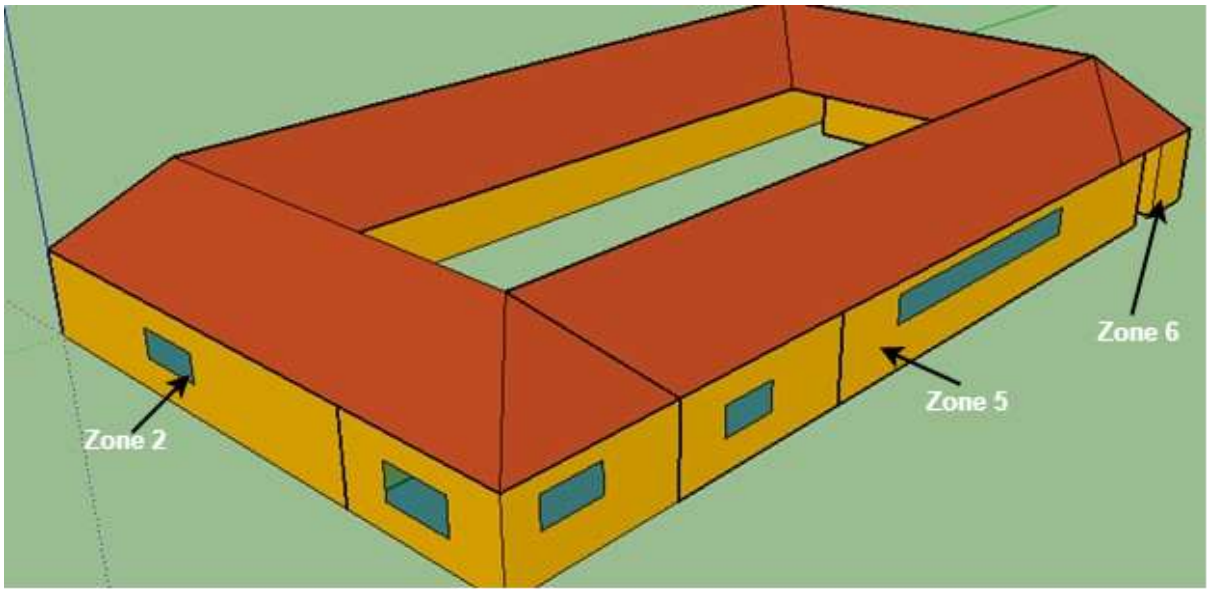


Figure 3.10. Equivalent building thermal zones developed using SKECH-UP

The formulated equivalent thermal zone of the building is then exported to TRNSYS 18 simulation studio, where the building materials are customised as specified in Table 3.1 and Table 3.2 is done using the TRNBUILD environment.

Table 3.1 Thermal properties of building materials

Building surface	**Layer**	**Total thickness (m)**	**Conductivity (kJ/hmK)**	**Capacity (kJ/kgK)**	**Density (kg/m^3)**	**Resistance (hm^{2}K/kJ)**
External wall	Insulation plaster	0.029	0.72	1	600	
	Concrete block	0.051	1.836	1	1400	
	hollow space					0.04
	Insulation plaster	0.029	0.72		600	
	Concrete block	0.051	1.836		1400	
External roof	Al-sheet	0.005	576	0.896	2800	
	TEPP	0.005	0.6	0.8	2800	
	KST	0.005	0.1	0.8	1600	
Building ceiling	Insulation board	0.01	0.198	1.29	288	

Table 3.2 U-values of building surfaces

Building surface	Total thickness (m)	U-value (W/m^{2}K)
External wall	0.16	1.206
External roof	0.015	2.63
Ceiling	0.01	2.8

Notably, when the SKETCHUP building model is exported to the TRNSYS simulation environment, the geometrical properties specified in Table 3.3, as well as the set-point temperatures for cooling and heating, become the basis for calculating the building energy required to cool or heat the building to setpoint temperatures based on the building's ambient condition. For this study, the comfort zone temperature was set at the more conservative side of 23.5ºC for cooling and 20ºC for heating. The occupancy period for which the heating and cooling are set is between morning hours from 8hrs to 18hrs, which corresponds to the period for high temperature and time during working hours of the health centre, as seen in Figure 3.11.

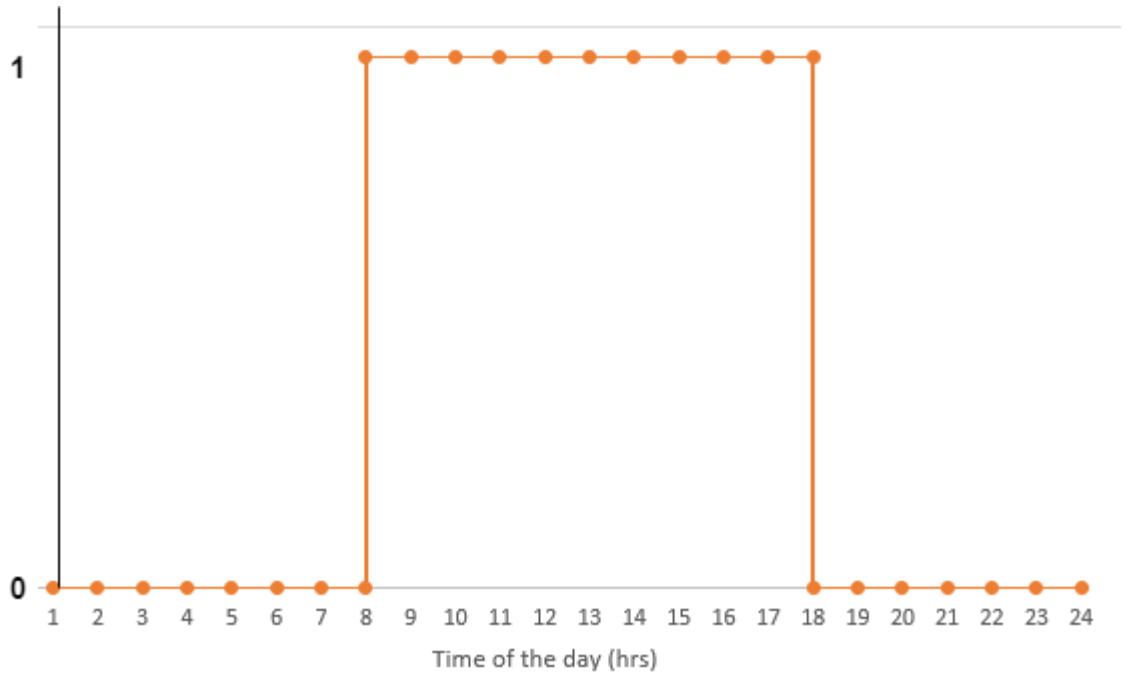


Figure 3.11. The occupancy period for HVAC heating and cooling control

The simulated temperature condition of each building zone is the basis for estimating the zone's cooling or heating power requirement. Table 3.3 shows zones' geometric and thermal characteristics of the zones with Heating and Ventilation Air Conditioner (HVAC) equipment. Zones 2, 5, and 6 present the building zones of emphasis because they require cooling or heating. Other zones do not require cooling or heating, and therefore no HVAC equipment is attached to the zones. Therefore, the power requirement of other zones is the power needed to power the appliances content in the zones only.

Table 3.3:Geometric and thermal properties of temperature zones.

Zones	**Volume (m^3)**	**Floor Area (m^2)**	**Capacitance (kJ/K)**	**No of windows**	**Window area (m^2)**	**Window orientation**
1	414.466	138.154	497.353	1	13.5	W
2	**168.691**	**56.23**	**202.429**	**1**	**2.5**	**S**
3	109.989	36.663	131.987	2	2.1 & 2.8	N E
4	63.873	21.291	76.648	1	2.00	E
5	**234.389**	**78.13**	**289.267**	**1**	**10.2**	**E**
6	**124.566**	**41.522**	**149.000**	**1**	**10.10**	**N**

.

The OFF/ON control strategy is implemented when the setpoint temperature is surpassed, using the temperature differential control, which generates a control function with a value of 1 or 0 to 'ON' and 'OFF' the HVAC equipment to estimate the HVAC power requirement within the occupancy period as shown in Figure 3.11. Under this control, the indoor zone temperature (Tzone) is compared with the setpoint temperatures, and whenever Tzone is higher than the cooling setpoint temperature of 23.5^{o}C within the occupancy period, the function outputs 1 to switch ON the cooling device. Cooling is continued the zone temperature drops below 23.5^{o}C. Similarly, the control function sends an ON signal to the heating unit when the zone temperature falls below 20 ^{o}C and switches off immediately when the zone temperature is heated to 20 ^{o}C. A schematic diagram to illustrate the operation and control of the heating device is shown in Figure 3.12 below. The building's annual HVAC demand is therefore obtained from the annual simulation of the building under the weather condition of Jos, Nigeria.

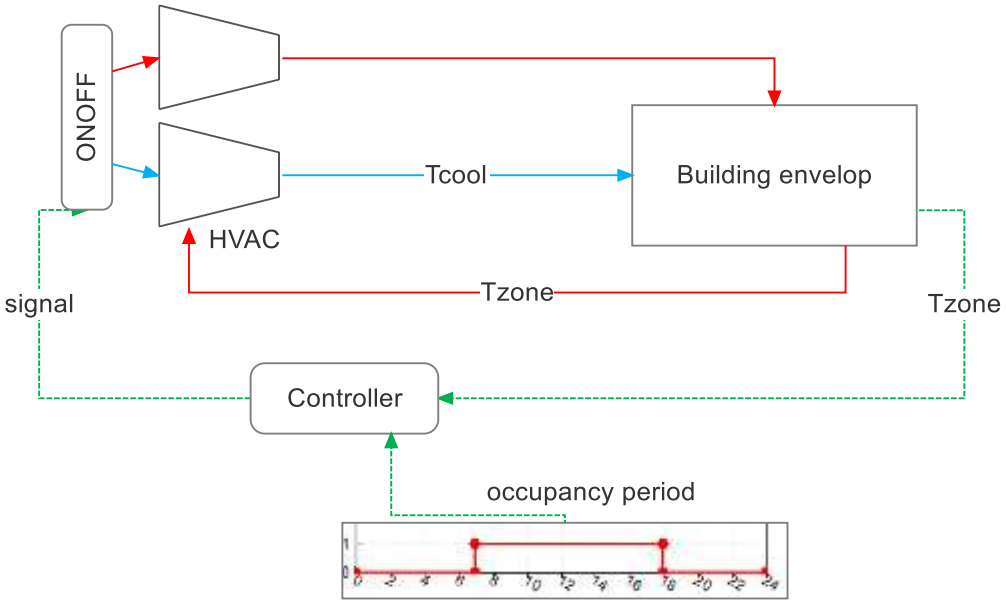


Figure 3.12: Operation and control of the HVAC device

The load is calculated only during the occupancy period. The energy consumed by the HVAC equipment is calculated as the energy required to keep the zones temperature within the setpoints. Eq(3.1) to Eq(3.3) calculate the cooling and heating load. The schematic of the model formulated in TRNSYS for calculating the building cooling and heating power requirement is shown in Figure 3.13.

$$Q_{cooling} = CAP(T_{zone} - Tset_{cool}) \qquad \text{Eq(3.1)}$$

$$Q_{heating} = CAP(Tset_{heat} - T_{zone}) \qquad \text{Eq(3.2)}$$

$$CAP = \rho_{air} V_{zone} C_{p_{air}} \qquad \text{Eq(3.3)}$$

where $Q_{cooling}$ is the quantity of heat required to cool the zone to cooling temperature setpoint

$Q_{heating}$ is the quantity of heat required to heat the zone temperature to the setpoint

T_{zone} is the temperature of the building zone.

$Tset_{heat}$ is the setpoint temperature for heating

$Tset_{cool}$ is the setpoint temperature for cooling.

CAP is the zone capacitance

ρ_{air} is the density of air

V_{zone} is the zone volume

$C_{p_{air}}$ is the heat capacity of air

Air infiltration is a significant factor that influences the building temperature and the power requirement to bring the building to the setpoints temperatures.

In this study, we assume an air exchange per hour (Air_{ACH}) of 5 as a standard. The mass flow rate of air infiltrating the thermal building zones was estimated from equation (Eq(3.4) below.

$$\dot{m}_{air} = \rho_{air} Air_{ACH} V_{zone} \qquad \text{Eq(3.4)}$$

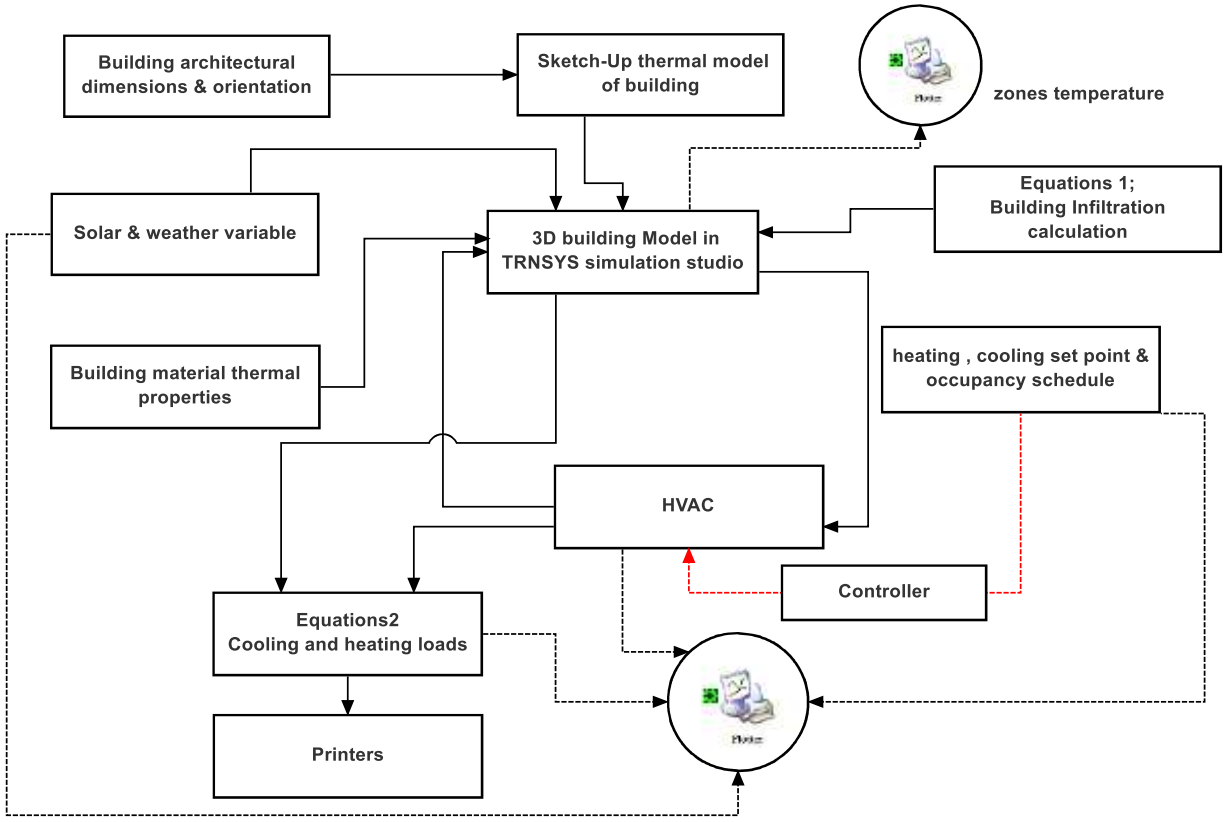


Figure 3.13: Schematic of the 3D building model developed in TRNSYS

3.5 Power and thermal energy demand estimation

The Service Availability and Readiness (SARA) survey tool designed by the World Health Organisation (WHO) to assess the readiness of health facilities [42] is employed to estimate the power consumption of the medical devices of the case study health centre. Under this method, the SARA data acquisition form is administered to the clinic to take inventory of the medical equipment and its power ratings and the hours of usage, as seen in appendix A. Based on estimations of these medical devices and appliance power requirements at various times of the day and night, a load profile for the health clinic was created. One assumption is that the formulated power profile based on the data collector for a week is repetitive for the entire year. This assumption is taken due to the absence of data on the daily power consumption for one year. A typical pattern of power profile for the medical equipment for health clinics based on the SARA methodology is shown in Figure 3.14. shows the power demand profile of the medical devices processed from the data obtained from the survey form found in the appendix A1-A2.

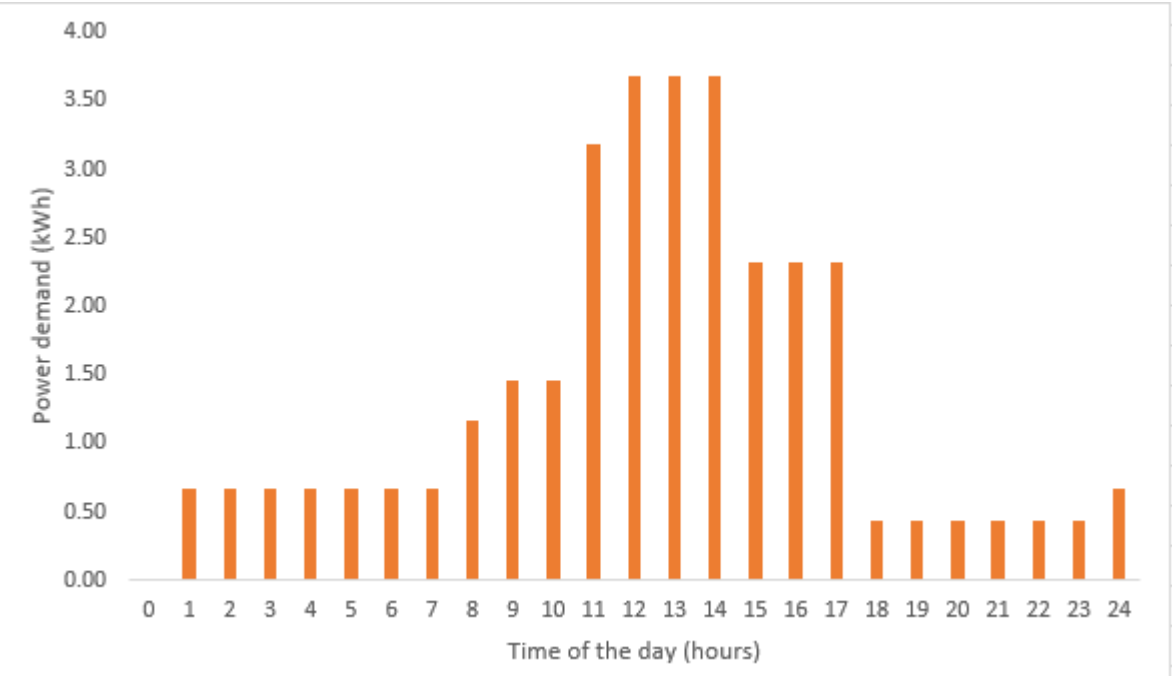


Figure 3.14. Medical equipment electric power profile of the health centre

Therefore, the building's total power demand is estimated as the sum of the power demand for cooling and heating and the power requirement to operate the facility devices.

Hot water consumption in health centres is intensive due to the many different hot water services provided in health facilities. For example, hot water requirements for equipment sterilisation are usually considered at 55 ^{o}C to 60^{o}C [173], [174]. For laundry purposes, hot water temperatures are required at 45 ^{o}C to 54^{o}C. According to Murphy [175] and Lima *et al.* [176], the hot water for bathing (postnatal service) is usually delivered at a temperature of around 37 ^{o}C to 45^{o}C. Interestingly, according to the investigation published by [177], the hot water thermal demand is significantly reduced by about 27% if hot water demand for different applications in the health centres are separated and met at their desired temperatures. An important factor that determines the performance of a solar water heating system is daily demand and the water draws distribution. Regrettably, limited hospital hot water consumption data are available for rural health centres, especially in developing countries. According to a recent study by Fuentes [171], the typical average daily hot water demand for residential buildings ranges from 20 to 94 litre/day per occupant and 80 to 150liter/bed/day for a typical hospital building. This study, therefore, adopts a conservative average daily hot water demand of 100L/bed/day for a ten-bed hospital. The water draw profile follows the typical normalised hourly profile found in a study conducted by [167] for hospitals, where peaks characterise the profile in the afternoon and low demand in the morning and evening.

Interestingly, this pattern is typical for most hospitals regardless of country and weather. This study, therefore, adopts the profile found from the study conducted by [167] with modification, as seen in Figure 3.15, as there are no significant consequences for the annual performance of the solar hot water system [178] [185].

The basic PVT hybrid configuration operates in a close loop. This type of system configuration is suitable primarily for hot water applications with a fixed desired temperature. However, there are several hot water applications in health centres at different temperatures. This study, therefore, proposes a new PVT thermal architecture that meets hospital applications of hot water for sterilisation, laundry, and postnatal services separately. The daily volume of the hot water demand of the facility is 1000L/day. Based on the study case health facility, the demand for sterilisation is 251L/day, the demand for laundry is 322L/day, and that required for postnatal services is 427L/day. One central assumption is that the daily hot water demand remains constant. The projected load profile is the worst-case scenario for the health clinic building demand to prevent the system's highest probable shortages. Furthermore, the hourly load profile adopted in this study is assumed to be constant throughout the year, as in some studies [180].

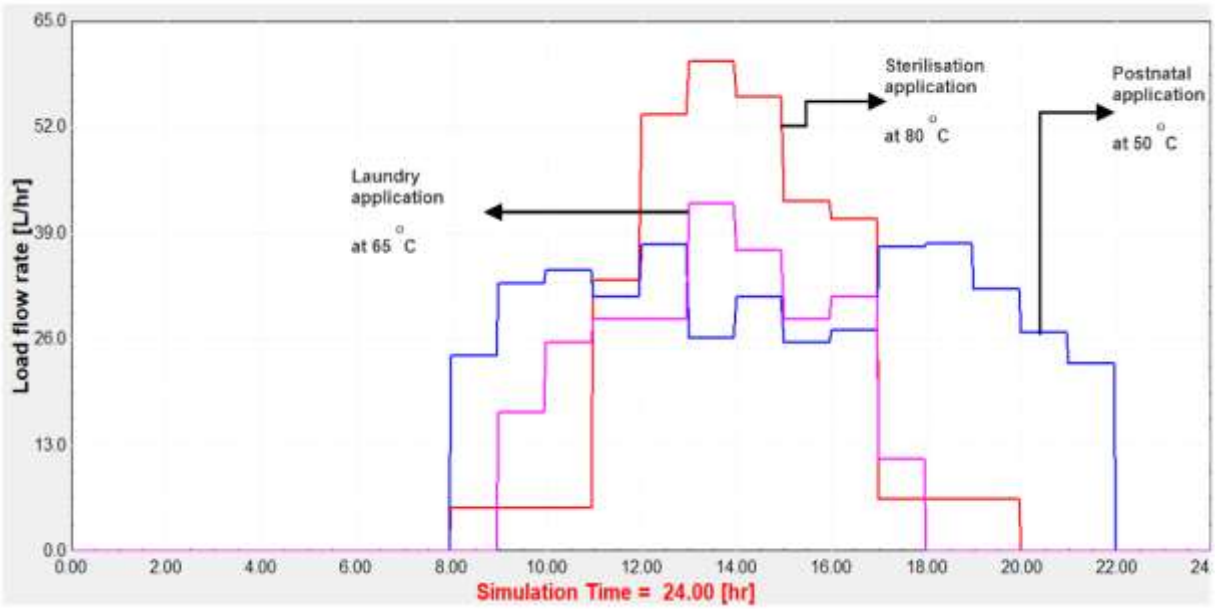


Figure 3.15 Daily hot water demand for the three applications

In this study, the hot water temperature for sterilisation is set at 80^{o}C, hot water services for postnatal are required at 50^{o}C, and needed for laundry services are demanded at 65^{o}C. The hourly hot water flow rate for the different hot water services is shown in Figure 3.15.

Accordingly, the hot water thermal hourly energy requirement is estimated based on the volume of hot water demand, as shown in Figure 3.15 using equations

$$\dot{Q}_{DHWL} = \dot{m}_L C_p (T_L - T_{mains}) \quad \text{Eq(3.5)}$$

$$\dot{Q}_{DHWS} = \dot{m}_S C_p (T_S - T_{mains}) \quad \text{Eq(3.6)}$$

$$\dot{Q}_{DHWP} = \dot{m}_P C_p (T_P - T_{mains}) \quad \text{Eq(3.7)}$$

Therefore, the total thermal energy demand rate is found from

$$\dot{Q}_{DHW} = \dot{Q}_{DHWL} + \dot{Q}_{DHWS} + \dot{Q}_{DHWP} \quad \text{Eq(3.8)}$$

where $\dot{Q}_{DHW}$ is the rate of thermal energy required to meet the load. $\dot{m}_L$, $\dot{m}_S$ and $\dot{m}_P$ are the demand flow rate for laundry, sterilisation, and postnatal services. C_p is the specific heat capacity of water, T_L , T_S and T_P are the load desired temperature for laundry, sterilisation and postnatal, respectively. and T_{mains} is the temperature of water from the mains. Whereas the hourly thermal output of the collector is calculated as:

$$\dot{Q}_{coll} = \dot{m}_{pump} C_p (T_{co} - T_{ci}) \quad \text{Eq(3.9)}$$

where $\dot{Q}_{coll}$ is the rate of useful energy from the collector, $\dot{m}_{pump}$ is the pump flow rate T_{co} and T_{ci} are the collector outlet and inlet temperature, respectively. The quantity of thermal energy delivered by the system to meet building hot water demand is estimated as:

$$\dot{Q}_d = \dot{m}_L C_p (T_d - T_{mains}) \quad \text{Eq(3.10)}$$

where T_d is the temperature of the hot water delivered by the system from the preheated water tank to the auxiliary heat tank. Since the extra energy to heat water to the desired hot water temperature is only required when the water temperature in the heater tank falls below the designed temperature, the required auxiliary thermal energy is calculated as:

$$\dot{Q}_{aux} = \max\left(\left(\dot{Q}_{DHW} - \dot{Q}_{d}\right), 0\right) \quad \text{Eq(3.11)}$$

The excess thermal energy dumped with no application is found in the expression

$$\dot{Q}_{dumped} = \max\left(\left(\dot{Q}_{d} - \dot{Q}_{DHW}\right), 0\right) \quad \text{Eq(3.12)}$$

The useful thermal energy $\dot{Q}_{useful}$ of the system generated by the collectors is estimated as

$$\dot{Q}_{useful} = \dot{Q}_{d} - \dot{Q}_{dumped} \quad \text{Eq(3.13)}$$

3.6 Modelling of proposed OPVETC System

One of the objectives of this study is to formulate a representative model of the proposed energy system for the performance simulation and evaluation. The formulated model will explain the entire system's power and thermal characteristics under the actual weather and the proposed energy management and control strategies. In this study, the transient system simulation tool TRNSYS 18 is selected for the system modelling, performance simulation, and evaluation. TRNSYS 18 is a modular software package with a comprehensive library of validated components like the PVT collector [187] [188] models that can be customised to any conceived energy solution and with great flexibility for adaptation for different applications. Its integration flexibility with other software like Sketch-Up, and the availability of the well-validated 3D building model[183] increased its wide applicability for building energy modelling and analysis, hence the broad flexibility of integrating energy systems with the building.

Additionally, its flexibility for users to formulate algorithms and logic that control the operation of the formulated models to adapt to specific control as desired by the user has made it suitable for studying different scenarios and control strategies [129]. Unlike other energy modelling software, its capability for transient system simulation and analysis has made it possible for system simulation for any specific length of time of interest. Moreover, all energy system

components models in the simulation studio of TRNSYS have been experimentally validated by a wide range of studies conducted in different climatic zones by different researchers and found to be valid with an excellent agreement [181], [182], [184].

A dynamic model (as seen in the appendix section) of the system, as depicted in the schematic as shown in Figure 3.7, is developed as a representation of the actual system to predict the system performance and evaluate the system's annual performance under the actual load and weather conditions of the case study using TRNSYS 18 software. This model consists of the various system components referred to as 'Type' found in the simulation library. The model components are connected in a manner that represents the actual working of the real system. From Figure 3.13, the earlier developed 3D building model that predicts and evaluates the building HVAC demand, the estimated equipment power profile (Type 14, forcing function 3) found using the SARA analysis tool, and the estimated hot water demand profile for the three different applications (Type 14, forcing function1 & 2) is now integrated with the developed system model. Energy management and different control strategies to coordinate the power elements and cooling flow control are modelled in the 'Equations blocks' and added to the developed system model.

Consequently, the operation of the modelled system is governed by the proposed energy management strategy and control. Interestingly, the Equation block can help calculate the system performance. Details of the energy management and control strategies are explained in separate sections in this chapter. Table 3.5 summarises the components ('Types') and their central actions in the model. In general, as shown in Figure 3.16, the model flow diagram represents the connection showing the connecting inputs/outputs between all components used in the model. The driving function for the simulation is the Typical Meteorological Year (TMY) weather and solar data for the study location obtained from the weather data library of

TRNSYS 18 software. The TMY weather data and the climatic condition is imported and processed in the weather data processor (Type 15) for the transient performance simulation of the energy system.

Table 3.4: OPVETC system components model and their functions

Name	**Type**	**Function/Action**
Weather processor	Type 15	It serves to process the weather data from an external weather data file at a given time step and make it accessible to other components of TRNSYS.
PVT collector	Type 560	The type 560 models an un-glazed sheet and tube PVT collector that produces both powers from the PV module and hot water from a fluid stream passing under the PV module used to cool it.
Evacuated Tube Collector	Type 71	This component models the thermal performance of a variety of an evacuated tube collector types using theory. The total collector array may consist of collectors connected in series and in parallel.
Solar pump	Type 110	The solar pump circulates the cooling water through the solar collectors. These component models a variable speed pump such that the output flow rate of this pump is controlled by input from other controllers.
Forcing function	Type 14	Models the hot water demand load profile. The output of this component serves the purpose of presenting the hot water drawn from the tank for the three hospital applications. It is also helpful in scheduling the occupancy period of the building envelope.
Diverter	Type 11	This component splits a fluid stream into two streams according to the user-specified ratio. Embedded in it is an input control signal to control the operation of the valve.
Battery storage	Type 47	Models a lead-acid battery storage system. The model accepts power as input to charge the battery and outputs power to meet the load. Interestingly, it can take in the control signal to control the charging and discharging operation of the battery storage.

Inverter/ regulator	Type 48	The function of this component is to convert the direct current (DC) to alternating current (AC). It also functions to regulate the charging of the battery.
Hot water storage tank	Type 158	This unit models the thermal behaviour of a vertical hot water storage tank with two inlets and outlets. Interacting with the hot fluid inside the tank and environment to predict the temperature of the fluid content.
Equation blocks	-	The equation blocks are not found in the library as the rest of the components. The equation block is a mathematical environment that enables the designer to model any control and develop a new component. It is equally valuable for evaluating the performance of the system

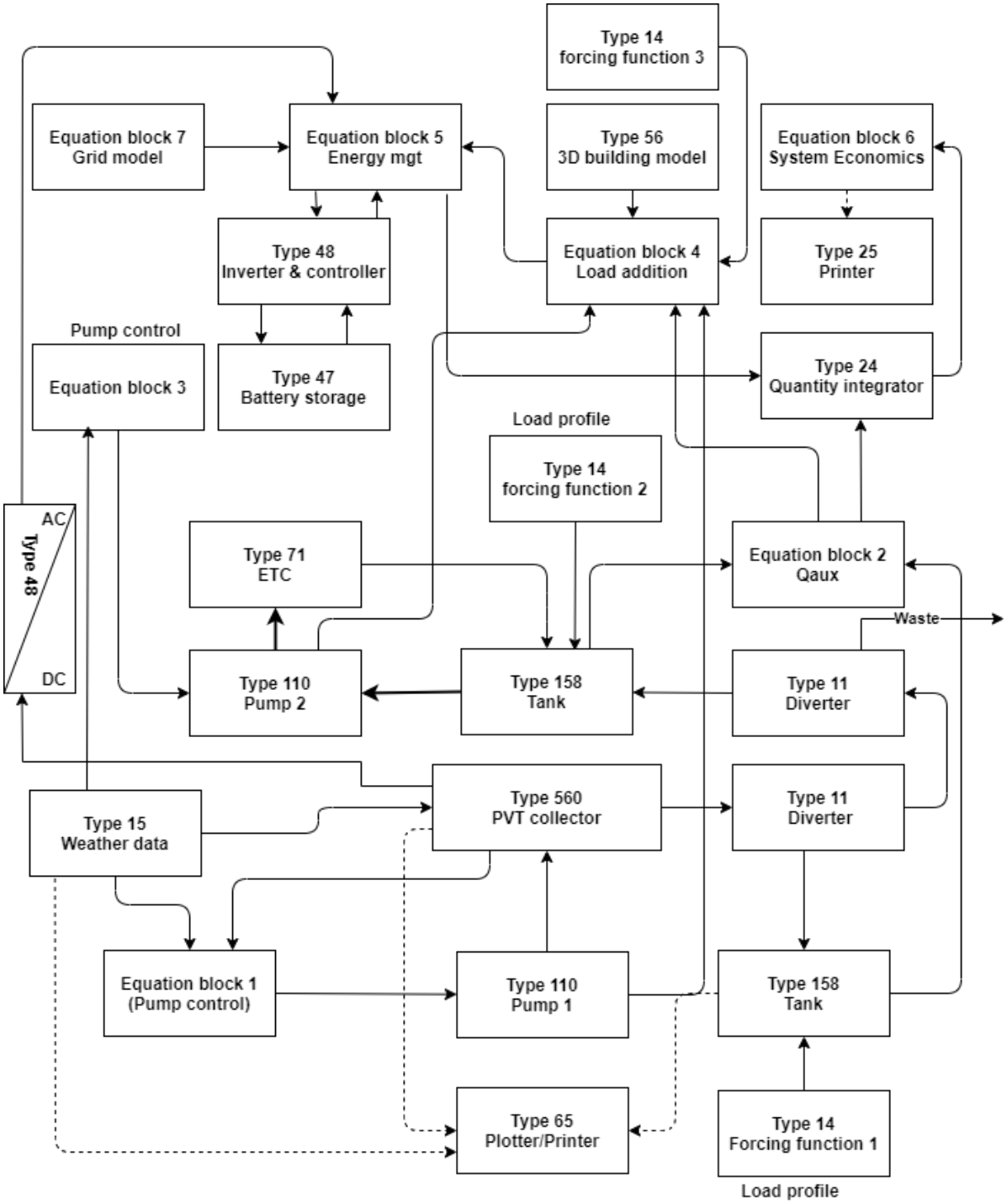


Figure 3.16. Process flow diagram of the proposed OPVETC TRNSYS model

3.6.1 Modelling of the PVT solar collector

The flat plate sheet-and-tube model of the solar collector in the simulation studio library of the TRNSYS 18 software was used to model the PVT collector. This component, 'Type 560', models an unglazed solar collector that produces both thermal and power from the combination

of solar cells embedded on an absorber plate and a fluid stream made to circulate underneath the absorber plate through tubes bonded to an absorber. The liquid passing underneath the solar cell is circulated first to cool the solar cells, and second, the exiting hot water could be used for many possible low-grade temperature applications. The power output of this model is correlated linearly with solar cell temperature and the solar radiation incident on the collector. The PV module is assumed to be operating at its maximum power point condition. In this study, the collector heat loss coefficient, which is a critical factor in determining the collector performance, is modelled as a function of the geometry of the collector and the solar and weather variables as expressed in Eq(3.14) - Eq(3.23) as opposed to assuming a constant value as stated on the technical datasheet of most manufacturers. The model developed for this hybrid system's collector coefficients is expressed in equations Eq(3.14) - Eq(3.23)[185]

$$U_L = U_t + U_b + U_e \qquad \text{Eq(3.14)}$$

$$U_e = \frac{(UA)_{edge}}{A_c} \qquad \text{Eq(3.15)}$$

$$U_b = \frac{K_{ins}}{t_{ins}} \qquad \text{Eq(3.16)}$$

Where K_{ins} and t_{ins} are the thermal conductivity of insulation material and thickness, respectively. $(UA)_{edge}$ is the area-coefficient product coefficient

$$U_t = U_1 + U_2 \qquad \text{Eq(3.17)}$$

$$U_1 = \left[\frac{N_g}{\frac{C}{T_{pm}} \left[\frac{T_{pm} - T_a}{(N_g + f)} \right]^e h_w} \right]^{-1} \quad \text{Eq(3.18)}$$

$$U_2 = \frac{\sigma(T_{pm} + T_a)(T_{pm}^2 + T_a^2)}{\frac{1}{\varepsilon_p + 0.0059 N_g h_w} + \frac{2N_g + f - 1 + 0.133\varepsilon_p}{\varepsilon_p} - N_g} \quad \text{Eq(3.19)}$$

where Ng is the number of the glass cover, Tpm and Ta are the mean plate temperature and the ambient temperature, ε_p band ε_g are the absorber plate and glass cover emissivity, where wind-heat transfer coefficient h_w , f and C are expressed as in Eq

$$h_w = 5.7 + 3.8V \quad \text{Eq(3.20)}$$

$$f = (1 + 0.089h_w - 0.116h_w)(1 - 0.07866N_g) \quad \text{Eq(3.21)}$$

$$e = 0.430\left(1 - \frac{100}{T_{pm}}\right) \quad \text{Eq(3.22)}$$

$$C = 520(1 - 0.000051\beta^2) \text{ for } \beta < 90^o \quad \text{Eq(3.23)}$$

Other technical parameters of the flat plate PVT collector as obtained from the datasheet of the commercially available PVT collector used for the design and simulation of the collector are specified in Table 3.5. These parameters are the manufacturer's technical test results of the commercially available 1.64m^2 TESZEUS PVT hybrid collector.

Table 3.5: Technical parameter of the TESZEUS flat plate PVT collector

SN	parameter	Value	Unit
1	Thermal Conductivity of the Absorber plate	1440	kJ/hr.m.K
2	Absorber plate thickness	4	mm
3	Fluid specific heat	4.190	kJ/kg.K
4	Reflectance of the collector surface	0.15	
5	PV cell reference temperature	25	^{o}C
6	PV cell reference radiation	3600	$kJ/hr.m^2$
7	PV efficiency at reference condition	0.12	
8	PV solar cell power coefficient	-0.065	$\%/^{o}C$
9	Collector slope	12.0	degrees
10	Area of single unit PVT module	$1650 \times 992 \times 50$	mm
11	Emissivity of plate	0.05	%
12	Collector tube internal diameter	10	mm
13	No. of the collector tubes	23	
14	No. of collector connected in series	33	-

For this study the PVT collectors are connected in series with the length of the collector (direction along the tubes) horizontally placed to reduce the height at which the cooling water is pumped to and hence the size and power consumption of the pump is reduced. The PVT and ETC collectors are tilted at 12 degree as this angle for optimal collection of energy on fixed collector surface located in Jos , Nigeria as conventional tilt angle based on the location as suggested in [186], [187]

3.6.2 Modelling the battery- inverter and charge controller system

The power output of the PVT and the battery storage is DC in nature; a power conditioning device is required to convert the power to an AC since the load, in this case, is an AC load. The 'Type 48', which models both the inverter and charge controller, is used. A regulator-charge controller system is necessary to regulate the power distribution between the battery and charge from energy sources. The battery storage is modelled using the 'Type 48'. Table 3.6 shows the technical parameters of the regulator-charge controller system used in the simulation model. The size of the inverter is determined by the maximum power demand rate as already determined in section 4. The commercial availability and cost of the battery determine the battery ampere rating and voltage choice. For a longer discharge period of more than 6 hours, battery charging was set at with constant charging current of 10% of battery current capacity based on the recommendation by [188]

Table 3.6 Other system components' design parameters for the proposed system

SN	Parameter	Value	Unit
	Inverter output power capacity	30,000	kJ/hr
	Inverter efficiency	0.98	fraction
	Battery ampere-hour rating	75	Ah
	Battery voltage rating	14.4	volt
	Battery charging /discharging current	7.5	Ah
	No in series	1	
	No in parallel	15	

3.6.3 Modelling of the evacuated tube collector (ETC)

Since water exiting the PVT collector is not redirected to the PVT collector and the temperature of the exiting water is conditioned to be no higher than 60^{o}C, the ETC is integrated into the solar thermal system primarily to reheat the preheated water to a temperature greater than 60^{o}C. This novel system architecture prevents the temperature of the PVT from rapidly rising due to recirculation of the preheated water in the cooling loop, which is especially important when the hot water temperature is desired at an elevated temperature of 80^{o}C, as considered in this study. Similarly, the collector area required to raise the preheated water temperature to a higher temperature will be greatly reduced. As a result, solar energy would be used to meet a large portion of the hot water demand for all services, with no compromise in the power production of the PV module collector, as is the case in a closed-loop direct cooling system. 'Type 71' is used to model the ETC, and its parameters are shown in Table 3.7.

Table 3.7: ETC technical and design parameters

Sn	Parameter	Value	unit
1	Flow rate at test conditions	72	kg/s.m^2
2	Intercept efficiency	0.81	
3	First-order efficiency coefficient	4.68	kJ/hr.m^2
4	Second order efficiency coefficient	0.0129	kJ/hr.m^2

3.7 Energy management and the dispatch strategy

The energy dispatch from the various power elements, the balance of energy produced and consumed, which power source to use to charge the battery and when to charge and discharge the battery, and finally, minimising excess thermal and electric power generated are some of the objectives of the proposed energy management and operating strategy in this study. The

proposed OPVETC hybrid energy comprises a PVT collector, randomly unavailable grid power, and battery storage as the power source elements. One of the objectives of this research is to develop an energy management strategy that coordinates the power from the PVT collector and the other power components with an unreliable grid power to meet load economically, reliably, and efficiently. For this study, the proposed energy management and dispatch strategy is based on the Follow-Electric-Load (FEL) control strategy that prioritises power from the PV module to meet the load. For this strategy, the various power elements in the system are set to produce the electric and thermal energy that follows the thermal power demand pattern and extra steps to ensure that excess of what is required is minimised. The PVT power production is first used to meet power demand, and the excess is used to charge the battery. Power from the grid is only taken when power from the PVT collector is insufficient to meet the load completely, and the battery power has been discharged to 20% of its storage capacity. In other words, when the PVT power is not adequate to meet power demand, the battery storage power is called to be used first and must be expended to 20% of the battery storage capacity before the grid power can be dispatched if available. In this study, the battery's maximum, and minimum state of charge (SOC) limits are set at 80% and 20%, respectively, in order to ensure its security to extend the battery life [189], [190]. Notably, for periods where the PV power is unavailable, the grid power is used to meet load and equally charge the battery until the battery is fully charged or the grid goes off due to outage.

Consequently, when the PV power is unavailable, the grid power dispatched is modelled as power sufficient to meet load demand and charge the battery until the battery state of charge (BSOC) is 100%. For a period with available power from PV, and the battery is fully charged or needs only a tapetr charge, the excess power from the PV is either sold back to the grid or dumped. However, in this study, the excess power generated is dumped when the load is fully

met and the battery state of charge is 100%, as this is the right scenario in most developing countries like with highly unstable grid power Nigeria, Uganda and Democratic Republic of Congo [10], [11] with no feedback tariff grid policy . The flow chart and the control logic for the energy management control and dispatch strategy are shown in Figure 3.17.

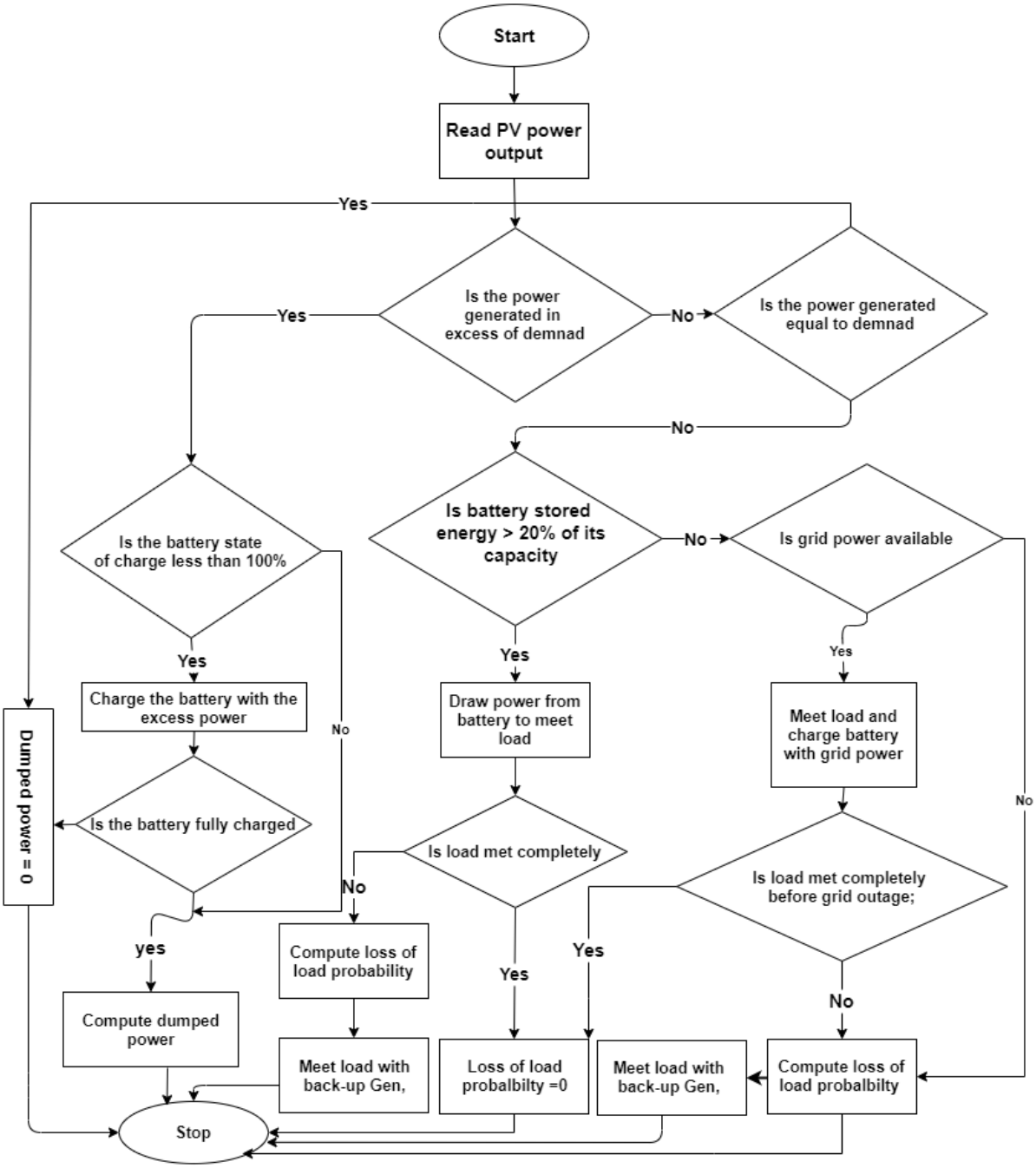


Figure 3.17. The detailed control logic and the modelled energy management strategy

Since grid energy is dispatchable when available, and the grid power source in this study is characterised by random failure, a model has also been developed that predicts the grid power dispatched. The developed model predicts the grid availability and unavailability and decides how much grid power is required at each step to avoid taking excess grid. Regrettably, power

from the PV source varies randomly, and it is not dispatchable, resulting in unavoidable excess power for a period of low load and power mismatch. Figure 3.18 is a flow chart of how the grid operation was modelled.

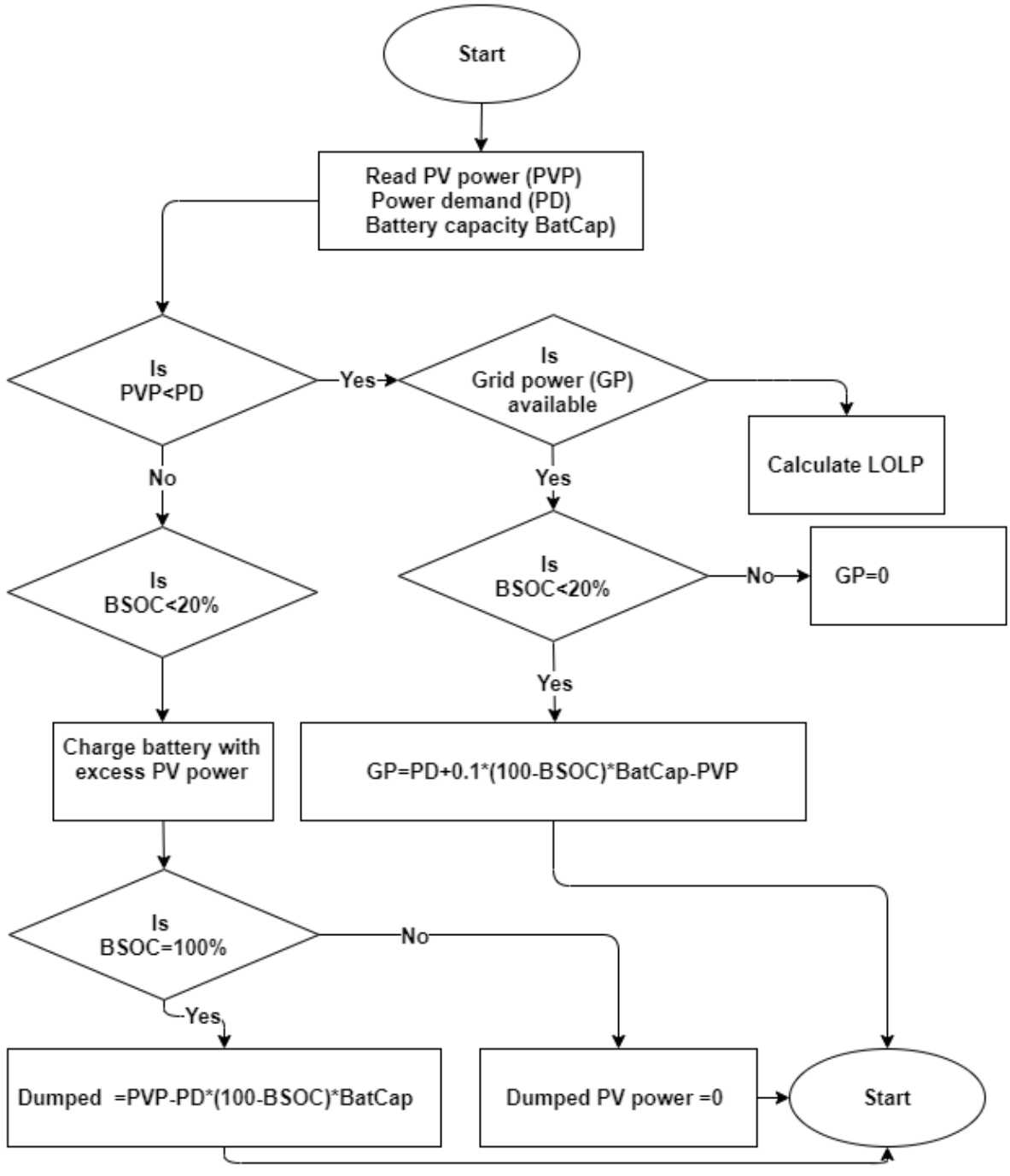


Figure 3.18. Flow chart model of grid power dispatch

Under this control operation, the grid power charges the battery only when there is no excess power from the PV, or the excess power is not sufficient to charge the battery to 100% of its capacity. In other words, for the period where the PV power is entirely unavailable, the grid power is modelled as the total electric power demand of all the building appliances plus the battery maximum charging power for a battery with a state of charge (BSOC) less than 100%. When the PV power is available, grid power can only be dispatched as the balance required to meet the unmet load by PV and the maximum charging power needed to charge the battery to 100% of its power capacity.

3.8 Modelling of the cooling water flow control

The time of operation and the flow rate of water from the pump are crucial factors for the effective cooling of the PV module to lower its temperature to enhance its power output. In this study, a unique flow control that controls the operation of the pump was developed (Appendix B). The control determines the proportionate cooling water flow rate required to cool the PV cell. By this control, the collector array cooling water exit temperature (T_exit) is desired not to exceed 60^{o}C. To achieve this desired temperature, the pump controller reads the instantaneous solar radiation (I_T) on the surface of the PVT collector array to estimate the total PVT array useful thermal energy (Q_{PVT}) based on the total array area (Ac_{PVT}) and the thermal properties of PVT collector (η_T) as expressed in Eq(3.24).

$$\dot{Q}_{PVT} = Ac_{PVT}\eta_T I_T \qquad \text{Eq(3.24)}$$

Based on the estimated useful energy $\dot{Q}_{PVT}$ the required flow rate of the cooling water is estimated from Eq(3.25)

$$\dot{m}_{req} = \left(\frac{\dot{Q}_{PVT}}{C_p\,(T_{exit} - T_{mains})}\right) \qquad \text{Eq(3.25)}$$

where C_p is the specific heat capacity of water.

Cooling the PV module with a flow rate equivalent to the domestic hot water (DHW) hourly demand rate is crucial for this unique cooling control. This condition is essential if the cooling water flow rate equally meets building hot water demand. Figure 3.19 explains the control logic and the practical way to implement the desired control of the cooling water to give the desired temperature of the collector exit water. Eq(3.26) represents the pump control signal modelled by the algorithm as illustrated in Figure 3.19 to meet the above condition.

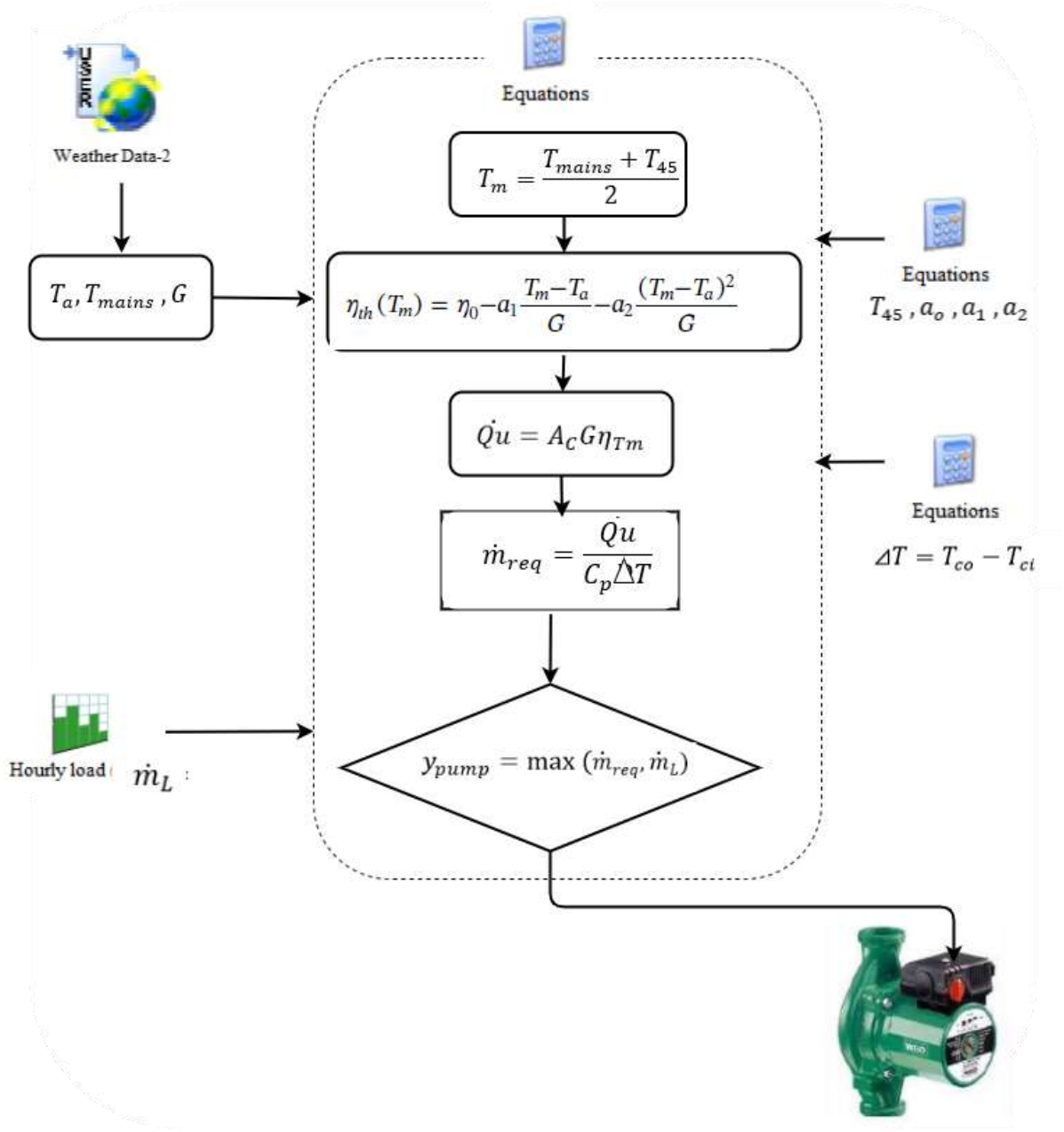


Figure 3.19. Cooling pump control flow and algorithm.

The water pump controller decides the maximum of the building hot water demand rate (m_{load}) and the estimated cooling water flow rate ($\dot{m}_{req}$) as expressed in Eq(3.26).

$$\boldsymbol{y_{pump}} = \max(\dot{m}_{req}, \dot{m}_{load}) \qquad \text{Eq(3.26)}$$

This control strategy operates the pump equally at the flow rate required to cool the collector module to around 50^{o}C only when solar radiation is available.

Table 3.8 explains the action of the developed control strategy on the cooling water pump. Since the PVT collector cooling water is required to meet the facility load at the required service temperature and volume., the cooling water is again redirected to be reheated before it is delivered to the building.

Table 3.8: Flow control and its action on the pump

Flow control model	Action on the pump
y_{pump} 	The control drives the water pump at the maximum flow rate between the building hot water demand rate ($\dot{m}_{load}$) and the estimated cooling water flow rate ($\dot{m}_{req}$)

Again, the operation of the diverter's valves is a vital part of cooling flow management that ensures the proper amount of water is provided first to fulfil the postnatal hot water requirement at Diverter1 and then the sterilisation and postnatal water need at Diverter2 as illustrated in Figure 3.20. For example, for the period of high radiation, the quantity of water required to cool the module to a temperature of about 50^{o}C, as desired in this study, may be higher than the domestic hot water demand of the building ($\dot{m}_{load}$). Consequently, allowing the entire preheated water used for the cooling of the PV module to be heated in the evacuated tube collector heating circuit will decrease the quality (temperature) of hot water delivered for sterilisation. Hence, the preheated water quantity ($\dot{m}_{req}$) exiting the PVT module array will have to be regulated to meet the building load using the controls valves of the diverters to deliver the correct quantity to be reheated. This way, only the appropriate quantity of water

required for hot water services of the health centre is heated, and the size of the collector required will significantly be reduced.

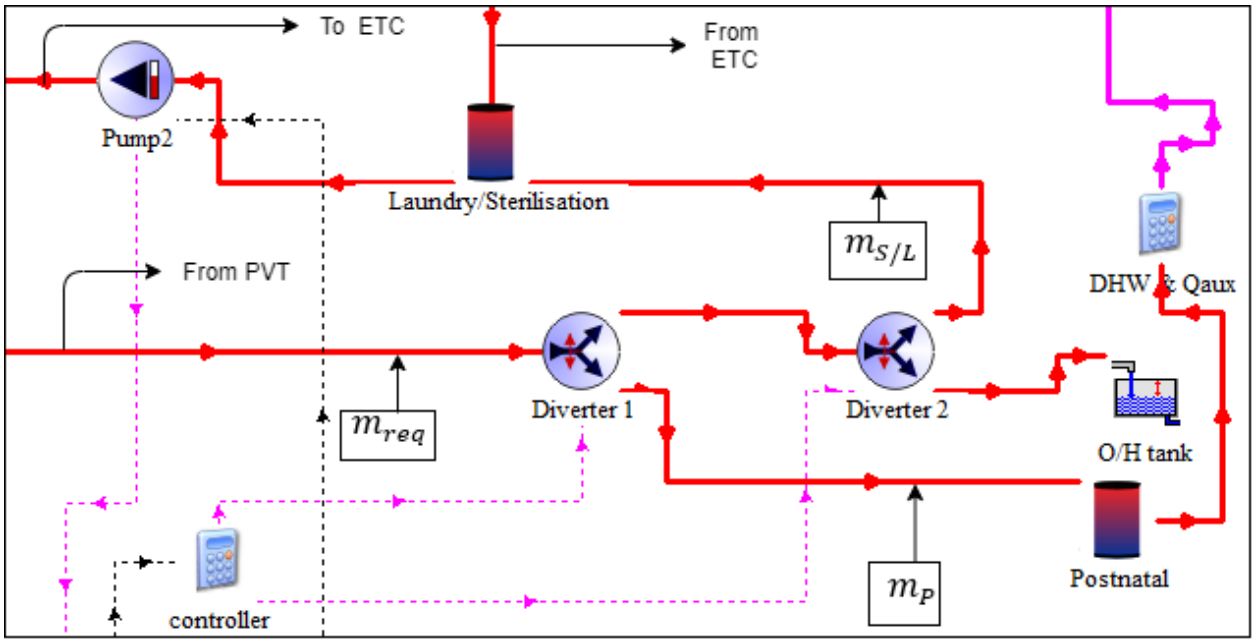


Figure 3.20: The reheated hot water flow network

From Figure 3.20, the function of the Diverter2 is to divert the required quantity of water needed for sterilisation and laundry services (m_{sL}) and the excess is sent to the overhead tank or an underground reservoir.

3.9 OPVETC parametric analysis and components sizing

The various components of the proposed OPVETC hybrid energy system must be appropriately sized to meet building thermal and electrical load with minimal losses. Remarkably, the size of the PVT collector, the battery storage, the pump, and the water storage tank in this study must satisfy both the technical and economic outlook of the energy project for the project to be competitive with other alternatives. For this reason, the simulation and parametric-based approach are adopted to size the system components to meet load demand satisfactorily in the most economical way. In this approach, a parametric analysis is conducted to study the effect

of various design parameters and components size on the system’s annual solar fraction and the total life cycle cost (TLCC) to select the sizes of the components that minimise the TLCC. The goal is to find the system parameters and components size that satisfactorily meet load allowing the maximum possible solar fraction penetration at the least total life cycle cost (TLCC). This way, the appropriate size and design parameters of the various components of the OPVETC are determined.

To conduct the parametric analysis, the TRNSYS model of the OPVETC developed in the simulation studio is prepared for the parametric analysis using the TRNedit program of the software. In the TRNedit environment, parametric tables of the various components' design parameters are prepared, and the system's annual performance is simulated based on these values of the parameters prepared in the parametric table in the simulation studio of TRNedit. The system's annual solar fraction, the useful thermal energy, and the total life cycle cost are the objective functions in this parametric analysis to determine the optimal flow rate, the appropriate volume of the storage tank, and the required number of the PVT collectors, respectively.

3.10 Performance assessment and analysis

Performance evaluation of hybrid renewable energy systems in terms of their energetic, economic, and environmental indices is essentially required to compare the proposed new energy solution to existing solutions. In this study, the method as adopted in previous studies [191]–[193] as defined by the equations (3.27) to (3.38) are the basis for the evaluation of the technical and environmental performance indices of the novel energy system proposed here in this study. To have a fair assessment of the performance of the proposed system in meeting with the objective of this study, the proposed system is compared to the baseline system in term of the thermal and electrical efficiencies as commonly used in most studies [194]. Others

important indicators for the assessment and comparison include the solar fraction, self-consumption ratio, loss of power probability, and renewable fraction etc are explained below with the equation used in the model to calculate these indicators.

The electrical and thermal efficiencies are the electrical and thermal gains divided by the solar irradiance and the total area of the collector as defined in (Eq(3.27 & Eq(3.28). The overall photovoltaic efficiency and thermal efficiency, or combined efficiency, determine the combined performance of the photovoltaic thermal collector PVT system.

$$\eta_{el} = \frac{\mathrm{PV_{power}}}{I_T A_C} \qquad \text{Eq(3.27) [68]}$$

$$\eta_{th} = \frac{\mathrm{Q_u}}{I_T A_C} \qquad \text{Eq(3.28) [195]}$$

Hence the total efficiency of the PVT collector is the sum of the thermal and electrical efficiency expressed as in Eq(3.1). These indicators reveal the collector's capacity to convert the solar energy that falls on it to power and thermal energy. A lower value indicates that most solar energy is lost.

$$\eta_{total} = \frac{\mathrm{PV_{power}} + \mathrm{Q_u}}{I_T A_C} = \eta_{el} + \eta_{th} \qquad \text{Eq (3.29)}$$

where $\mathrm{Q_u}$ the useful thermal energy from the collector is. The Hottel–Whillier equation Hottel and Whillier equation defines Qu as the difference between thermal heat losses and the absorbed solar irradiance expressed as;

$$Q_u = A_c F_R (S - U_L (T_i - T_a)) \qquad \text{Eq(3.30) [196]}$$

The ESR is a metric that compares the new system to the reference system in terms of renewable energy savings. It is defined as shown in the equation below. A positive value of the (ESR) indicates that the adoption of the new energy solution has resulted in increased energy savings compared to the reference system. The greater the positive difference, the greater the proposed system's energy-savings capacity relative to the reference system. On the other hand, a zero value indicates that both systems can save the same amount of energy.

$$ESR = 1 - \frac{ES_{basicPVT}}{ES_{OPVT}} \qquad \text{Eq(3.31) [197]}$$

Another technical performance indicator is the solar fraction (SF). SF is the fraction of energy demand met from the solar system to the total demand expressed in Eq(3.32). The SF value demonstrates the contribution of the PVT in meeting the total energy demand [198] [191]

$$SF = \frac{Tota\ load\ met\ from\ rnewable\ energy\ source}{Total\ energy\ demand} \qquad \text{Eq(3.32) [199]}$$

Technical matrices that measure system reliability indices are the Loss of Power Probability (LOLP), the Renewable Energy Fraction (REF), Self-consumption ratio (SCR) and Load Cover Ratio (LCR). The LOLP is the probability that the energy system may not supply energy to meet demand at any given length of time. It is expressed as in equation Eq(3.33)

$$LOLP = \int_0^t \left(\frac{energy\ deficit}{energy\ demand}\right) dt \qquad \text{Eq(3.33) [180]}$$

The REF measures how much the renewable energy sources in the hybrid energy system displace the conventional energy sources in meeting the load. It is expressed as in Eq(3.34) [201]. A higher value indicates the energy savings and the amount of emission displaced [200].

$$REF = \left(1 - \frac{PL_{conventional}}{PL_{renewable}}\right) \qquad \text{Eq(3.34) [201]}$$

To evaluate the renewable hybrid energy self-reliance in meeting demand, the annual average renewable energy SCR is calculated by Eq(3.35.) [202]

$$SCR = \frac{Onsite\ RE\ to\ load}{Total\ RE\ generated} = \frac{E_PVT_{load} + E_PVT_{batt}}{E_{PVT}} \qquad \text{Eq(3.35.) [202]}$$

where E_PVT_{load} is the power from the PVT collector to load E_PVT_{batt} is the PVT supply to charge the battery storage. Similarly, the load cover ratio (LCR) of the electrical Load, also known as the Self Sufficiency Ratio (SSR), is defined in Eq(3.36). [202]

$$SSR = \frac{Onsite\ RE\ to\ load}{total\ electric\ load} = \frac{E_PVT_{load} + E_PVT_{batt}}{E_{load}} \qquad \text{Eq(3.36). [202]}$$

One of the goals of this study is to assess the environmental impact of the system in reducing emissions like CO_2. To assess the mitigation impact of the proposed energy system, the avoided carbon dioxide (ACO_2) emission displaced by the system is calculated based on the type of fuel substituted from Eq(3.38) [203]. Even though there are other energy-related emissions, since car dioxide dominates the other emission and of primary in the energy market and road map to reducing global warming, the environmental mitigation impact of this study considers the level of CO_2 as an environmental index. Therefore, the CO_2 reduction ratio RR_{CO_2} as defined in Eq(3.37) [197] is adopted to compare the new study with the reference system to measure the relative improvement in reduction of CO_2 in the energy mix.

$$Avoided_{CO_2}\ Ratio = \frac{ACO_{2_{prop}}}{CO_{2_{ref}}} \qquad \text{Eq(3.37)}$$

$$ACO_2 = Amout\ of\ fuel\ displaced\ \times Emission\ factor\ of\ fuel \quad \text{Eq(3.38)}$$

Recommended emission factors of 0.439kgCO_2/kWh for grid power and 2.6kg CO_2/L for diesel generators in the case of Nigeria [203].

3.11 The reference and the baseline systems

The primary aim of hybrid renewable based poly-generation energy system projects is to ensure reliability, and profitability with an acceptable level of greenhouse gas in the energy mix. The realisation of this objective can only be measured if the performance of any hybrid renewable based poly-generation energy system is gauged against the reference energy system which are conventional energy technologies like the grid and diesel power generators[204]–[206]. In this study therefore, the overall performance of the proposed hybrid OPVETC energy system used in meeting power and hot water demand of the case study building is assessed and its advantage over the reference energy source (diesel generator) in terms of profitability and environmental protection is compared.

Furthermore, in this study, the baseline energy system is the currently commercially available hybrid PVT energy system. To evaluate the efficacy of the proposed OPVETC over the widely and currently adopted commercial conventional hybrid PVT energy system, the performance of the new system (OPVETC) is further gauged relative to the current conventional hybrid PVT energy system in meeting power and hot water demand of the same case study building. In this study, the electric power and hot water demand of the case study health facility is first met using the diesel generator and the economics and environmental indicators now form the reference matrix for the performance comparison of the currently commercially available hybrid PVT energy system (Base line system) and the new proposed energy system (OPVETC)

.

Notably, for a fair comparison, the size and parameters of the baseline system and the proposed system are identical and both systems are coordinated based on the same energy management to meet the case study electric power and hot water demand. Figure 3.21 below is a schematic and summary of the modelling and performance evaluation method.

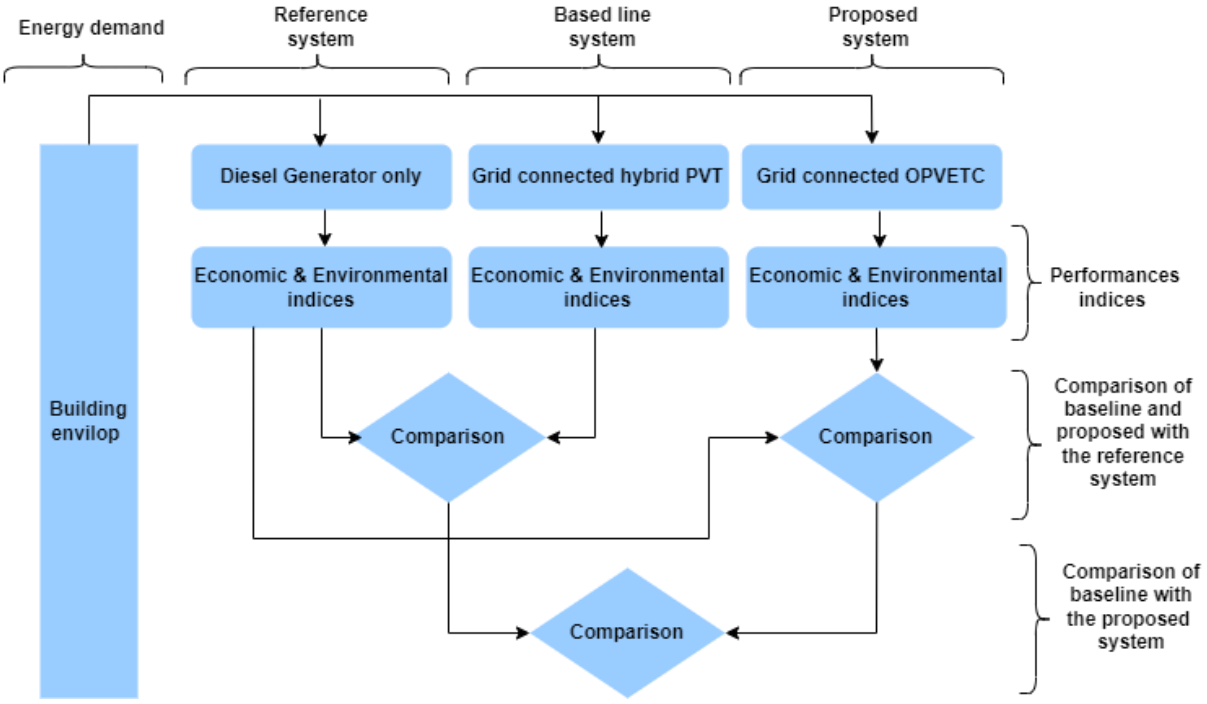


Figure 3.21. Summary of modelling approach

3.12 Modelling of the basic PVT hybrid system (The baseline)

To assess the efficacy and significance of the proposed OPVETC in terms of the technical, energetic, economic, and environmental benefits based on the developed energy management strategy, and flow control in this study, an equivalent model of the conventional hybrid PVT energy system as seen in

Figure 3.22 is developed using TRNSYS software. This way, the contribution of the proposed energy system and cooling technique will be measured relative to the widely adopted system configuration and cooling architecture as found in most literature[207], [208]. For the much-

consolidated traditional PVT hybrid energy system, the cooling liquid is repeatedly circulated in a closed-loop circuit to cool the PV module. The cooling fluid is circulated at a constant flow rate in most cases. The cooling water is primarily to cool the PV module. In this study, therefore, the conventional hybrid system connected to the grid and operated based on a randomly unavailable grid power control strategy is equally used to meet the power and hot water demand of the study case health centre based on an identical load scenario under the same weather and climatic conditions. To ensure that the comparison is fair, all components of the conventional hybrid PVT system are modelled using the same design parameters and sizes. Notably, the basic PVT collector area is $57m^2$ compared to the collector area in the proposed OPVETC, which is $55m^2$ for the PVT collector and $2m^2$ for the evacuated tube collector. This measure ensures that the total collector area is the same in both the conventional and the OPVETC. Aside from that, the parameters and sizes of all other components are the same. Table 3.9 compares both systems based on the various components they are made of.

The proposed OPVETC hybrid energy system is equivalent to the basic PVT hybrid system model. The power components and building load are coordinated for both models based on the previously developed energy management control strategy. The module cooling method is the primary distinction between the basic PVT hybrid and OPVETC. The basic PVT hybrid energy system is cooled using the closed-loop basic flow control (CLCCS) strategy that has been used in most studies, whereas the OPVETC model is cooled using the developed open-loop cooling control strategy (OLCCS).

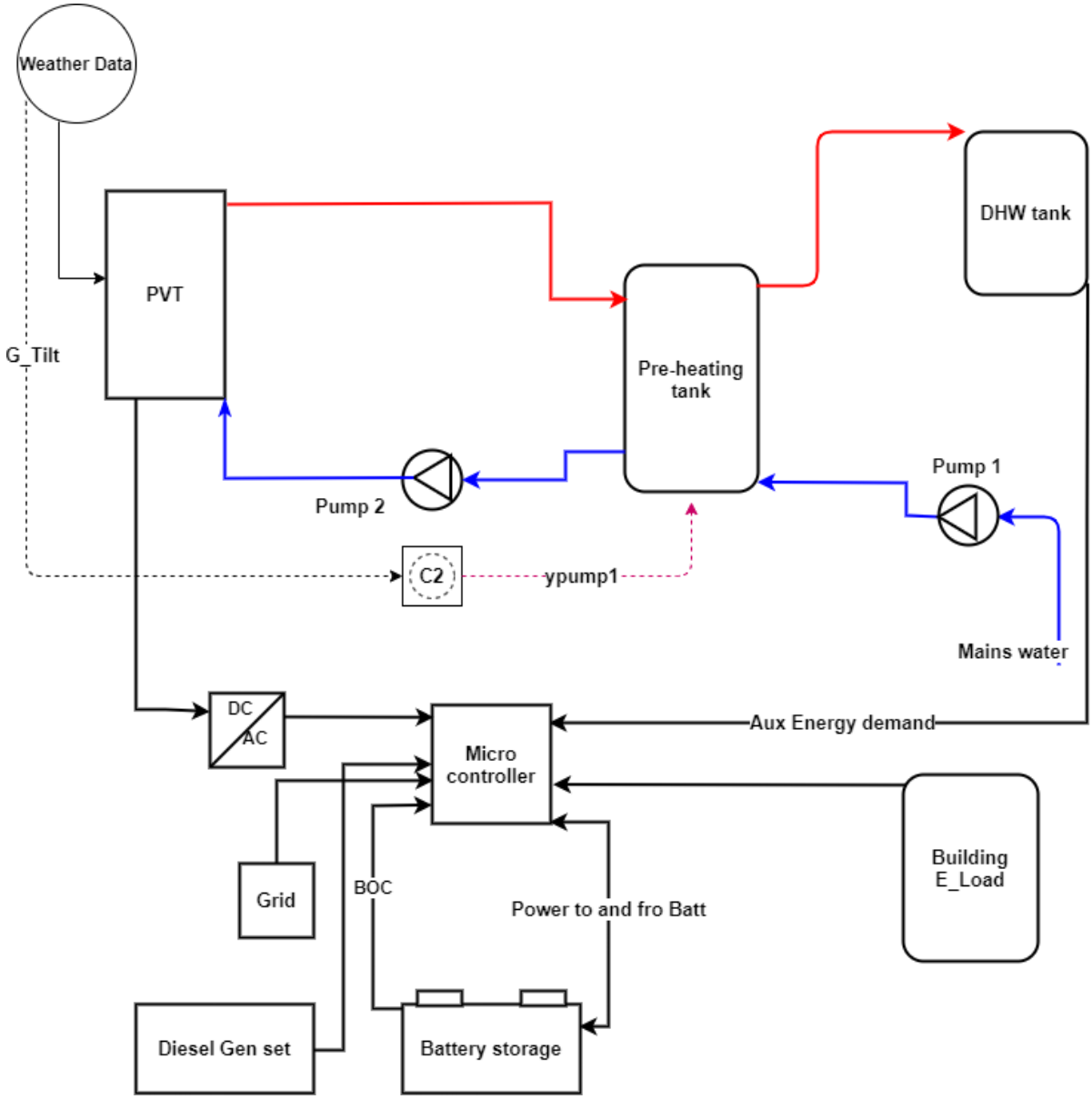


Figure 3.22: The basic PVT: Equivalent of the proposed OPVETC

Moreover, the hot water demand for the different health services is supplied through a single tank in the basic PVT, whereas in the OPVETC, the water demand is delivered separately from the two tanks. Table 3.9 compares the proposed OPVETC and the basic PVT hybrid energy system, showing similarities and dissimilarities.

Finally, the annual performance of the modelled conventional system used as the benchmark is simulated, and a comparative evaluation of the technical, environmental, and economic performance of the basic PVT is undertaken under similar performance indicators as previously described in this chapter.

Table 3.9: The Basic PVT and the OPVETC components size

SN	Parameter	Basic PVT model	OPVETC model
1	Total numbers of PVT collectors (1.63m^2)	36	33
2	Total area of ETC (1.63 m^2)	-	3
3	Total number of tank (0.3 m^3)	1	2
4	Total number of diverters	1	2
5	Total number of pumps	1	2
6	Total number of pump controller	1	2
7	Total number of battery (75Amp), 14volts)	15	15
8	Total number of inverters (8kW)	1	1

From Table 3.9 it is evident that the comparison of the both the baseline system and the proposed OPVETC are based on the same component size. Particularly, for fair comparison, the total collector area for both the basic PVT and the OPVETC models are 36m^2.

3.13 Validation and verification of simulation model

It is a common practice to determine whether a formulated system model and its outputs are valid and, to a large extent, represent the actual system and its outputs. One strategy used in most research is comparing the model's simulated output with empirically measured performance. In this way, the concern of how reliable the model is at predicting actual system performance is thus addressed. A technique that compares the model output with the

experimental result of a similar system published in the literature is analogous to comparing model output with measured system performance. Because of the complexity, the huge financial cost, and time constraints required to set up the experimental rig, validation of the model by comparing its outcome to the experimental result is not conducted in this study. Moreover, no published works found in the literature have the experimental result of an exact or similar system to what is proposed in this study.

In this study, therefore, the verification and validation (V&V) methodology as used by Sigarchian [197] to validate a small-scale polygeneration energy system, which includes several renewable energy sources for cooling and heating and power generation is adopted. By this technique, the closeness of the conceptual model to the actual system and its outputs are ascertained. The V&V verification approach compares component-by-component outputs of the formulated components of the modelled system to the description of the expected theoretical behaviour as found in the literature [209]. Interestingly, the verification steps are even the initial step that finetunes the system model to the desired output and expected behaviour desired by the designer during the model development. The flow chart in Figure 3.23 illustrates the model verification approach.

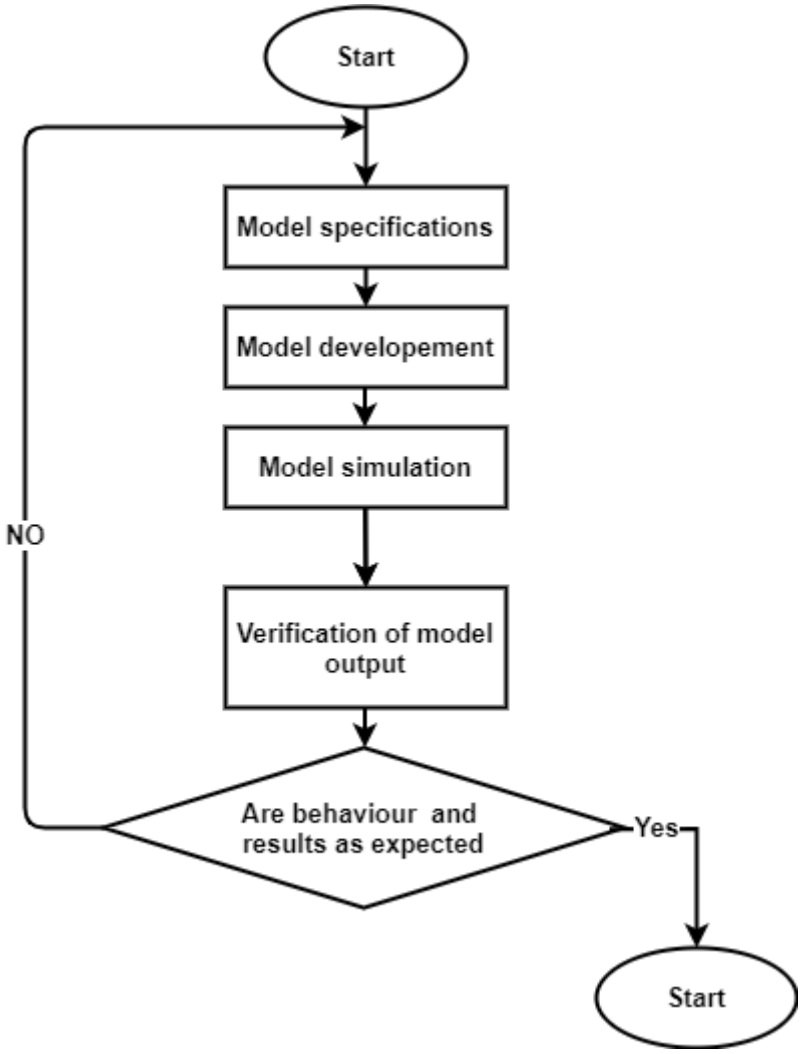


Figure 3.23. Verification and validation flow chart in model development

In verifying the model performance output, the first consideration of the formulated system model is based on components that have long been validated and accepted in science. To this end, different studies have experimentally validated the Type 560 of the PVT collector model found in the simulation library of TRNSYS [181], [182], [210]–[212]. Similarly, Type 56 of the 3D building model found in TRNSYS have been experimentally validated in other studies[183], [213]. Furthermore, the simulated output of the evacuated model (Type 73) was found to be 13.7% variance with the experimental result under a quasi-steady state in a study conducted by [214]

To this end, in this work, the unglazed TRNSYS model of the PVT collector (Type 560) was compared against the most commonly and widely well-validated numerical model published by Sun et al.[215] and Pantic et al. [216] as expressed in Eq(3.39). to Eq(3.41).

$$T_c = T_a + \frac{G}{G_{NOCT}}(T_{NOCT} - 20) \quad \text{Eq(3.39).}$$

where Sun et al.[215] showed that in an unglazed PVT collector, the Nominal Cell Operating Temperature (NOCT) is found from Eq(3.40).

$$T_{NOCT} = 509.5\frac{T_{fi} - T_a}{G_T} - 0.7352\dot{m}_f + 36.94 \quad \text{Eq(3.40).}$$

$$P_{max} = P_{max,STC}(1 - \gamma(T_c - 25)\frac{G_T}{G_{NOCT}} \quad \text{Eq(3.41).}$$

where Ta is an ambient temperature (^{o}C), G_T is a measured solar radiation intensity (W/m^2) and G_{NOCT} is the standard test condition solar radiation intensity of 800 W/m^2.

To evaluate the compliance of the fitness of the TRNSYS model with the above equations, the model prediction is compared, and the results are variance from the Eq is based on the R^2 correlation and mean absolute percentage error (MAP_{err}) defined as in Eq(3.42).

$$MAP_{err} = \frac{1}{n}\sum_{t=1}^{n}\left|\frac{A_t - F_t}{A_t}\right| \quad \text{Eq(3.42).}$$

A_t is the predicted result from the reference equations and F_t is the fitted result from the TRNSYS model. n is the number of readings.

After the component-by-component validation with an empirically established model of the component, the next consideration is verifying whether the entire system model outputs and

characteristics are in accordance with the designed logic or control strategy. This expected logic is inspected by graphically following the outputs and dynamic model behaviour, considering the expected characteristics. This study monitors the dispatch strategy of the various power elements based on the FEL control for 24 hours a day and 365 days. Additionally, the system's operation should give a logical trend when simulated under a certain condition's increasing or decreasing effect.

In addition, two more approaches are employed to validate the model formulated in TRNSYS for assessing the proposed hybrid energy system architecture. First, an energy balance analysis to check the relative accuracy of the formulated system model was conducted utilising an energy balance subroutine (Type 28) obtained in the TRNSYS library. This subroutine (Type 28) checks and compares the energy flows across the system boundary and determines if the flow across the system boundary is balanced. Energy flows (losses and gains) of several components of the entire system are linked to this component specifying whether it’s a loss or a gain. For this method, the system power and thermal boundaries of system components are analysed separately, as shown in Figure 3.24 and Figure 3.25, respectively. The yellow arrow shows all gains across a component boundary with direction pointing into the boundary. Likewise, all losses are indicated by the arrow pointing outwards of the boundary. All losses have a negative convention for analysis, and all gains are assigned positive values. The simulation summary subroutine (Type 28) performs the monthly and annual arithmetic on all energy quantities connected to it. Consequently, if the energy balance between the system gains and losses is within a 2% error, then the formulated model is appropriately set up, and the simulated model converges within the specified time step and tolerance error; otherwise, a warning will be issued in the *.lst and *.log file [217].

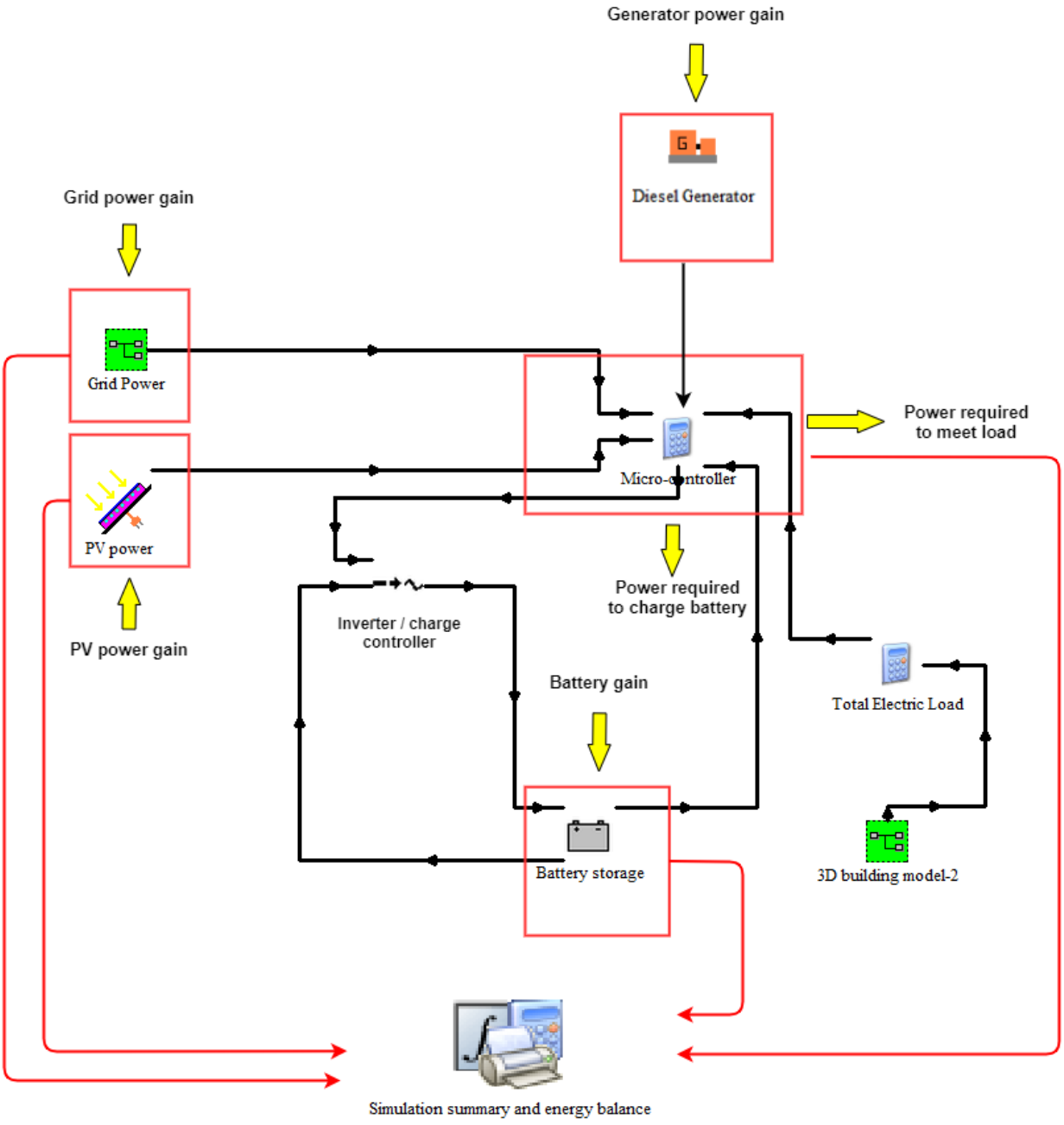


Figure 3.24. System's power model energy balance

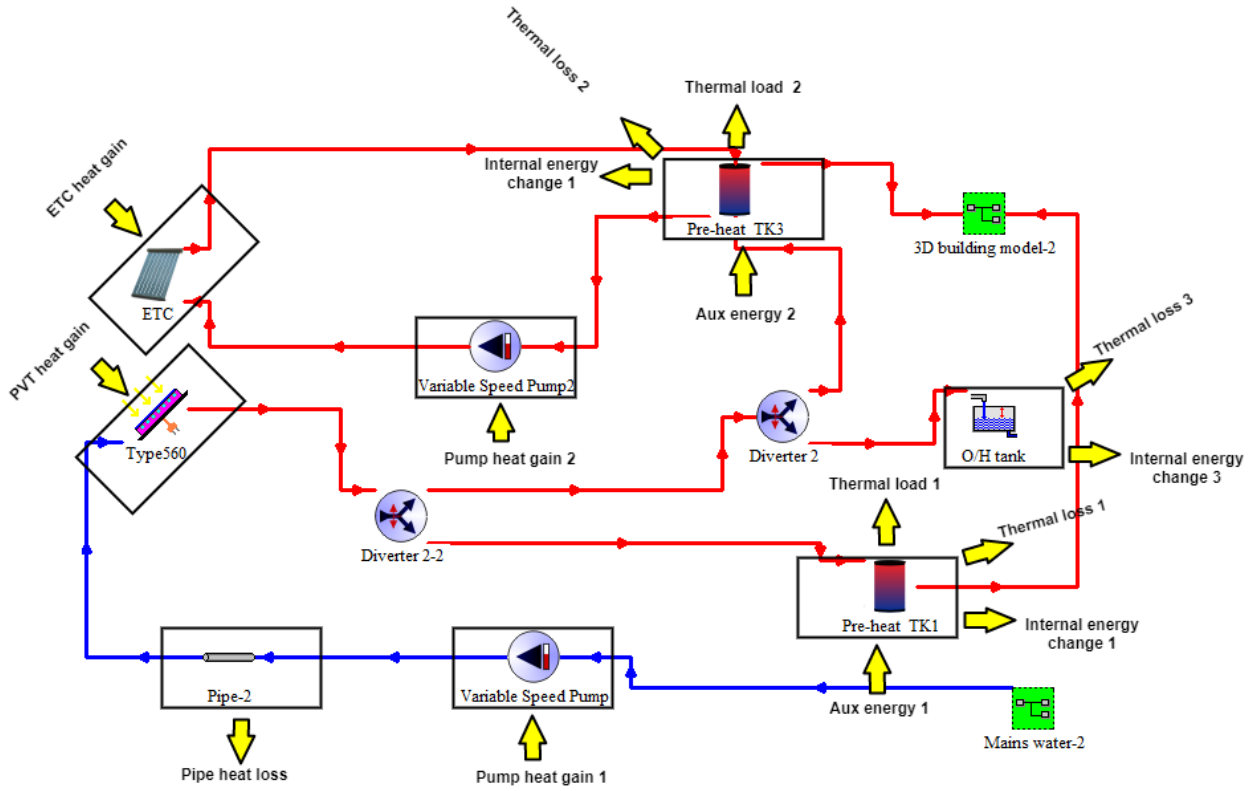


Figure 3.25. System's thermal model energy balance

Secondly, the building envelops zone temperature was experimentally measured, 20 at a time step of 15minutes, and the measured temperature was statistically compared with the predicted zone temperature. The measured indoor temperature from 9/01/2020 to 14/01/2020 (see appendix D) was obtained using the Elitech GSP-6 Digital Temperature and Humidity Data Logger. The GSP-6 detachable dual probes device measures temperature from –40^{o}C to 65^{o}C with maximum accuracy up to ±0.6^{o}C. In addition, an MS-602 pyranometer with an accuracy of ±10watt kept on a horizontal surface outside the case study building is used to measure the solar radiation. To statistically assess the correlation and agreement of the model with the reference model and experimentally measured data, the Root Mean Square Error (RMSE) as defined in Eq(3.43) and the R-Squared correlation is employed.

$$RMSE = \sqrt{\frac{\sum_i^n (x_{,i} - y_{,i})^2}{n}} \qquad \text{Eq(3.43)}$$

3.14 Methodology for the project economic assessment

There are different economic indicators for measuring the monetary value of renewable energy projects. Several factors determine the choice of the appropriate evaluation matrix. These factors are dependent on one or a combination of different considerations. The government regulations and risks associated with the investment are suitable assessment matrices to first consider by investors. Assessment matrices that evaluate financing, project cash flow, and the comparative benefit of the project over mutually exclusive alternatives are good assessment tools after the risk and government policies are assessed. Usually, it is good to assess the viability and profitability of an energy project based on two or more criteria using different economic indicators. The choice of the indicator must be appropriate as specific economic indicators are inappropriate for some investments. For example, adopting the internal rate of return to assess and compare two projects that are in all aspects different in their returns over time may result in inappropriate assumptions regarding the rate of return available through reinvestment of the cash inflow. It will be inappropriate to compare projects based on the Levelized Cost of Energy and payback period for mutually exclusive projects. The economic indicators described in the subsequent section are those selected in this study since the goal is to measure the cost-effectiveness of the proposed reconfiguration over the basic grid-connected hybrid PVT. For this reason, the choice of the total life cycle cost, the Levelized cost of energy, payback period, return on investment, and the net present value are appropriate and considered adequate for the economic assessment of the proposed energy system.

Since renewable energy projects usually have a life span of more than 25 years, the economics of renewable projects is assessed based on the future value of the investment. For example, the cost of capital for components and the operation and maintenance that will occur in the future is assessed considering the time value of money. In this study, the commonly used time analysis for the time value of cash flow in most investments is adopted as the present value (PV) of money. Therefore, project economics is evaluated and analysed based on the theoretical framework established in the subsection below. The economic results are presented and discussed in this chapter's result and discussion section.

3.14.1 The present value method

The present value (PV) analysis calculates today's worth of monitory transaction that occurs in the future to account for changing money worth. In other words, the present value of revenues produced, or expenses incurred today is a measure of the future value of those revenues or expenses. Therefore, the present worth (PV) of an investment from the future worth (F_n) is calculated from Eq(3.44) and Eq(3.45)

$$PV = PVIF_n \times F_n \qquad \text{Eq(3.44) [218]}$$

$$PVIF_n = \frac{1}{(1+d)^n} \qquad \text{Eq(3.45) [218]}$$

This formula is used to assess the present value of cash flow, considering what happens in the future from now. where PV is the present value of cash flow, $PVIF_n$ is present value interest factor, d is the annual discount rate, n is the base year of analysis after year zero and F_n is the assumed or expected cash flow in n years in the future. The expected cash flow in the case of a renewable energy project is the savings arising from the load demand met using renewable energy sources. This study assumes that the energy project is operational with no increase in load for 25 years. Therefore, all expected revenues in the future that occurred during the

lifetime period (25 years) are estimated based on the PV analysis method using the current dollar cash flow method [218]. Consequently, the project economic matrices are evaluated based on the present value analysis method

3.14.2 Total Life-Cycle Cost (TLCC)

The TLCC sums all expenses that occur right from the installation, operation, and maintenance, minus the worth of the project at the time of expiration of the life of the project [176]. For renewable energy projects, the TLCC estimates the overall cost of the energy technology, starting with the installation costs (IC), fuel costs (FC), operating and maintenance costs (OMC), replacement costs (RC) and residual values (PSV) [176]. These costs are estimated as cash outflows except for the residual values (PSV) which is considered as cash inflow. The TLCC is a valuable economic matrix for comparing expenses between energy project alternatives. In computing expenses that occur during the entire lifetime of an energy project, the costs incurred at any time are discounted to the base year at which they occurred using present value analysis[176]. The scrap value revenue generated from the resale of the investment is also discounted to the base year in which the project is disposed of. This scrap value is subtracted from the total expenses discounted at present value costs. Importantly, TLCC is not a matrix for deciding whether to accept or reject an energy investment since the total cost of an investment has no frame of reference for what is acceptable and what is not acceptable [176]. However, if in comparing energy alternatives, and these projects have the same economic indicators other than the TLCC, the TLCC can be used to rank the investment. For renewable energy projects, the TLCC analysis consists of distinct categories of outflows, as depicted in Eq(3.47) [219][176]. The expenses must be discounted based on the appropriate year; otherwise, the analysis will be flawed. For renewable energy projects, a simple expression for the TLCC is equation Eq(3.46)

$$TLCC = IC + RC + OMC + FC - PSV \qquad \text{Eq(3.47) [176]}$$

RC is the cost of replacing system components that have a shorter life than the project lifetime. OMC is the operation and maintenance cost. This cost includes the cost of battery and PVT collector maintenance, diesel generator service, and system repairs. The fuel cost FC includes the cost of diesel fuel and energy purchased from the grid. This study adopts the current dollar method for which cash outflows and cash inflows are discounted at the nominal discount rate. Therefore, the lifetime operation and maintenance cost OMC_T after year zero with an annual inflation rate i is estimated as:

$$OMC_T = OMC(1+i)^n \times PVIF_n \qquad \text{Eq(3.48) [176]}$$

Similarly, the total replacement cost RC_T. The total fuel cost FC_T and the total salvage value PSV_T are calculated using Eq(3.49), Eq(3.50) and Eq(3.51)

$$RC_T = OMC(1+i)^n \times PVIF_n \qquad \text{Eq(3.49) [176]}$$

$$FC_T = FC(1+i)^n \times PVIF_n \qquad \text{Eq(3.50) [176]}$$

$$PSV_T = OMC(1+i)^n \times PVIF_n \qquad \text{Eq(3.51) [176]}$$

where n is the base year for which the cash flow occurs and $n \geq 1$. OMC is the annual cost of maintenance. N is the analysis period; d is the annual nominal discount rate. Equations Eq(3.49) to Eq(3.51) are added to arrive at the entire system's total life cycle cost as depicted in equation (6). Worthy of note is that the discounted cost, whether cash inflow or cash outflow, is evaluated on the appropriate present value interest factor (PVIF) depending on the year cash

flow occurs. The initial investment cost is an area or unit dependent cost that is incurred at year zero of the lifetime of the technology. For this project, it is expressed as.

$$OIC = C_c + C_{instal} \quad \text{Eq(3.52)}$$

where C_c is defined as;

$$C_c = N_{coll}C_{opvetc} + N_{tk}C_{tank} + N_{pump}C_{pump} + N_{cont}C_{con} + C_{inv} + N_{batt}C_{batt} \quad \text{Eq(3.53)}$$

where N_{coll} N_{tk} , N_{pump}, N_{cont}, and N_{batt} are the units of collectors, storage tanks, pumps, controllers, and batteries, respectively. C_{opvetc}, C_{tank}, C_{pump}, C_{cont}, C_{inv}, and C_{batt} are the unit cost of the collector, storage tank, pumps, controller, inverter, and battery, respectively. The system installation cost C_{instal} is taken as 10% 0f the total investment cost [220]

3.14.3 Life cycle savings (LCS)

The total solar fraction (both thermal and electrical) fulfilled by the energy system is translated to equivalent income by multiplying the saved energy with the unit cost of the replaced conventional energy, in this case, diesel power, to determine the annual cash inflow of the energy project [221]. As stated earlier, the annual system revenue is then discounted using the current dollar approach. Assuming that the annual saving of the system is E_s and the power degradation factor is δ then the value of the LCS evaluated in any base year n is found from Eq(3.54)

$$LCS = E_s(1-\delta)^n(1+i)^n\, PVIF_n \quad \text{Eq(3.54) [221]}$$

The total system revenue during the project's entire lifetime is found by the addition of all the annual revenue for the system's entire lifetime. Eq(3.55) is the project cash inflow discounted based on the current dollar method.

3.14.4 Net Present Value (NPV)

The NPV of a project measures the project's profitability at any time of interest but is evaluated chiefly at the end of the project life. This indicator shows the worth of the project based on the PV analysis method [222]. The NPV is a suitable matrix for comparing projects and even mutually exclusive projects. In simple terms, it is the worth of the project when all expenses have been deducted, as expressed in Eq(3.55).

$$NPV = Cash_{inflow} - Cash_{outflow} \qquad \text{Eq(3.55) [152].}$$

The $Cash_{inflow}$ is the total revenue obtained from the energy saved, while the $Cash_{outflow}$ is equal to the system $TLCC$

The general rule is to “Accept” if NPV >0, “Reject” if NPV<0, and “Accept” if NPV=0 considering other benefits [218].

3.14.5 Levelised Cost of Energy

The Levelised Cost of Energy (LCOE) describes the unit cost of energy produced by the project. It sums up all the expenses that occurred during the project's entire lifespan and divides it by the total kilowatt-hour of energy produced by the system discounted at the present value interest factor as shown in Eq 3.56 [6]. This indicator, in other words, is the minimum cost for which the energy produced must be sold to recover the investment. Therefore, the energy cost for a business purpose must be sold at $/kWh, not less than the LCOE of the project. There is no benchmark for this indicator; it only shows the comparativeness of the project with other alternatives [218]. Projects with lower LCOE are usually more preferred by investors since consumers prefer to pay a lower cost for energy consumed. However, an energy project with low LCOE does not necessarily mean good environmental conservativeness. For hybrid energy systems combining renewable energy sources with conventional energy sources, in most cases,

lower LCOE comes with a trade-off in the conservative capacity of the energy system expressed below.

$$LCOE = \frac{TLCC}{E_p\ PVIF_N} \qquad \text{Eq(3.56) [6]}$$

where E_p is the energy produced by the system in year N equal to the period of analysis

3.14.6 Return on investment (ROI).

This indicator assesses the project's profitability in terms of the percentage of the total life cycle cost of the project [218]. The profit is gauged against the total cost and expenditure during the project's entire life cycle. For comparative analysis of exclusive energy projects, the ROI is not recommended. It is a practice to use more than one indicator to judge in this case.

3.14.7 Payback period (PBP).

The payback period (PBP) is when the net cash flow of the energy project is at break-even and the initial investment has been fully recovered[222]. For this study the investment and expenditure are discounted to arrive at the payback time for discounted PBP. PBP is a quick reference for when an investor's investment is at risk. Projects with lower payback times are at lower risk than projects with more extended payback periods [222]. The analysis considers the time axis in the cash flow diagram where the NPV value is zero to find the PBP. The following subsection is the result of the economic evaluation of the OPVETC hybrid energy system compared with the basic hybrid PVT energy system. Remarkably, both systems are operated based on the same condition and load scenario, making the basis for comparison rational

3.15 Chapter Summary

The numerical model and performance evaluation of the proposed OPVETC is estimated based on the system model formulated using TRNSYS 18 software. TRNSYS 18 is the transient system simulation tool selected in this study for system modelling, performance simulation, and evaluation. TRNSYS 18 is a modular software package with a large library of validated components models, that can be tailored to any conceived energy solution and has great adaptability for different applications and control.

The first step in this study is the establishment of the methodology to identify the energy needs that the system is intended to satisfy and the approach to estimate this load. In contrast to the intuitive approach, where the air conditioning load is estimated by multiplying the power rating of each air conditioning unit by the estimated time of use, in this study, the air conditioning load is estimated based on the 3D building model of the case study building envelope formulated in TRNSYS. This numerical approach is based on the method where the air conditioning and ventilation energy demand and their dynamic characteristics are evaluated more accurately as a function of weather and occupancy period.

The World Health Organization's (WHO) Service Availability and Readiness (SARA) survey tool, designed to assess the readiness of health facilities, is used to estimate the power consumption of the medical equipment of the case study health centre. As shown in appendix A1- A2, the SARA data acquisition form is administered to the clinic to take inventory of the medical equipment, its power ratings, and the hours of usage. This way the electric power demand of the health centre can be obtained by multiplying each equipment power rating with its time of usage and the sum of each equipment power requirement is evaluated as the power demand for medical equipment of the health centre. The air conditioning load is then added to the medical equipment power demand to arrive at the total power demand of the health centre.

For this study, the proposed energy management and dispatch strategy is based on the Follow-Electric-Load (FEL) control strategy that prioritises power from the PV module to meet the load. For this strategy, the various power elements in the system are set to produce the electric and thermal energy that follows the thermal power demand pattern and extra steps to ensure that excess of what is required is minimised.

The method to appropriately size the various components of the proposed OPVETC hybrid energy system to avoid over or under sizing is clearly explained. Remarkably, the size of the PVT collector, the battery storage, the pump, and the water storage tank in this study are the sole target and the parametric analysis approach use used to satisfactory size the components to meet both the technical and economic outlook of the energy project for the project to be competitive with other alternatives.

In this study, therefore, the verification and validation (V&V) methodology as used by Sigarchian [197] to validate a small-scale polygeneration energy system, which includes several renewable energy sources for cooling and heating and power generation is adopted. By this technique, the closeness of the conceptual model to the actual system and its outputs are ascertained. The V&V verification approach compares component-by-component outputs of the formulated components of the modelled system to the description of the expected theoretical behaviour as found in the literature [209].

Finally, the commonly used time analysis for the time value of cash flow in most investments is adopted to evaluate the system economic performance for the system life span of 25 years. Therefore, project economics is evaluated and analysed based on the Total Life cycle cost (TLCC), System solar fraction (SF), Net Present Value (NPV) Levelised Cost of Energy (LCOE) Return on Investment (ROI) and the project Payback Period (PBP). The methodology

to assess the viability of the proposed system in other geographical locations other than the study case location is explained.

Chapter 4: Results and Discussion

4.1 Introduction

This chapter presents and discusses the findings of the procedures developed in chapter 3. The first subsection discusses the thermal characteristics of the case study building, which serves as the foundation for estimating the HVAC load and medical equipment power demand of the building. The monthly average daily domestic hot water characteristic is also discussed in its daily distribution. In another section, the dynamic behaviour of the modelled system is presented based on the proposed unreliable grid energy management strategy and the open-loop cooling control strategy to reveal the implications and technical potentials of the energy system configuration and control strategies in enhancing the cooling of the PV component and net energy harvesting. The discussion explains how the appropriate component size was determined based on the parametric analysis. Finally, to evaluate the study's improvement, the technical performance indicators of the proposed energy system and the conventional PVT hybrid are presented and compared. The implications of energy balance and statistical analysis are discussed to ensure that the model is properly set up and valid.

4.2 Thermal characteristics of building zones

After the 3D building model is developed, as seen in Figure 3.13, the annual thermal characteristics of the thermal zones are simulated under the typical meteorological (TMY) weather data of the study area (Jos, Nigeria).

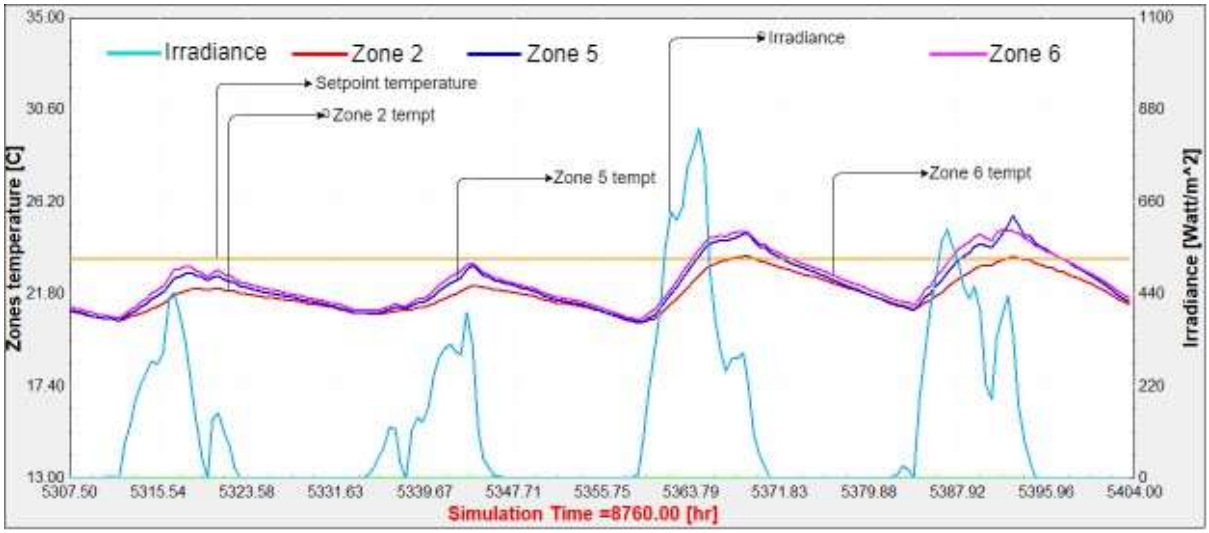


Figure 4.1.Zones' uncontrolled temperature on typical cloudy days 10/8/21 to 14/8/21

shows the uncontrolled temperature variation of the zones on typical cloudy days in August. It could be observed that the zones temperatures are slightly higher than the setpoint temperature of 23.5^{o}C. Notably, zones with the same orientation have shown a similar trend in temperature variation. Zone 5 and 6, which have a West-East orientation, seem to show higher temperatures than zone 2 with a North-East orientation. On typical days with a high amount of solar energy, as seen in Figure 4.2, zone 5 shows higher temperatures than zone 6 even though they have the same orientation. This difference in thermal characteristics of zone 5 and 6 is attributed to the difference in the thermal volume of the zones. Zones with higher volume have higher capacitance and, therefore, higher temperature. Zone 5, in this case, has a higher volume than zone 6, and therefore it is seen in to have a higher temperature.

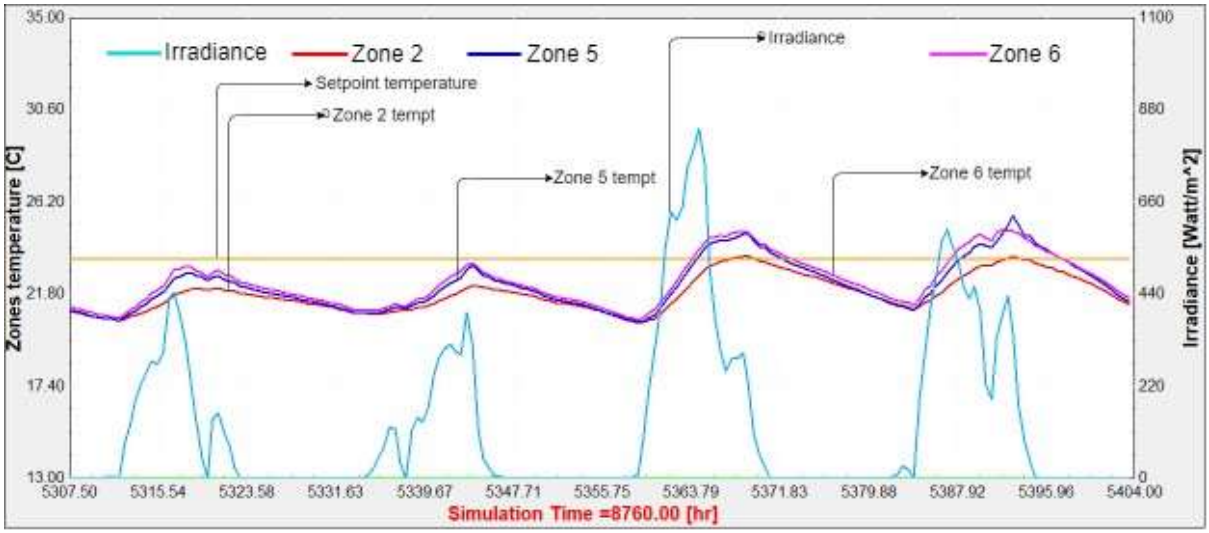


Figure 4.1.Zones' uncontrolled temperature on typical cloudy days 10/8/21 to 14/8/21

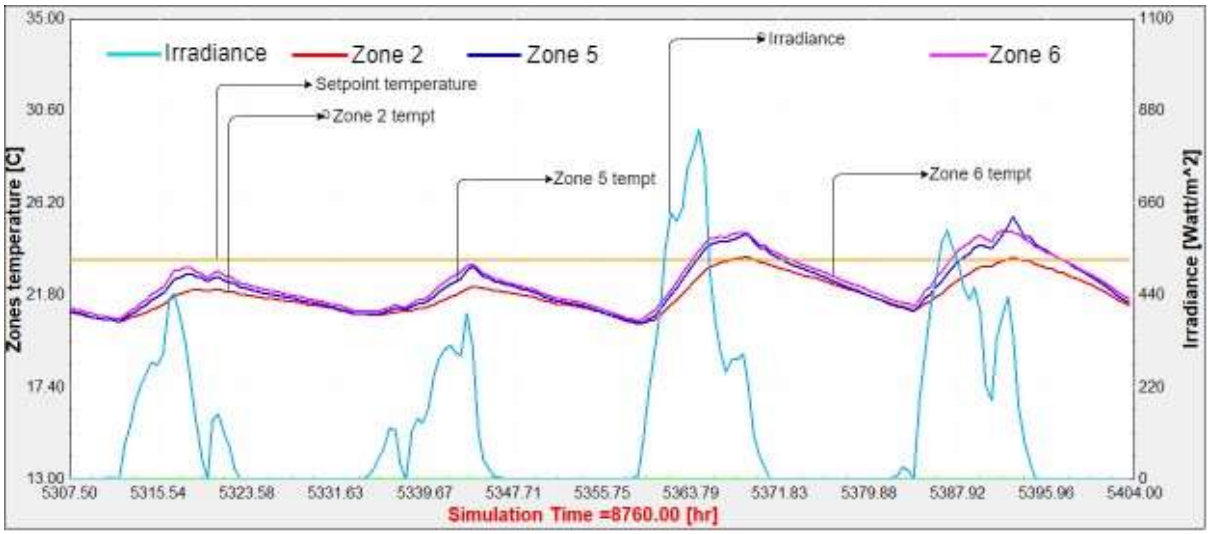


Figure 4.1.Zones' uncontrolled temperature on typical cloudy days 10/8/21 to 14/8/21

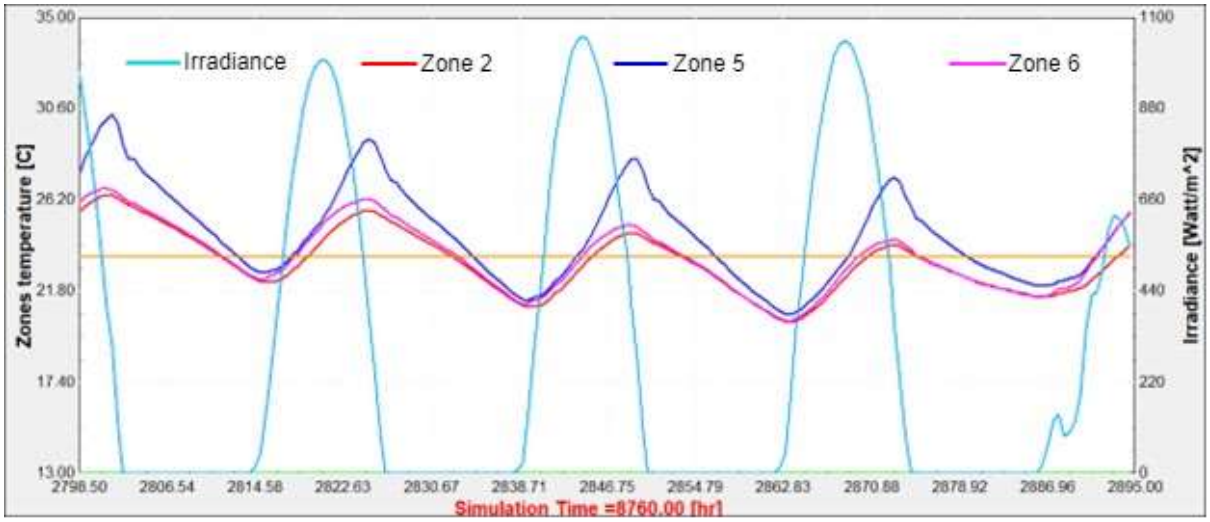


Figure 4.2:Zones uncontrolled temperature on typical sunny days 28/4/21 to 30/4/21

Figure 4.3 shows the temperature characteristics of the zones with the HVAC equipment cooling the thermal zones within the occupancy period as modelled in the HVAC controller. Since the building is an outpatient health facility, the occupancy period, in this case, falls only within working hours of 8 am to 6 pm. Consequently, the cooling or heating equipment operates from 10 am to 6 pm. This control strategy means that the HVAC is operated for 8 hours, and energy is only consumed when the zones temperature rises above the setpoint of 23.5^{o}C within 10 -18 hours daily. A similar trend with the temperature of zones flattening between 10 am to 6 pm is observed even on days with low irradiance and where zones' temperature rises above the setpoint temperature.

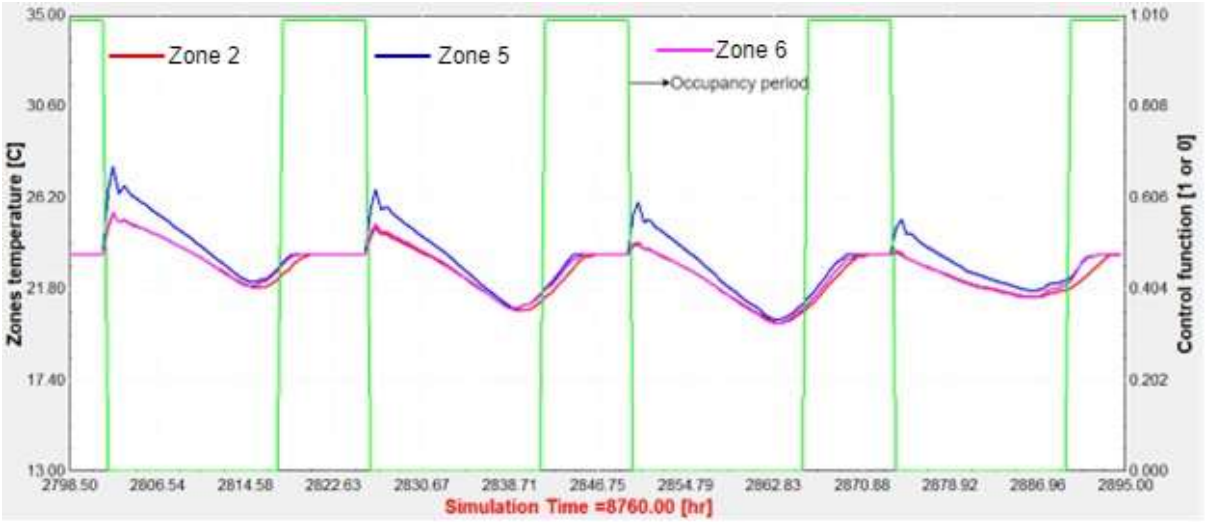


Figure 4.3. Zones controlled temperature on typical sunny days in April

Even though the controlled temperature behaviour of the thermal zones flattens during the control period for both cloudy and sunny days, the energy consumption of the HVAC equipment needed to bring the zones to the set temperature significantly differs, as seen in Figure 4.4 and Figure 4.5. The brown line in both figures indicates when the HVAC control is implemented.

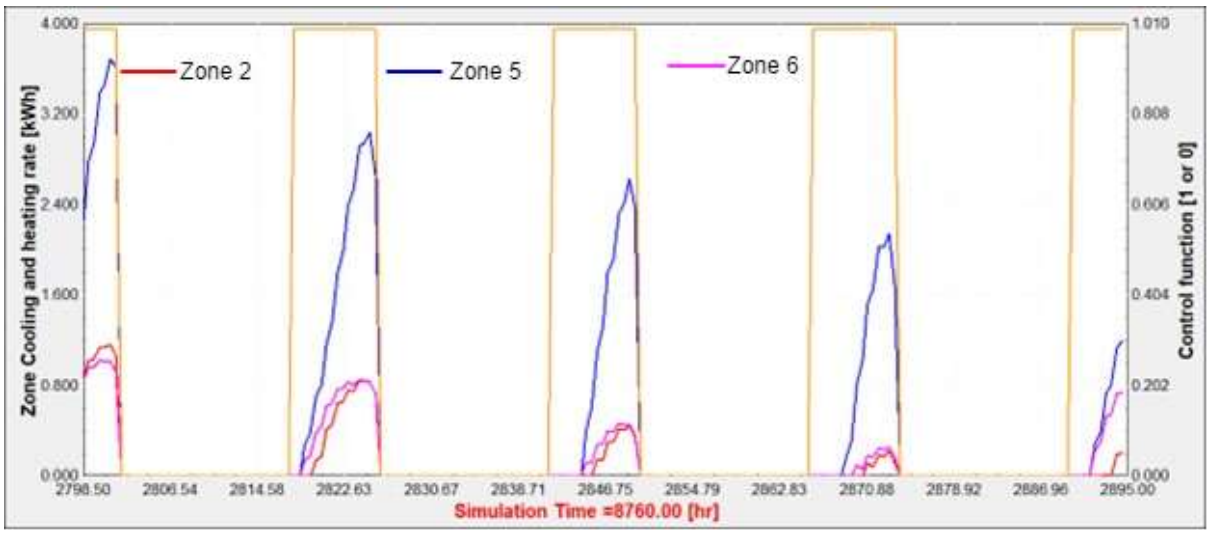


Figure 4.4 Zones HVAC power demand on typical sunny days

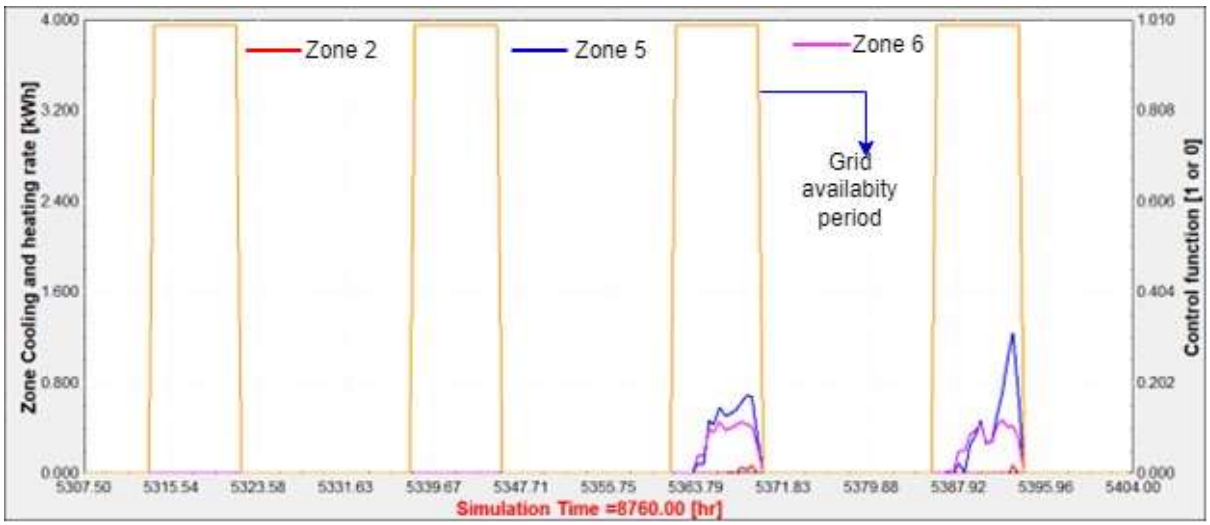


Figure 4.5: Zones HVAC power demand on typical cloudy days

Interestingly, months with low solar irradiance have lower energy demand. Likewise, months with very high cooling demand comparatively have a higher level of solar radiation, as seen in Table 4.1. Table 4.1 is the extract of the simulated performance of 3D building envelop model as shown in Figure 3.13 of the case study health centre. The trend implies that solar energy systems' output matches building load demand, and therefore photovoltaic hybrid energy systems are a promising and viable alternative for building energy demand.

Table 4.1: Monthly averaged daily maximum cooling and heating demand

Maximum zone temperature (°C)				**Average daily HVAC demand (kWh/day)**			
Month	Zone 2	Zone 5	Zone 6	Zone 2	Zone 5	Zone 6	Total
Jan	24.05	27.65	29.58	0.51	3.56	6.21	10.28
Feb	25.76	29.61	29.21	0.90	5.35	5.22	11.47
Mar	27.08	30.28	28.64	3.32	10.91	6.64	20.87
Apr	27.99	31.95	28.89	4.29	12.75	5.85	22.89
May	27.51	30.49	28.64	4.32	11.15	6.19	21.67
Jun	27.36	29.64	28.20	2.76	7.22	3.92	13.90

Jul	26.74	29.24	26.57	1.03	4.55	2.45	8.03
Aug	25.20	28.95	26.47	0.58	3.96	1.94	6.48
Sep	25.66	29.50	26.56	0.86	5.98	3.03	9.87
Oct	26.36	29.61	28.83	1.84	8.42	6.38	16.65
Nov	25.07	28.71	29.62	0.30	6.13	8.36	14.79
Dec	23.82	27.34	29.72	0.34	3.45	7.15	10.95

The cooling load as specified in Table 4.1 is obtained based on the building model developed based on the geometrical and roofing configuration, building construction type, and building materials as in Table 3.3, U-value of building materials as in Table 3.2, occupancy period and cooling and heating control as in Fig 3.12 and the all the comfort temperature of 23.5^{o}C required for the calculation of cooling load are all stated in the methodology Section 3.4

4.3 Estimating the total power and DHW demand

The building energy demand and the actual load profile are valuable inputs for the accurate design of energy systems to cover the building energy requirement. These energy demands include the electric power to run the medical equipment, the flowrate dependent power to operate the cooling water pump, varying domestic hot water (DHW) demand and the air conditioning cooling and heating demand. The power demand for cooling and heating is estimated from the formulated 3D building model of the case study building as seen in Figure 3.13 based on equation The demand for cooling or heating the building constitutes a sizeable portion of the load, and this demand varies seasonally and even monthly. In the same way, the power required to run the cooling water pump is dependent on the flow rate and its hours of operation. Similarly, the domestic hot water auxiliary energy is a function of the hourly performance of the thermal system. Consequently, to predict these loads with a close to accurate approximation, the dynamic characteristics of these loads are predicted using the TRNSYS 18 model of the building envelope and system model, as seen in Figure 3.13 using

equations Eq(3.1).1 to Eq(3.4). Figure 4.9 is the predicted building's maximum hourly heating and cooling rate. As shown in Table 4.2, the total power demand is higher for months with higher solar irradiance and lower for months with low solar irradiance. The DHW demand shows a similar yearly trend as the power.

The reason is that summer for this location starts in March, and the temperature gets remarkably high, consequently requiring much energy to reduce the zones temperature to the setpoint. Equally, winter is experienced around November to January, and therefore the ambient temperature is relatively lower; again, the cooling load is lower. One limitation in this study is that the appliance's load profile obtained from the analysis of the administered SARA form (Appendix A1to A2) as in seen in Figure 4.6 and Table 4.2 is assumed to be constant each day in every month. This assumption is used since there is no data available on the electric power consumption for medical equipment for the case study health facility.

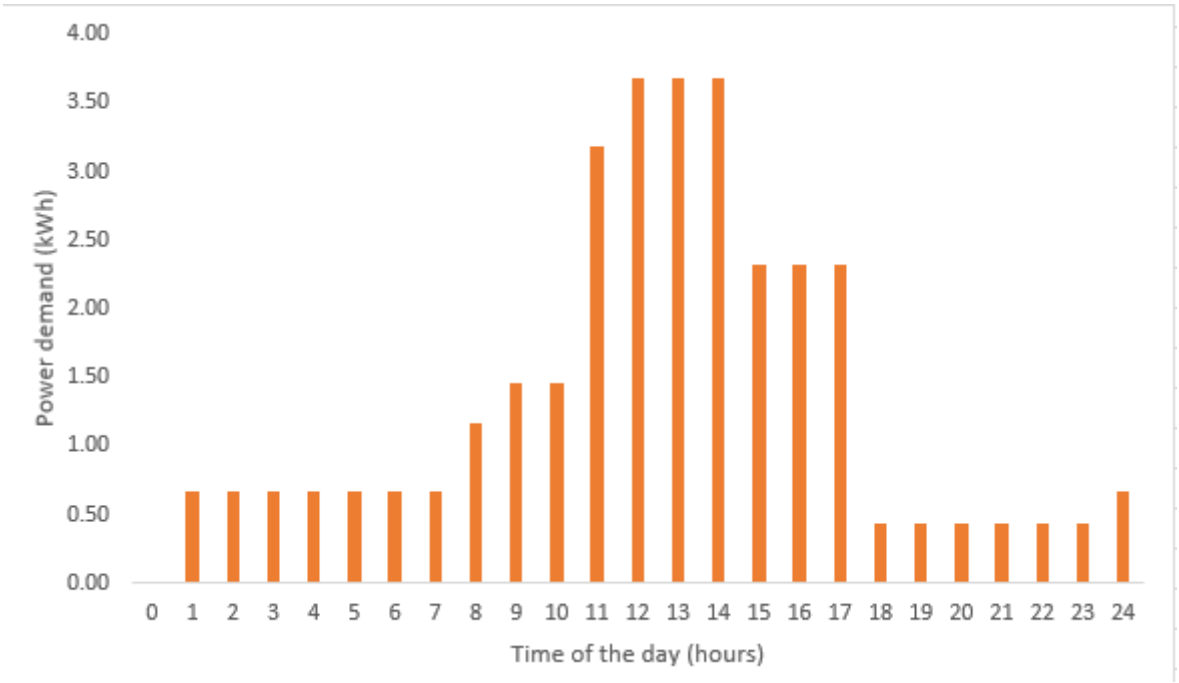


Figure 4.6. The health clinic equipment power demand profile

Even though the volume of hot water is assumed to remain constant, the monthly average daily thermal energy varies, as seen in Figure 4.7 and Figure 4.8. This fluctuation is due to changes

in the monthly average mains water temperature. Months with higher mains water temperature have lower thermal requirements to raise the water temperature to the desired temperature.

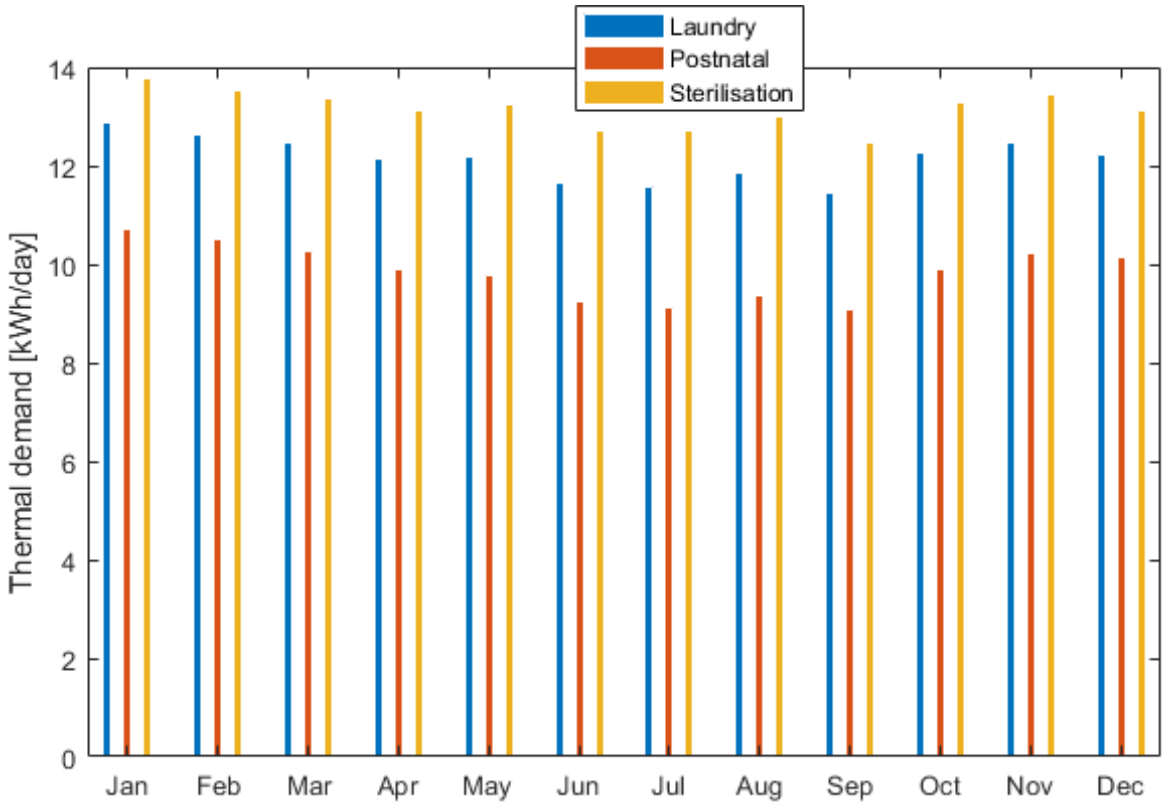


Figure 4.7: Monthly average daily hot water demand

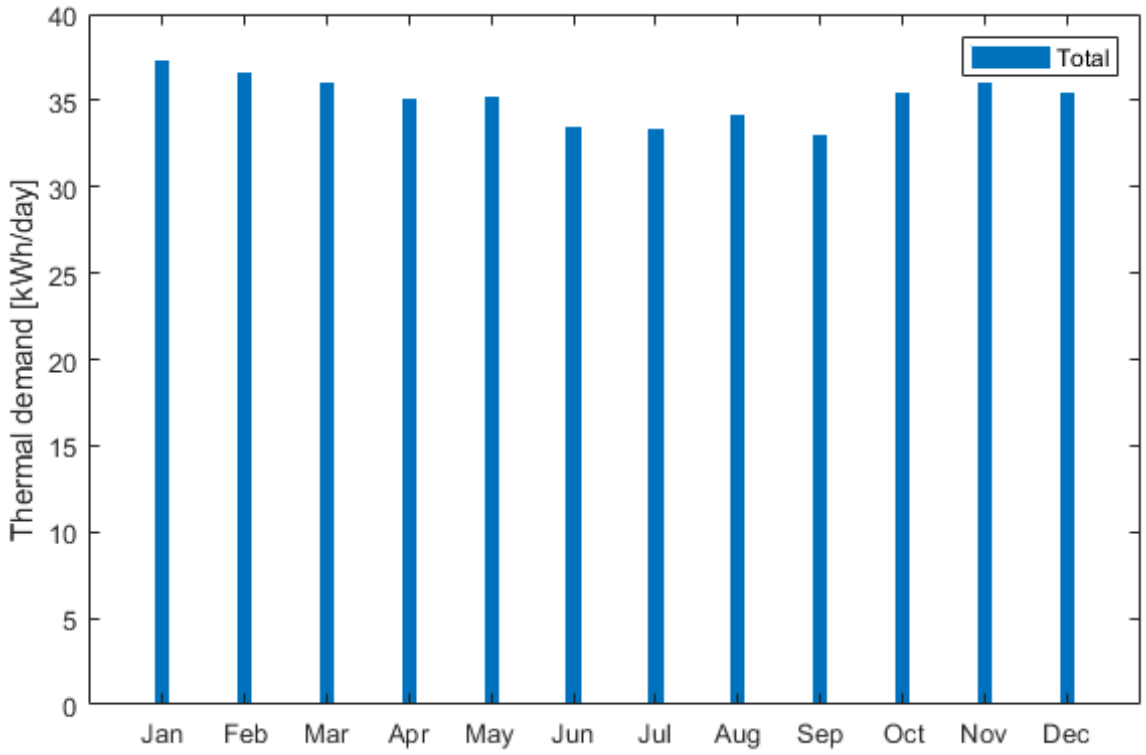


Figure 4.8:Total monthly average daily hot water demand

Table 4.2 is the monthly average daily appliances, air conditioning, and DHW energy demands obtained from the simulated performance entire system model in the simulation studio based on methodology and equations as in section 3.5. From Table 4.2, the annual average daily electrical and DHW load for the study case-building is 47.9kWh/day and 35.15kWh/day. The average daily power consumption of the building is 47.9 kWh/day which fall within the energy demand of health facility classified as hospital by World health Organisation (WHO) [42]. For this case study, the air conditioning load constituting about 28% of the total power demand. The specific heat capacity of building materials, their thermal conductivity, the requirements of the heating, ventilation, and air conditioning (HVAC) system, as well as regional weather variations and occupant energy consumption patterns, are factors that influence the consumption of this energy as concluded in the study [223]. In this case, the power demand is about 26.6% higher than the energy demand for hot water. Therefore, for system reliability, the

proposed energy system must be sized to cover a minimum of 48kWh/day for power demand, 35kWh/day demand for DHW, and the additional power demand for the pumps and controllers' operation. Comparing the monthly average building power consumption of 119.9kWh of an office building in Malaysia, the difference is significance as a result of the difference in weather condition and building material properties and occupancy and life style [224] .

The required hourly average maximum heating and cooling rate for the entire building is given in Figure 4.9. This information forms the basis for sizing the HVAC device needed to regulate the building zones temperature to setpoint as desired in this study. As seen in Figure 4.9 the 3.74kWh is the maximum cooling demand rate per hour required to cool the entire building to the setpoint temperature of 23.5 ^{o}C.

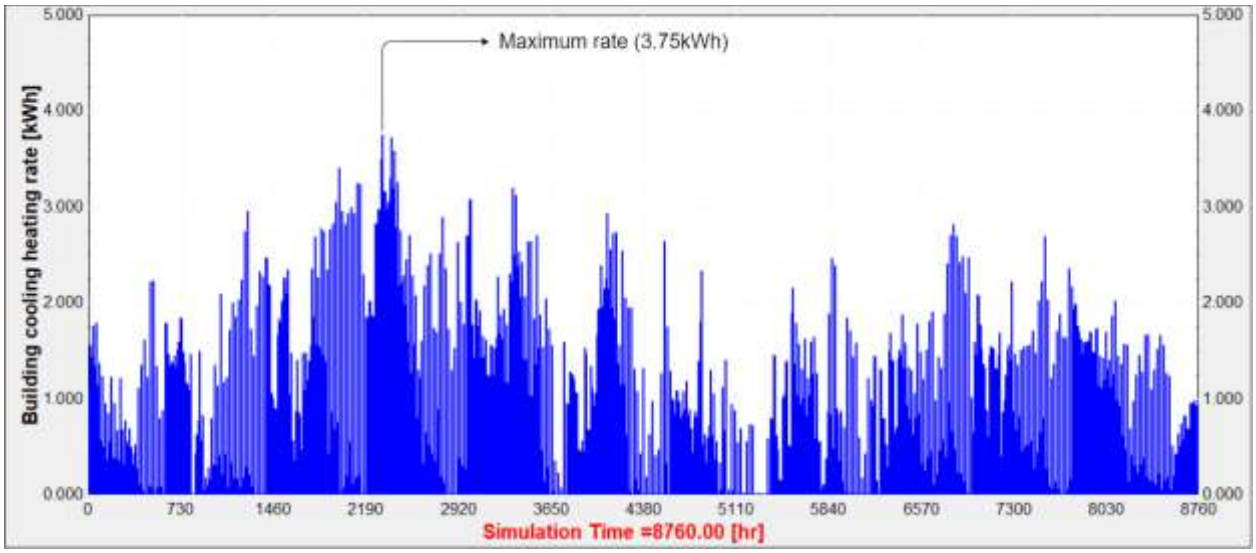


Figure 4.9: Building annual hourly cooling and heating rate

This required power consumption rate of 3.75 kWh per hour is the peak demand that only occurred on 2nd April. Therefore, if heating and cooling is to be done centrally, and the maximum energy demand per hour of 3.75kWh on the 2nd of April must be satisfied, the cooling device must be sized adequately to provide the demand of 3.75kWh. For this study therefore,

the cooling and heating equipment for entire building is sized to a capacity of 4.0kW. A central air conditioning unit of power rating of 4kW is the appropriate size to satisfactory meet cooling requirement even for months with the highest energy demand (2nd April). It is essential not to undersize the HVAC equipment, as doing so will make the equipment cool the zone longer than required. Critical is the fact that grid power for this study is intermittent. Furthermore, if the cooling is not centralised, then the monthly average hourly maximum cooling demand of each zone is the size of the HVAC to be considered.

Table 4.2:Monthly average power and hot water demand of the building

month	Appliance's load (kWh/day)	HVAC load (kWh/day)	Total power (kWh/day)	Total DHW load (kWh/day)
Jan	33.91	10.28	44.19	37.40
Feb	33.91	11.47	45.38	36.67
Mar	33.91	20.87	54.78	36.10
Apr	33.91	22.89	56.80	35.13
May	33.91	21.67	55.58	35.23
Jun	33.91	13.9	47.81	33.58
Jul	33.91	8.03	41.94	33.43
Aug	33.91	6.48	40.39	34.20
Sep	33.91	9.87	43.78	33.01
Oct	33.91	16.65	50.56	35.45
Nov	33.91	14.79	48.70	36.12
Dec	33.91	10.95	44.86	35.50
Annual Average	**33.91**	**13.99**	**47.90**	**35.15**

4.4 System response to energy management and flow control strategies

The dynamic behaviour of renewable energy systems is the system's response to the weather condition, energy management and control strategy. It provides the means of understanding the system characteristic under the different conditions as a check to the appropriateness of the system behaviour compared to the control inputs and strategy. Since weather conditions that determine the performance of solar energy systems vary randomly with time throughout the year, it is important to understand the system behaviour based on the formulated energy management and control strategies under different extreme conditions of the weather. Moreover, as earlier stated in section 3.2, the weather condition of the study area experienced an overcast and cloudy sky for about 83days, and for the rest of the days, the sky was clear with good solar energy level. Therefore, it is important to understand the performance and the implication of the proposed energy management and flow control under extreme weather conditions.

Figure 4.10 is the solar radiation characteristic of typical the overcast day (6^{th} July to 7^{th} July) cloudy day (10^{th} July to 11^{th} July) and sunny day (21^{st} December to 22^{nd} December). These selected days are selected because the performance of the proposed system on gives an idea of the daily performance characteristics on days with extremely poor radiation level, average radiation levels and high radiation level. Importantly, the performance characteristic on days with extremely poor level of solar radiation is an indication of how much auxiliary energy will be required for days with poor amount of sun energy. As seen in Figure 4.10, the sunny and overcast days exhibit extreme high and low solar energy levels compared to the cloudy day. It is essential to quantify the effect of this extreme on the dispatch and cooling flow control strategy. The following subsection explains the influence on the dispatch and cooling flow control strategies.

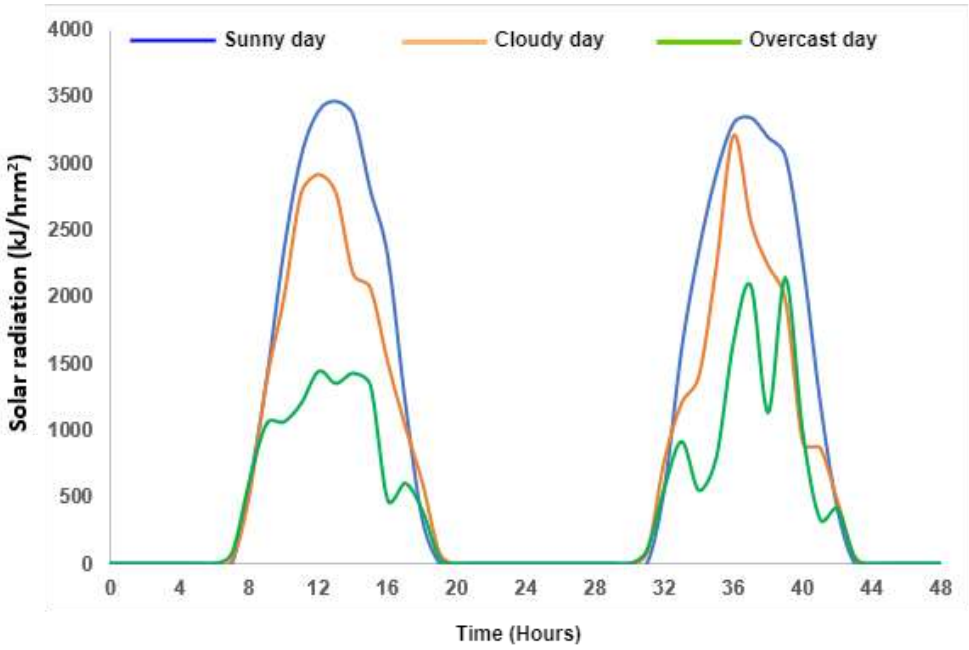


Figure 4.10. Solar radiation of typical sunny, cloudy, and overcast day

Two days with consecutive overcast days and sunny days are deliberately selected to ensure that the observations that will be typical of the weather condition are repeated.

4.4.1 Energy management and operating strategy

The energy management strategy formulated to coordinate the various power elements is designed to allow maximum possible penetration of renewable energy with a minimal injection of conventional energy into the energy mix. Under this strategy, the grid is only dispatched to meet load when energy from the PV is not sufficient. It is relevant to estimate the reliability of this strategy in meeting the electric load under extreme weather conditions, especially since the grid is highly unreliable. Figure 4.11 is the dynamic performance of the system based on an overcast sky in July as stated on page 12. Even though grid power is only available for about 18 hours out of 48 hours, or 37.5% of the time, PV power and stored energy in the battery cover about 67% of total electric demand, and the battery is only discharged to a minimum of about 25% of its full capacity for about one hour, or 2% of the time of its usage in two days, under extremely low average radiation as low as 250 watts. Surprisingly, the battery's fractional state

of charge (FSOC) is kept above 50% for more than 79% of its use. As a result, the battery life is elongated. This result is promising, indicating that even for a period with an extremely poor level of radiation as low as 250W, with just 37.5% of grid power availability, the proposed model can meet up to about 67% of the total electric load, which comprises both power demand for electrical equipment and the auxiliary power for hot water. As a result, even on days when the sky is foggy, the system's size is sufficient to meet electricity demand with low power loss. Again, even for a period where the grid is dispatched to service power demand, power from the grid accounts for only less than 33% of the total power demand for the two days. A relevant conclusion drawn from this result is that even on a day with an overcast sky, the modelled system shows good potential for significant energy saving with a good displacement of conventional energy resulting in a minimum solar fraction of about 67%. A minimum solar fraction of 67% is even far above the minimum acceptable solar fraction of 30% recommended by NREL for reasonable economic performance with a fast payback period [225], [226]. Furthermore, a critical analysis of system reliability reveals that even without a generator backup system, 100% system reliability can be achieved with just 9 hours of grid availability

per day (18% grid availability) and good energy savings of about 67% of the total hot water and power demand of the health centre.

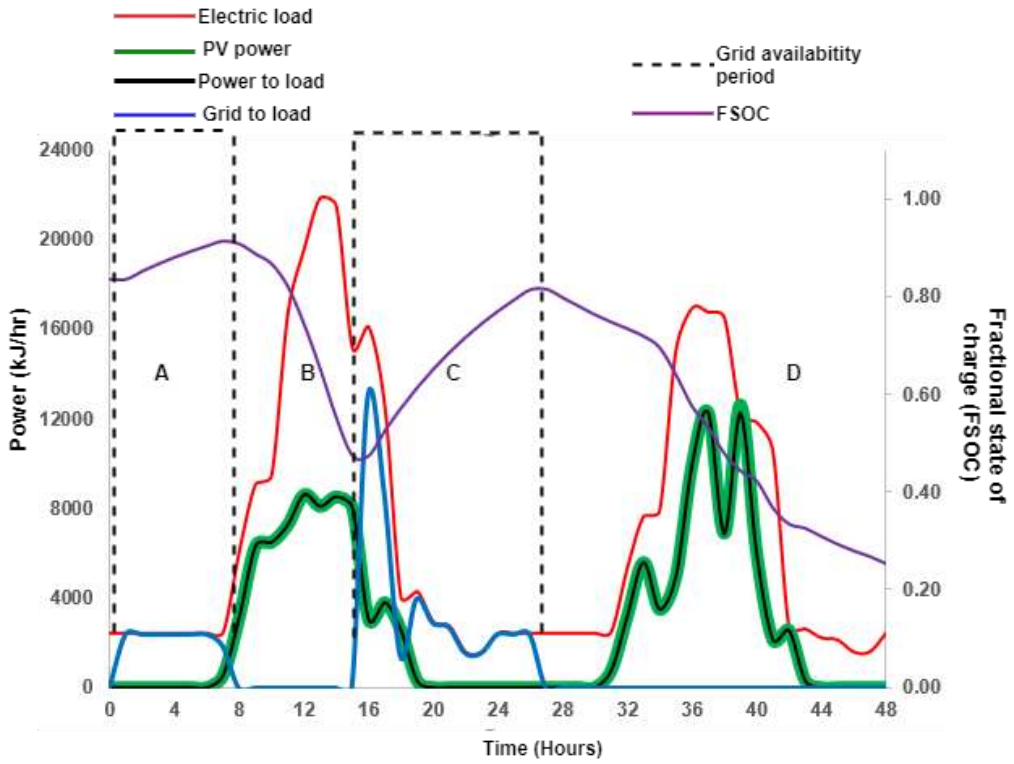


Figure 4.11 Dynamic performance of the system on an overcast day

Further consideration examining the dynamic performance on the 27th of July cloudy day with average solar radiation of about 450 W/m^2 indicates that the proposed energy system has a saving of about 79%, with 66% of the savings contributed from energy from the PV array and 13% is from the energy stored in the battery. This ratio of saving from the battery and battery storage is expected since the PV module is the central power component contributing to the health centre's thermal and electrical power for hot water and power applications, respectively. As seen in Figure 4.12, the grid power is available for just 9 hours in 2 days (48hrs) from 16 hours to 26 hours (evening to the next morning). Because the time when the grid is available does not match the time when demand is high, grid electricity is only used to meet 5% of total

power demand across the two days, and a significant part of the grid is taken to charge the battery. Consequently, the PV plus the stored energy from the battery is used to meet a large portion of the power demand. As a result, the battery's FSOC is maintained at 41% on average, with a low FSOC of less than 30% for the first 18 hours of operation.

Furthermore, analysis reveals that the system has a grid power availability of 9 hours out of 48 hours, reliability of 94%, and a LOLP of 6%. Indicating a 6% higher generator use if the load must be fulfilled compared to a scenario where grid power is available for around 9 hours per day. In conclusion, it is inferred that optimal hours of grid time usage for each day match the system dependability need while also increasing system economic viability.

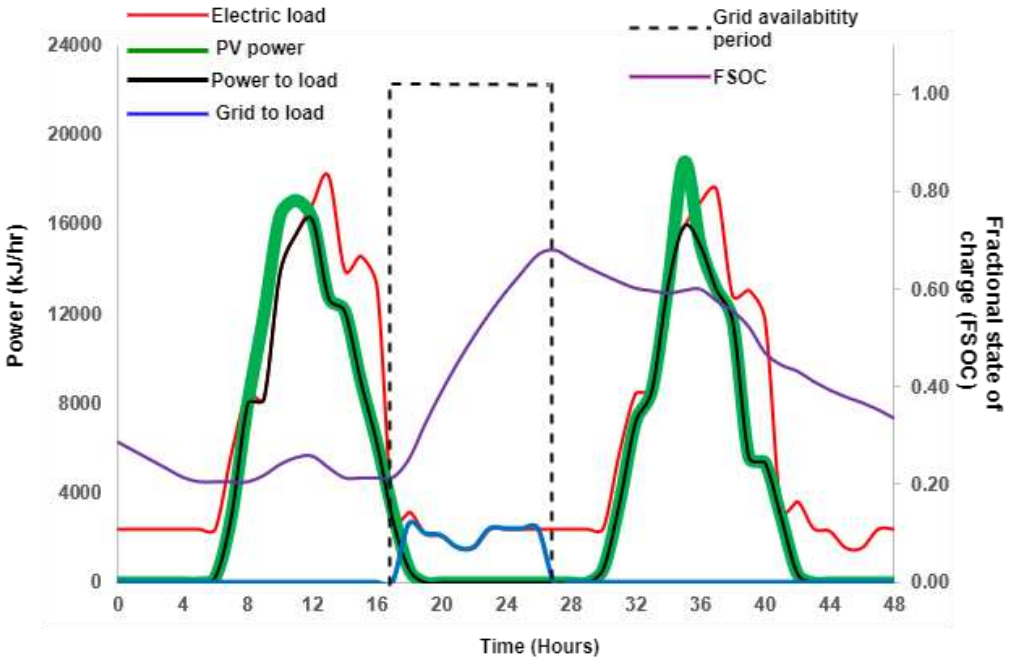


Figure 4.12 Dynamic performance of the system on a cloudy day

Similarly, the dynamic performance on the 24th of December, a day with a clear sky and sunny average daily solar radiation of about 612 W/m^{2,} shows that the grid availability in 48 hours is about 60%. However, it is evident from Figure 4.13 that except for periods where the power demand falls outside solar hours, a substantial portion (82%) of the total load is covered by the

renewable energy sources with the PV accounting for about 74% and battery meeting only 8% of the demand. Again, indicating a sizing method and dispatch strategy that priorities PV power and minimal injection of conventional energy. It is also clear that the strategy only uses grid power in a time where PV power is not adequate to meet both load and battery charging demand, as seen from the blue line in Figure 4.13 in periods where the PV power is more than electric demand (14 to 20hrs on the first day and 27 to 44hrs on the second day). Interestingly grid power usage to meet load only represents about 11% even though the grid's availability is highest compared to the two other days discussed earlier.

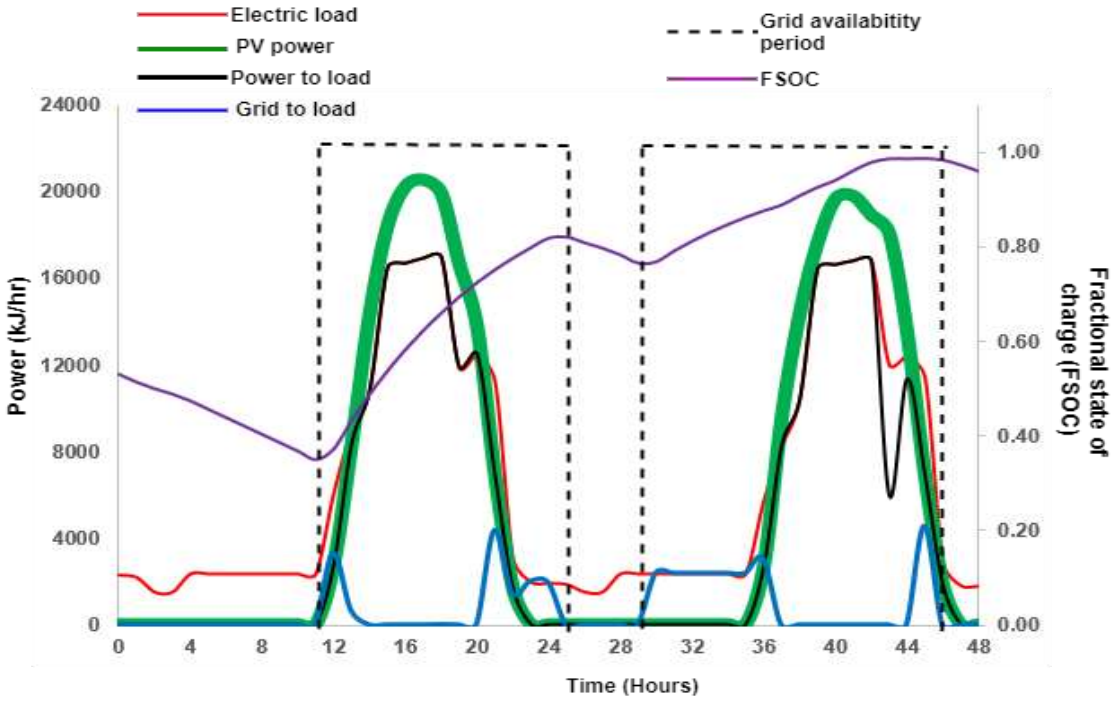


Figure 4.13. Dynamic performance of the system on a sunny day

Again 78% of the time of use of the battery, the battery FSOC is above 60%. Suggesting that weather with a good number of sunny days, the need to increase battery storage is not as demanding as in cloudy, and the benefit of stability is seen in this case. The further evaluation shows that the excess power produced from the PV is 2.2% of the total power demand. Again, this indicates that the size of the collector is appropriately sized to minimise excess power

generated since excess power has no benefit for this scenario because of the No-Feed-Back, a scenario associated with the study area.

4.4.2 Cooling method and flow control strategy

Apart from effective energy management, which ensures that the PV's power output is effectively used to boost the renewable energy penetration in meeting total power demand, it is also highly desirable in this research to improve the system's energy output to increase its economic viability, particularly in the health centres. As a result, a new system configuration and PV module cooling strategy were created. The cooling method and system configuration cool the PV for better power output while ensuring that the system's thermal energy output quality and quantity are both increased. The implication of this new approach on the power and thermal characteristics on days with overcast, cloudy and sunny days is presented and discussed in this subsection. Figure 4.14 is the dynamic response of the cooling pump to the developed flow control strategy on an overcast day, cloudy day and sunny day and the illustration of the domestic hot water load-sharing technique developed to boost thermal energy harvesting and PV power production. In health centres, the demand for hot water varies from a low-temperature demand of 45-55oC for dishwashing, bathing, and laundry. Hot water temperature may be desired for sterilisation above 80oC. Producing temperatures as high as 90oC with the PVT may decrease its power production. Therefore, a new technique to increase thermal system output with minimal loss in power is created, as illustrated in Figure 4.14. Under this method, the cooling water from the collector (Figure 4.14a) is diverted at the flow rate required to meet the thermal demand for postnatal services at 50oC (Figure 4.14b) and the excess water from the collector is diverted at a flow rate equal to hot water demand for laundry and sterilisation as shown in (Figure 4.14c) to be reheated by the evacuated tube collector as already explained in chapter 3. The cooling pump operation and control are such that the cooling water will exit at a temperature close to that required for postnatal application. As seen from Figure 4.14a, the

cooling water pump is operated at a higher rate than on days with overcast or cloudy days for days with high solar energy.

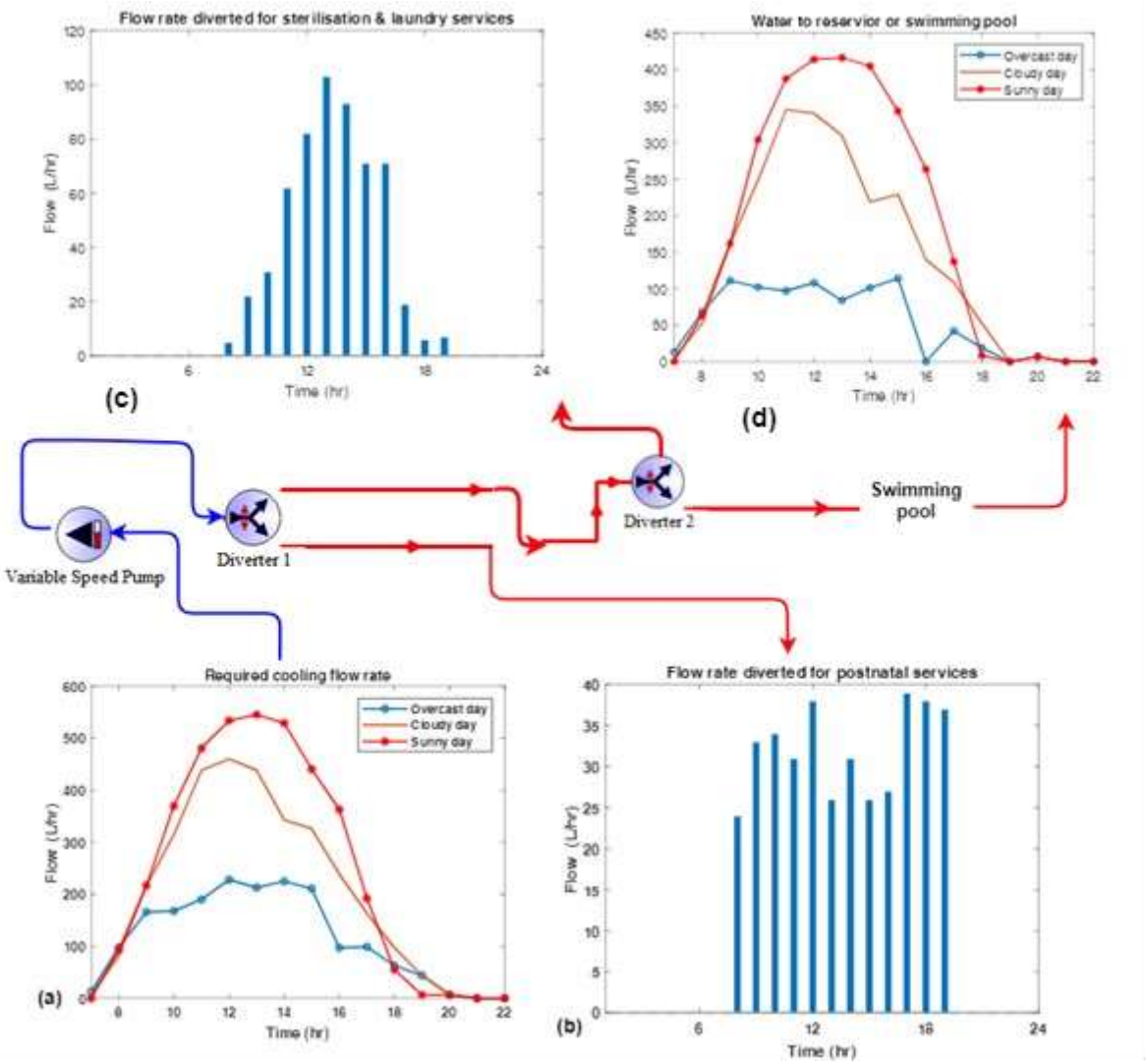


Figure 4.14. Dynamic flow characteristics based on the proposed strategy

This higher flow rate on days with a higher level of solar energy is explained by the fact that on a day with a high level of solar energy, the amount of heat trapped in the collector is higher since the solar cell can only convert less than 30% of the incident solar energy on the collector. As a result, a higher flow rate is required to extract the trapped heat to keep the collector exit water temperature at about 50oC. On the other hand, on days with clouds or an overcast sky, the cooling water flow rate is lower since the level of solar radiation is lower; as such, the

trapped heat is lower; hence the pump is operated at a lower flow rate. This type of pump operation strategy has the benefit of reducing the power consumed by the pump on days with cloudy or overcast sky conditions since the power consumed by the pump is a function of the flow rate. On the other side, on days with a high level of irradiance, the pump consumes a higher amount of electric power to circulate the cooling water at a rate required to maintain the collector temperature at a maximum of 60oC and to keep the PVT cooling fluid outlet temperature to about 50oC as desired in this study. Besides, it is worth noting that this approach may be detrimental if the flow rate required to keep the PVT module at the desired maximum temperature may eventually result to lower net PV power due to the high power demand for running the pump, as seen in Figure 4.15. As seen from this figure, a flow rate beyond 642L/hr will rather decrease the network than increase it. This reduction is due to the PV module's low sensitivity to the circulating water's cooling impact; as a result, the rise in electrical efficiency is sluggish, and as the pump's power increases with the increase in the flow rate, the power demand for the pump finally outweighs the increase in the PV power.

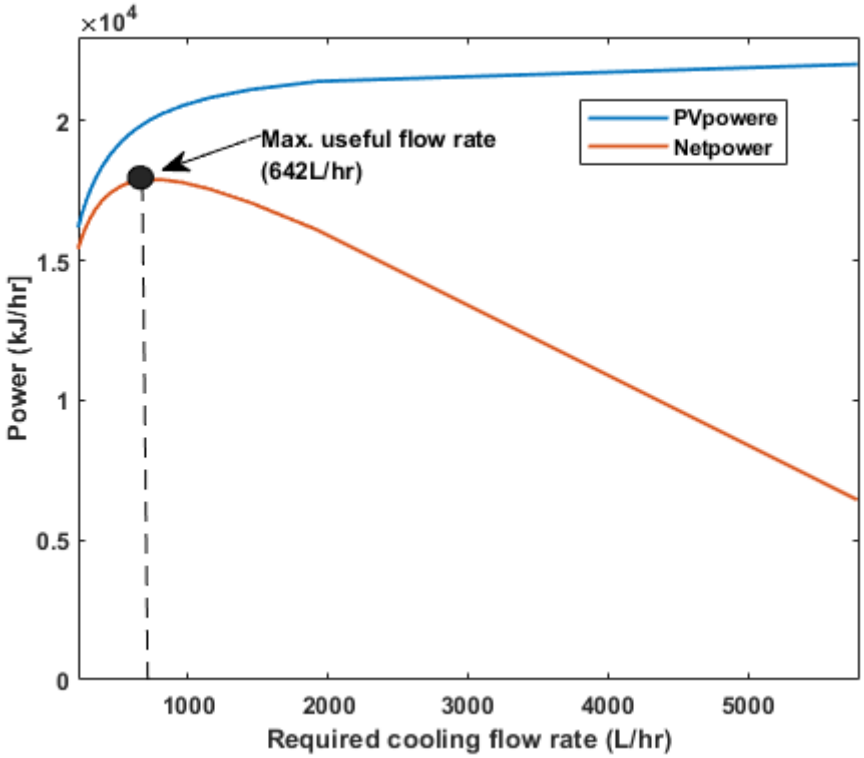


Figure 4.15 Effect of pump flow rate on the net PV power produced

As a result, the net power starts to drop once the flow rate reaches 642L/hr. It, therefore, means that for the desire to meet hot water demand for postnatal services from the hot water from the PVT collector outlet, as illustrated in Figure 4.14, the choice of keeping the outlet collector water temperature at 50oC was a careful choice to meet thermal for postnatal hot water services with minimal 0.98% trade-off in PV power as seen in Figure 4.16.

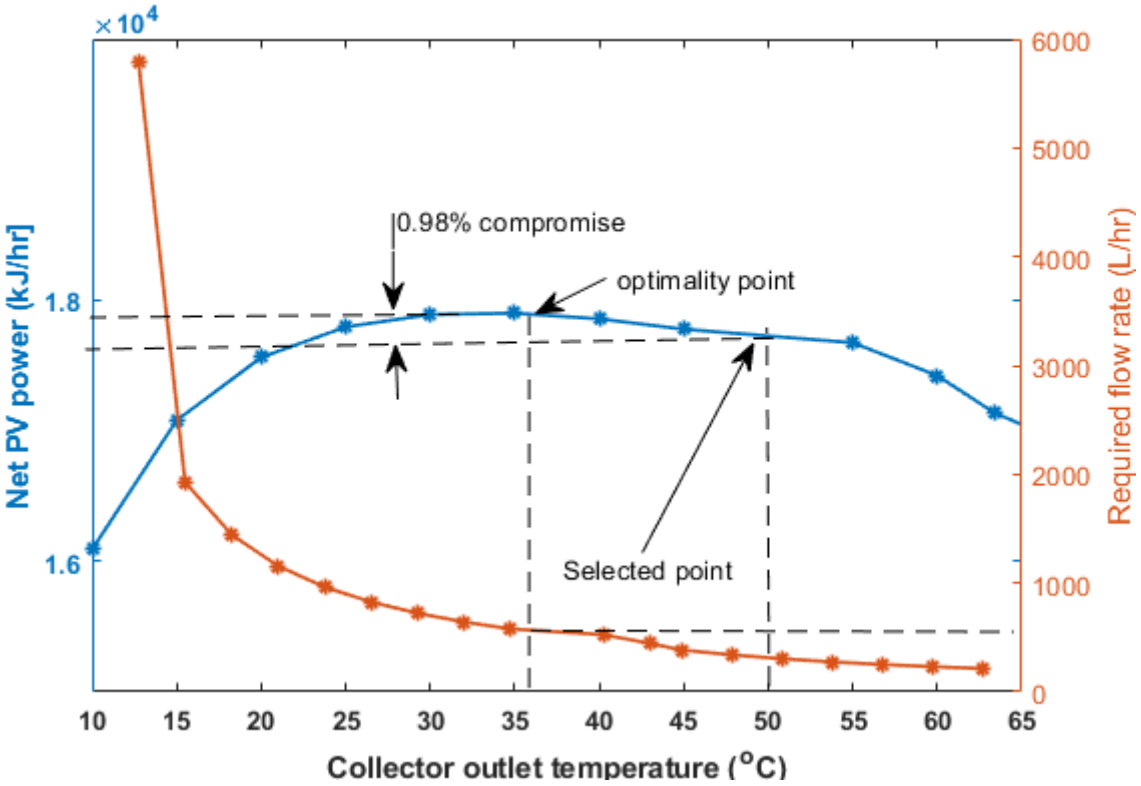


Figure 4.16. Effect of collector outlet temperature on net power of the PV module

4.4.3 Delivered hot water temperature characteristic

The temperature of the delivered hot water from the thermal power element is a measure and indicator of the effectiveness of the proposed system configuration and flow control strategy in meeting the thermal energy demand of the health centre. The tank outlet temperature is an indication that the demand for hot water is met at the desired temperature, or it will require additional energy to raise its thermal energy to the desired energy level and quality. Figure 4.17 and Figure 4.18 show the temperature of the delivered hot water on typical overcast, cloudy and sunny days for the three applications relative to the desired temperatures for the three different applications within the hours of demand from 7.00hrs to 22.00hrs. On an overcast day, the hourly average daily hot water temperature delivered for postnatal services is around 8.4^{o}C lower than the desired temperature of 50^{o}C. They provided hot water for laundry and

sterilisation have a higher hourly average daily hot water temperature difference of 10.4^{o}C and 24.5^{o}C, respectively.

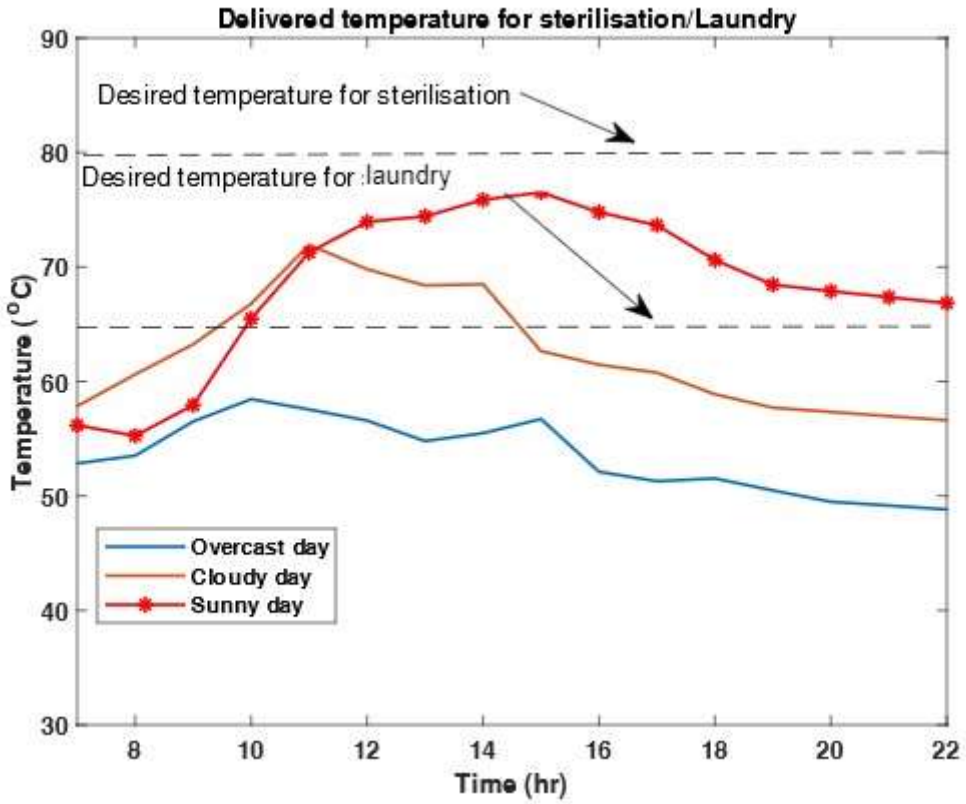


Figure 4.17. Temperature variation of sterilising and laundry hot water

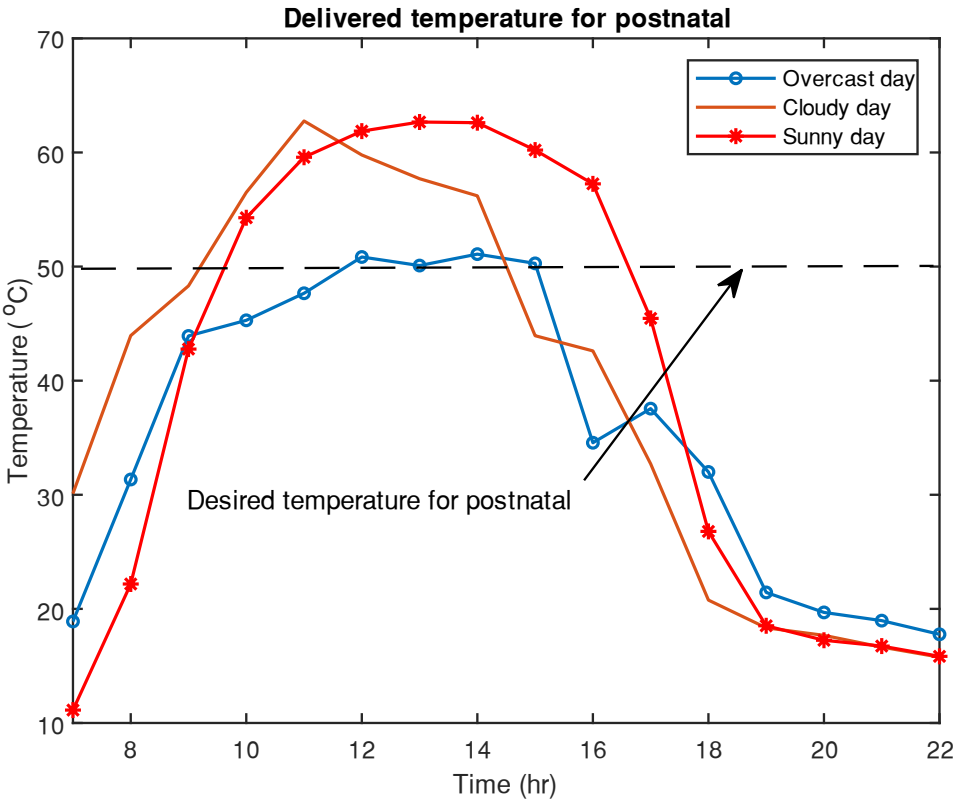


Figure 4.18. Temperature variation of the DHW delivered for postnatal

This bigger temperature differential for laundry and sterilising is due to a lack of accessible solar energy on days with low irradiance to satisfy the targeted hot water temperatures of 65°C and 80°C for washing and sterilisation. The gap in delivered hot water temperature means that additional energy from the conventional sources will be required to raise the temperatures of the service hot water to specified points for these uses, as seen in Table 4.4. For postnatal services, hot water temperature is desired at 50°C; the auxiliary energy demand to fulfil the 8.4°C temperature difference is about 34% of the total daily energy demand for postnatal services. By this, it means that about 66% of the total hot water demand at the desired temperature of 50°C is supplied for postnatal services from the solar system even with a poor level of solar radiation of less than 300W/m^2 on this day. An energy savings of about 66% is adequate for quick payback and good return on investment (ROI). This result suggests the suitability of this system for low-temperature applications, even in locations with a significant

part of the year with an overcast sky. Furthermore, as the sky condition improves, as seen in Table 4.3, for a cloudy and sunny day, the average temperature difference is reduced to 3.6°C for cloudy and 5.6°C for a sunny day. Interestingly, the cloudy day with average daily solar irradiance of 450W/m^2 shows a lesser gap between the desired temperature and the delivered temperature than the sunny day with average irradiance of about 650W/m^2.

Table 4.3. Hot water load and temperature difference between demand and supply

Weather condition	Q_p (kJ/hr)	Q_L (kJ/hr)	Q_S (kJ/hr)	ΔT_p (°C)	ΔT_L (°C)	ΔT_S (°C)
Overcast	2802	4145	6055	8.4	10.4	24.50
Cloudy	2788	4132	6041	3.6	0.9	10.76
Sunny	3185	4480	6403	5.6	1.7	16.43

where;

$\boldsymbol{Q_p}$ is the hourly average daily demand for postnatal

$\boldsymbol{Q_L}$ is the hourly average daily demand for Laundry

$\boldsymbol{Q_S}$ is the hourly average daily demand for sterilisation

$\Delta \boldsymbol{T_p} = \boldsymbol{max}\left((\boldsymbol{T_D} - \boldsymbol{T_p}), \boldsymbol{0}\right)$ is the average temperature gap between the supplied and desired temperature for postnatal

$\Delta \boldsymbol{T_L} = \boldsymbol{max}\left((\boldsymbol{T_D} - \boldsymbol{T_L}), \boldsymbol{0}\right)$ is the average temperature gap between the supplied and desired temperature for laundry

$\Delta \boldsymbol{T_S} = \boldsymbol{max}\left((\boldsymbol{T_D} - \boldsymbol{T_S}), \boldsymbol{0}\right)$ is the average temperature gap between the supplied and desired temperature for sterilisation

This observation can be explained by the fact that the selected cloudy day is in July and the typical sunny day is in December. As seen from the monthly average daily mains water variation in Figure 4.19, the monthly average daily mains water temperature in July is 28.25°C

which is about 3ºC higher in temperature than the mains water temperature of 25.25ºC in December.

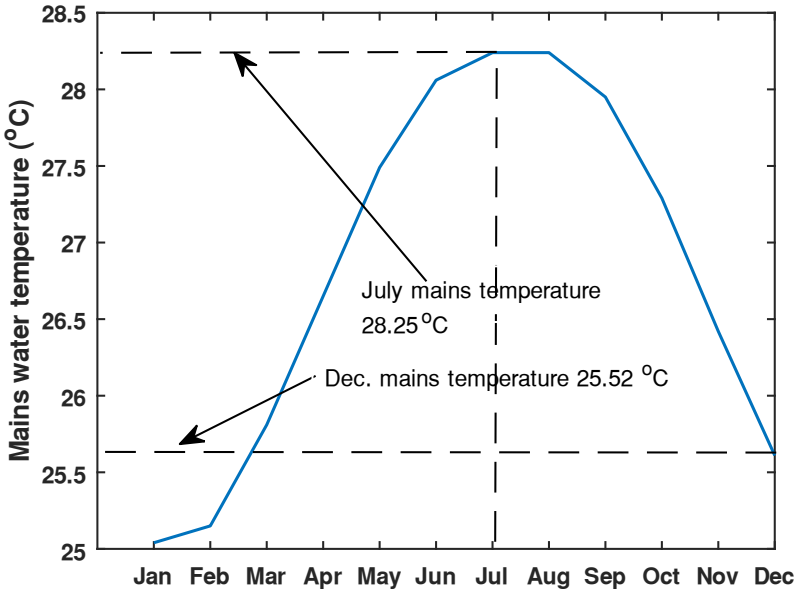


Figure 4.19. Monthly average mains water temperature variation

These figures (Figure 4.17 and Figure 4.18) indicate that the mains water temperature used to cool the PVT collector will exit the collector at a higher temperature, particularly in the morning when radiation is lower in July and December. However, as the difference in irradiance between cloudy (July) and sunny days (December) increases towards the afternoon period, the collector water exit temperature for sunny days is now higher than that for cloudy days (July), as shown in Figure 4.18. A similar observation is seen in Figure 4.17 for hot water temperature for laundry and sterilisation on a cloudy and sunny day. Overall, the temperature difference between the targeted and delivered temperatures for all three applications on a cloudy day (July) is lower than that on a sunny day (December). Consequently, the thermal auxiliary energy demand is lowered for all hot water applications in July (cloudy day) than in December (sunny day), as seen in both. Another factor that explains the observation is the fact that in December for this location, the sky is dusty and therefore, the diffuse part of the total

radiation in December (cloudy day) is high and therefore, the thermal performance of the collector is reduced since flat plate performance is better with the beam component of the radiation. It is concluded from this result that the thermal performance of solar hot water system is improved in months with higher mains water temperature. This improvement is because the energy required to increase the water thermal energy will be smaller than the energy required to increase the temperature of the same mains water with a lower temperature. On the other hand, the PV module temperature will be higher for days with higher mains water temperature, as seen from the PV temperature in the early hours in Figure 4.20.

Since hot water demand for laundry and sterilisation is required at 65 and 80^{o}C, respectively, the demand for both services is supplied from a hot water storage tank in the ETC reheating circuit. This approach is conceived to prevent an increase in the temperature of the PV module. Because the supply for both services comes from the same source, the hot water for the laundry and sterilisation is delivered at the same temperature even though they are required at a different temperature, as seen in Figure 4.17. Furthermore, for high-temperature hot water demand like hot water demand for sterilisation desired at 80^{o}C, as seen from Figure 4.17, the temperature gap between the hourly average daily hot water temperature supply is 16^{o}C even on the sunny day. The biggest shortfall in temperature of hot water demand for sterilisation is seen on days with overcast sky conditions. This result shows that about an average of 32% of the average total daily demand for hot water for sterilisation is supplied from the grid or diesel.

Table 4.4 Hot water auxiliary energy demand based on the weather condition

Weather condition	$Qaux_P$ (kJ/hr)	$Qaux_L$ (kJ/hr)	$Qaux_S$ (kJ/hr)	$\left(\frac{Qaux_P}{Q_{load}}\right)$ (%)	$\left(\frac{Qaux_L}{Q_{load}}\right)$ (%)	$\left(\frac{Qaux_S}{Q_{load}}\right)$ (%)
Overcast	1081	1095	2845	34	28	47
Cloudy	444	21	1176	16	3	21
Sunny	719	299	1975	22	4	30

Where;

$Qaux_P$ is the hourly average daily auxiliary for postnatal

$Qaux_L$ is the hourly average daily auxiliary for laundry

$Qaux_S$ is the hourly average daily auxiliary for sterilisation

$\left(\frac{Qaux_P}{Q_{load}}\right)$ is the auxiliary energy for postnatal as a percentage of the average load

$\left(\frac{Qaux_L}{Q_{load}}\right)$ is the auxiliary energy for laundry as a percentage of the average load

$\left(\frac{Qaux_S}{Q_{load}}\right)$ is the auxiliary energy for sterilisation as a percentage of the average load

An indication that the proposed cooling control strategy is delivering the desired objective of limiting the maximum temperature of the PV module to about 60^{o}C is seen in the variation of the PV module temperature, as observed in Figure 4.20. As observed in Figure 4.20, the maximum temperature of the PV module, even on a sunny day, is about 60^{o}C. The target here is to improve power production of the PV module by preventing temperature rise on sunny days yet achieving the desired hot water temperature for postnatal services using the PVT collector. On an overcast day, the solar radiation falling on the PV module is not adequate to cause a temperature rise; as such, the PV module temperature is below the maximum allowable temperature rise in this study. One benefit is the saving in pump power consumption as in

strategy; the flow rate is adjusted based on the level of solar energy to deliver hot water to a maximum temperature of 50^{o}C.

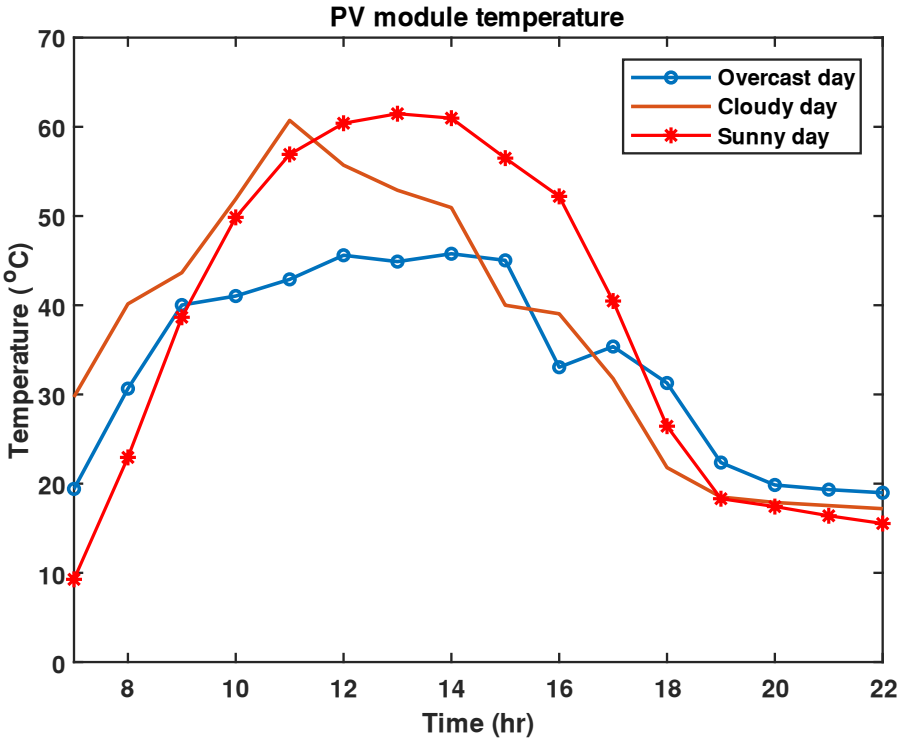


Figure 4.20. Variation of PV module temperature

Therefore, the proposed system configuration, energy management, and cooling strategy interaction are desired in this study, as evidenced by the dynamic features of the system as stated in the results above. Surprisingly, the result demonstrates good potential, as the thermal element of the system saves roughly 60% of energy even on overcast days. For this study location, the sky is clear for a large part of the year, around 278 days, with average daily radiation of above 450 W/m^2 for a minimum of 7 sunny hours [227]. This implies that the system holds good potential in the long run.

4.5 Optimal system sizing and parameters determination

The choice of the appropriate component size and design parameters contributes significantly to improving the system's power and thermal energy production. For this study and system, one important parameter in improving power and thermal energy utilisation is the water flow rate and hot water storage tank size. Other important in meeting the desired power and hot water with good reliability in the most economical and environmentally friendly way is the collector size and the number of the battery. The subsection shows the results and how each parameter and component size is determined.

4.5.1 Optimal system flow rate and pump selection

The flow rate of the circulating cooling water conveyed by the water pumps is crucial to improving the net energy harvesting for this system. Since the appropriate flow rate depends on the load scenario and weather conditions, it was important to find the flow for which the harvested thermal energy will be improved. The choice of the pump will now be based on the desired flow rate. Therefore, a parametric study was conducted based on the case study load profile under the actual weather condition of the study location to find the optimal flow rate. In this study, the effect of the flow rate on the solar fraction is investigated to determine the flow rate required to give optimal solar fraction based on the load and weather scenario of the study health centre. Figure 4.21 is the variation of the solar system fraction under different pump flow rates for the ETC closed loop. The result obtained shows that the highest solar fraction is obtained at a flow rate of about 160L/hr. As the flow rate increases, the system thermal solar fraction also increases, reaching a maximum value of 0.883 at a flow rate of 160L/hr.

Beyond a flow rate of 160L/hr, the solar fraction is observed to decrease at a slow rate. Therefore, for this configuration and load profile of the study case, the optimal water flow rate

required for optimal delivery of hot water for sterilisation and laundry services by the evacuated tube collector circuit is 160L/hr. Therefore, the solar pump with a 160L/hr rated flow rate is selected for the ETC loop. The pump in the ETC loop is operated at a constant flow rate of 160L/hr when solar radiation is available. On the other hand, the selected pump for circulating the water required for cooling the PV module is a variable speed pump with a maximum flow rate of 600L/hr selected based on the simulated flow rate that is required to maintain a PV temperature of about 60^{o}C even in month with highest solar energy.

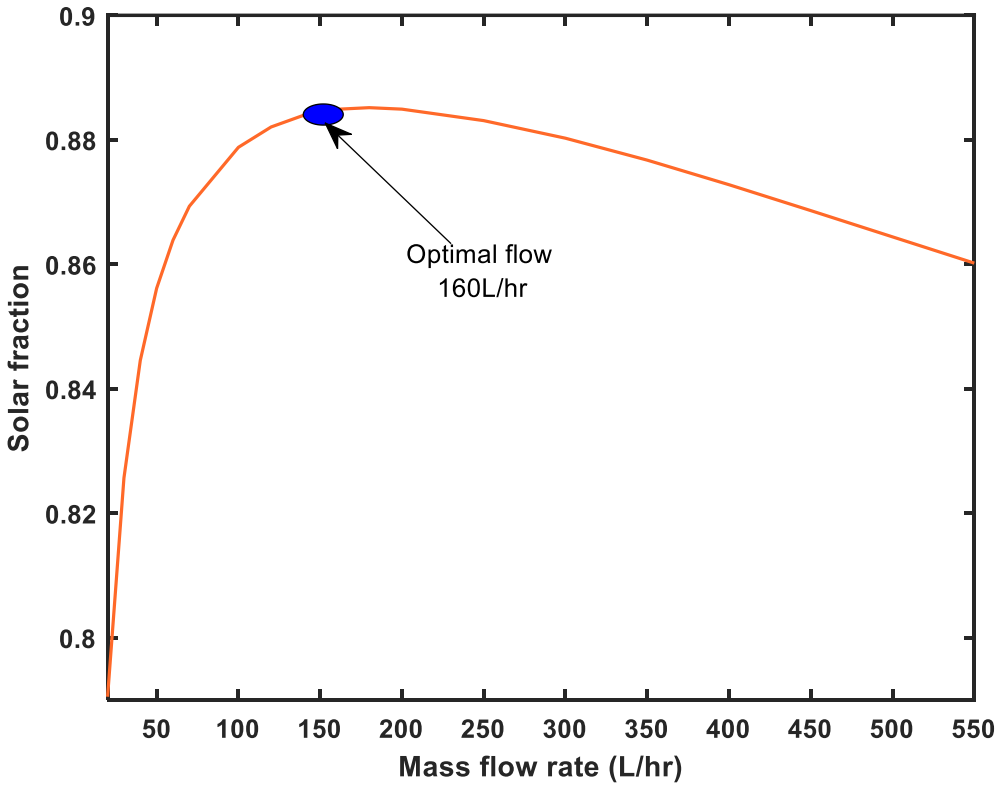


Figure 4.21: Effect of flow rate on the system thermal solar fraction

4.5.2 Determination of the number of PVT collector

The size of the PVT collector is an important design parameter that must be carefully sized if the goals of reliability and economic viability are to be met. Because this study aims to meet both thermal and electrical demand with the highest possible penetration of renewable energy,

the size of the PVT considered satisfactory is that which meets total energy demand while saving money. It is useful to determine the appropriate number of each component that reliably meets load at the lowest possible cost to increase system viability. The variation of the solar system fraction with the total life cycle cost (TLCC) and the number of PVT collectors is shown in Figure 4.22. It is seen that the solar fraction increases while the total life cycle cost decreases for every unit addition of the PVT collector in the system. It is equally seen from the graph that the solar fraction is maximum, and the TLCC is minimum when the number of PVT collectors reaches 33. When the PVT collector is more than 33, the solar fraction is observed to remain constant while the TLCC starts to increase. This trend can be explained; thus, with the increase in the number of PVT in the system, the additional PV power is used to meet the load, and the savings are equally increased. However, a point is reached where the additional power from the additional unit of PVT collector is only dumped. The power is dumped because the load is completely met, or the additional power does not match the load. This way, the cost of the system continues to rise with additional units of the PVT collectors with no corresponding savings since the power generated is dumped. The coordinate of the point where the TLCC curve changes direction is the appropriate size of the PVT collector required to meet load efficiently and economically. The sizing method used in this study is focused on minimising the production of excess electrical power and domestic hot water to the greatest extent possible because excess power generation in the scenario of interest is a waist since is not fed back into the grid for any compensation. In this study, if the number of the PVT is more than 33, the additional energy produced by the PVT has no use since the excess power is not fed back to the grid, and therefore the system viability will be compromised.

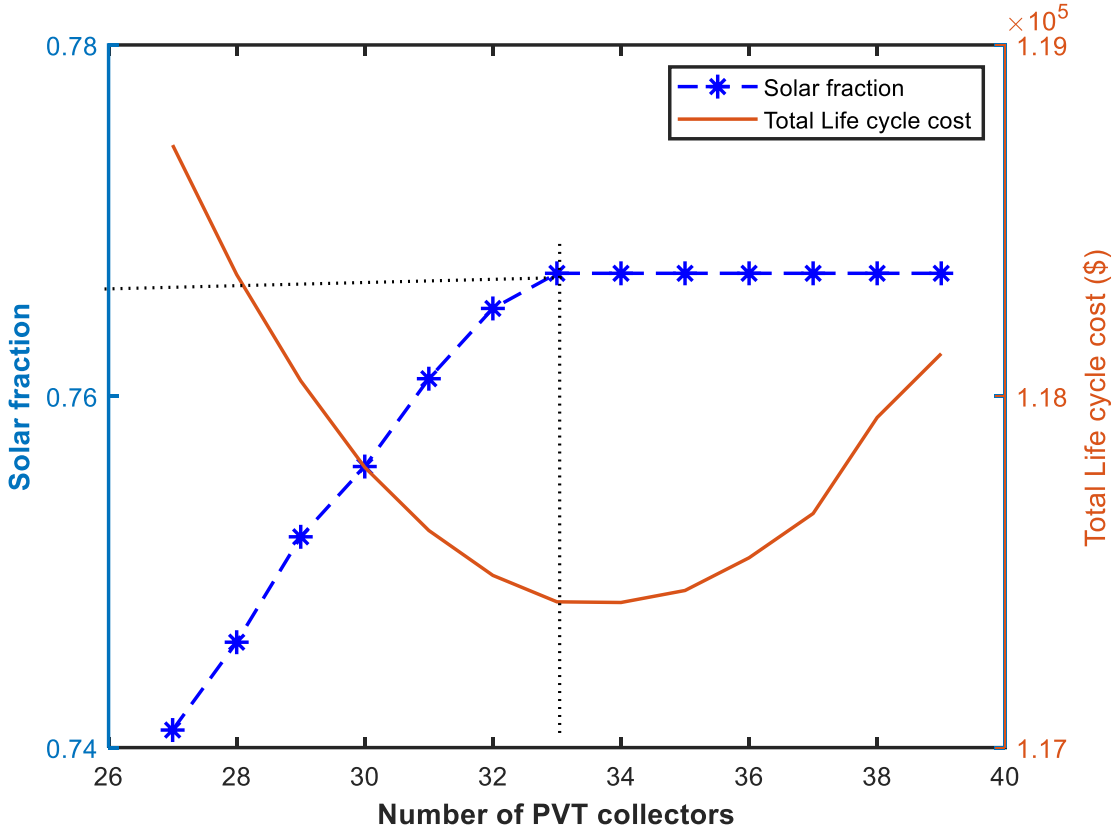


Figure 4.22:Effect of the number PVT on TLCC and solar fraction

4.5.3 Sizing the hot water tanks

The volume of the hot water storage tank is one of the factors that determine the heat loss of the water stored in the tank and hence the amount of energy required to raise the water temperature to the desired temperature. Poor hot water storage results from poorly sized tanks resulting in a high loss coefficient and hence the tank's energy loss. Figure 4.23 depicts the relationship between tank volume and thermal energy of the water for both the sterilisation and postnatal tanks. The thermal energy of the water in the storage tank is sensitive to the change in tank volume. For the postnatal water tank, the hot water thermal energy is a maximum volume of 0.7m^3. Therefore, the selected volume for the postnatal tank is 0.7m^3.

Similarly, from the graph, the appropriate tank volume for sterilisation and laundry services is 0.3 m^3. A critical observation shows that the required tank volume for sterilisation and laundry

services is smaller than the volume required for the postnatal purpose, even though the hot water quantity (0.571m^3 /day) needed for sterilisation and laundry services is higher than that required for postnatal services (0.427m^3 /day). Since the load profiles (see Figure 3.15) for sterilisation and laundry services are centred around solar noon, a critical deduction that can be drawn from the results obtained in this analysis is that the required hot water tank volume for hot water demand is centred around solar noon should be less than the total hot water demand per day. Likewise, for the hot water demand profile with peaks in the morning and evening, the volume of the hot water tank should be slightly higher than the volume of total hot water demand per day. Increasing or decreasing the size of the tank will lead to a loss in the thermal energy of the hot water, as seen in Figure 4.23.

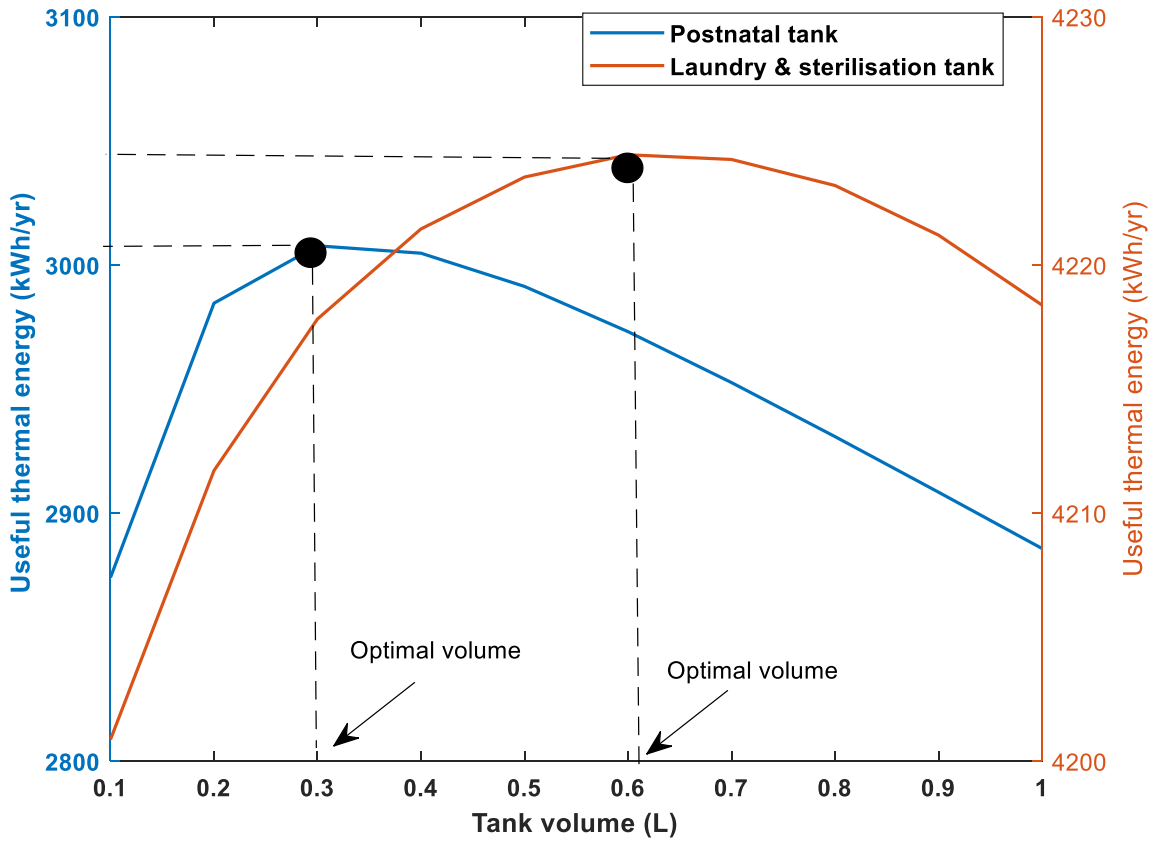


Figure 4.23. Effect of tank volume on tank delivered useful energy

Overall, the interacting visual interface of TRNSY software and its open-endedness allows for the measurement of system output based on any selected system size against load demand at any time step, even for an entire year. As a result, the final system size is determined through iterative simulation and gauging the size against the load distribution until the appropriate size that meet the load with satisfactory with the least excess power product is found.

4.6 Comparison of the basic PVT and the OPVETC hybrid energy system

Weather data, which is a driving function for solar energy systems, varies greatly with time and season of the year. As a result, it is critical to compare and comprehend the dynamic behaviour of the proposed OPVETC with the basic hybrid PVT on both the hourly average and the monthly and annual on days with extreme weather condition of overcast and Sunny days as already justified in section 4.4. The hourly dynamic simulation is tailored at exposing the factor that significantly influence the overall energetic performance of both the OPVETC and the basic PVT hybrid energy system. The characteristic of irradiation of a typically sunny and overcast day 20th April and 8th August of the study location (Jos, Nigeria) is depicted in Figure 4.24. The performance of both the basic hybrid PVT and the OPVETC these days with extreme weather condition serves the purpose of estimating the effectiveness of the cooling control strategy on both systems.

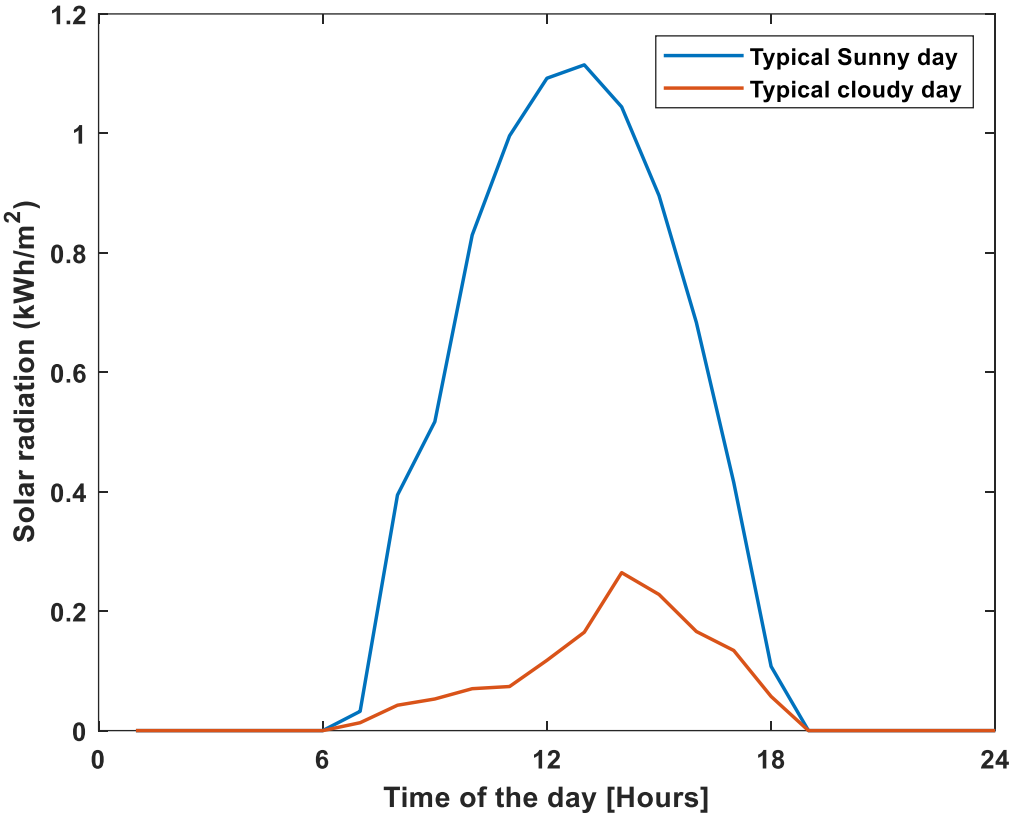


Figure 4.24: Solar irradiation for a typically sunny and cloudy day in April and August

4.6.1 PV power production and pump power consumption

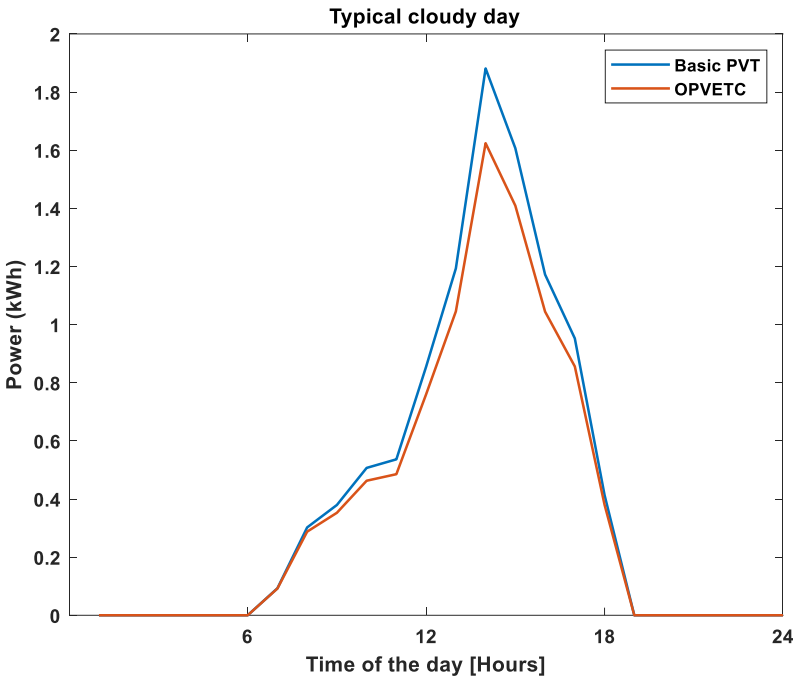
The advantage of the hybrid PVT collector over the uncooled PV module is the dual and simultaneous production of both power and thermal energy. However, for substantial improvement in power production, the cooling strategy must be appropriate for any collector module. Therefore, it will be more beneficial where the thermal output is improved without compromising the power output. Figure 4.25 compares the power output of the hybrid energy system based on the traditional system configuration and the proposed system architecture. It is seen that on sunny days, the power production of the OPVETC is significantly higher than that of the basic PVT system architecture. It is also seen that on days with poor solar radiation (cloudy days), the difference in the cooling method in both the basic PVT and OPVETC shows no considerable influence on power production. The power output of the two systems on cloudy

days is almost identical. This observation can be explained by the fact that on days with a high level of solar energy, the heat trapped in the collector is high, and since the cooling water in the conventional hybrid configuration is conveyed and circulated in a closed-loop, the water in the water tank eventually mixes up, and the stratification is destroyed. Therefore, the water in the tank is uniformly hotter since the top of the tank and the bottom has an equal temperature. Hence, the heat extraction from the absorber when water is passed underneath the collector is now reduced.

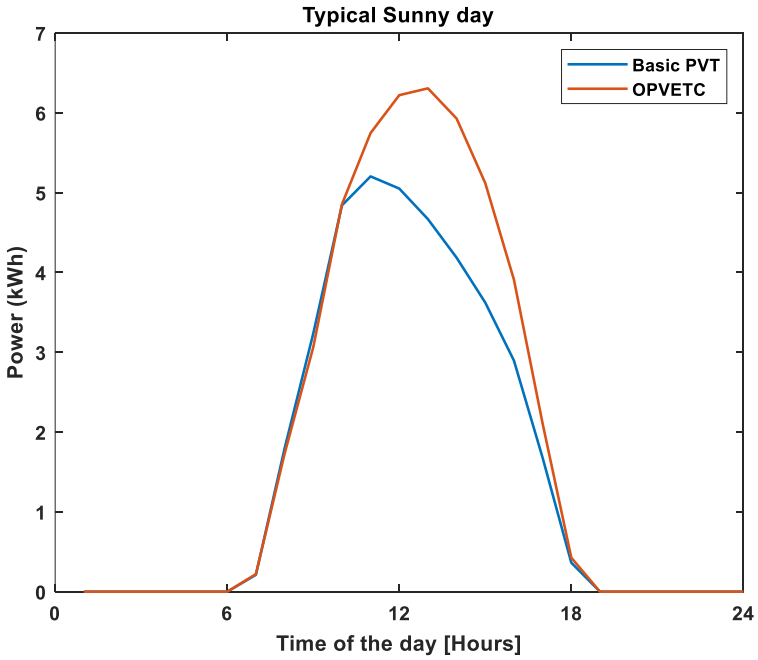
On the other hand, the power output of the proposed system is higher first because the control is set to increase the flow rate of the cooling water to match the flow required to adequately extract the trapped heat in the collector. Secondly, the cooling water is not recirculated and hence the cooling heat removal factor is higher than the conventional system configuration. Since the proposed flow control of the OPVETC is modelled to operate the pump to discharge cooling water at a flow rate just sufficient to cool the module temperature to about $60^{o}C$, the pump consumes lower power on cloudy days than the basic flow control as seen in Figure 4.26. Even though the pump's power consumption for the proposed flow control consumes higher power on days with a high level of solar radiation, the benefit is that the power production is substantially, and the higher pump power consumption is negligible compared to the improved power.

On the other hand, the basic flow control cools the PV module at a $72L/hrm^2$ constant flow rate within hours of available solar radiation. For this cooling method, even on days with low solar irradiance, the pump continues to consume the same amount of power aa seen in Figure 4.26 since the pump power depends on flow rate and operation time. Notably, the power output of the conventional system configuration is slightly higher than that of the proposed OPVETC system on a typical day with a cloudy sky as observed in Figure 4.25. This observation shows

that the proposed cooling strategy moderates the cooling water for the cooling of the PV module such that the cooling water leaves the PVT collector at a higher temperature of about 50^{o}C as desired in this study to meet the temperature for postnatal services. It means that for days with a low level of solar energy, the flow rate of the cooling water pump operated based on the proposed strategy is less than 72L/hr.m^{2,} and therefore the power production is compromised. As a result, the heat needed to be extracted from the PV module was not completely removed, and therefore, a drop in power was observed. However, the adjustment to a low flow rate as proposed is required to boost the thermal production of the collector to ensure that the demand for hot water is improved,

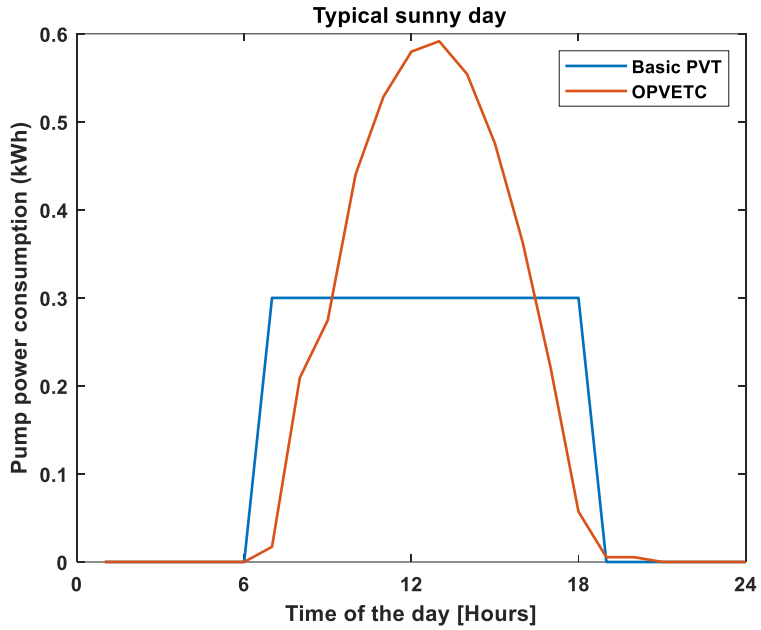


(a)

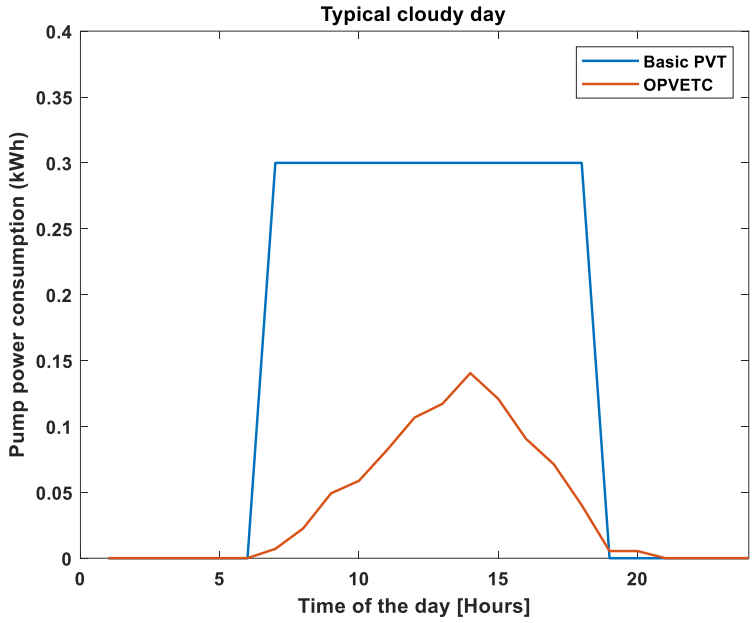


(b)

Figure 4.25: Comparison of the PV module power output



(a)



(b)

Figure 4.26: Comparison of the pump power consumption

On the other hand, since the basic flow control sets the cooling flow rate at a constant flow rate, its power production will not be compromised on a day with a low level of solar energy as seen on a cloudy day, but the thermal production of the collector will be traded-off with a low-grade temperature that may require more energy to upgrade to the desired temperature for

postnatal services. Even though the basic PVT cooling technique was observed to cool the PV module better, resulting in higher power output on days with an overcast sky as observed in Figure 4.25, a stark contrast is observed even in months with poor levels of solar energy from June to August as seen in Figure 4.27. As seen, for these months, the monthly average daily power output of the OPVETC system configuration is higher than that of the basic PVT, even in months with low radiation. It implies that if the number of days with an overcast sky is fewer than cloudy days and sunny days in the month, the OPVETC hybrid energy system outperforms the basic PVT energy system configuration in power production in all the months. One advantage of the proposed OPVETC hybrid architecture over the simple basic PVT hybrid architecture is its capacity for higher power production in months with high solar irradiance with equally good thermal output. The higher performance (both power and thermal) in months with good solar energy is because the cooling flow control will moderate the flow rate such that the cooling water is adequate for higher power production, and the cooling water exiting the PVT collector exits at a higher temperature, and this flow rate is adequate to reduce the thermal demand and raise the temperature to the desired temperature for the postnatal application desired at temperatures of 50^{o}C.

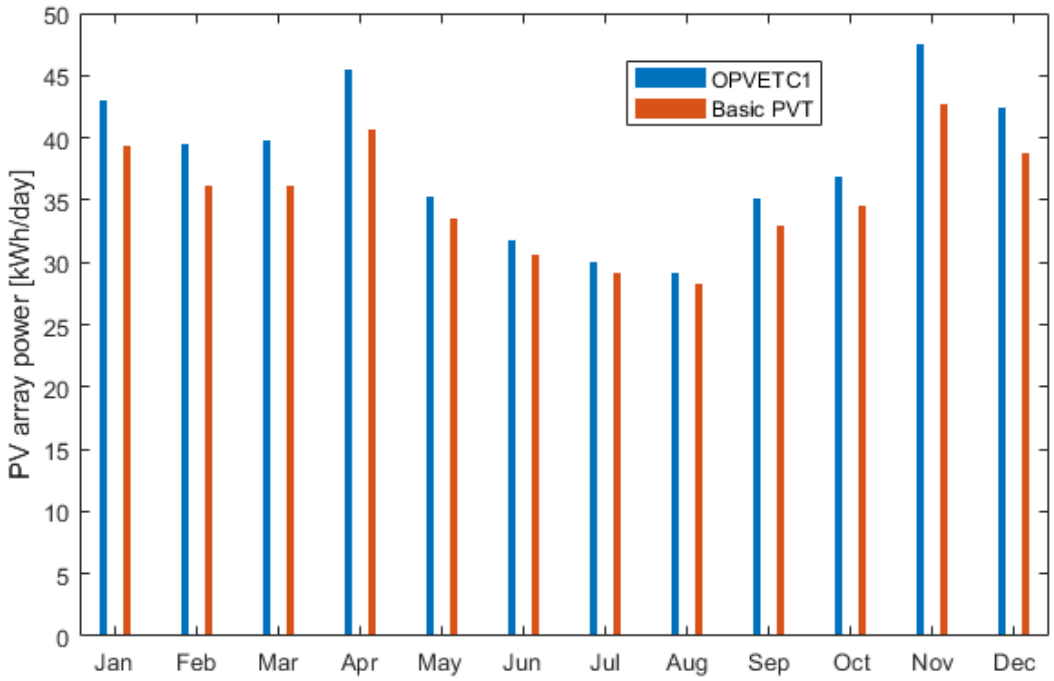


Figure 4.27:Monthly averaged daily PV array power production

Even though the OPVETC hybrid configuration requires higher pump power in months with higher solar energy, as seen in Table 4.5, its net power production is higher in all months than the basic PVT configuration. Overall, the net power production of the OPVETC hybrid configuration is 9.25% higher than that of the basic PVT configuration.

It is also observed from Table 4.5 that the cooling benefits of the proposed cooling method over the basic cooling method are evident in months with higher solar energy. This observation implies that for climate with extremely high temperatures like in the Northern part of Nigeria, the adoption of the basic PVT system will lead to a significant loss in power production, especially if the hot water demand is not appropriately sized to affect the proper kind of cooling as already shown in Ref. [228] a paper published as part of this study that supports this claim. An average pump power consumption of 3.3kWh/day of the OPVETC hybrid architecture represents 9% of the total power production of 38kWh/day. Similarly, despite a lower power production of the basic PVT system configuration, the power required to run the pump

consumes about 10% of the total power produced. An important conclusion that can be drawn from this result is that the net power production of the PV module is better enhanced when cooled based on the proposed system configuration than the traditional closed-loop system architecture. Overall, the proposed system configuration leads to higher power production of about 9.4% compared to the basic, widely adopted PVT hybrid system in most homes for domestic applications. This improvement could lead to the better economic viability of the OPVETC than the basic hybrid PVT energy system.

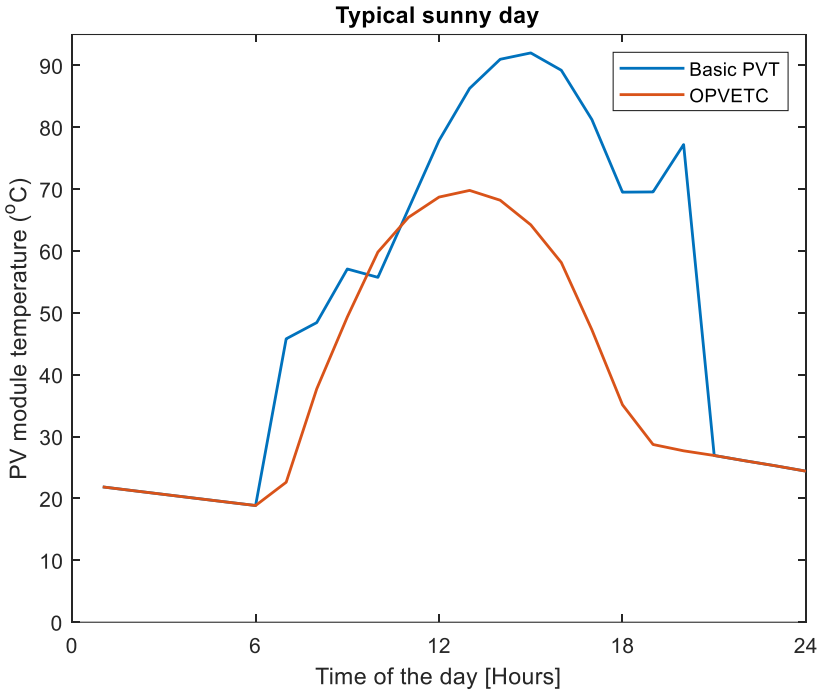
Table 4.5: Comparison of power production of OPVETC and basic PVT

	OPVETC (kWh/day)			**Basic PVT (kWh/day)**			
month	PV power output	Pump consumption	Net power	PV power output	Pump consumption	Net power	Diff btw basic and OPVETC (%)
Jan	43.11	3.62	39.49	39.47	3.30	36.17	9.19
Feb	39.51	3.33	36.18	36.23	3.29	32.94	9.82
Mar	39.94	3.43	36.51	36.22	3.42	32.80	11.30
Apr	45.49	3.97	41.52	40.80	3.60	37.20	11.62
May	35.30	3.16	32.13	33.56	3.77	29.79	7.88
Jun	31.88	2.92	28.96	30.74	3.86	26.88	7.74
Jul	30.09	2.76	27.33	29.24	3.83	25.41	7.57
Aug	29.18	2.67	26.50	28.34	3.76	24.58	7.82
Sep	35.22	3.16	32.06	33.02	3.59	29.43	8.93
Oct	36.97	3.26	33.71	34.55	3.58	30.97	8.83
Nov	47.60	4.08	43.52	42.83	3.55	39.28	10.81
Dec	42.53	3.60	38.94	38.83	3.29	35.54	9.56
Annual aver	**38.07**	**3.33**	**34.74**	**35.32**	**3.57**	**31.75**	**9.25**

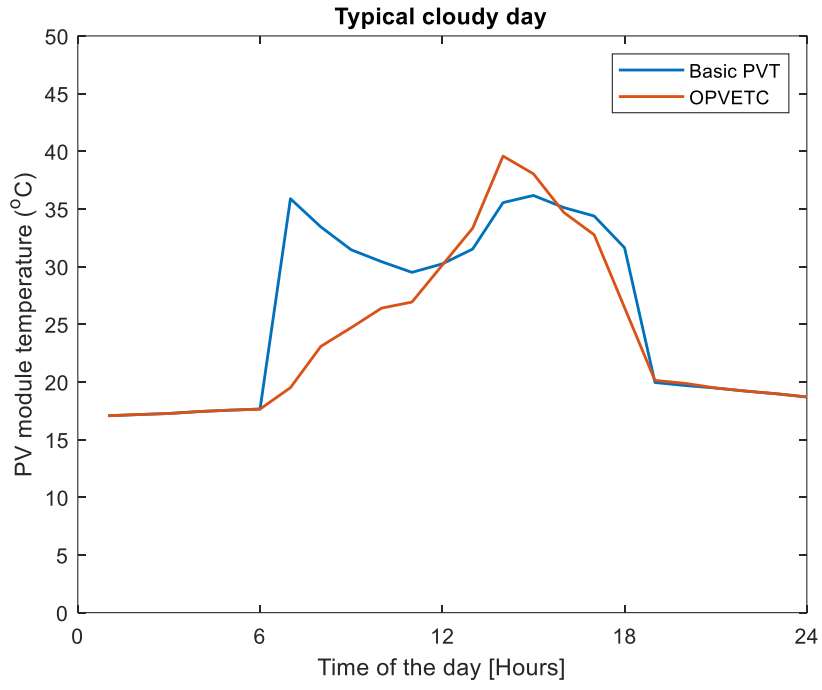
Furthermore, what is yet not known at this stage is the utilisation of the power generated in meeting the power demand of the health centre. In further analysis, the capacity of each system in self-consumption of the power generated is further analysed to see how well the production on both strategies coincides with the power demand. This attribute signifies the self-reliability and potential of good economic viability

4.6.2 PV module temperature characteristics

The primary objective of the cooling method is to lower the temperature of the PV module. The cooling water circulated under the absorber plate mainly removes the trapped heat in the module, thereby lowering the PV module temperature. It is, therefore, important to understand the effect of the cooling control strategy on the PV module temperature under different weather scenarios. Figure 4.28 compares the variation of the PV module temperature on typical sunny and cloudy days for the OPVETC and the reference Basic-hybrid PVT system. As seen in Figure 4.28, the module's temperature in the basic system architecture hybrid system could rise to about 90^{o}C on days with high solar radiation. For the proposed OPVETC system architecture and flow control strategy, the maximum PV module rise in temperature is limited to about 60^{o}C. As already explained, the module's temperature is higher for days with a higher level of solar energy for the basic hybrid system than the OPVETC because of the cooling strategy of operating the cooling water pump at a constant flow rate of 72L/hr.m^{2}. This flow rate is not adequate for cooling the PV on days with a high level of solar energy, and hence the PV module temperature is observed to increase. At the same time, the OPVETC cooling strategy cools the PV with a cooling flow rate adequate to maintain the temperature of the PV at about 60^{o}C. As observed again, on days with overcast sky conditions, the PV cooling approach has no significant effect on the PV module temperature since the trapped heat in the module is low. Since the objective of this study is to reduce the PV module temperature to increase its power output, the proposed flow control and cooling strategy will be more beneficial in maintaining the temperature of the PV module while harvesting higher power than the conventional and currently used basic system configuration. Besides improving the module power efficiency, the module solar cells are prevented from damaging due to the high rising temperature of the PV module.



(a)



(b)

Figure 4.28: Comparison of the PV module surface temperature

An analysis of the annual simulated performance of both the basic PVT hybrid system architecture and the proposed OPVETC hybrid system architecture shows in Figure 4.29 that

the OPVETC configuration and cooling control method can limit the PV module temperature to an average of about 60^{o}C even in months with high solar energy. On the contrary, module temperature could rise to about 80 ^{o}C for the basic PVT in months with high solar energy. The results shown in Figure 4.29 imply that the power production of the PV module will be higher in all months for the OPVETC system configuration than the currently available and adopted the architecture of the hybrid PVT energy system, as seen in Figure 4.27.

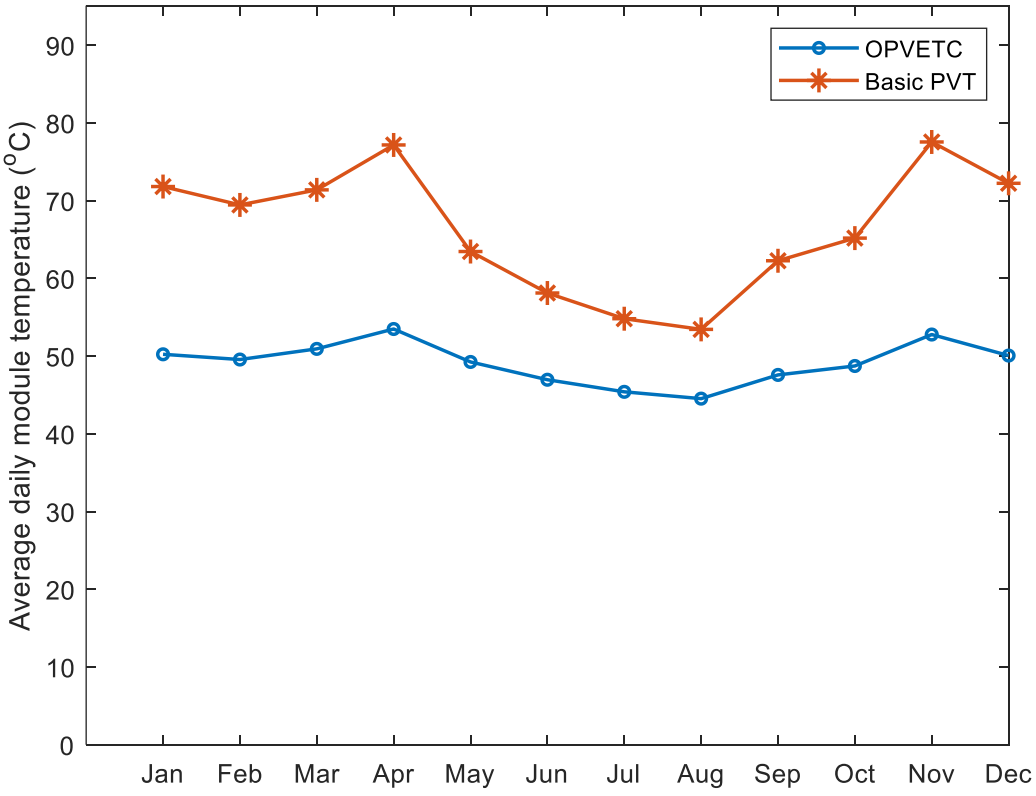


Figure 4.29 Monthly averaged daily module temperature from 11 am to 4 pm

The consequence of high module temperature is not only a reduced power production, but it can also reduce the life span of the PV module leading to poor viability with loss in profitability and a long payback period. Even if care is not taken, the power output may even be lower than the uncooled PV module for system cooled based on the conventional system architecture. Since the basic hybrid PVT system shows elevated temperature on days with a high level of

solar energy, the economic performance of the OPVETC will be higher than the basic hybrid PVT system since the power production of the basic hybrid system, which is the saving, will degrade over the years due to higher temperature.

It is worth noting here that the control strategy developed for the OPVETC hybrid system varies the generated cooling flow rate required to keep with the hot water temperature as desired. Therefore, one benefit of the OPVETC hybrid system as proposed is its flexibility for adoption in all weather conditions and adjustable goals. This means that the goal can be adjusted to shift from meeting 50:50 thermal and electrical energy in this study to a higher or lower portion in any targeted energy as desired based on need. That can be done only by deciding the temperature difference across the collector, and the controller in the flow control circuit regulates the flow based on the incident solar energy to achieve the set temperature difference as desired.

4.6.3 Thermal characteristics of service hot water

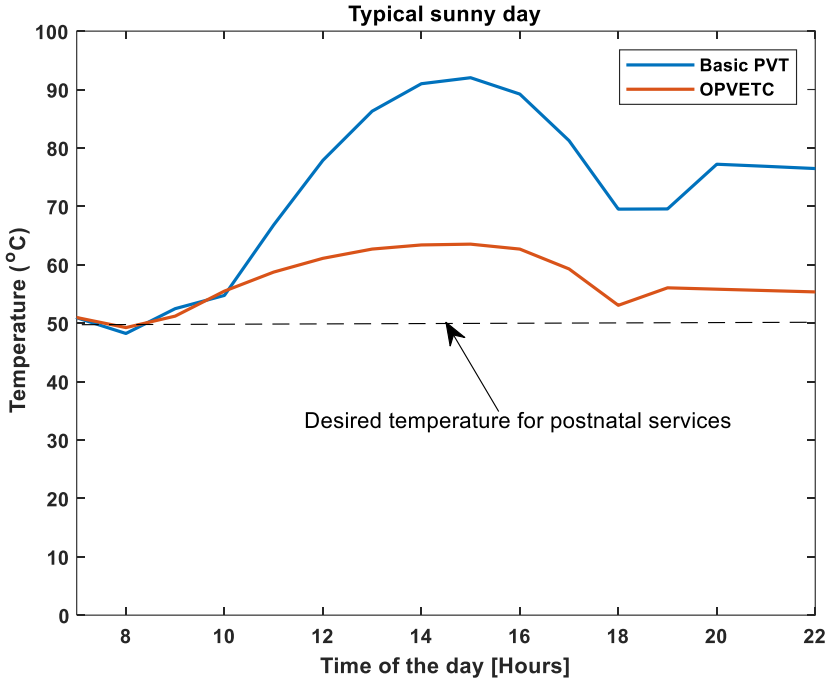
The provision of hot water for postnatal, laundry, and sterilisation services in energy-constrained health centres buildings was the target application for the proposed hybrid energy system. For these applications, the hot water temperatures are desired at 80 ^{o}C for sterilisation, 65 ^{o}C for laundry, and 50^{o}C for bathing services. This study aims to deliver the required hot water at these desired temperatures using the sun's energy most economically with the minimum requirement for conventional auxiliary energy. For this reason, the hot water demand for bathing required at the lowest temperature of 50^{o}C is separated and met from the PVT collector preheated tank. A separate hot water storage tank is used for the hot water demand for sterilisation and laundry. This concept ensures that the PVT cooling water is not recirculated back to the PVT at a higher temperature since the demand for sterilisation is required at about

80^{o}C. To achieve this temperature, the preheated cooling water is reheated in the ETC loop to a higher temperature for sterilisation and laundry. Again, the performance of the proposed OPVETC and the basic hybrid PVT in meeting the objective of harvesting the maximum thermal energy for the three hot water services in the studied health centre is evaluated and compared. Figure 4.30 compares the delivered hot water temperature for postnatal services within the time of demand (7.00 -22.00hrs) on a typical sunny day in April.

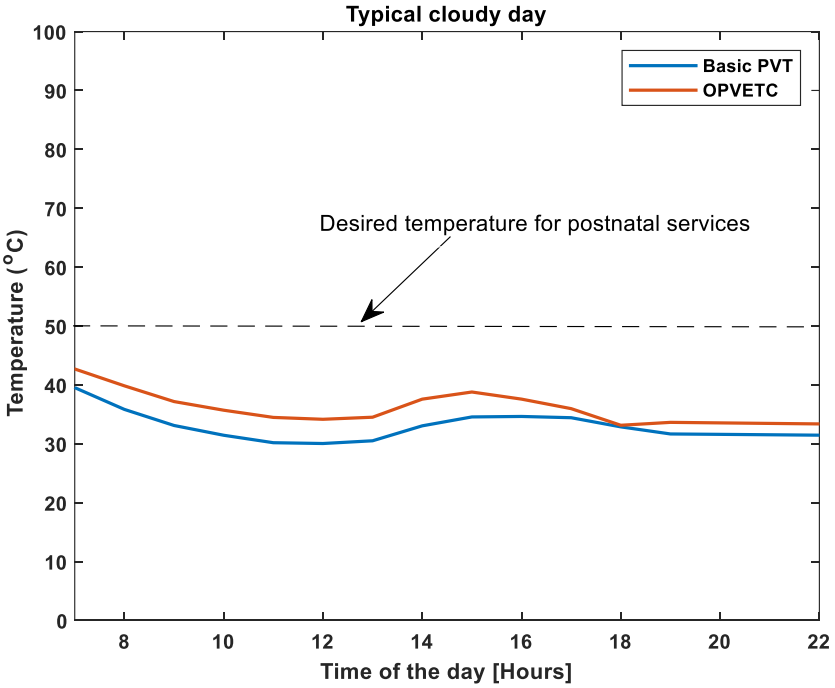
Interestingly, both the reference system and the proposed system delivered the hot water at a temperature even above the desired temperature for postnatal services even though the basic hybrid PVT water temperature is higher than that of the proposed system for most of the day, as seen in Figure 4.30a. This observation indicates that for both systems, the thermal energy requirement for postnatal hot water services is fully covered by both systems with no auxiliary energy demand on a typical sunny day like the one in April.

However, for a typical overcast day like in August, both system configurations delivered the hot water below the desired temperature, as seen in Figure 4.30b. As seen from the hot water is delivered at a higher temperature for the proposed system than the basic hybrid PVT system on days with an overcast sky similar to August. On days with an overcast sky, the solar energy is lower, and the heat absorbed by the collector absorber plate is lower; therefore, for a rise in temperature of the cooling, a lower flow rate proportionate to the absorbed heat of the absorber plate is needed. Since the basic hybrid PVT cools at a constant flow rate, the exit temperature of the cooling water will be lower than 50^{o}C in instances where the flow rate goes above the required flow rate. By implication, since water is delivered at a temperature lower than the desired temperature for postnatal services, additional energy will be required to fulfil the temperature requirement. It then means that the auxiliary energy demand will be lower in

months with an overcast sky with the adoption of the proposed system compared to the basic hybrid PVT.



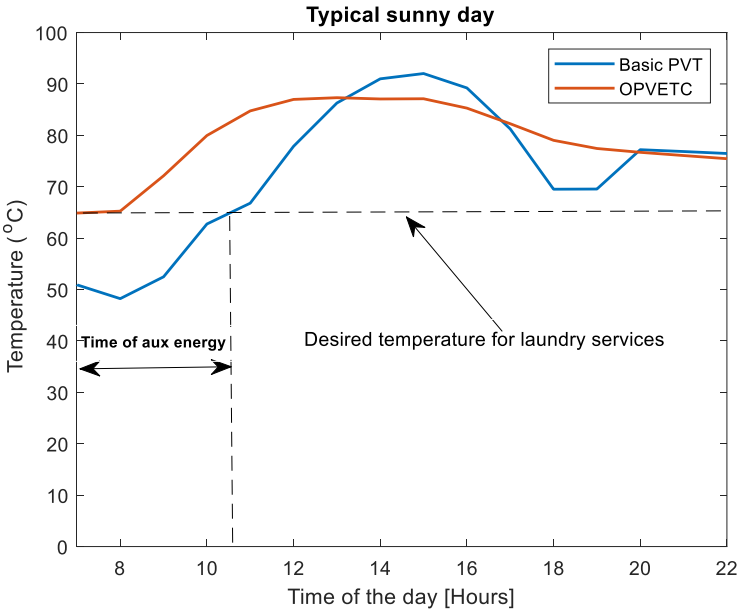
(a)



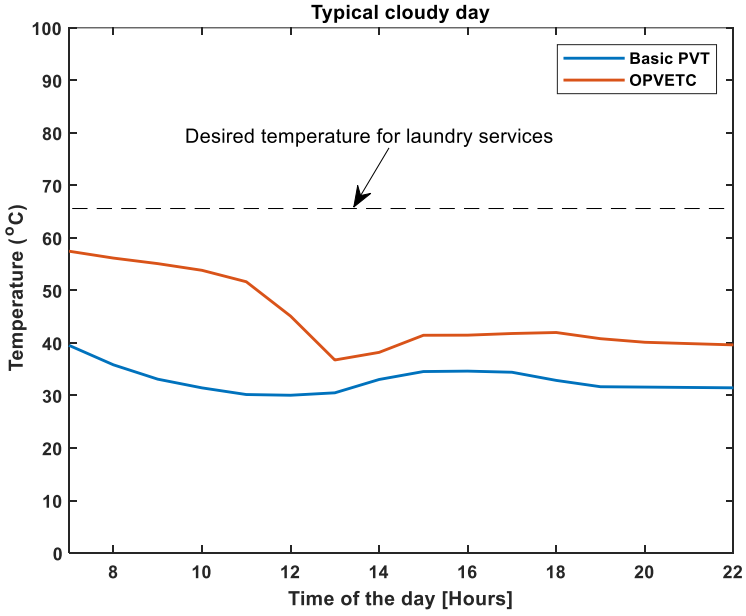
(b)

Figure 4.30: Load delivered hot water temperature for postnatal services

An observation similar to the trend and variation of the temperature of the hot water delivered for postnatal services for both systems on sunny and cloudy days is also seen in Figure 4.31and Figure 4.32. An important observation is observed as the required hot water temperature is demanded at a higher temperature, like in the case of laundry (65^{o}C) and sterilisation (80^{o}C). A startling revelation seen in Figure 4.31and Figure 4.32 shows that the basic hybrid system's capacity to supply the hot water at the required temperature diminishes more and more as the service hot water temperature increases from 65^{o}C to 80^{o}C. As seen from the indicated lines, the hours for which the hot water temperature is below the desired temperature on a typical sunny day is higher for the basic hybrid energy system in Figure 4.31 than in Figure 4.32. This means that as the temperature for hot water applications increases the gap in energy savings between the proposed system relative to the basic hybrid PVT energy system becomes wider.

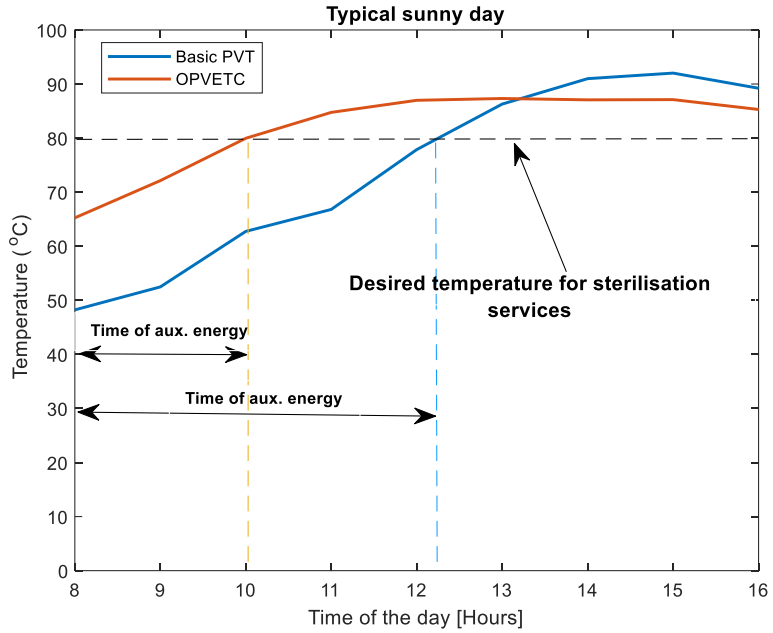


(a)

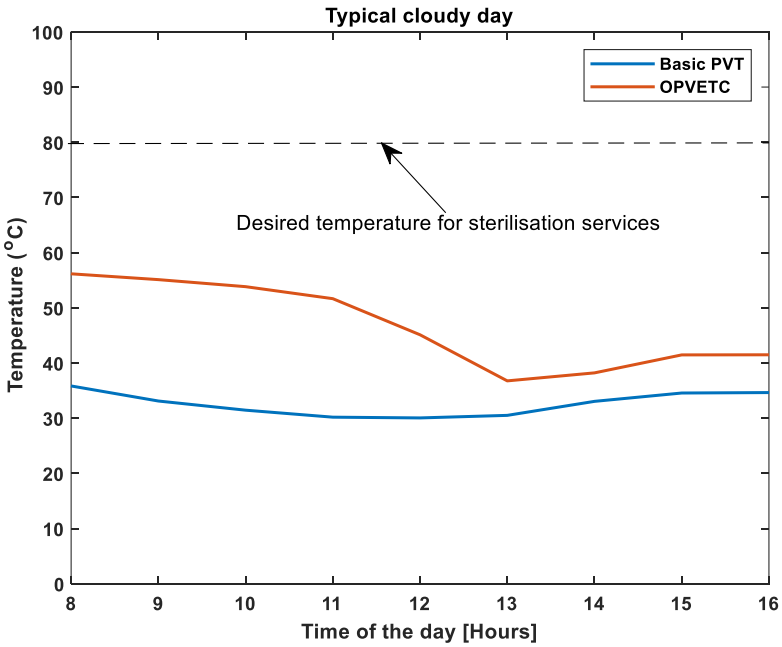


(b)

Figure 4.31:Load delivered hot water temperature for laundry services



(a)



(b)

Figure 4.32:Load delivered hot water temperature for sterilisation services

In conclusion, the proposed OPVETC system outperformed the basic hybrid PVT energy system to meet the goal of higher hot water demand on both sunny and overcast days. However, the basic hybrid PVT energy system delivers water at a higher temperature for postnatal applications, which results in more dumped thermal energy and reduces the system's power

conversion and harvesting efficiency on days with a high level of solar energy. These conclusions are drawn from assessing both system performances on sunny and cloudy days. Since the number of days with different sky conditions varies, a fair conclusion based on the monthly and annual performance of the systems will be beneficial in understanding the system's performance in different seasons of the year since Nigeria has different climatic conditions at different times of the year. The monthly performance may even be the basis for another control that may be further investigated to improve system performance in some months. The next subsection presents the monthly performance of the proposed and the basic hybrid energy systems.

4.7 Monthly average daily system performance analysis

The impact of the suggested energy management and cooling flow control strategies in section 3.7 on the monthly average daily thermal and electrical energy production of both the reference basic hybrid PVT and the proposed OPVETC hybrid energy systems are examined and compared in the subsections below. In the following subsection, the impact of the energy management and flow control strategies on the grid and diesel generator power usage is evaluated and compared on a monthly and annual basis to determine the monthly and yearly CO_2 contribution of both the basic hybrid PVT and the OPVETC hybrid system architecture.

4.7.1 Monthly average daily thermal performance assessment

The monthly average daily thermal performance measures the thermal system capacity in meeting the hot water demand for all three applications in the health centre. For this study, the total hot water production and its effective utilisation in meeting hot water demand for all three applications are assessed and compared for both the basic and the OPVETC hybrid systems. The goal here is to understand and compare the effectiveness of basic and the OPVETC hybrid system architecture in meeting the demand for hot water for all three hot water applications

based on the cooling flow control strategies. Figure 4.33 shows the monthly average daily thermal power production for both the basic and the OPVETC hybrid energy systems in relation to the actual power demand for domestic hot water for health care services. It is seen that for both systems, the thermal power production exceeded the actual power demand in the months (January to April) and (October to November) with good levels of solar energy. The thermal power production is seen to be higher in months with good levels of solar energy for the basic hybrid PVT than the proposed OPVETC hybrid system. However, in months with overcast and cloudy sky conditions, the thermal power of the OPVETC system is higher than the basic hybrid energy system. This behaviour confirms the repeatability of expected thermal characteristics as already explained in earlier subsections above for typical extreme weather conditions.

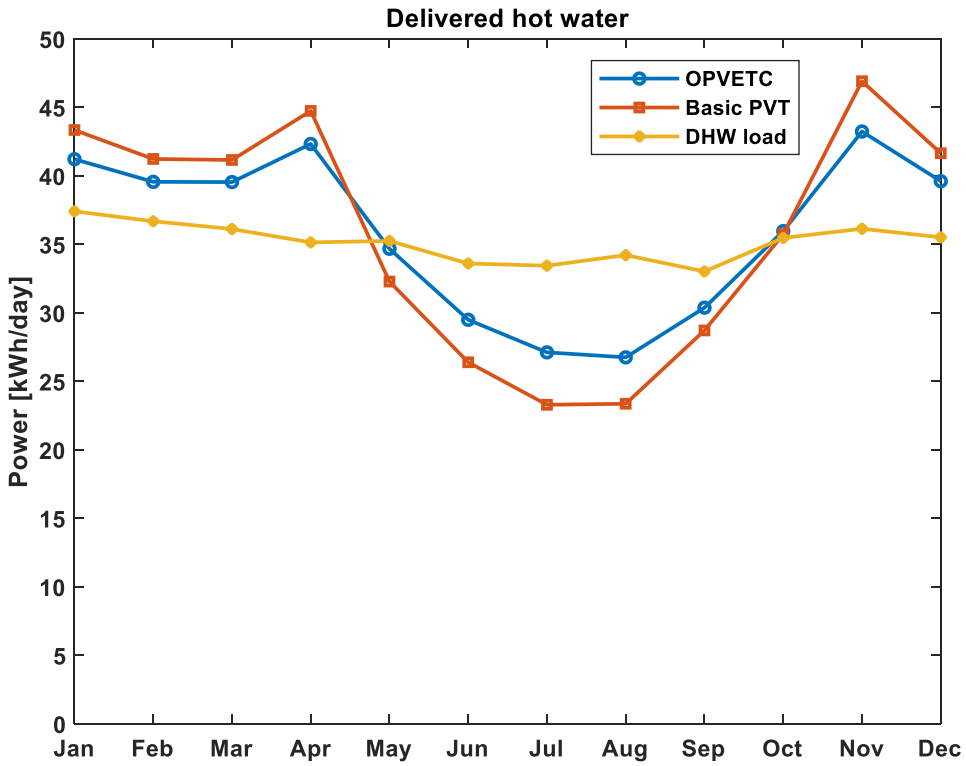


Figure 4.33. Comparison of monthly average daily delivered thermal energy

A more detailed analysis of the amount of thermal power produced that fulfils the health centre's thermal need reveals that even in months with excess thermal power, as shown in Figure 4.33, the useful thermal power is insufficient to meet demand. Notably, the OPVETC hybrid system is observed to have higher useful thermal power in all the months than the basic hybrid PVT energy system, as seen in Figure 4.34 and Table 4.7, with an overall higher useful thermal power of about 9.5% than the basic hybrid PVT system. This observation can be explained by the fact that even in months with high levels of solar energy, the flow rate at which cooling fluid in the basic hybrid PVT cools the collector in the morning period (7-12 noon) is at a rate that the cooling fluid energy gain is not enough to cause a rise in temperature of the cooling water. The cooling fluid exiting the collector at a low-grade temperature means that the basic hybrid system's useful thermal power in the early hours is lower than the OPVETC hybrid energy system. The low gain in the morning is because the available solar energy during the early hours of the day is relatively lower than that in the late hours of the day, and the cooling flow rate exceeds that required to cause a rise in the cooling water temperature in the morning hours.

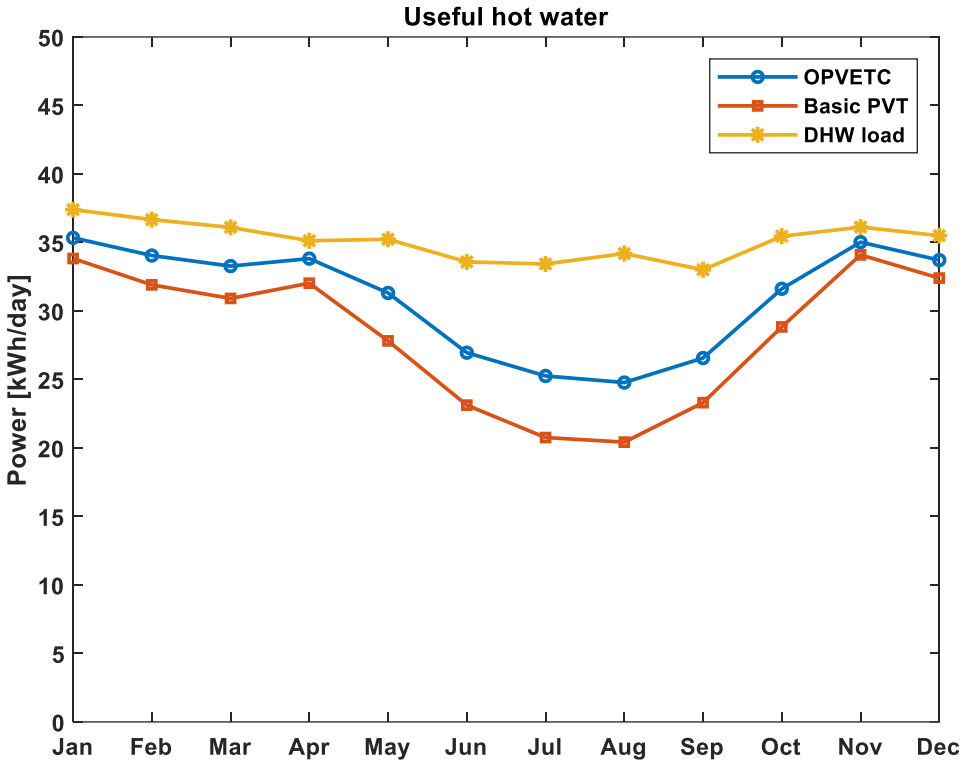


Figure 4.34. Comparison of monthly average daily useful thermal energy.

And during the afternoon period, the amount of solar energy is increased. As a result, the cooling fluid of the basic hybrid system thermal gain is significantly higher since the cooling water repeatedly circulated at a flow rate adequate to extract higher amounts of thermal energy from the collector than that of the OPVETC hybrid energy system. However, a good portion of the thermal gain exceeds the demand for hot water during this period of high gain; therefore, the basic system has about 34% more dumped thermal energy with no useful value annually, as seen in Table 4.7. That is why even though the delivered thermal power is higher than that of the OPVETC, the useful thermal power for the basic hybrid system is seen to be lower than that of the OPVETC hybrid system.

A critical assessment of even the delivered thermal power of both systems on an annual basis show that overall, the annual average daily thermal output of both systems is about 34kWh/day.

As seen in Table 4.7, even though the basic hybrid PVT system shows better delivered thermal power in months with a good level of solar energy, the thermal power production is lower than that of the OPVETC in months with low levels of solar energy. Since the OPVETC hybrid system configuration has a 9.5% more useful thermal power gain than the basic system, its means that the auxiliary energy demand for supplementing the thermal hot water demand will be 28% lower than that required for water heating based on the basic system configuration as seen in Table 4.6.

Table 4.6. Comparison of monthly average auxiliary energy demand

	OPVETC			Basic hybrid		
Month	**DHW Aux energy demand (kWh/day)**	**Pump power energy demand (kWh/day)**	**Total Aux energy demand (kWh/day)**	**DHW Aux energy demand (kWh/day)**	**Pump power energy demand (kWh/day)**	**Total Aux energy demand (kWh/day)**
Jan	2.1	3.6	5.7	3.6	3.3	6.9
Feb	2.6	3.3	6.0	4.8	3.3	8.1
Mar	2.8	3.4	6.3	5.2	3.4	8.6
Apr	1.3	4.0	5.3	3.1	3.6	6.7
May	3.9	3.2	7.1	7.4	3.8	11.2
Jun	6.6	2.9	9.5	10.5	3.9	14.3
Jul	8.2	2.8	10.9	12.7	3.8	16.5
Aug	9.4	2.7	12.1	13.8	3.8	17.5
Sep	6.4	3.2	9.6	9.7	3.6	13.3
Oct	3.8	3.3	7.1	6.6	3.6	10.2
Nov	1.1	4.1	5.2	2.0	3.6	5.6
Dec	1.8	3.6	5.4	3.1	3.3	6.4
Average	**4.2**	**3.3**	**7.5**	**6.9**	**3.6**	**10.4**

As a result, the electric power demand for the health centre will be higher if the basic hybrid PVT energy system is used to meet the demand for hot water and power compared to the proposed OPVETC system. It is equally seen in Table 4.6 that the proposed approach shows better thermal power utilisation and proved to have lower pump power consumption. Implying that the total electric power demand for the health centre will be lower if the power and hot

water need are supplied based on the new hybrid energy system integration and cooling approach.

Table 4.7. Comparison of monthly average daily thermal energy utilisation

	OPVETC				Basic hybrid			
Month	**Collector thermal power (kWh/day)**	**Thermal power used (kWh/day)**	**Solar Fraction**	**Dumped fraction**	**Collector thermal power (kWh/day)**	**Thermal power used (kWh/day)**	**Solar Fraction**	**Dumped fraction**
Jan	41.20	35.34	0.86	0.14	43.33	33.83	0.78	0.22
Feb	39.55	34.05	0.86	0.14	41.21	31.91	0.77	0.23
Mar	39.53	33.28	0.84	0.16	41.14	30.92	0.75	0.25
Apr	42.31	33.82	0.80	0.20	44.72	32.03	0.72	0.28
May	34.66	31.32	0.90	0.10	32.27	27.82	0.86	0.14
Jun	29.48	26.95	0.91	0.09	26.38	23.12	0.88	0.12
Jul	27.10	25.26	0.93	0.07	23.28	20.76	0.89	0.11
Aug	26.74	24.77	0.93	0.07	23.35	20.42	0.87	0.13
Sep	30.36	26.56	0.87	0.13	28.70	23.30	0.81	0.19
Oct	35.95	31.62	0.88	0.12	35.72	28.84	0.81	0.19
Nov	43.22	35.02	0.81	0.19	46.89	34.10	0.73	0.27
Dec	39.60	33.71	0.85	0.15	41.64	32.40	0.78	0.22
Average	**35.81**	**30.98**	**0.87**	**0.13**	**35.72**	**28.29**	**0.80**	**0.20**

The increase in the electric power demand of the health centre is because the hot water auxiliary energy, which is higher for the basic system, is added to the electric power that will be required to be supplied by either power from the PV module or the power from the grid and diesel generator used as a backup. By implication, it equally means that for periods where the PV power fails to meet all the power demand plus hot water auxiliary power demand, the basic hybrid energy system will depend on 33% more conventional power than the OPVETC hybrid system, as seen in Table 4.8

Table 4.8. Comparison of monthly average daily fossil fuel energy utilisation

	OPVETC			Basic hybrid		
Month	**Grid power usage (kWh/day)**	**Diesel power usage (kWh/day)**	**Total conventional power usage (kWh/day)**	**Grid power usage (kWh/day)**	**Diesel power usage (kWh/day)**	**Total conventional power usage (kWh/day)**
Jan	6.3	0.1	6.4	9.3	0.7	10.0
Feb	8.1	1.1	9.2	11.8	2.8	14.6
Mar	10.5	1.3	11.7	14.6	5.3	19.9
Apr	9.0	0.3	9.3	14.2	2.7	16.8
May	9.8	5.7	15.5	13.7	10.7	24.4
Jun	13.1	5.8	18.9	15.7	10.8	26.5
Jul	16.1	3.0	19.2	20.0	6.3	26.3
Aug	14.4	5.7	20.1	17.4	9.5	26.9
Sep	11.1	4.6	15.7	13.7	8.1	21.8
Oct	10.3	4.1	14.4	12.6	8.4	20.9
Nov	4.3	0.0	4.3	7.3	0.5	7.7
Dec	6.6	0.0	6.6	10.2	0.1	10.2
Average	10.0	2.6	12.6	13.4	5.5	18.8

These observations indicate that the profitability and environmental conservation of the proposed OPVETC will be higher than the currently used basic hybrid PVT energy system. It also means that the diesel generator's hours of operation when integrated with the basic hybrid PVT energy system will be about 50% higher than when used as a backup for the new proposed OPVETC hybrid system configuration. Economically speaking, it also means that the diesel fuel and replacement cost will be double when the basic hybrid PVT is used in supplying the energy demand of the health centre for a project life cycle of 25 years.

4.7.2 Comparison of the monthly average daily power production

Because the proposed OPVETC system's goal is to improve PV module power production while also increasing thermal output, it's critical to see if the energy management strategy and cooling flow control technique are suitable for achieving satisfactory results even in months with extreme weather conditions, as has already been determined for thermal power output. The power output is critical for satisfying the power demand of the health centre and the

auxiliary hot waterpower requirement. Figure 4.35 is the PV module's monthly average daily power output for the basic and the OPVETC hybrid energy systems. Again, the power output of the OPVETC hybrid system is improved relative to the basic hybrid PVT. The power production gap is more pronounced in the early four months and the last four months. These months are months with higher levels of solar energy than the middle four months

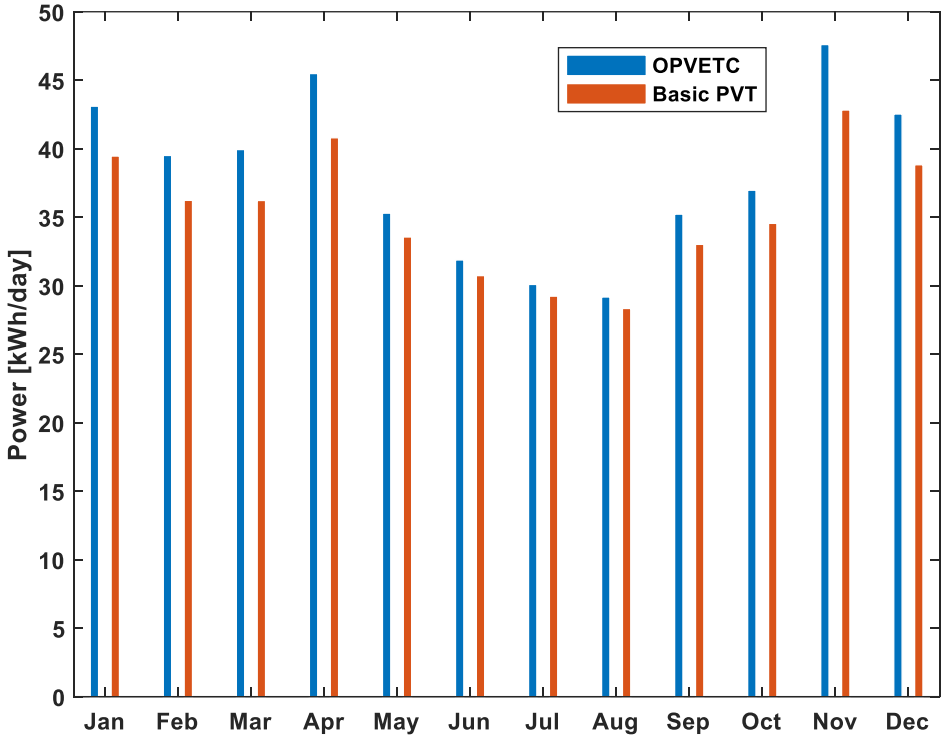


Figure 4.35.Comparison of monthly average daily PV array power output

In months with higher levels of solar energy, the gap in power production between the two systems is wider because, during these months, the thermal production of the basic hybrid PVT is improved due to repeated circulation of the cooling water. On the other hand, the heat removal capacity of the cooling water is impaired since the cooling water enters the collector at a higher temperature as a result of destroyed stratification in the cooling water tank due to repeated recirculation in the closed-loop. As a result, the module surface temperature increases, reducing the PV module's power production. The cooling method for the OPVETC hybrid

system is based on an open-loop cooling and flow control strategy, in which the flow required on days with higher solar energy levels is moderated to match the need for cooling to a specific temperature. Because the cooling water does not return to cool the PVT collector, the PVT collector inlet water enters at a lower temperature, equal to the mains water temperature. As a result, heat removal is improved because the inlet water enters at a lower temperature than in the case of the basic hybrid PVT energy system. This again indicates, as seen in Table 4.9, that the proposed system configuration and cooling method has improved the power production of the PVT collector by an average of 7.7% relative to the basic case widely adopted hybrid PVT energy system used for power and thermal application in most residential buildings. As earlier mentioned, since the useful thermal energy of the OPVETC is higher than that of the basic hybrid PVT, the auxiliary energy required to fulfil the health centre thermal demand is lower when the OPVETC is adopted compared to the currently used basic hybrid PVT system configuration. Table 4.9 indicates that the dumped power from the basic PV module is 4% lower than that of the OPVETC hybrid energy system. This result is expected since the power generated from the PV module is used for medical equipment power demand and to meet the higher auxiliary energy demand for hot water demand created by the poor thermal performance of the basic hybrid energy system. As a result, the PV power usage is high, resulting in lower dumped power, as seen in Table 4.9, since the system is struggling to meet the higher power demand.

Table 4.9. Comparison of monthly average daily power generation and utilisation

	OPVETC				Basic PVT			
Month	**Average Power demand (kWh/day)**	**Average Power output (kWh/day)**	**Average Power used (kWh/day)**	**Solar Fraction**	**Average Power demand (kWh/day)**	**Average Power output (kWh/day)**	**Average Power used (kWh/day)**	**Solar Fraction**
Jan	44.0	43.1	39.4	0.89	46.7	39.47	38.44	0.82
Feb	45.5	39.5	36.8	0.81	49.6	36.23	35.57	0.72
Mar	49.9	39.9	38.2	0.77	55.6	36.22	35.81	0.64
Apr	50.3	45.5	42.7	0.85	55.6	40.80	40.13	0.72
May	51.1	35.3	35.3	0.69	58.6	33.56	33.56	0.57
Jun	48.3	31.9	31.8	0.66	55.0	30.74	30.74	0.56
Jul	49.7	30.1	29.1	0.59	56.7	29.24	28.72	0.51
Aug	48.5	29.2	28.5	0.59	54.8	28.34	28.30	0.52
Sep	47.9	35.2	33.5	0.70	53.1	33.02	32.48	0.61
Oct	48.6	37.0	34.9	0.72	54.3	34.55	34.11	0.63
Nov	46.0	47.6	42.3	0.92	48.9	42.83	41.27	0.84
Dec	44.0	42.5	38.3	0.87	46.7	38.83	38.11	0.82
Aver.	47.8	38.1	35.9	0.75	53.0	35.32	34.77	0.66

Furthermore, a critical assessment of Table 4.9 shows that the health centre's monthly average daily power electric load demand is 47.8kWh/day for the OPVETC system and 53kWh/day for the basic hybrid system. This value indicates that even though the equipment load, which comprises the power demand for cooling and heating of the health centre building, and the power for operating the medical equipment are the same, the total electric demand for the health centre will be about 10% lower if the new OPVETC system is used rather than the current basic hybrid energy system. Adopting the new system reduces the total electric demand since the electric demand for hot water auxiliary energy and pump operation is lower, as already explained above. In addition to the 7% gap in average daily thermal power utilisation as seen in Table 4.7, it again revealed that the proposed new system integration and flow control technique resulted in about a 9% increase in the average daily utilisation of the power produced from the PV panel than the basic hybrid PVT system configuration operated under the same scenario and controls. Overall, these findings are an indication that the new configuration will

improve the business outlook of using the PVT collector hybrid energy system for residential energy demand.

4.8 Comparison of system performance indicators

Renewable energy technologies are becoming increasingly popular to mitigate the negative effects of fossil fuel energy production, which necessitates a technical evaluation of the annual performance of renewable energy projects to determine their sustainability and profitability and compare their advantages over other alternative renewable sources of energy technologies [229]. For comparing the environmental sustainability and financial viability of the reference basic hybrid PVT system with the new OPVETC hybrid energy system, in this section, performance metrics such as Solar Fraction (SF), the system Loss of Load Probability (LOLP), Avoidable CO_2 Ratio (ACO_2_Ratio), Self-Consumption Ratio (SCR) and the Self-Sufficiency Ratio (SSR) as performance indicators that are pointers to the environmental sustainability and economic viability of these energy systems are evaluated and discussed.

4.8.1 System solar fraction (SF)

Buckles and Klein [230] defined solar fraction as the percentage of the solar energy generated from the solar energy system that meets energy demand in any application. Therefore, SF is a superior performance indicator since it measures the part of the energy demand met by the sun's energy free from emission. It is also an indication of the energy and cost savings of the system. Figure 4.36 compares the annual solar fraction of the basic PVT configuration and the OPVETC hybrid system architecture. It is seen from Figure 4.36 that the proposed system reconfiguration has an 6% and 7% improvement in the average daily thermal and electrical solar fractions relative to the basic hybrid energy system. It also implies that the annual Renewable Energy Fraction (REF) of the OPVETC of hybrid system architecture indicates that its overall energy saving is 6% higher than the basic hybrid PVT system configuration.

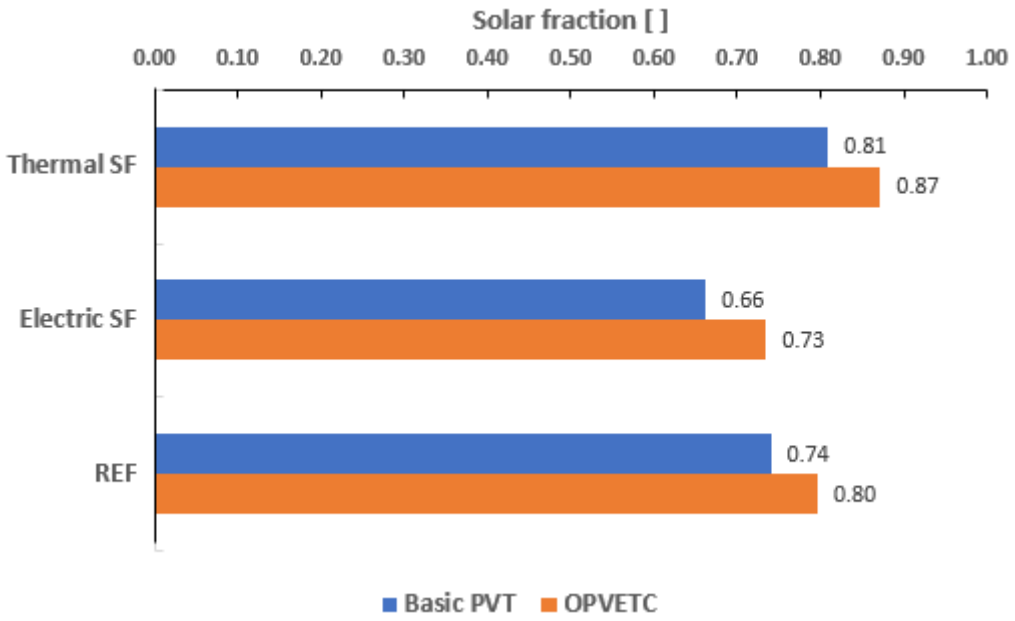


Figure 4.36. Comparison of systems solar fraction

Since the solar fraction indicates energy savings and profitability, it is inferred at this stage that the proposed system architecture may have better economic returns than the traditional system architecture. Lastly, the annual thermal solar fraction for both system configurations is above 60%, indicating that the solar fraction of the system is within the acceptable range (30% to 90%) of solar system solar fraction for good payback and economic profitability as recommended by the National Renewable Laboratory (NREL) guideline for the design of solar water heating systems [231].

4.8.2 Collector efficiency

Another evaluation indicator that does not consider whether the energy produced by the collector matches demand is the system efficiency. Using this evaluator gives an idea of how well the system converts the total incident energy to electrical or thermal energy without concern for its usefulness[232]. Again, the solar collector thermal efficiency of the proposed OPVETC is 50%, and that of the basic PVT architecture is 39%, as seen in Figure 4.37. This result means that the capacity of the PVT collector to convert the solar energy incident on its

surface is increased by about 11% when the collector is cooled based on the cooling technique as proposed in this study compared to the cooling approach and system architecture of the

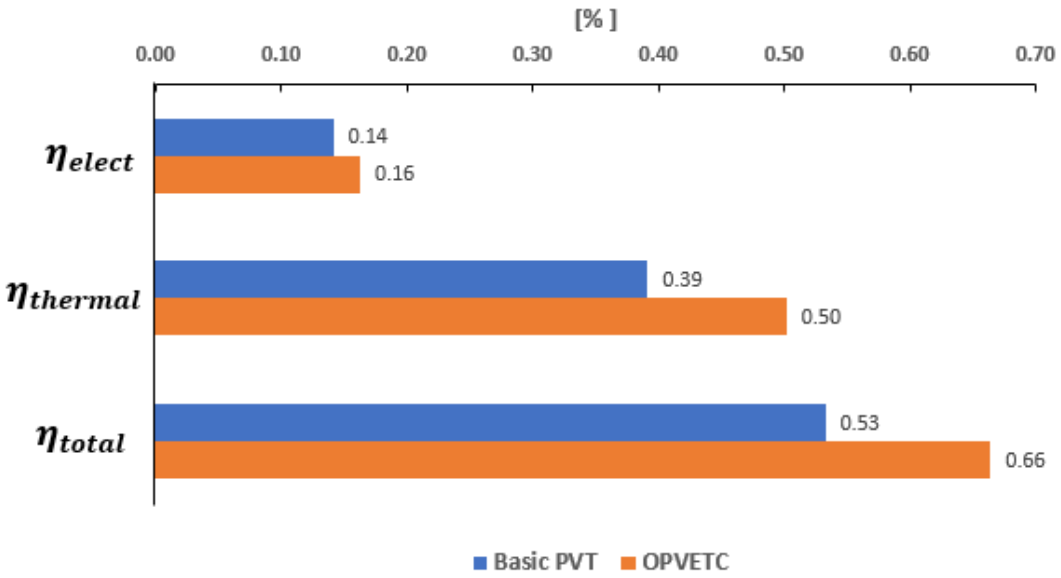


Figure 4.37. Comparison of PVT solar energy conversion efficiency

traditional hybrid PVT energy system. For the basic PVT hybrid system configuration, the cooling of the PVT collector is carried through the continuous circulation of the cooling water in a closed-loop. By this method, the cooling water from the water tank at a point is almost in equilibrium with the surface temperature of the PVT collector, and as such, the heat removal capacity of the cooling is greatly reduced. Hence the collector conversion efficiency of the solar radiation incident on its surface is reduced due to the small temperature gradient between the cooling fluid and the PVT collector surface. In addition, the thermal efficiency for the basic configuration is lower due to the smaller volume of water that is recirculated to cool the collector in a closed loop. This is already corroborated by a portion of this study that has been published [228], investigating the influence of hot water demand volume on the efficiency of the solar collector, which findings showed that the heat removal factor of the collector decreases when a small volume is circulated repeatedly in a closed loop[228].

4.8.3 System reliability

Since modern energy systems must equally meet the goal of system reliability, the Loss of Load Probability (LOLP) is a suitable performance matrix to assess the system's reliability. The LOLP is the chance that the proposed HRES system may not meet the load requirement at any given time in a year. This performance is of interest to the end-user and the investor. In this study, the hybrid energy system consists of a PVT collector, the grid power source, and a battery storage system sized to meet the design load. In this instance, the LOLP is the probability that these power elements may not meet the load at any given time. Table 4.10 is the monthly and annual evaluation of the loss of the load probability for both the basic PVT system architecture and the OPVETC hybrid system architecture. It is seen from Table 4.10 that in months with a high level of solar energy, the monthly average system reliability is higher than system reliability in months with a low level of solar energy.

Interestingly, the LOLP is zero for both hybrid system configurations for November and December. This observation is due to the elevated level of solar energy and less frequent grid power outage in these months. Overall, the OPVETC system architecture has an annual LOLP of 5.4%. An annual LOLP of 5.4% means that the system requires backup energy for 477 hours in a year (8760 hours) to be completely reliable. Consequently, for a diesel generator set used as a backup, as in this study, the gen-set is only operated for 477 hours per year.

Similarly, the annual LOLP of the basic PVT configuration is 9.7%, indicating that the system requires that the backup system be operated for 848 hours in a year. On the other hand, because the LOLP is an indication of the amount of time during which the generator is used as a backup to ensure that the system is 100% reliable, the LOLP for both systems revealed that the OPVETC hybrid is a proposal that has the potential to reduce CO_2 emissions from the backup

system (diesel generator) by up to 44% when compared to the basic hybrid PVT energy system. It is possible that the unreliability of both systems observed from May to August is related to grid outages and, to a greater extent, to the low level of solar energy reported during these months. Lower diesel operation and maintenance costs are financial benefits of the proposed configuration over the basic system configuration since its operation hours are 44% decreased compared to the basic hybrid PVT energy system. For the diesel generator used as a backup, the OPVETC configuration consumes a lower quantity of fuel and takes a long time before maintenance operation is carried out on the backup system. This benefit can improve the profitability and sustainability of the hybrid energy system.

Table 4.10: Comparison of LOLP between the basic PVT and the OPVETC

	Basic PVT			**OPVETC**		
Month	Electric power demand (kWh/month)	Unmet electric power demand (kWh/month)	LOLP (%)	Electric power demand (kWh/month)	Unmet electric power demand (kWh/month)	LOLP (%)
Jan	1449	14	1	1364	5	0
Feb	1388	70	5	1274	31	2
Mar	1723	151	9	1546	39	3
Apr	1667	72	4	1509	10	1
May	1816	314	17	1584	176	11
Jun	1706	303	18	1498	174	12
Jul	1700	181	11	1492	94	6
Aug	1700	283	17	1504	177	12
Sep	1593	230	14	1437	139	10
Oct	1683	244	15	1507	127	8
Nov	1466	11	1	1381	0	0
Dec	1449	1	0	1365	0	0
Annual Average	1612	156	9.7	1455	80.9	5.4

Furthermore, the backup diesel generator in the basic system configuration will be replaced twice before the backup power system of the OPVETC is replaced during the entire project life

span. Since the time of operation of the diesel backup generator set of the basic hybrid system configuration is about twice that of the OPVETC system, the OPVETC system's contribution to the mitigation of carbon dioxide released into the atmosphere is more than that of the basic PVT configuration.

4.8.4 Self-consumption ratio (SCR) and self-sufficient ratio (SSR)

The SCR and SSR are two important evaluation matrices determining how much renewable energy generated by the hybrid energy system is utilised. These evaluators are beneficial for comparing alternative hybrid energy systems regarding their conservativeness and economic benefit. The SCR is the ratio of the total renewable energy generated with useful applications. For this study, the SCR is the ratio of the system's renewable energy utilised in meeting the health centre's hot water demand, the electric power demand, and the power for charging the battery system to the total generated renewable energy. The SSR is the ratio of the utilised renewable energy from the energy system to the total energy demand.

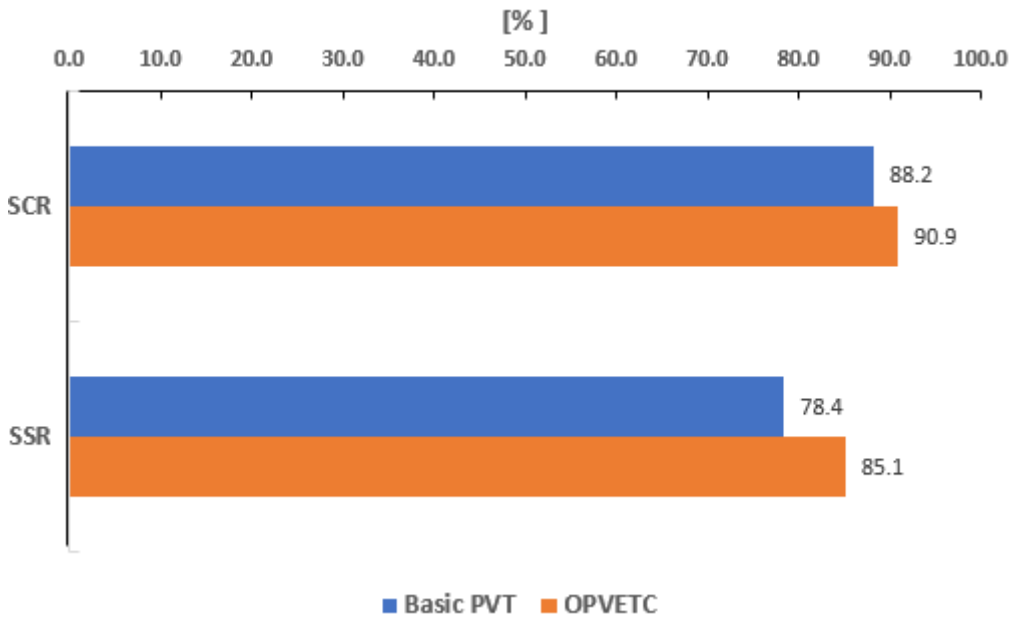


Figure 4.38. Comparison of annual system self-reliability

These performance matrices indicate the independency of the hybrid energy system from the conventional power element in fulfilling the load requirement of the health centre. A higher value shows lesser dependence on the conventional power element in meeting total energy demand. Figure 4.38 compares the basic hybrid PVT SCR and SSR with the proposed OPVETC hybrid energy system. In Figure 4.38, the SCR values are 0.82 and 0.91 for the basic and OPVETC hybrid systems, respectively. The SCR values indicate that both systems operated following the suggested energy management resulting in maximum use of renewable energy generated, with just 18% and 9% of the generated energy being dumped without being used by the basic and OPVETC energy systems, respectively. Compared to the OPVETC hybrid energy system, the basic hybrid PVT has 50% more dumped energy. This is primarily due to the excess thermal energy generated by the recirculation of the cooling water, which has no advantage but also heats the PVT collector rising its surface temperature, thereby reducing the power output.

Similarly, since the SSR performance matrix is an indicator that gauges the useful energy with the energy demand, its main concern is an assessment of the capacity of the system to satisfy the energy demand. Again, the OPVETC hybrid system configuration SSR is 0.85, and that of the basic hybrid PVT is 0.78. These values show that the OPVETC system under the flow control and energy management approach has a lower demand for auxiliary energy of about 15% of its total energy demand, and the basic hybrid system's demand for auxiliary energy will be about 22% of its total energy demand. By implication, the energy demand for the health centre is higher by about 22% when the supply is based on the basic system configuration compared to the OPVTEC configuration due to a higher pump and auxiliary hot water demand. Higher auxiliary energy by about 22% for the basic will lead to higher operating costs and higher emissions than the OPVETC system.

4.8.5 Avoidable carbon dioxide ratio (ACO_2 Ratio)

The avoidable carbon dioxide ratio (ACO_2 Ratio) is a measure of the mitigative contribution of the renewable energy system to reducing the amount of CO_2 in the energy mix as a pathway for renewable energy technologies in the decarbonisation effort as required by the Paris Agreement (PA). A higher ratio of the ACO_2 Ratio is promising and shows the percentage of the reference energy CO_2 that is replaced by the renewable energy system. In this study, the reference energy system is the diesel generator. The CO_2 emission from the diesel generator is the baseline for measuring the ACO_2 Ratio of the basic hybrid PVT and the OPVETC energy systems. Table 4.11 compares the avoided CO_2 emission from both systems and the evaluated ACO_2 Ratio of both the basic and the OPVETC systems.

Table 4.11. Comparison of systems CO_2 emission and the computed ACO_2 Ratio

System configuration	ACO_2 (kg/yr)	ACO_2_ratio (%)
OPVETC	59137	78.8
Basic PVT	56030	71.5

As seen in Table 4.11, the basic hybrid PVT energy system has 56,030kgCO_2/yr translating to an ACO_2 ratio of 78.8%, while the OPVETC hybrid energy system has a higher avoided CO_2/yr of 59,139kg/yr with an avoidable CO_2 ratio of about 78.8%. Even though the proposed hybrid energy system has higher avoided CO_2/yr, the evaluated ACO_2 ratio of both systems indicates the hybrid PVT energy system, when used in the residential building, has great potential for emission reduction in the energy mix.

Again, since the roadmap to limit global warming to +1.5^{o}C requires that global emissions be cut down by about 7.6%/yr between 2020 and 2030 [233], an ACO2 ratio of above 70%/yr as revealed in this study, shows that hybrid PVT collectors integrated with conventional energy

sources are more than enough to cut the emission from the building sector. Since building energy consumption represents about 49% of Nigeria's total energy demand [234], the adoption of this technology in residential buildings could be a potential area for the country to target to keep to its CO_2 reduction target and make an effort to increase access to power in rural communities.

4.9 Model validation

As earlier mentioned, the validation of the simulation output against the behaviour of a real system was not possible due to a lack of an experimental setup. Furthermore, the literature identified no exact simulated and appropriately validated system while looking at available models. As a result, for validation and verification (V&V) purposes, a combination of relevant methodologies as found in the literature is adopted. For this approach, the goal here is to ensure that the conceptual model is appropriately modelled and can represent the actual system to a great extent. First, the major system component model is verified against established theoretical and experimentally validated models. However, the indoor simulation is experimentally validated against measured data for the building model. Second, the logic and control of the dynamic characteristic of the whole system based on the designed operation are graphically verified. Lastly, the model appropriateness is tested by conducting system energy balance. The results are discussed in detail in the subsections below.

4.9.1 Component-by-component V&V

In this study, the Type 560 PVT model found in the simulation studio is used to model the unglazed sheet and tube, water-cooled PVT collector. Hence, to validate and verify this component, the power output of the unglazed TRNSYS model of the PVT collector (Type 560) was compared to the most extensively used and well-validated numerical model published by Sun et al.[215] and Pantic et al. [216], a method recommended by Sigarchian [197]. For this

comparison, a hypothetical TRNSY model system similar to that found in the study by Sun et al.[215] and Pantic et al. [216] are replicated and simulated under the same weather and load condition. Figure 4.39 compares the power output to the Type 560 model of unglazed PVT collector and the empirically validated PVT collector power model as published by Pantic et al. [216] for 3 days in January. The details of the parameters and configuration are as in [216]. It is seen that the power output of the two models shows a similar and close trend. The power output from the model proposed by [216] shows higher power output on all three days. This observation is expected since the Pantic model is simple and does not account for detail losses as in the case of the TRNSYS model. Overall, it is clear that the power out of the TRNSYS model is modelled based on established and proven equations in the field of science.

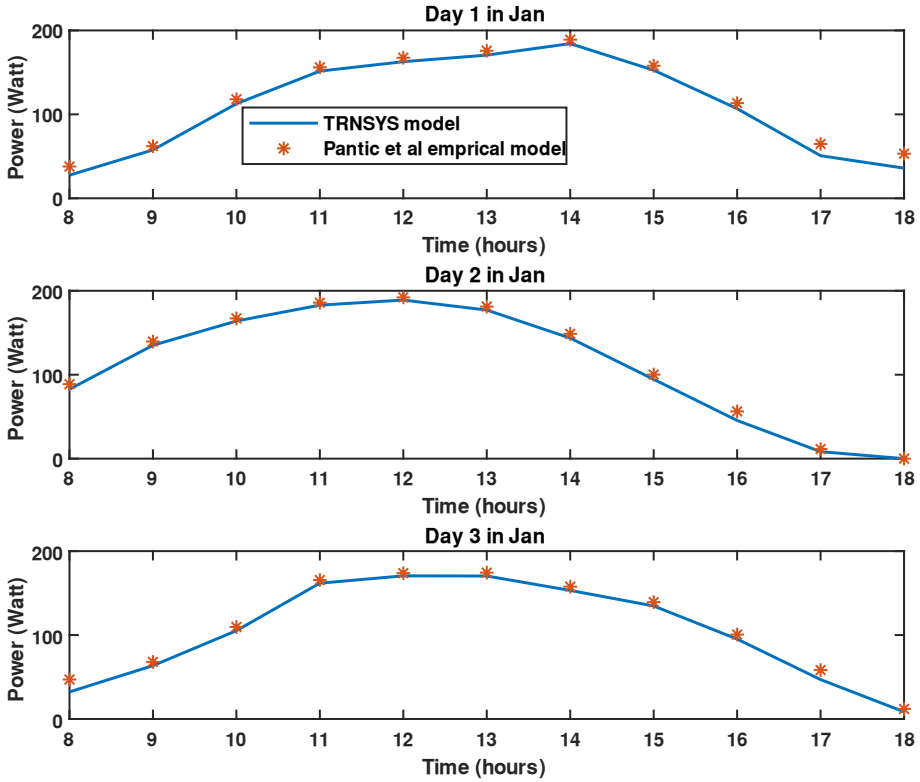


Figure 4.39. Comparison of TRNSYS and Pantic et al.'s PVT power model

To answer the question, 'to what extent these models are close', a statistical analysis of the power prediction of the two models is evaluated. Figure 4.40 is the difference between the two

models along a regression line 1:1 for the best relation fit. The R-squared measures how close the relationship between the power output from the TRNSYS model and the reference model to the best line regression line is. A value of 0.997, as obtained in this analysis, indicates that the relationship between the TRNSYS model and the reference model is significantly close, with more than 99% similarity. The Root Mean Square Error (RMSE) of 5.7 in this study indicates that the two models' power output predictions disagree by an average of 5watts. This difference is quantitatively translated to a Mean Average Percentage Error (MAPE) of roughly 9.3%, lower than the 12.9 % RMSE error percentage difference discovered in the study done by [235].

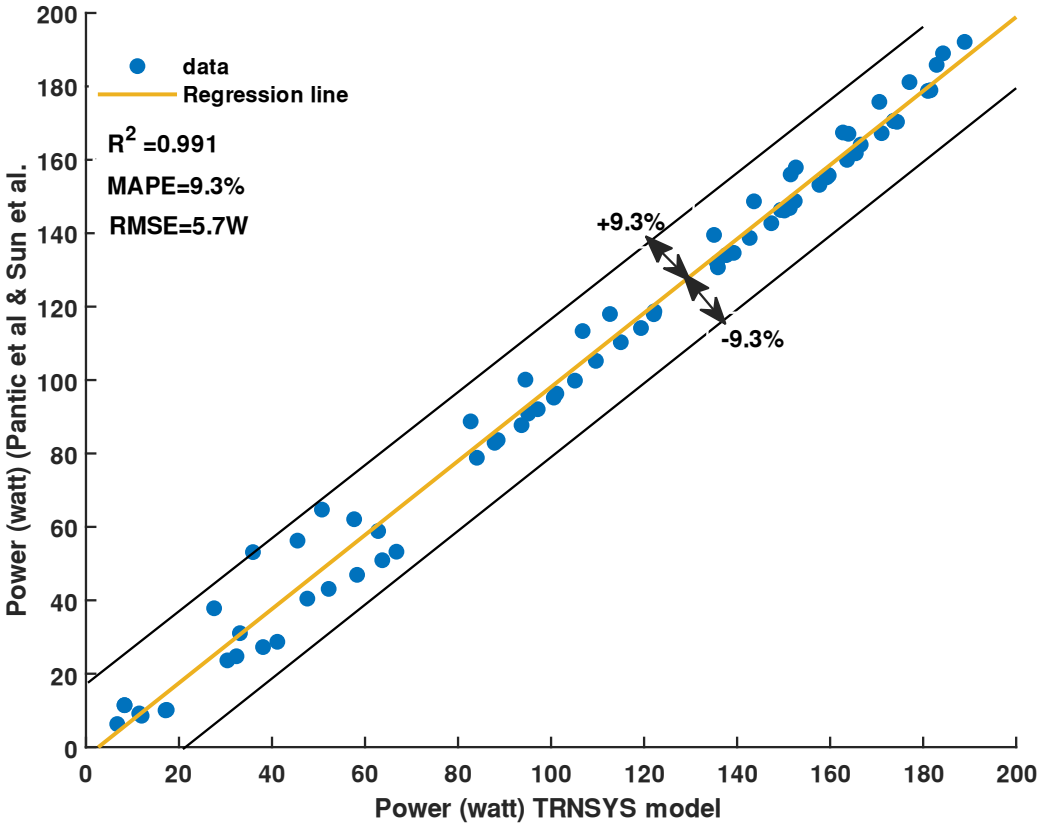


Figure 4.40. Statistical analysis of TRNSYS and Pantic et al.'s PVT model.

4.9.2 Experimental verification of the building model

The indoor temperature of a building zone significantly determines the amount of power required to cool or heat the zone to set-point comfort conditions. Therefore, to validate the 3D building model used to estimate the heating and cooling energy of the case study building, the building envelops zone ambient temperature was experimentally measured, and the measured temperature was statistically compared with the predicted zone temperature. The measured indoor temperature from 9/01/2020 to 12/01/2020 (see appendix section) was obtained using the Elitech GSP-6 Digital Temperature and Humidity Data Logger. The GSP-6 detachable dual probes device measures temperature from –40^{o}C to 65^{o}C with maximum accuracy up to ±0.6^{o}C. Figure 4.41 to Figure 4.43 compares the measured uncontrolled indoor building temperature with the predicted temperature from 9/01/2020 to 11/01/2020.

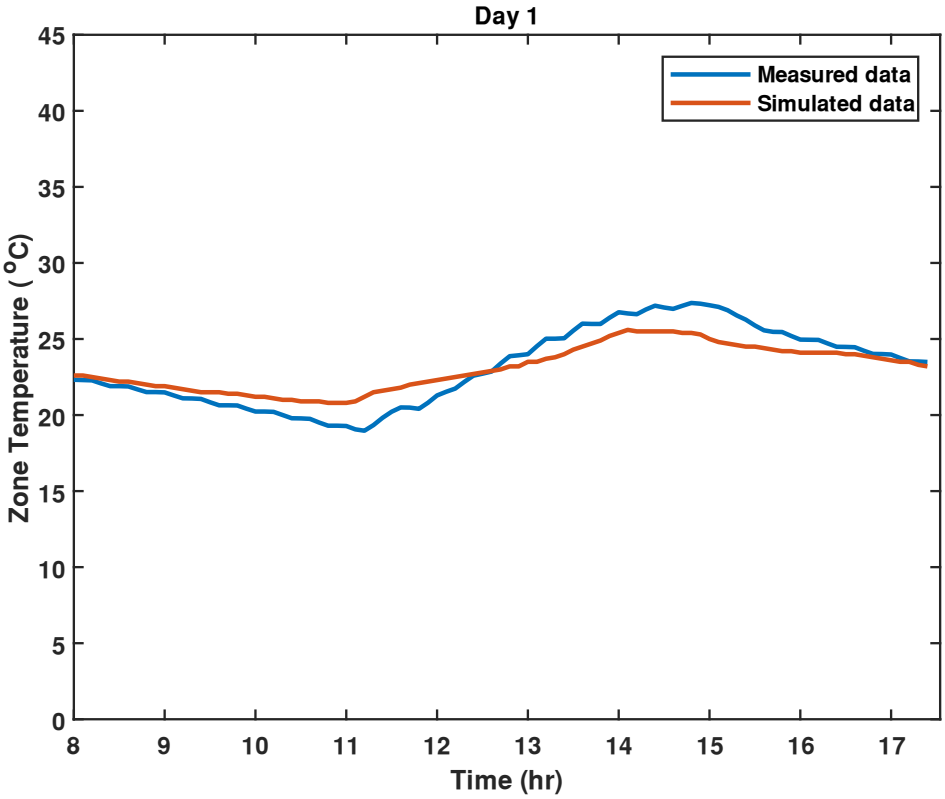


Figure 4.41. Comparison of the temperature of the case study building on 9th/01/ 2020

Even though the TRNSYS building model is seen to show a similar trend to the experimental results as seen in Figure 4.41 to Figure 4.43, a critical observation reveals that for the three days, the TRNSYS model consistently overestimated the zone temperature in the morning to about past noon and underestimate the zone temperature relative to the measured temperature from noon to about 5.00 pm. This observed difference in the predicted and the measured temperature (even though not much) is because the weather data used to drive the simulation are based on the Typical Meteorological Year data (TMY), which is the average data for more than 20 years.

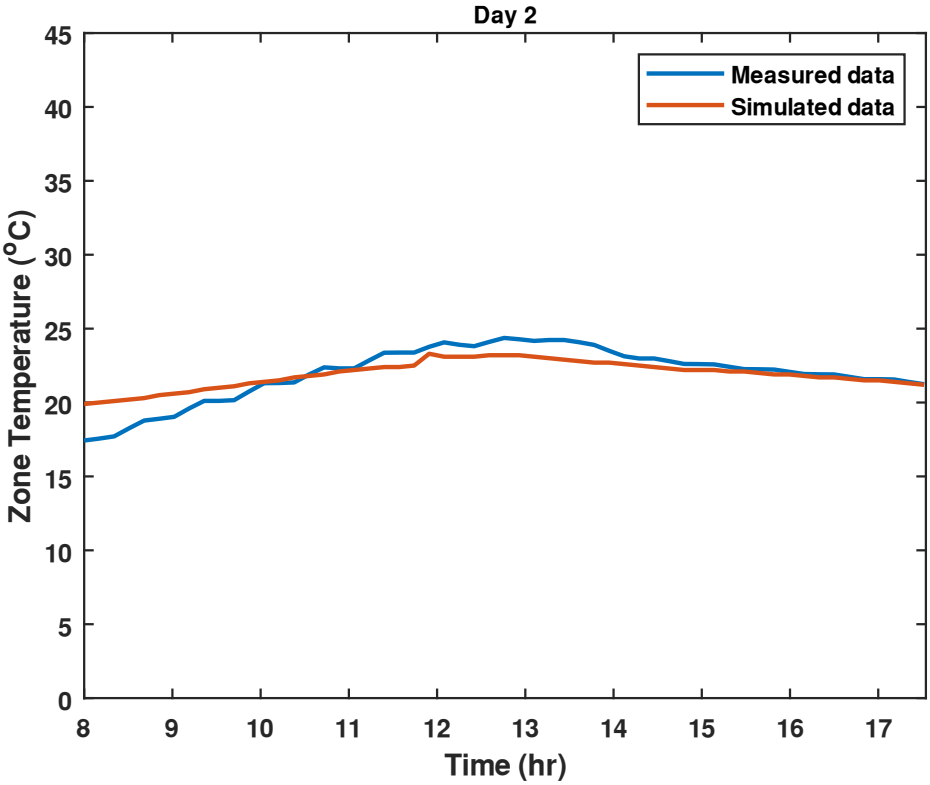


Figure 4.42 Comparison of the temperature of the case study building on 10th/01/ 2020

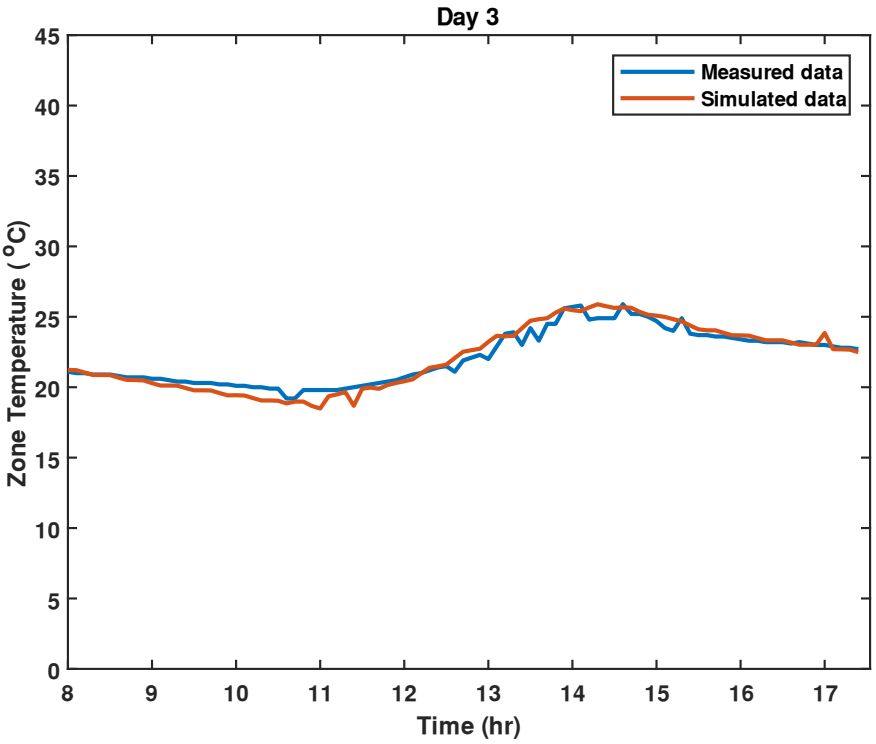


Figure 4.43. Comparison of the temperature of the case study building on 11th/01/ 2020

As observed in Figure 4.43, the gap between the predicted and the measured temperature is smaller than in Figure 4.41 and Figure 4.42. As a result, it implies that if the analysis and comparison are conducted for extended days, the average simulated temperature will better predict the actual building zone temperature. This assertion is evident, as seen in Figure 4.44. The analysis based on the three statistical tools shows that the RMSE is 0.955, indicating that the average error difference in the predicted and experimental zone temperature is less than 1^{o}C, with an average percentage error of about 3.4%. Notably, this has also remarkably explained why the percentage error in predicting the PVT power output using the TRNSYS Type 560 compared to the widely used PVT power model is as high as about 9.3%

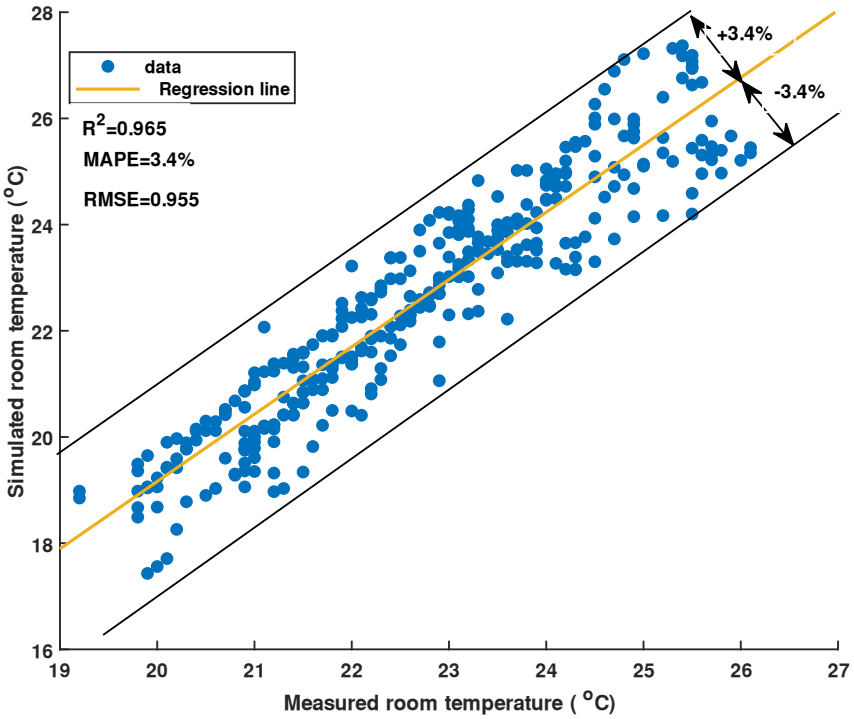


Figure 4.44. Analysis of simulated and measured building temperature

4.9.3 System model output and control logic

The formulated system model can equally be validated and verified based on the expected dynamic performance of the entire system coordinated and controlled based on the developed energy and flow control strategy, as explained in chapter 3. Figure 4.45 is the graphical representation of the dynamic characteristic of the modelled hybrid energy system under the weather conditions of the study case area. The overall power consumption (red line) includes power needed for cooling, heating, and operation of the health centre equipment. It also includes the hot water auxiliary power required to raise the temperature of the hot water to the desired temperature when the thermal collector cannot completely meet the hot water demand. The energy management and control strategy size the renewable power components to meet the load most reliably and economically.

For this reason, the Fellow-Electric-Load control strategy is implemented. Under this strategy, the renewable power component is sized to deliver sufficient power to meet the load. For periods where the excess power generated is unavoidable due to load mismatch, the excess generated is used to charge the battery. Grid power is only dispatched as the exact power required to meet the load completely for where the grid is available, and the energy from a renewable source is not sufficient to meet all demands. Notably, for the period that the grid is available, and the power from the PV module is not sufficient to meet load, the grid power is used to meet both electric load and charge battery when the battery state of charge is less than 100%. A careful observation of Figure 4.45 shows that the dynamic behaviour meets all the mentioned requirements indicated by the different parameters. From this Figure 4.45, the green line shows the power used to charge the battery storage. The battery is only discharged only in periods when the grid and PV power are not available, as evident by the downward decrease of the battery fraction stare of charge (FSOC) as shown in the graph. The power to the battery (green line) shows an exponential decrease when it is charged by the grid power. This behaviour is in fulfilment of charging with only 10% of the battery capacity to ensure a longer period of discharge. Overall, the dispatch control strategy is successfully implemented. Therefore, the developed model for the simulation of the actual system, to a reasonable extent, mimics the expected behaviour and control strategy

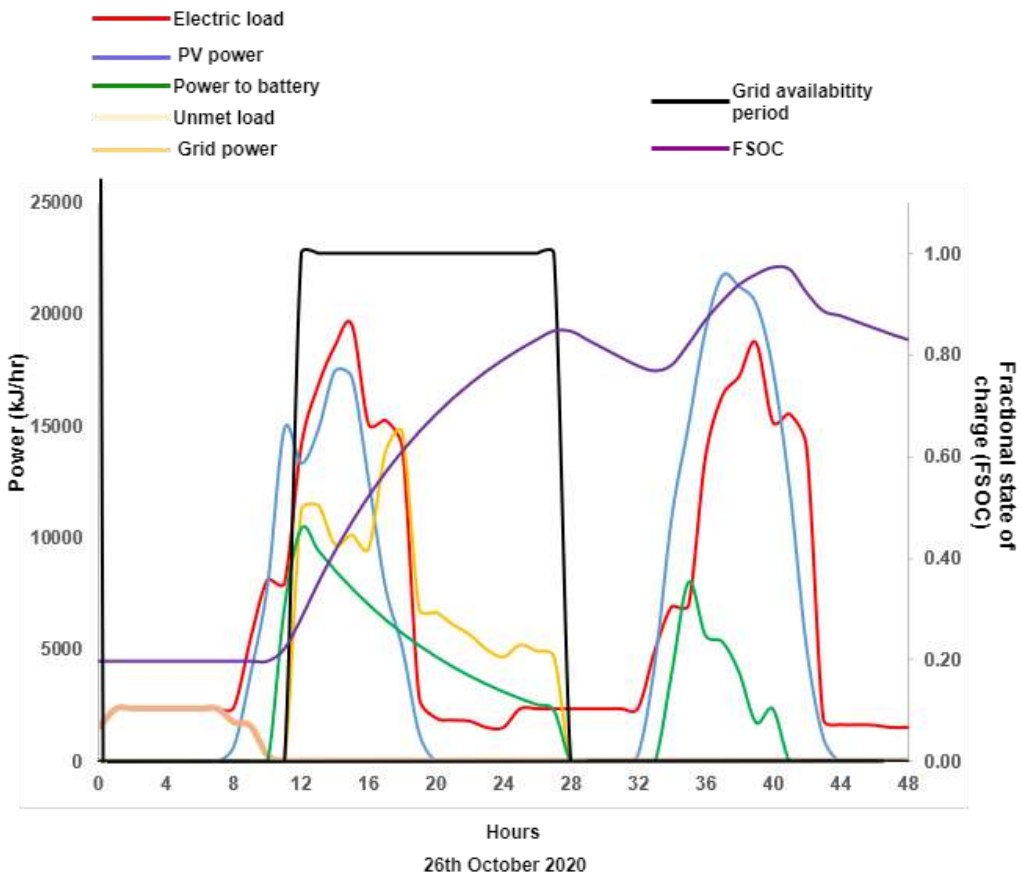


Figure 4.45. System behaviour on days with grid availability and grid outage

Furthermore, the battery is set to discharge a maximum of 80% of its capacity in prolonged grid outages corresponding to a period with poor PV power generation due to cloudy and overcast sky conditions. It is also evident in Figure 4.46 that this requirement is fulfilled. That is why in Figure 4.46, the line representing the unmet load is not flat but interestingly shows the amount of power required to completely meet the load for periods with insufficient power from the PV module. Remarkable and startling evidence that the system model work as needed is seen in point marked 'A' in Figure 4.46. It is clear from point 'A' that the moment the power generated from the PV is more than the load, the excess is used to charge the battery if the FSOC of the battery is less than 100%. This inspection can also help fine-tune until the desired condition is met based on the reliability and economic objectives.

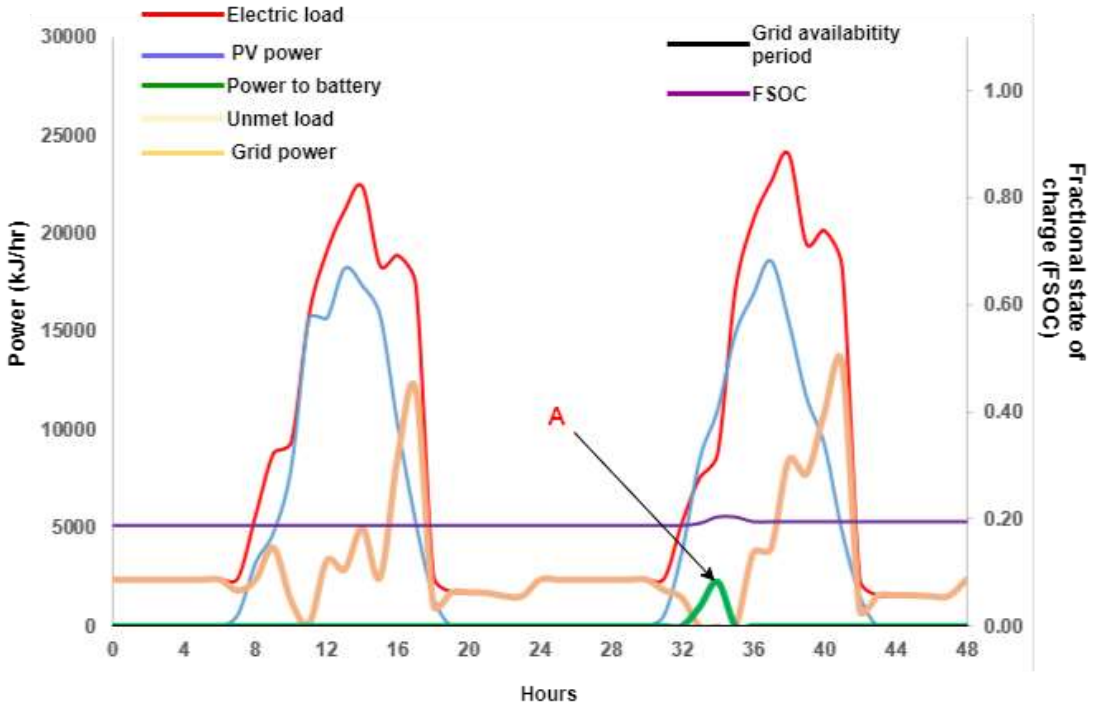


Figure 4.46. Dynamic behaviour of the system on days with no grid power

Another important control strategy proposed to fulfil the goal of this study is the effective control of the cooling water to meet both cooling of the PV module and demand for hot water with minimum consumption of pump power as the constraint. To achieve this goal, the proposed system is configured to be diverted at 2 points (i.e., diverters 1 and 2) to ensure that the appropriate flow rate is diverted to satisfactorily meet the flow rate necessary to meet the separated hot water demand. The separation of hot water demand met at different temperatures, and flow rates is a new method to improve the thermal solar fraction of solar water heaters published as part of this research work [177]. In this paper, it was demonstrated that this novel configuration, which meets the hot water demand for different services at their different required temperatures, is advantageous and that it increased the thermal solar fraction of hot water met by the solar collector by about 27% when compared to the case where the different hot water demand is supplied at a single delivered hot water temperature, as is common in most solar thermal water heating systems. For this study, the variable speed pump is programmed to

deliver the water required for cooling the PVT collector at a rate that results in a temperature difference of about 50^{o}C between the PVT collector water inlet and out. For this flow control, the variable speed pump is required to increase the cooling water flow rate on days with high solar energy to maintain the PV module's temperature at the design 50^{o}C. This control is evident in Figure 4.47 and Figure 4.48. the flow rate is about 50% higher in Figure 4.47 than in Figure 4.48. The implication of this strategy is the maintenance of the PV module temperature at about constant temperature, ensuring higher electrical efficiency and supplying water at minimum temperature for postnatal services in the health centre.

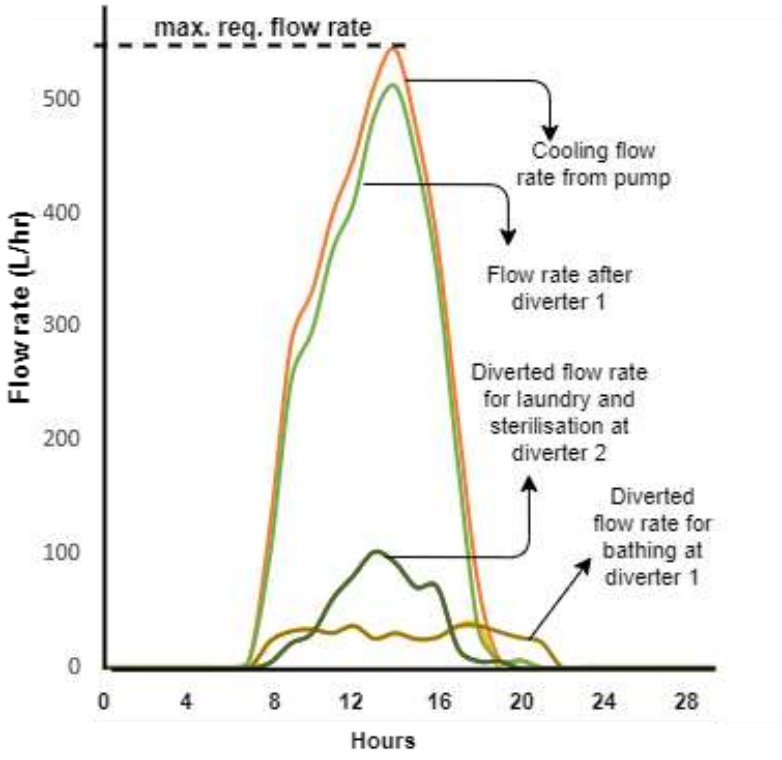


Figure 4.47. Dynamic cooling water flow characteristic on a day with good irradiance

This way, the dual objective of meeting both thermal and power demand is achieved with minimum compromise in the power output of the PV module. Importantly, the flow rate required for postnatal and sterilisation services must be controlled at diverter 1 and 2. From

both Figure 4.47 and Figure 4.48, it is evident that the flow control strategy is delivering the right dynamic behaviour.

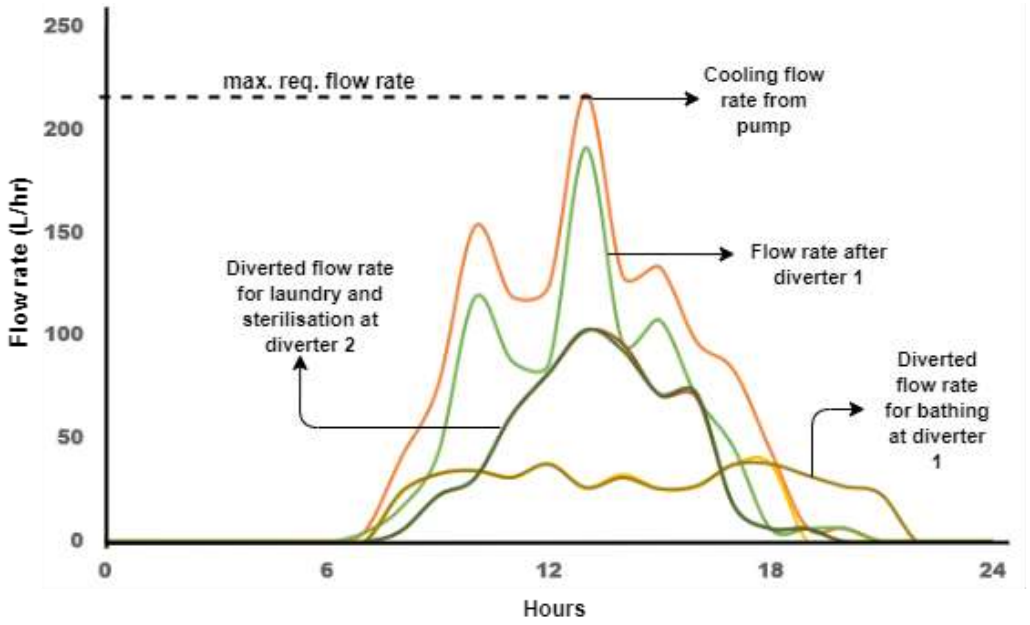


Figure 4.48.Dynamic cooling water flow characteristic on days with low irradiance

4.9.4 System model energy balance analysis

For energy system modelling with the target of meeting a specific load, the model requirement is that the energy supply across all system boundaries should be balanced. This requirement is to check if the model is appropriately set up regarding power supply and demand. Table 4.12 is the monthly and annual summary of the energy balance error obtained from the energy balance subroutine (Type 28) based on the electrical energy flows across the system boundary. From Table 4.12, the difference between all electrical gains and losses across the system boundary is 1.28%. This value is below the 2% tolerance benchmark, implying that the model is appropriately set up with not much excess electrical energy introduced into the system.

Similarly, Table 4.13 shows an energy balance error of 1.49%, implying that the components are appropriately sized and modelled to meet the thermal load with not much excess thermal energy introduced into the system. On the other hand, it equally implies that the energy sources are not undersized, resulting in system unreliability.

Table 4.12. Analysis of the formulated model power energy balance

Months	Gains (kWh/month)				Losses (kWh/month)			
	Diesel power	PVT power	Grid power	Power to battery	Electrical Load	Battery power to load	Dumped energy	Energy balance (%)
Jan	4.6	1363.6	194.1	282.1	1364.2	227.1	115.7	1.54
Feb	31.1	1128.9	227.6	284.9	1273.9	270.0	76.2	1.38
Mar	38.9	1263.4	324.1	349.4	1546.5	347.2	52.4	1.29
Apr	10.1	1392.5	270.3	349.5	1508.7	296.6	83.5	1.43
May	176.3	1116.5	303.5	303.2	1584.2	314.5	0.9	1.18
Jun	173.5	975.9	392.1	330.8	1497.6	307.7	1.2	1.07
Jul	94.0	952.0	499.8	360.0	1492.3	355.9	30.0	1.02
Aug	177.1	922.9	446.5	335.1	1504.3	331.2	19.7	1.00
Sep	138.6	1078.3	333.0	348.0	1437.0	309.5	52.6	1.18
Oct	126.6	1169.5	318.8	314.4	1507.0	293.3	63.3	1.24
Nov	0.0	1457.3	130.5	311.2	1380.5	292.4	159.3	1.56
Dec	0.0	1345.5	204.7	291.4	1365.4	263.7	130.2	1.50
Sum	**970.8**	**14166.1**	**3645.1**	**3860.0**	**17461.6**	**3609.0**	**784.8**	**1.28**

Table 4.13. Analysis of the formulated model thermal energy balance

Months	Gains (kWh/month)		Losses (kWh/month)				
	Collector thermal gain	Auxiliary heat	Thermal load	Tank loss	Pipe loss	Internal energy	Energy balance (%)
Jan	4645.35	63.74	4518.01	103.50	1.36	0.0081	1.85
Feb	3895.36	73.41	3817.31	92.32	1.26	0.0000	1.47
Mar	4487.57	87.56	4367.05	105.34	1.48	0.0008	2.24
Apr	4979.88	39.14	4759.34	113.47	1.49	0.0012	2.93
May	3597.17	121.45	3600.80	96.57	1.52	0.0009	0.53
Jun	2934.76	198.90	3035.48	83.07	1.44	0.0000	0.44
Jul	2691.36	253.32	2867.83	80.71	1.45	0.0005	0.18
Aug	2591.38	292.06	2809.87	76.73	1.42	0.0005	0.16
Sep	3359.81	193.29	3415.67	89.21	1.41	0.0005	1.33
Oct	3836.80	118.84	3827.20	95.49	1.48	0.0004	0.80
Nov	5119.98	32.98	4903.79	105.54	1.41	0.0005	2.80
Dec	4579.71	55.31	4450.56	103.80	1.37	0.0016	1.73
Summary	**46719.12**	**1530.01**	**46372.92**	**1145.76**	**17.09**	**0.0056**	**1.49**

4.10 Results and discussion of economic assessment

One major barrier to the rapid deployment of renewable energy technologies, especially photovoltaic -solar thermal hybrid energy systems, in meeting energy demand in buildings is the high initial investment and long-term payback period. Because of the unfavourable economic prognosis for the renewable energy system, investing in this technology is considered a high-risk adventure. Therefore, the economic performance indicators of renewable energy systems are major decision variables for both end-users, investors, and policymakers alike. As already mentioned in the methodology section, the diesel generator set is the baseline for the economic analysis since it is the energy system operated in rural communities with poor access to electric power and the power system used in our case study health centre as back-up. The economic analysis compares the proposed energy system with the basic hybrid PVT energy system from the investment stage, breaking it down into component-by-component initial cost analysis. Furthermore, the analysis includes a detailed comparison of the total operating cost

and replacement cost. Finally, both systems are compared based on vital economic indicators, which are the basis for important economic decisions for end-users and key stakeholders.

4.10.1 Components cost and system economic parameters

The methodology established earlier in section 3.14 of this research is the basis of the economic model developed and integrated with the system models in TRNSYS. The economic model developed as part of the system model receives inputs from the simulated performance, the annual system energy saving (solar fraction), the amount of power used from the grid, and a diesel generator to service the load to compute the economics of the systems. Other inputs in the economic model are the economic variables based on the study location and the unit cost of each component that constitutes the energy system. Table 4.14 shows the cost of each component of the energy system. As observed in Table 4.14, the proposed OPVETC system configuration has a slightly higher number of components to achieve the functionality desired in this study. Notably, the number of PVT collectors in the basic system is 2 more than that of the OPVETC system. The reason for the additional 2 no. of PVT collectors is to equal the total solar collector area since the OPVETC has, in addition, the ETC collector integrated as part of the new configuration.

Table 4.14:System components and the current market prices of system components

SN	Parameter	Qty Basic PVT	Qty OPVETC	Unit cost (USD)	Reference
1	PVT collectors (1.63m$^{2)}$	35	33	480	[236] [237][32]
2	ETC (1.63 m^2)	-	2	295	
3	Hot water tank (0.3 m^3)	1	2	380	[238]
4	Diverters	1	2	11.8	[238]
5	Pumps (170kg/hr discharge) 100watt, 12 meters head	1	2	6	[238]
6	Controller	2	2	210	[238]
7	Battery (75Amp, 24volts)	15	15	380	
8`	Inverters (8kW)	1	1	960	[24]
9	Gen set 20 kW	1	1	1580	[238]
10	Installation cost			$0.1 \times Cost_{PVT}$	[159]

Therefore, the total initial cost of OPVETC system configuration is slightly higher than that of the basic PVT system architecture, as seen in Figure 4.49. Even though the two system architectures differ in the number of components, the analysis of the initial investment show close similarity in the capital investment and the percentage of each component cost, as seen in Figure 4.49. Consequently, Figure 4.49 confirms that the systems are identical with the same initial investment, making it appropriate to compare both system architectures.

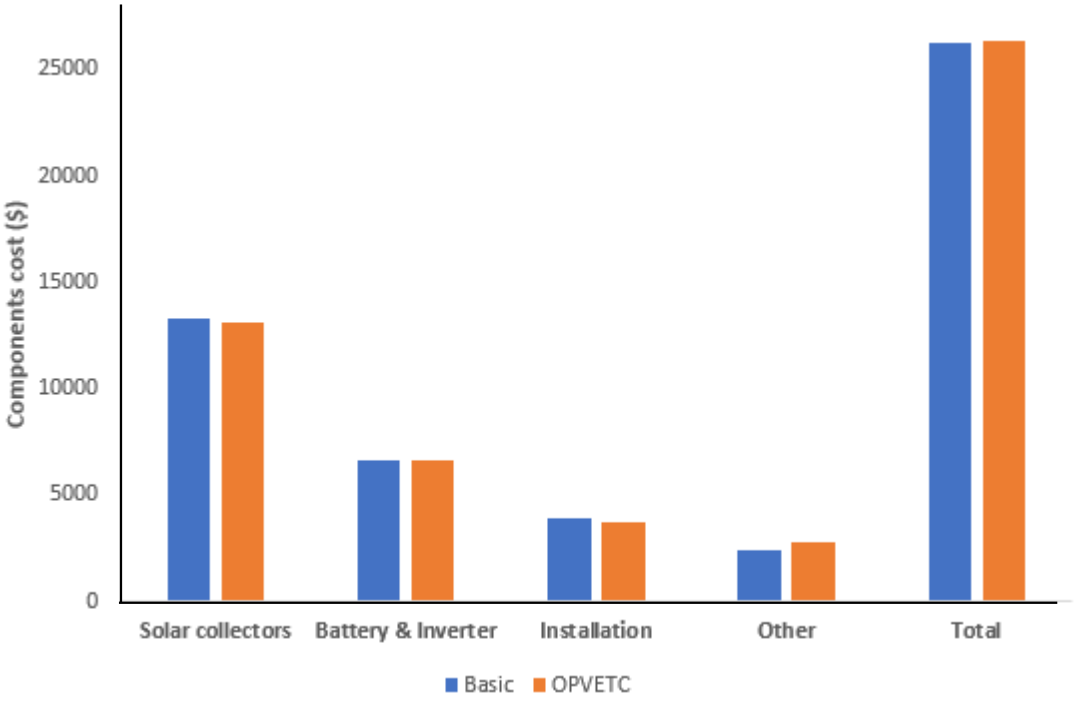


Figure 4.49. Comparison of system components cost

Table 4.15 shows some standard and local economic variables used in assessing the economics of the energy systems. Table 4.14and Table 4.15 form the constant inputs to the economic model developed and integrated with the simulation model in the TRNSYS simulation environment.

Table 4.15: Parameters for system economics and CO_2 impact

SN	Economic index	Value	Unit	Reference
1	Inflation rate	14	%	[6]
2	Annual discount rate	6	%	[6]
3	Degradation factor	0.5	%	[238] [239]
4	Cost of diesel fuel	0.48	$/L	[240]
5	Cost of grid power	0.10	$/kWh	[238]
6	Battery lifetime	5	years	[236] [241]
7	inverter lifetime	10	years	[236] [242]
8`	Diesel gen lifetime	15000	hours	[242]
9	Gen. maintenance rate	0.05	$/kWh	[242]
10	CO_2 per litre of diesel	2.6	Kg/L	[243]
11	The reference baseline LCOE	0.2456 (Diesel generator)	$/kWh	[244] [245]

The component's lifetime indicates the number of times the components are replaced before the entire project lifetime of 25 years, as typical with most photovoltaic energy systems [246]. Consequently, from Table 4.15, the battery storage is replaced four times before the expiration of the project's lifetime. Similarly, the inverter component is replaced twice, i.e., first in the 10th year and the 20th year after the start of the project. When calculating the replacement cost, the inflation and the present value interest factor are used. As seen in Table 4.15, the inflation rate is double-digit, and it is assumed to remain unchanged for the period of analysis of this study.

4.10.2 Component replacement cost

Unlike energy projects with a short life, photovoltaic collectors have a very long useful life. However, other components used along with the collector do not have a long life as the PVT collector. Therefore, these components will have to be replaced in some cases more than twice before the expiration of the project lifetime. Figure 4.50 compares the replacement cost of components of the two system architectures. The battery replacement cost constitutes above 80% of the replacement cost for both system configurations. This result implies that the battery storage cost significantly influences the system life cycle cost, as revealed even in the study conducted by [160]. Again, it is observed from Figure 4.50 that in the OPVETC system architecture, the generator is not replaced during the lifetime of the entire project, whereas in the basic PVT system configuration, the generator is replaced before the end of the project life. The non-replacement of the diesel generator in the proposed system shows that the hours of usage of the diesel generator did not exceed the generator's lifetime in the OPVETC configuration. Even though the OPVETC has a higher cost of other components than the basic system architecture, as seen in Figure 4.49, its total replacement cost is lower due to using the

generator less frequently and no replacement for the entire project lifetime. The major replacement (i.e., replacement of the battery, inverter, and generator set) costs are incurred for both systems in the 5th, 10th, 15th, and 20th years. Notably, the replacement cost all year for both system configurations increases as the project lifetime increases. The cost is the same except in the 15th year. This year, the generator is replaced for the basic PVT with no replacement for the OPVETC system architecture.

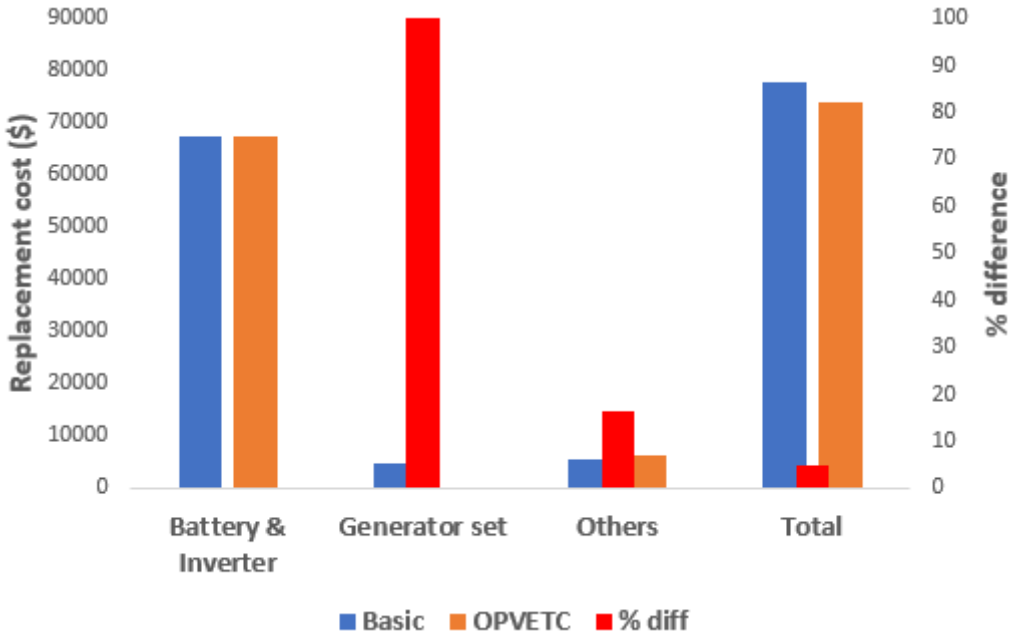


Figure 4.50. Component's replacement cost

Minor system components such as the solar pump and diverters are replaced annually in this study. Since the minor cost is by far less than the major replacement cost, the advantage of fewer components in the basic PVT configuration does not cover the benefit of no replacement of the generator set in the OPVETC configuration. Hence, the benefit of the lower total replacement cost of the OPVETC over the basic PVT configuration is depicted in Figure 4.50, as the percentage difference is shown by the red bar.

4.10.3 Evaluating the system operating costs

The system operating costs are expenses incurred in operating the system to ensure power demand is made satisfactorily and the energy system's capacity is prevented from fast deteriorating throughout the project life. These costs include the fuel cost and maintenance for the diesel backup, the cost of power purchased from the grid and the overall yearly cleaning of the collector surface to remove dust and dirt that may shade the radiation from the collector. Figure 4.51 shows that the operating cost of the basic hybrid system configuration is higher for all three operating costs. For the fuel cost, the cost is higher for the basic system since it has higher unmet power demand that the backup generator is used to service the load. Meeting this unmet load will consume higher fuel, and the hours of usage of the generator will be higher and hence more frequent services and repairs as reflected in the O&M cost in Figure 4.51. Overall, the total operation cost of the OPVETC hybrid energy system is about 48% lower than that of the basic hybrid PVT system.

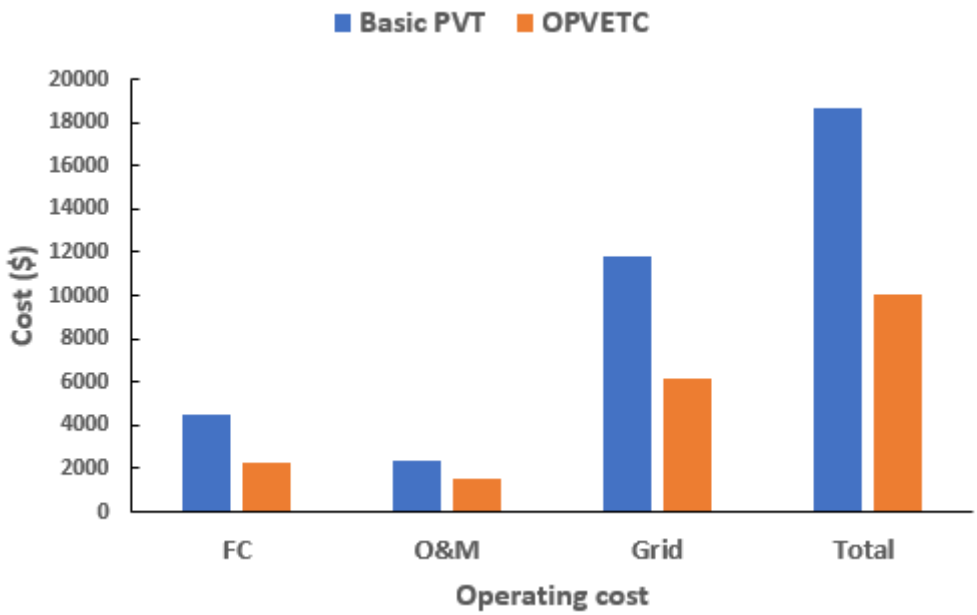


Figure 4.51. Comparison of operating costs between the OPVETC and basic PVT

The system operating cost is important to both the end-user and the investor since it represents the expenses incurred after the initial capital investment. For a decision on an alternative energy system, end-users will prefer power installations with lower operating costs since lower operating costs result in better net cash flow.

4.10.4 Analysis of project Net present Value (NPV)

The project cash flow diagram is the yearly net difference between the revenue and the project's expenditure during the project's entire lifetime represented on a life cycle timeline of the project. Positive values on the graph show revenue, while negative values on the diagram indicate expenses. The cash flow analysis is employed in this study to compare the cash flow of the proposed reconfiguration with the basic PVT configuration. Figure 4.52 shows the cash flow associated with the basic PVT and OPVETC system architectures. As seen from the graph, the basic hybrid PVT configuration has annual revenue of $4.472, while the OPVETC prove to have higher annual revenue of $5,168. This result means that the inclusion of the ETC and the open-loop cooling technique of the OPVETC system architecture has improved the system's annual revenue by about 15.5% higher than the basic system architecture cooled based on the traditional flow control technique. This result is expected since the OPVETC configuration from the technical evaluation shows better energy saving which is the source of the annual revenue for the project. As observed from Figure 4.52, the downward bars indicate major expenses incurred in the 5th, 10th, 15th, and 20th years to replace worn-out system components. It was observed that the expenditure increases as the project lifetime increases. Notably, the expenses for the basic PVT during the entire life are, on average, 17.75% higher than that of the OPVETC system architecture. As already established, the considerable difference in the expenses between the basic PVT and OPVETC configuration in the 15^{th} year results from replacing the diesel generator set in the basic PVT configuration. It is seen from

Figure 4.52 that there is a significant spike in revenue for both system configurations in the 25th year of the project. This spike in revenue results from the sale of residual project components at the end of the project life. Again, the higher revenue of the OPVETC configuration is a result of the higher energy savings of the system due to the proposed cooling configuration and method.

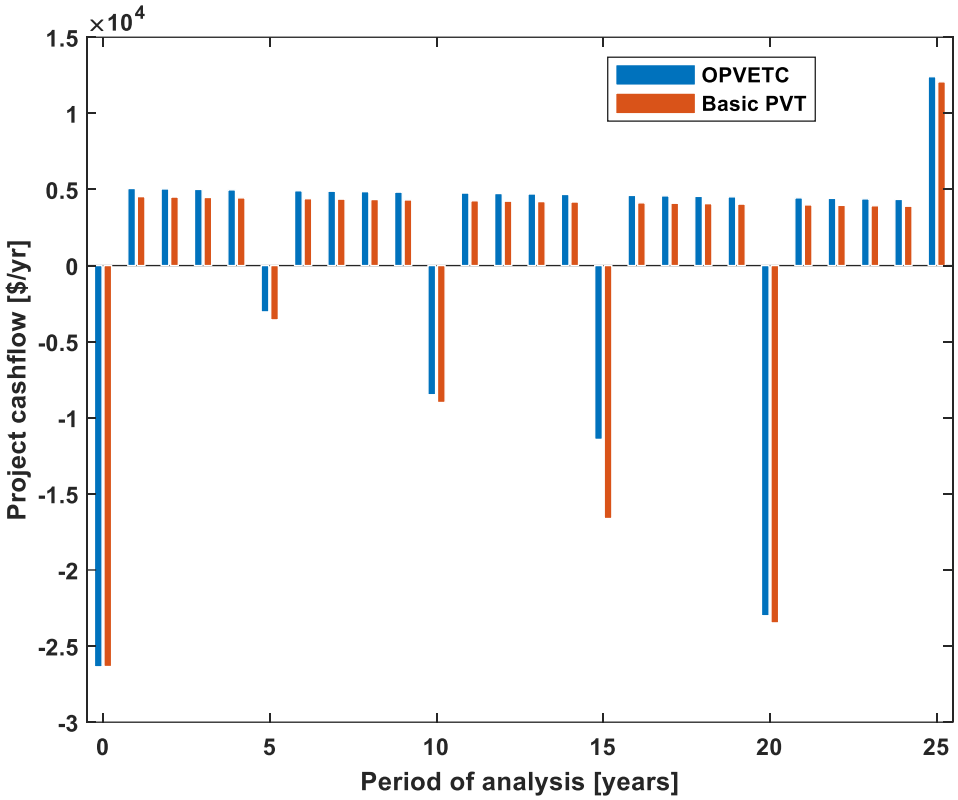


Figure 4.52. Comparison of the basic PVT and OPVETC cash flow

The cumulative cash flow diagram is another way of examining the worth of the project at a specific period for the entire duration of the project lifetime. Figure 4.53 compares the cumulative cash flow of the basic PVT and the proposed OPVETC system architecture. As observed from Figure 4.53, the net present worth (NPV) is negative for both configurations in the early part of the project lifetime before the payback period. This implies that the project profitability starts only after a minimum of six years for both configurations. Importantly, the

net worth of the project declines at any time the components are replaced. As observed, the net present worth of the OPVETC configuration at the end of the project lifetime is $36,985, and that of the basic PVT architecture is $17,359. These values imply that the novel reconfiguration and energy system integration has increased the system's net worth by about 130% relative to the system's worth based on the much-consolidated basic system configuration. For rational economic decisions, the proposed system will be preferred since it's even twice more viable than the basic system configuration.

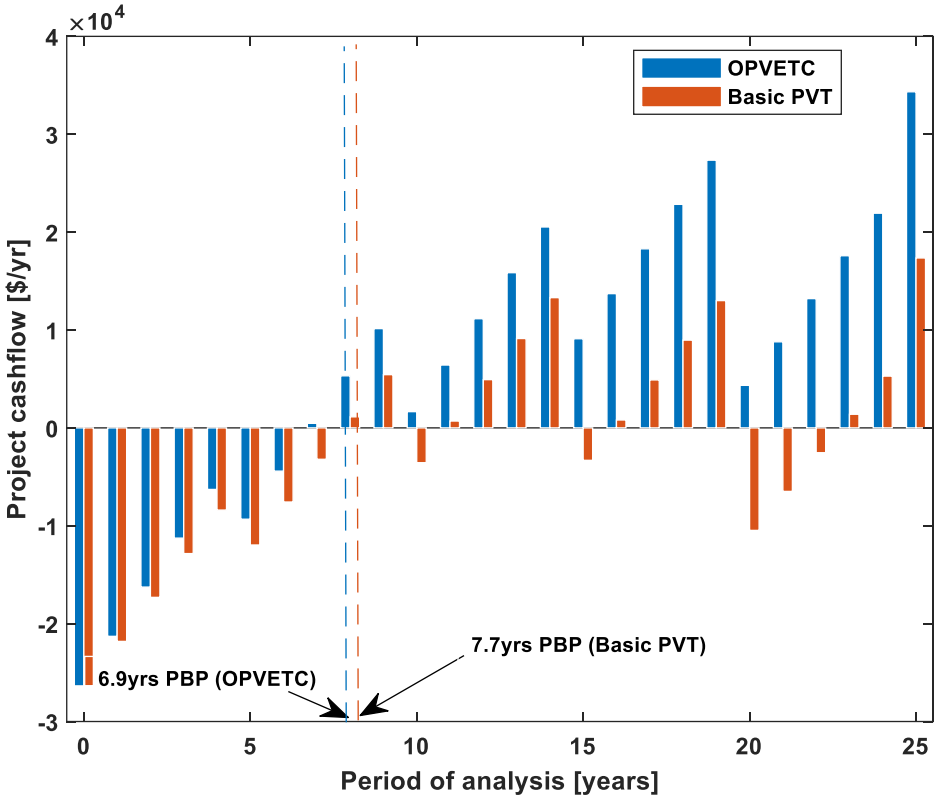


Figure 4.53. Comparison of the basic PVT and OPVETC cumulative cash flow

A critical observation of Figure 4.53 shows that the basic hybrid PVT net worth still drops to negative values in the 10th, 15^{th,} and 20th years even after the project had paid back its initial investment in the 7th year of the start of the project. This drop in the net worth of the project in these years is a result of the replacement cost of the battery every five years, the inverter every

10 years, and the diesel generator in the 10th year. Remarkably, the NPV after the battery is replaced in the 10th year and the battery and the inverter are replaced in the 15th year takes only one year to return to a positive value. This observation is explained by the fact that the yearly revenue from the sale of the energy saved was enough to offset the replacement cost of the battery within one year. However, in the 20th year, when the battery, the inverter and the generator set were replaced, the NPV returned to a positive value only after three 3 years. This observation is also because the yearly revenue from the energy savings cannot easily offset the expenses in the 20th year, so it took 3 years to recover.

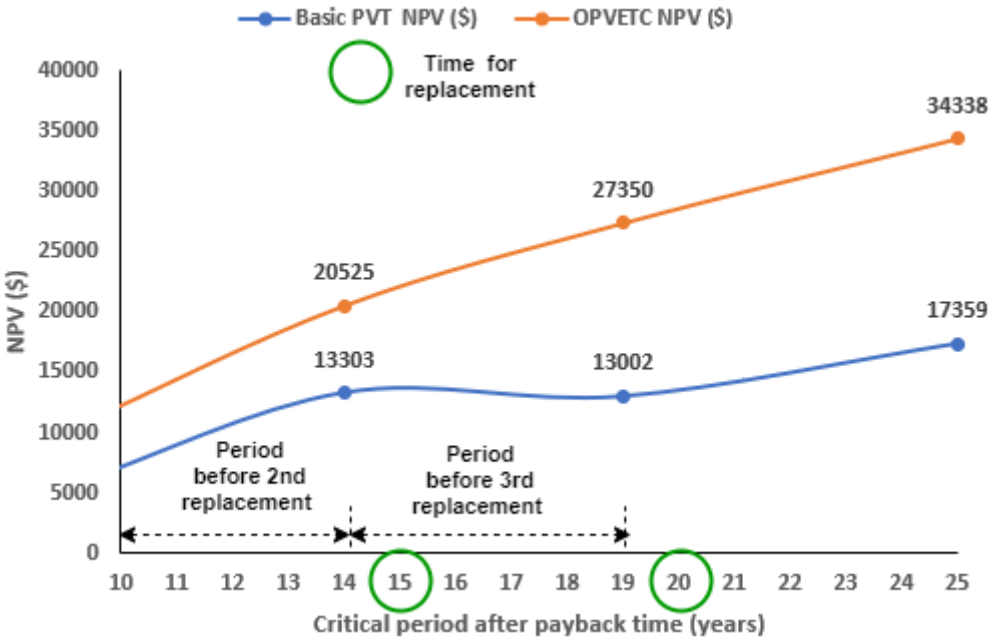


Figure 4.54. The net worth of the project based on different periods of analysis

A startling revelation reveals that the net present value (NPV) of the basic hybrid PVT in the 14th year is $13,303, while it is $13,002 in the 19th year, demonstrating that the project's net worth has not only remained constant but has also decreased by approximately 2.2% when compared to its worth in the 14th year. In this case, the continuous investment beyond the 14th year in the case of the basic configuration is a critical decision that must be considered carefully

since the net worth will only improve significantly after 10years, as seen in Figure 4.54. OPVETC hybrid energy system, on the other hand, exhibits a consistent increase in the net present value (NPV) throughout the same period, as illustrated in Figure 4.54. These findings demonstrate that the proposed cooling and system architecture improves the technical performance of a hybrid PVT energy system and increases the system's lifetime while maintaining good economic viability even beyond the 25-year life span that is typically assumed for PVT collectors in most analyses.

4.10.5 Project Payback Time (PBT) and Return on Investment (ROI)

The project payback time is when the investment in the energy system is at risk. In contrast, the ROI indicates the returns relative to the investment. In most cases, choosing an energy system among different alternatives may require combining more than one indicator to arrive at a final decision. These indicators are gauged against the acceptable standard for rational choice. Figure 4.53 shows the net cash flow (NPV) time frame analysis for both energy systems. A cumulative cash flow analysis indicated for both systems in Figure 4.53 shows the point on the time axis where the positive incremental cash flow marks the payback period. The graph shows that the cumulative cash is negative from year zero until 6.9years and 7.7 years for both the OPVETC and the basic PVT, respectively. A payback period of 6.9 and 7.7yrs demonstrates that the risk in investment in both alternative configurations is remarkably lower than 11.2 years as in Ref. [157], and 12years in Ref.[36] for similar technologies in Osmar and Cyprus, respectively. This finding is a contribution that reveals the business potential in adopting this technology, particularly the OPVETC configuration, especially in health centres where the demand for both hot water and power is considerably high. Overall, the analysis shows that the payback time for the basic hybrid system configuration is reduced, and its economy is better if integrated with the evacuated tube, as demonstrated in this study.

Since the payback time does not say anything further about project returns after payback time, it does not conclusively suggest that one project is economically and environmentally better. Therefore, further analysis is required to compare energy projects with close payback time. Figure 4.55 is the return-on-investment (ROI) of both hybrid energy systems.

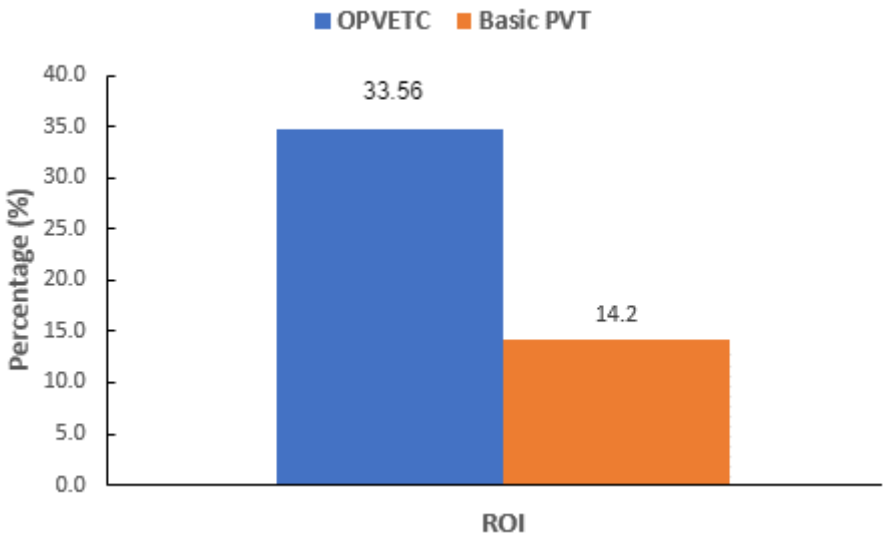


Figure 4.55. Comparison of ROI between the basic and OPVETC

Again, this study shows that cooling the PVT collector, as proposed here in this study, has significantly increased the ROI of the traditional PVT hybrid energy system from 14.17% to 33.56%, representing an improvement of over 100% in the profitability of basic PVT configuration. Since initial investment in each configuration is about the same, it is therefore revealed in this study that the proposed integration and cooling method improves the business scenes of photovoltaic hybrid energy systems.

4.10.6 Levelised Cost of Energy (LCOE)

The LCOE is an indicator that indicates the kWh cost of energy produced from the energy system. For business purposes, the LCOE is the unit kWh cost at which energy produced from energy systems must be sold to make any profit. Therefore, for an investor, the LCOE of any

energy system is compared with other alternative systems for the decision to invest or not to invest. The proposed system configuration and the basic hybrid system architecture have LCOE of $0.154/kWh and $0.165/kWh, respectively, and as demonstrated in Figure 4.56, the LCOEs are both higher than that of the grid in the study location, indicating that PVT energy technology in the study location has not reached parity. In most cases, an individual decision to accept an alternative technology is mostly considered relative to the unit cost of energy from the grid. However, in this case, both the basic and the OPVETC system configuration are economically viable alternatives compared to the diesel generator, whose LCOE ranges between $0.24/kWh to $0.33/kWh and, for now, the most preferred since grid power in this location is unreliable and grossly inadequate to meet with demand [245][247].

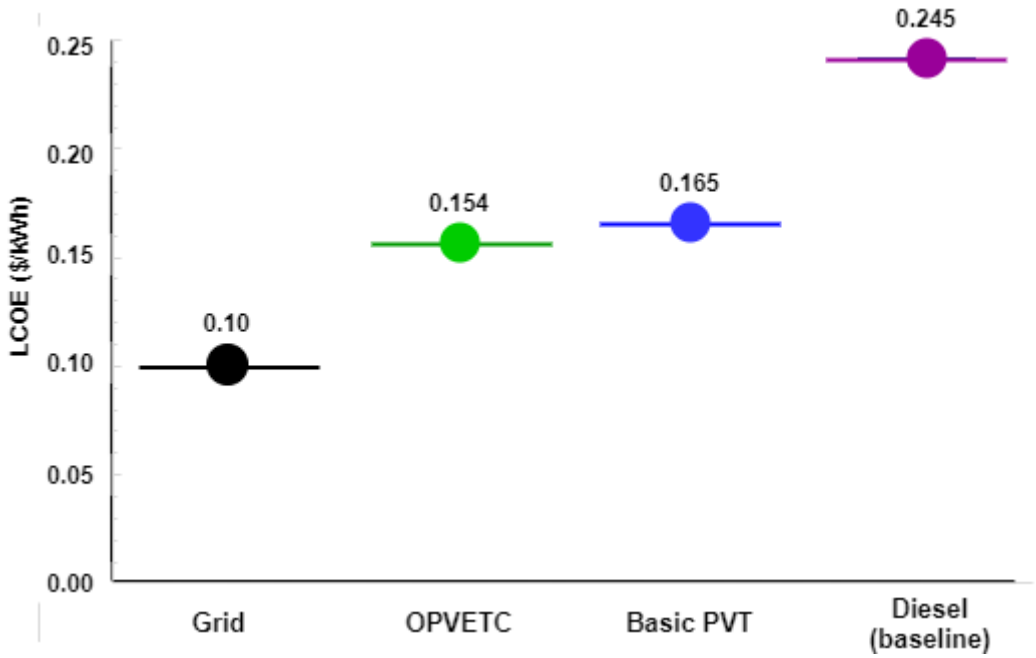


Figure 4.56. Comparison of the OPVETC, Grid and diesel generator LCOE

Since the Levelised cost of energy from diesel generators (the base case energy scenario) is higher than the minimum cost of $0.154/kWh of energy produced from the proposed system integration, the proposed energy option is an attractive option considering the business outlook. One of the goals of this study is to increase energy access in energy-constrained communities;

the proposed energy system is a reliable energy source and a more economical and sustainable energy option for a health centre in remote communities. In general, the economic matrices of both the basic and OPVETC hybrid systems as evaluated are within a reasonable and acceptable range that points to the acceptance of the energy project with good sustainability and environmental protection. Notwithstanding, the OPVETC hybrid energy system has shown superior performance both technically, environmentally, and economically than the basic hybrid PVT system architecture cooled based on the traditional method cooling based on the close lose cooling technique

4.11 Economic sensitivity analysis of proposed system

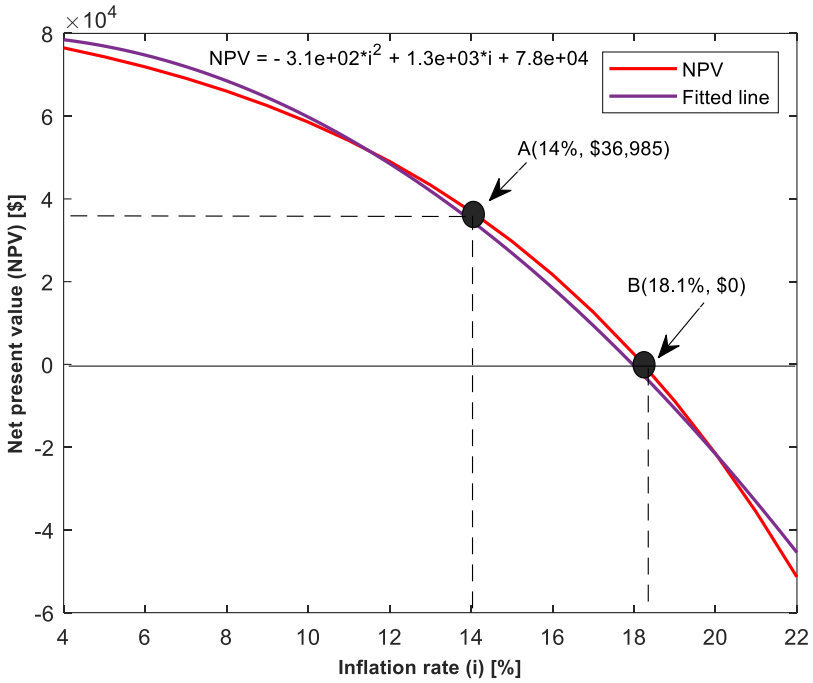
The economic indices used in the current economic study are based on the values in effect when the research was conducted. If these economic indices shift in any direction, one question that may arise is, 'what happens if they change in either direction?". Therefore, an economic viability analysis of the energy project's susceptibility to change in these economic indices is necessary. In the next subsection, the impact of changes in inflation, which determines changes in the cost of system components and the operating cost, is analysed in relation to some key economic indicators. The key input to the economic sensitivity analysis performed in MATLAB environment are the technical performance outputs of the both the basic hybrid PVT and the OPVETC obtained from the system model developed. The In Furthermore, because this system is primarily intended for use in healthcare facilities, the end-user (healthcare institutions) may choose to implement it based on the volume of hot water that they require. As a result, the sensitivity study also includes the effect of a change in the volume of the hot water demand on the system's economic performance.

4.11.1 Change in inflation rate

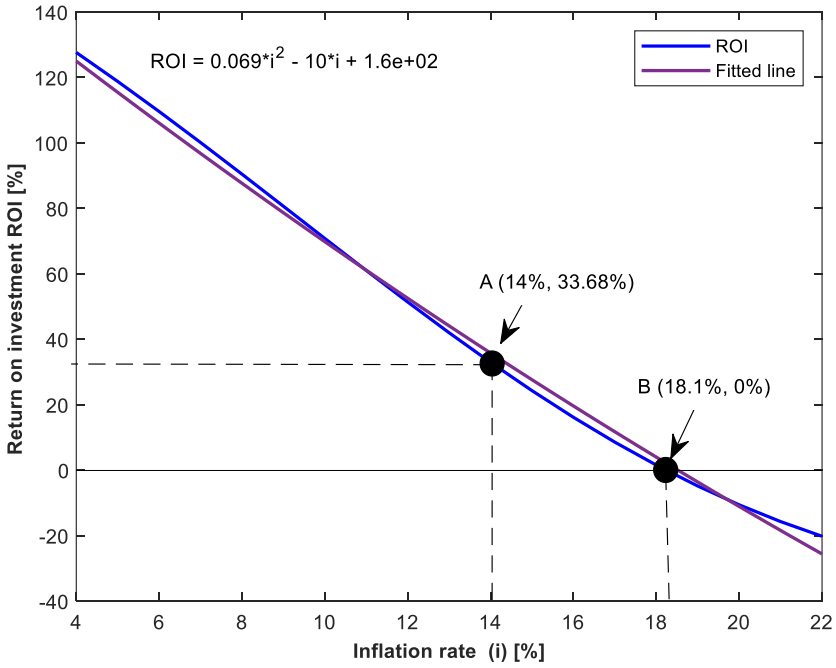
Energy project economic and environmental benefits are major factors influencing government, individual, and business person decision to accept or reject a project proposal [248]. Ironically, the future economic benefit evaluation is based on the long run. However, this future benefit may be susceptible to changes due to fluctuations in the market prices of goods due to inflation. It is, therefore, necessary to evaluate the effect of this uncertainty in the market price on the project's economic benefit for better decision-making considering the possibility of risk in the future. Figure 4.57 shows the sensitivity and the effect of inflation on the NPV and the ROI. At the current condition, denoted by the letter 'A' in Figure 5.9, the net present value (NPV) is $36,985 at the current inflation rate of 14%, resulting in an ROI of 33%. NPV worth of the energy system will decline as the inflation rate moves to the right of point A towards point B. On the other hand, as the inflation rate moves to the left of point A, the system economy improves. Judging based on the net worth of the energy project and taking into account the quick payback time of below 8 years as already stated, this energy system is worth considering for meeting residential building energy demand since the predominant energy demand in the building is power and hot water demand.

For quick evaluation of the business outlook of the energy system at any inflation rate, the NPV and ROI models based on the inflation rate are developed, as seen in Figure 4.57. These models are economic models that are useful for the quick rational decision on the risk of investment since the inflation rate is bound to change for a country with an unstable economy, especially a developing country like Nigeria. Overall, since the economic evaluation was assessed based on a change in inflation rate per year of 14%, it will be necessary to maintain this rate or, at worst, keep the percentage increase to at most 0.1% per year to make the investment in this project attractive. If inflation rises by more than 0.1% above the previous year's rate, the

project's net worth will quickly deteriorate to negative values before the project's life, resulting in a massive loss of investment.



(a)



(b)

Figure 4.57. Sensitivity of project ROI and NPV to the inflation rate change

From Figure 4.57, it is seen that as the inflation increases from zero to 18%, the percentage decrease of the NPV follows an exponential trend, as seen in Figure 4.58. The NPV decreases

exponentially, reaching a minimum of about $2,494 when the inflation rate rises to 18%. When the inflation rate rises above 18.1%, as shown in Figure 4.58, the percentage decline of the net present value (NPV) of the energy project changes stiffly, eventually leading to negative NPV, as depicted in Figure 4.57, implying that investment in the system will result in a loss if the inflation rate rises above 18%.

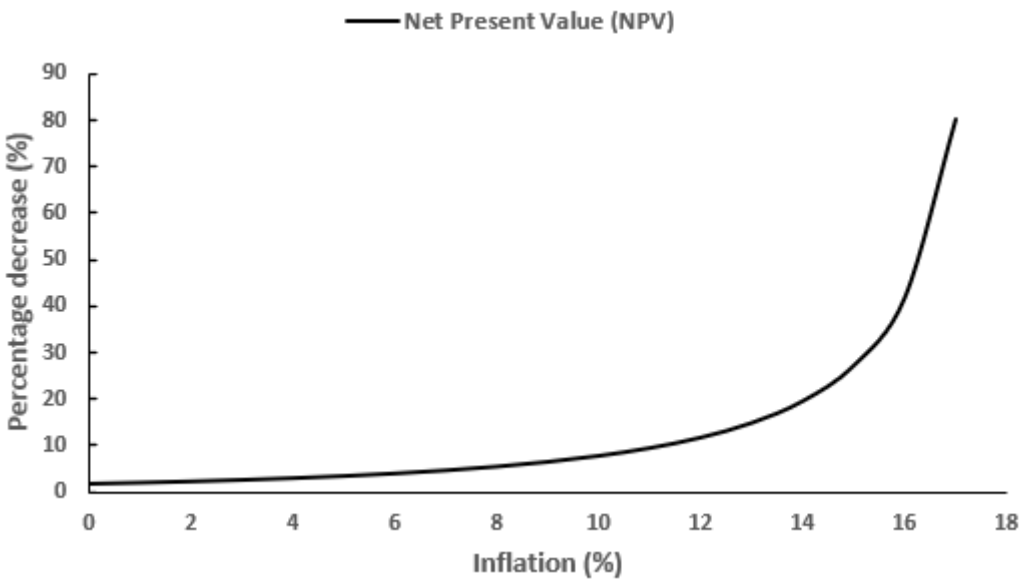


Figure 4.58. Effect of change in inflation rate on the NPV

Currently, the LCOE of power from the diesel generator is considered for this study at $0.246/kWh [244]. Hence, if the inflation rate rises to 18%, the unit cost of energy based on the proposed system becomes $0.23/kWh, as seen in point ‘B’; in Figure 4.59. Consequently, if the LCOE is $0.23/kWh, the unit cost of energy must be sold at a minimum of $0.23/kWh to recoup the investment in a reasonable amount of time. As a result, the LCOE of the proposed system is no longer competitive with the kWh cost of electricity generated by diesel generators.

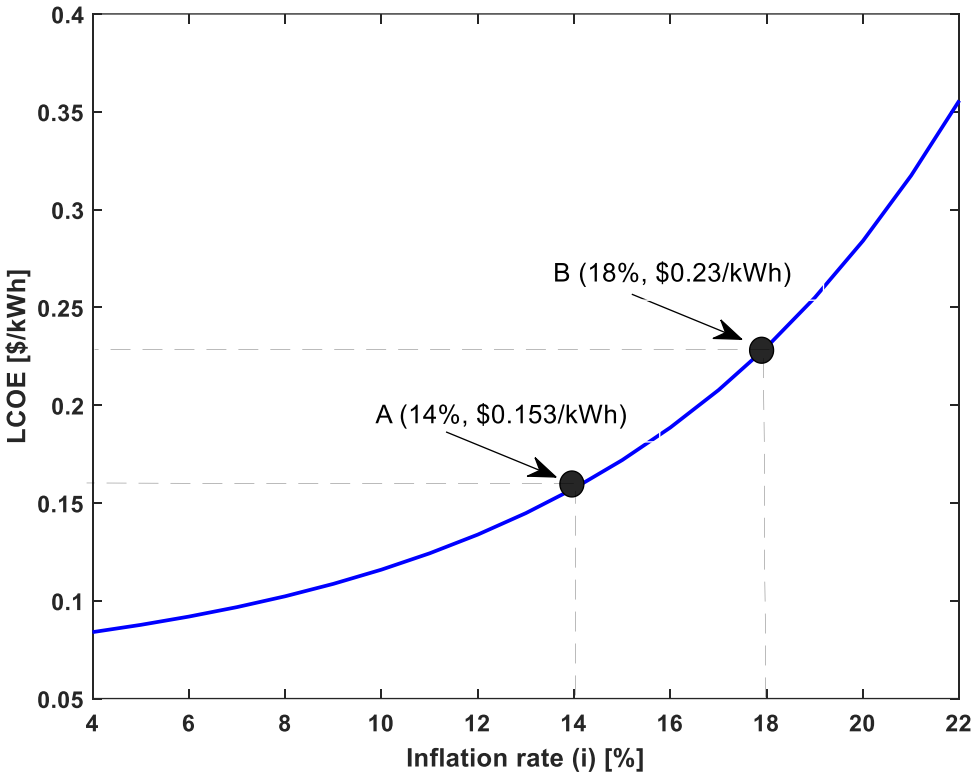


Figure 4.59. Effect of change in inflation rate on the LCOE

Consequently, the proposed energy system becomes less attractive due to its high initial investment than diesel power generation. Reasonable consideration will imply that the project should be rejected for a critical decision if there is the slightest chance that the inflation rate within the project's lifetime will increase to 18%.

The government, particularly policymakers, can encourage massive deployment of renewable energy, even if not for building domestic applications but for critical sectors like health facilities, by checking and ensuring that inflation is checked and kept at a minimal level that will encourage investment in energy projects, especially renewable.

4.11.2 Change in domestic hot water demand volume

It is important to note that, even though the total hot water demand volume of 1000L/day, as indicated in point A on the graph in Figure 4.60, is the primary basis for sizing and analysing the proposed OPVETC energy system, the actual hot water demand volume will most likely vary depending on how much hot water is required in each location where the system is used. Figure 4.60 shows the effect of change in hot water demand volume on the overall system solar fraction (SSF) and the economic and environmental implications as indicated by the ROI and the CO_2 emission on the graph. As observed from the graph, even though the SFF is seen to decrease with an increase in the volume of the hot water demand, the return on investment (ROI) is seen to increase at a decreasing rate to a maximum of 68% at point B before it starts decreasing.

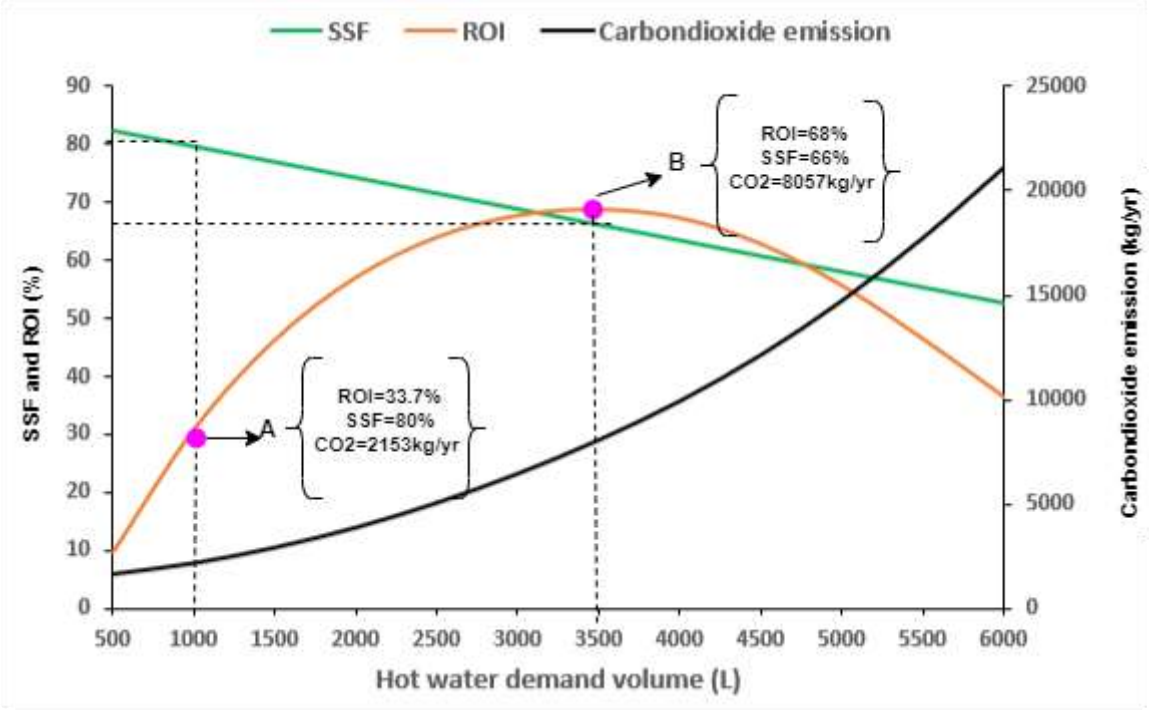


Figure 4.60 Effect of hot water demand volume on ROI, CO_2 emission and SSF

An explanation for this trend is that for every increase in the volume of hot water demand, it is necessary to increase the collector area to increase the thermal energy available to meet the

increased demand. Because there is no increase in the size of the collector, the amount of thermal energy produced by the collector is insufficient compared to the demand. A consequence of this is an increase in the auxiliary energy demand requirement, which leads to an exponential increase in the cash outflow, as illustrated by the graph in Figure 4.61. Moreover, to meet the total hot water demand, more energy must be supplied from either the grid or the diesel generator, increasing the system's CO2 emissions.

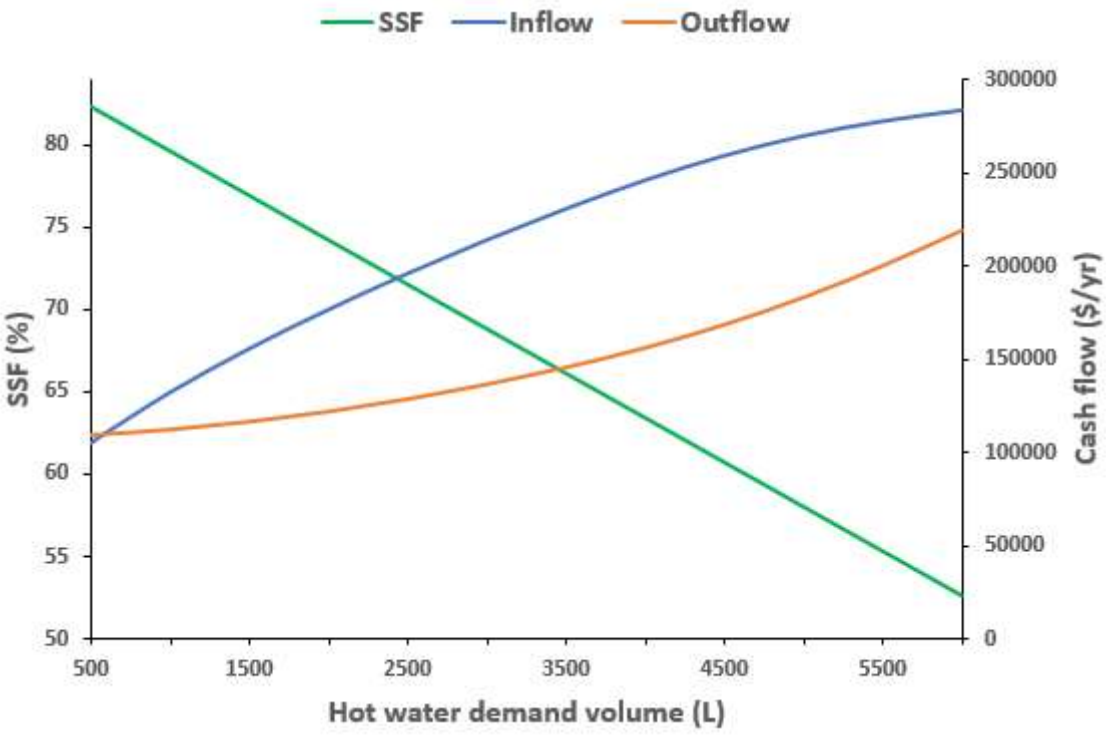


Figure 4.61. Effect of change in the size of the hot water demand volume

Even though the solar fraction decreases as the volume of hot water increases, on the other hand, the quantity of useful thermal energy is increasing. As a result, the total energy savings of the system is increased, leading to a beneficial income revenue (cash inflow) from the increased energy saving in the system. Notably, this increase in revenue is also accompanied by an increase in the auxiliary energy demand due to the inability of the system to meet up with the increase in the thermal demand of the hot water. An increase in the auxiliary energy demand

to meet up with the increased thermal energy demand for hot water subsequentially leads to a higher operating cost arising from the cost of diesel and grid power utilised to meet the increasing auxiliary hot water demand. Consequently, as the operating cost increase, a point is reached (point B) where the operating cost outweighs the slowly increasing revenue, and the net worth of the project starts to decrease. Further increase in the volume beyond 6000L will reduce the net worth since more conventional energy will be purchased to supply the increasing auxiliary energy for hot water. As seen in Figure 4.60, increasing the ROI comes with a consequential increase in CO_2 emission.

In conclusion, as shown in Figure 4.60, these results can be the basis for specifying the maximum power demand that the proposed system can be used to meet the specific economic and environmental targets required by policy. The ROI of 33.7% and SSF of 80% with minimal CO_2 emission of 2153kg/yr from the system for this present study, as indicated by point B in Figure 4.60, shows that the energy management and system sizing aligned with the multi-objective economic viability and environmental protection as earlier stated from the objective of this study.

4.11.3 Effect of change in price of diesel fuel

One of the economic parameters taken into account in this study for the evaluation of system viability and profitability is the price of diesel fuel, as shown in Table 4.15 of Section 4. Based on the current market price in Nigeria's market economy, the price of diesel for this study is $0.48 per litre [240]. The impact of fluctuating diesel prices on Return on Investment (ROI), Net Present Value (NPV), and Levelised Cost of Energy (LCOE) is depicted in Figure 4.62. The price of diesel per litre at the time of the study in 2019 is shown at Points A1 and A2 on Figure 4.62. Figure 4.62 shows that the ROI and NPV of the project are observed to linearly decrease from 33.56% to 33.33% and $37016.8 to $36827.7, respectively, as the price of diesel

increases from the current $0.48/L to $1.5/L, signifying a price increase of more than triple (above 300%) the original price. From the observation in Figure 4.62, even though the price of diesel increases from $0.48 to $1.5, an increase of more than triple (over 300%), the ROI and NPV are only observed to decreased by 0.70% and 0.5% respectively. On the other hand, the LCOE is observed to increase with increase in the price of diesel. This increase is also seen to be not sharply sensitive to the change in the diesel price. As seen in Figure 4.62b the LCOE only increased by 0.2% even with the huge change of diesel price of over 300%. This response of the ROI, NPV and ROI to change in diesel price is very sluggish and not significant. This observation implies that the economic viability of the energy system is less susceptible to change in diesel price.

One issue investors face in most developing nations, such as Nigeria, is the high risk of losing their investment due to erratically fluctuating prices of goods as a result of high inflation rates. [6], [249]. A surprising finding is that the economic indicators (NPV, ROI, and LCOE) are less than 1% sensitive to any change in the price of diesel from the current study location, as shown in Figure 4.62. This result suggests that diesel power generator backup integrated with renewable energy project are not significantly impacted and that there is very little risk of investment in this energy project due to fluctuating diesel price for the study location Nigeria. Even though this interesting finding is for the study location of Jos in Nigeria, it might be applicable to any place with weather similar to Nigeria's and a market economy.

.

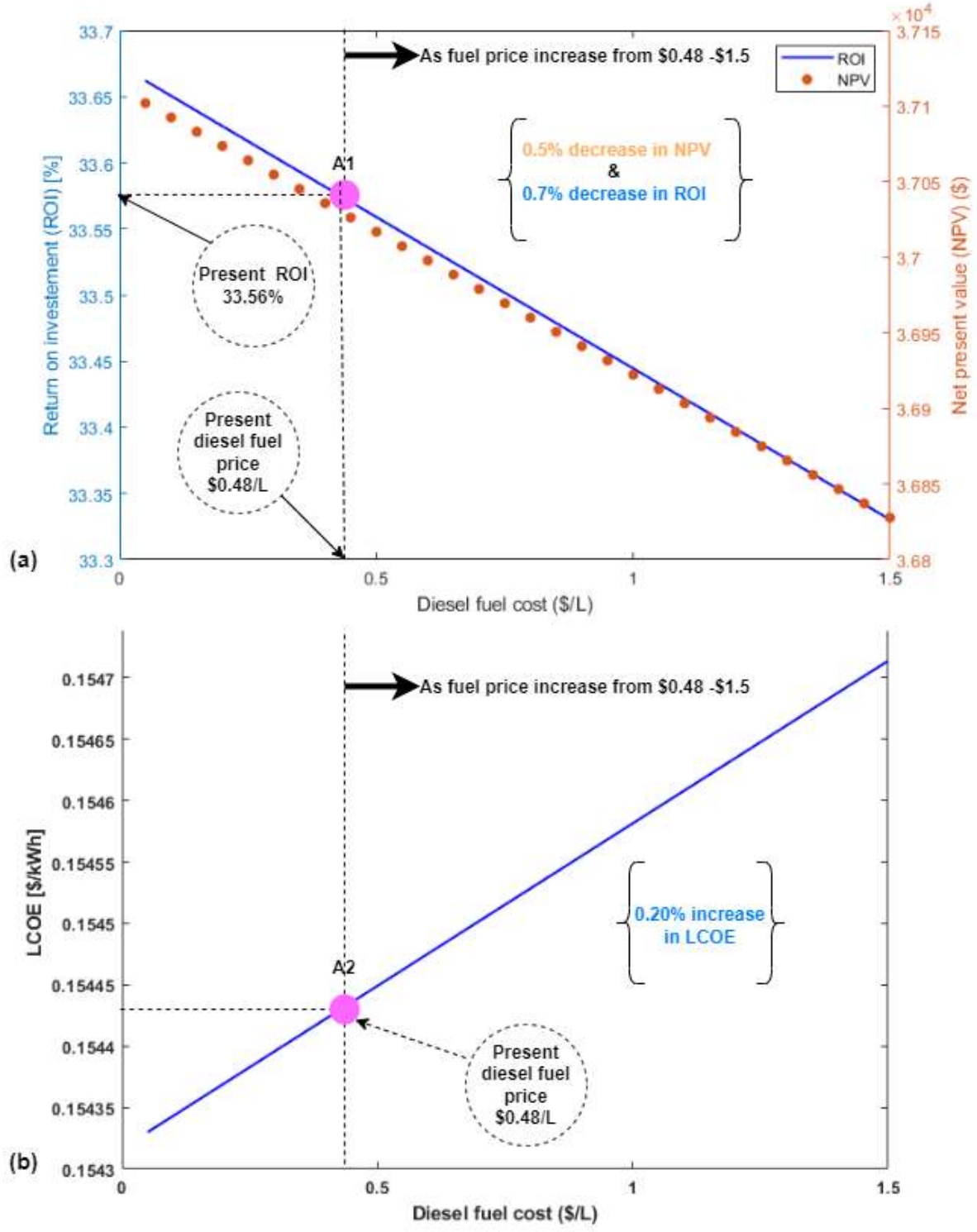


Figure 4.62. Effect of change in diesel fuel price on (a) NPV & ROI and (b) LCOE

4.12 Geographic mapping of economic system viability

Since several factors, including geographic location, and weather conditions, determine the performance of a solar energy system, as proven in many feasibility studies [53], [97], [58], one key question that seeks an answer is whether the proposed energy system is a viable alternative in other energy-constrained communities order than the case study location. This study, therefore, extends and maps the techno-economic of the proposed energy system for application in other six communities, namely, Benin, Ilorin, Kano, Maiduguri, Minna, and Portharcourt, spread in three sunshine belts of Nigeria as depicted in Figure 4.64 [6]. The techno-economic mapping is for the benefit of policymakers, potential investors, and sources of information for health facilities that privately wish to cut energy costs. Figure 4.63 shows the location and the name of each selected community.

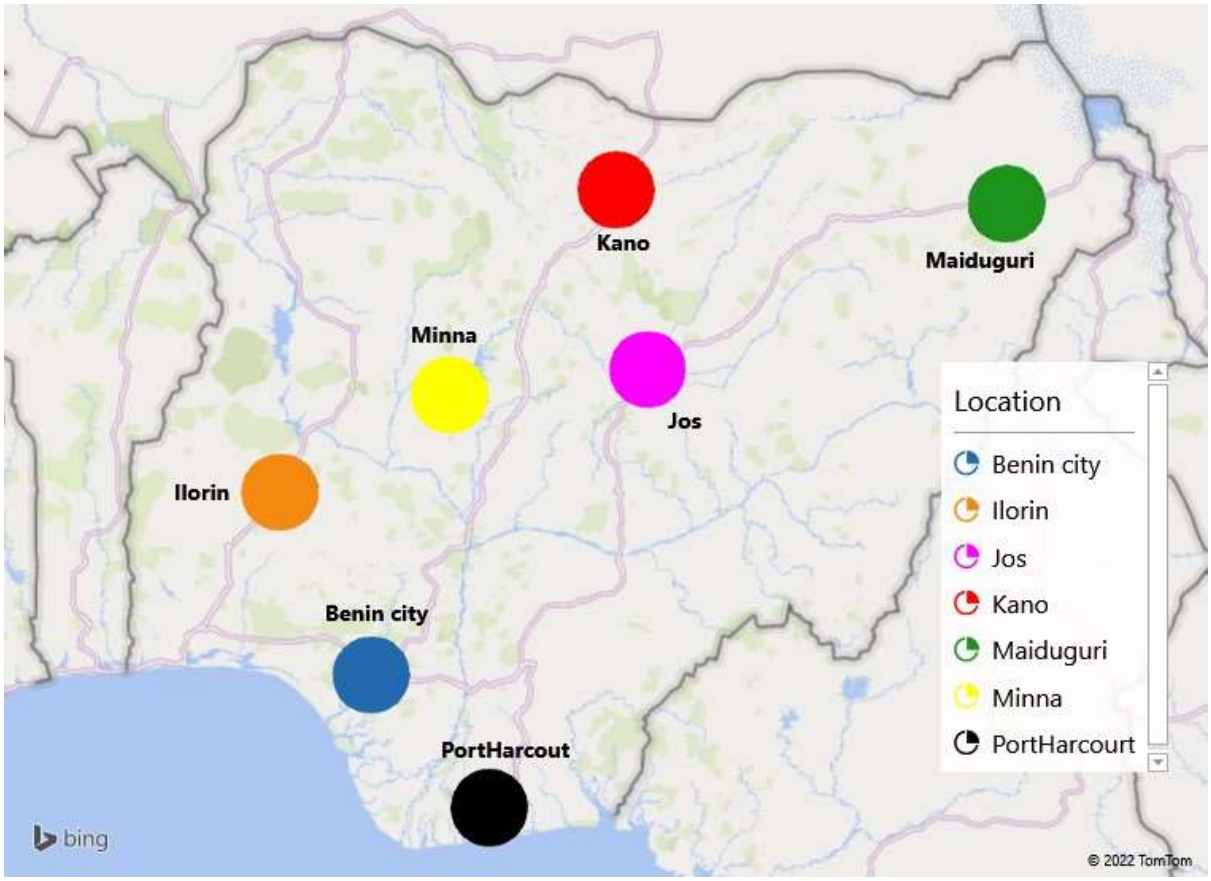


Figure 4.63. Geographical locations for the energy project mapping

Zone I is characterised by high temperatures and solar radiation of 6.0kWh/m^2.day on average. The temperature in Zone II is moderate, with a monthly averaged daily solar energy potential of 5.6kWh/m^2.day. Zone III is a mangrove swamp with daily solar irradiation of 4.5 kWh/m^2.day. The developed model was simulated using weather data from six locations spread in these zones, as shown in Figure 4.63, using identical load conditions as in the study case to assess the proposed hybrid energy system's economic viability.

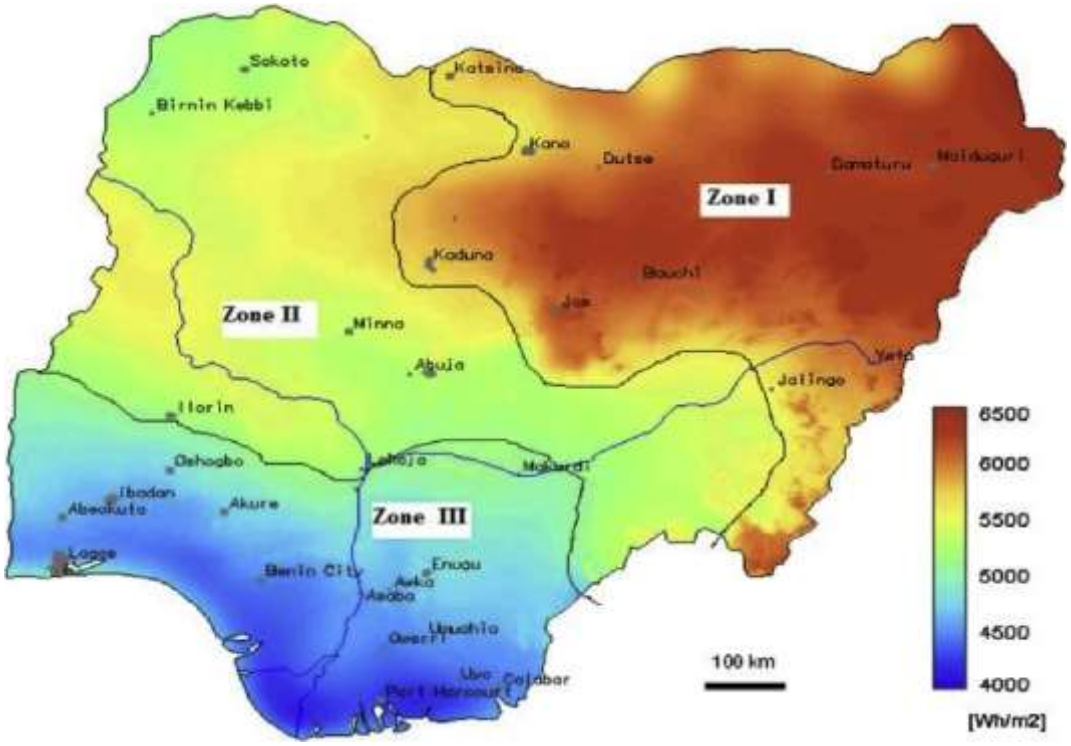


Figure 4.64. Nigeria solar irradiance demographic information

Figure 4.65 shows the evaluated NPV of the energy project under the weather data of the six locations in the three solar belts. As seen from the chart, the system's net present worth (NPV) increases from a minimum of $21,428 in PortHarcourt in the southmost part of Nigeria to a maximum of $61,396 in Kano in the Northmost of Nigeria. A return of investment of 53% and 16.6%, as shown in Table 4.16, indicates that the project is most viable in Kano and has the lowest profitability in PortHarcout, respectively

Table 4.16 Economic performance mapping of the OPVETC in different locations

Location	NPV ($)	ROI (%)	LCOE ($/kWh)
Kano	61,396	53.0	0.143
Maiduguri	58,338	49.1	0.143
Minna	41,948	34.1	0.154
Ilorin	37,824	30.7	0.157
Jos	36,985	33.56	0.154
Benin city	29,922	23.7	0.161
PortHarcourt	21,428	16.6	0.166

This trend shows that regions with higher solar irradiance have higher NPV than those in the southern regions. Higher NPV in regions with higher solar irradiance is due to better system solar fraction met by the system in these regions. A general conclusion that can be drawn is that renewable energy projects are viable energy alternatives in Nigeria. However, these energy technologies are about 36% more profitable in the Northern part of Nigeria than in the south part of Nigeria.

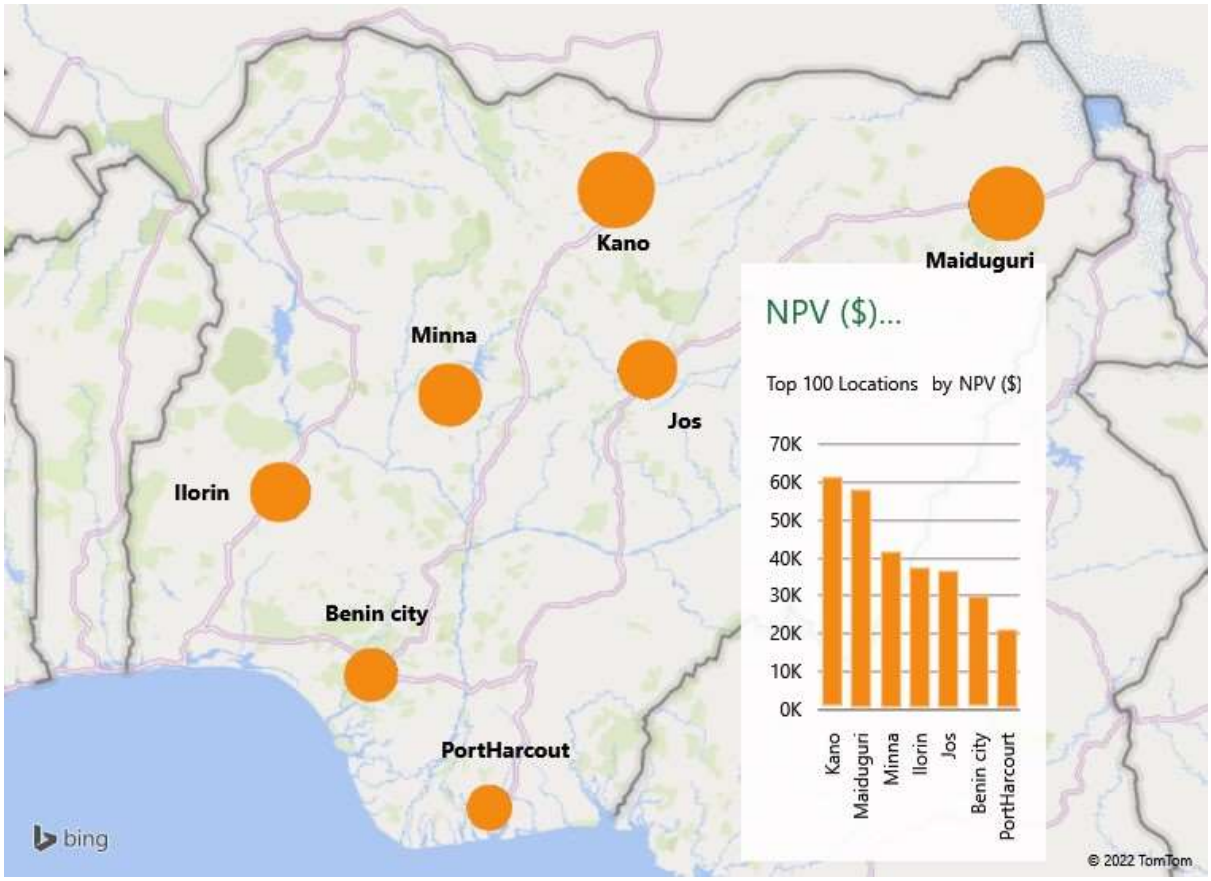


Figure 4.65. Mapping of project NPV by location

Interestingly, the NPV in all locations is positive. Since the NPV in a location with the worst solar radiation (Portaharcout) is positive, it means that the hybridisation of the PVT collector with the ETC collector based on the open-loop cooling control strategy for randomly unstable grid communities is an economically and environmentally viable alternative to solve poor power access in these communities. Therefore, it would be beneficial for private and government alike to promote the wide adoption of this proposed OPVETC in meeting the power demand of health facilities since even in locations with poor solar irradiance like in Portharcourt, as seen in the solar demographic in Figure 4.64. the project has an LCOE of $0.166/kWh as seen in Figure 4.66, which is about 33% cheaper than the unit cost of energy of $0.246/kWh from diesel in this location. Overall, this unit energy cost is of energy based on the new hybrid energy system in all the locations is still cheaper than the average cost of power

of $0.32/kWh of the traditional diesel generator adopted in most communities with poor access to the grid power in Nigeria.

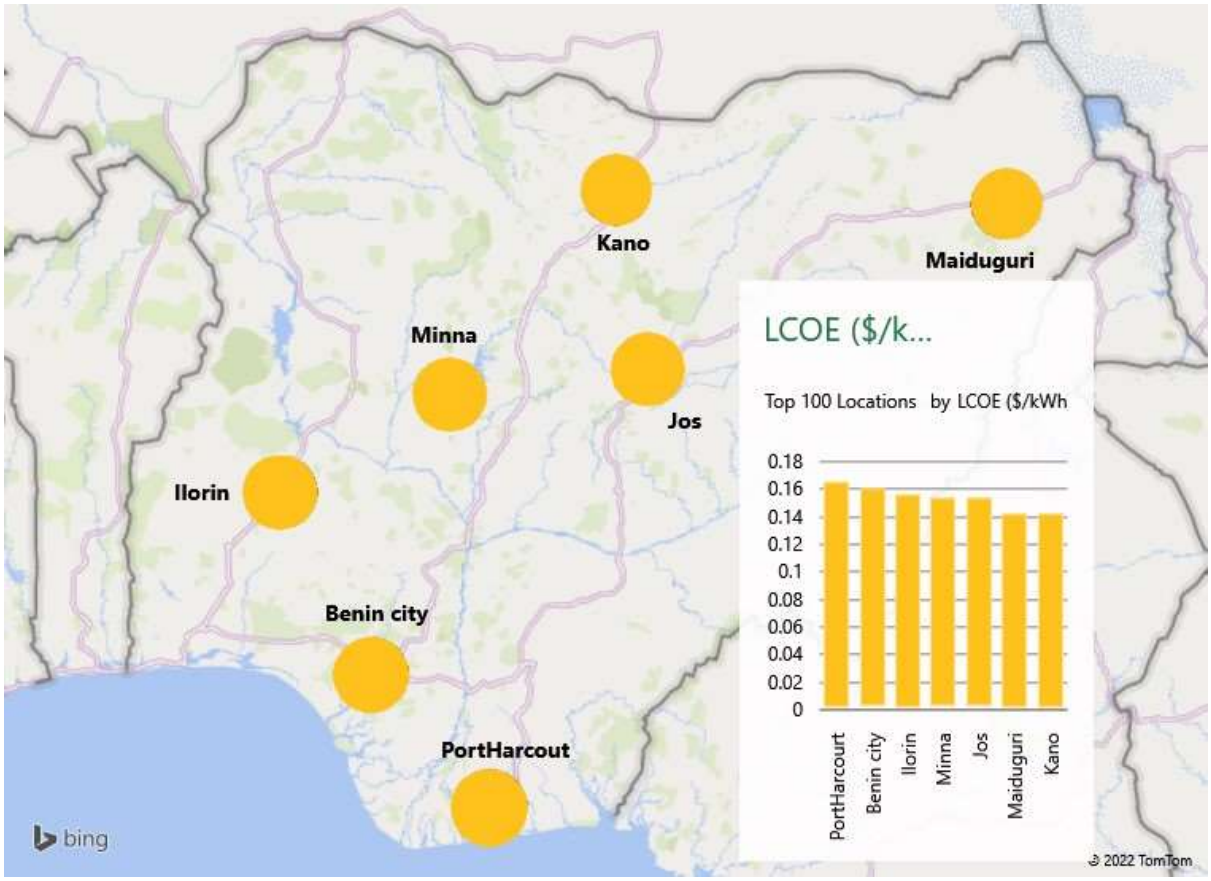


Figure 4.66. Mapping of energy project LCOE by location

Overall, the economic indices as assessed in this study in a different part of Nigeria shows that OPVETC hybrid energy system is a promising investment option since, in all regions, the net worth of the project is positive with lower LCOE than the baseline energy system in all these locations. However, it is more profitable in the Northern region than in its southern region since the Northern region has higher solar irradiance than the southern part of Nigeria.

4.13 Chapter summary

In this study, the grid-connected hybrid OPVETC is appropriately sized to meet the energy demand consistently and reliably for a case study health centre, which has a monthly average daily demand for hot water and electricity of 35kWh and 47.9kWh, respectively.

The optimal number of a 1.63m^2 PVT collector with an electrical efficiency of 17.3% was found to be 33 using the parametric sizing method with the solar fraction and Total Life Cycle Cost (TLCC) as objective functions. The optimal number for the 1200Wh battery capacity was discovered to be 15. Based on the optimal flow rate of 160L/hr. determined by the sensitivity analysis, a pump with a maximum flow rate of 160L/hr. was also chosen.

One objective in this study, is the reduction of the surface temperature of photovoltaic solar panel with the sole aim of reducing the panel degradation and increasing electrical power efficiency. From the result found in the chapter, it is evident that the surface temperature of the solar panel based on the innovative OPVETC energy system is 30^oC lower than the conventional basic hybrid PVT. Evaluating the power and thermal energy production of the proposed OPVETC system relative to the baseline basic hybrid PVT energy system, it is evident that the power and thermal energy utilization of the proposed OPVETC higher than the basic hybrid PVT energy system with an average daily power and thermal energy production gap of 7.7% and 9.5% respectively.

Solar fraction (SF) is one of the performance indices to measure the technical performance of solar energy systems. SF is a superior performance indicator since it measures the part of the energy demand met by the sun's energy free from emission. It is also an indication of the cost savings of the system. It is equally revealing from the results in section 4, that the proposed system reconfiguration proved to have better average daily energy saving of 6% over the

basic hybrid system owing to higher average daily thermal and electrical solar fractions. The evaluation of the collector efficiency which is a measure of the capacity of the system in converting the free solar energy into power and thermal energy before utilisation, revealed that the total PVT collector efficiency based on the new OPVETC system configuration and cooling strategy is increased by about 13% relative to the basic hybrid PVT energy system.

Meeting the power demand reliably and economically with minimal negative impact of the energy production to the environment is another critical objective in this study. The loss of load probability (LOLP), Avoidable carbon dioxide ratio, are good pointer to the reliability and environmental protector indices of the energy system. The Net present value and the Return on Investment are pointers to profitability of the energy system. A critical assessment of performance of the OPVETC hybrid energy system compared to the basic hybrid PVT based on these critical matrices, showed that the basic hybrid PVT energy system LOLP is 44% higher relative to the that of the OPVETC. Since the LOLP is an indication of the system's dependency on the expensive and high emission diesel backup system, its means that the new OPVETC is 44% less dependent on the expensive and high pollution diesel backup system used in this study.

Overall, the new cooling and system architecture is over 100% more profitable with a $36,985 Net worth compared to $17,359 net worth of the basic hybrid at the expiration of the project life after 25 years. A critical evaluation of the proposed system in different geographical locations in Nigeria revealed that the system is viable in all part of Nigeria with the North being the most viable location.

Chapter 5: Conclusions and future work

5.1 Introduction

In this chapter, general conclusions on the study are drawn and summerised based on the key findings of this research in relation to the study aims and objectives. The theoretical and practical implication of key finding are stated along with the key findings. The novelty and contribution and as well as the limitations of the study are reviewed in this section. The potential for additional research to enhance the findings of the current study is also suggested in this section. This section concludes with recommendations for government and decision-makers in the energy sector.

5.2 Summary of key findings

This study challenged the conventional hybrid PVT energy system, claiming that the proposed system (OPVETC) will result in better cooling of the PV module as well as higher power production and utilisation, resulting in improved technical, economic, and environmental indicators. The aim of this research is to develop a numerical model for the performance simulation and evaluation of a novel Open-loop Photovoltaic solar thermal Evacuated tube collector hybrid energy system (OPVETC) for application in health clinic in communities with randomly unstable grid power in Nigeria. The result of the analysis of the formulated model based on the R^2 value indicates that the numerical model is successfully developed and it's a good representation for the annual evaluation of the model performance

Overall, the findings based on the results suggested hybridisation and cooling configuration and flow control strategy has resulted in higher annual renewable power generation and utilisation by about 10% compared to the basic hybrid PVT cooling method and system configuration.

Further critical examination shows that, while the new hybrid system (OPVETC) configuration has a better lifetime Self-consumption ratio (SSR) of 85% than the basic hybrid PVT system SSR of 74%, the SSR values for both systems show that the new developed energy management strategy in this study has met the goal of prioritising renewable energy while a significant reduction in CO_2 emissions from the energy mix well above the minimum energy savings (30%) specified by NREL for good system economic viability [225], [226].

An economic study of the new system demonstrates that the new technical upgrade system configuration and energy management strategy as proposed in this study has resulted in significant economic savings, cutting the system's operating expenses by around 48% and increasing annual income by nearly 15%. This annual revenue rise increases the basic PVT energy system's return on investment (ROI) from 14% to 33% and its net worth (NPV) by over 100%.

The result further indicates that the proposed energy system is a viable energy alternative for domestic application especially in the health centre for energy-constrained communities in most regions of Nigeria. The viability of project grows as the project moves northward in Nigeria, with a maximum ROI of 53% in Kano. An interesting deduction that can be drawn from the economic sensitivity analysis is that that the economic worth of the project in the study location is not sensitive (less than 0.8%) to change in diesel price which in most cases is the fear of most investors. However, the sensitivity study of the project economic performance on the change in inflation rate suggest that the inflation rate must not exceed 18% during the entire lifetime of the project of 25years. Beyond an inflation rate of 18% the project worth becomes negative and unattractive scaring investors away.

5.3 Novelty and contributions

The following are the main accomplishments and contributions: A new numerical model for the performance simulation and techno-economic evaluation of a novel hybridisation of the basic PVT system operated on a unique energy management and control strategy that coordinates the new system with a randomly unavailable grid has been successfully developed and validated as a contribution to the knowledge field.

The ability to tailor the desired preference performance of the PVT to either prioritise the thermal or electrical performance is one of the most appealing features of the flow control strategy. Another completely new aspect of this research is that the domestic hot water is delivered at three different temperatures to match the hot water demand of the health centres for diverse services, unlike in majority of studies where the hot water is delivered at a single temperature[141], [208], [252]. Interestingly, the negative compromise in either power or hot water production, as in the conventional hybrid photovoltaic solar thermal energy system, is significantly minimised in the proposed OPVETC hybrid energy system. For the proposed OPVETC hybrid energy system, the PV module's power output does not significantly reduce when hot water demand at elevated temperatures is met.

In addition, this research provides a new prospect in applying hybrid PVT for health centres applications in energy-constrained communities. Besides, it provides an enhanced means to meet health power and hot water demand with significant energy savings. The study equally reveals the proposed system's business outlook exposing the profitability of the proposed hybrid photovoltaic energy system in the health centres in different geographical locations of the study country. The findings of this studies are the bases for good decision making for both government and renewable energy investors. These results will equally serve as catalyst to promote, the fast deployment of hybrid PVT energy system for domestic application even in

locations with poor solar energy. The economic viability of the new hybrid PVT system in different regions of the study country will serve as a bonus for individual operators of health centres in Nigeria who wish to have reliable energy sources with a significant cut down in their energy costs.

5.4 Limitations of study

Despite the success demonstrated with results suggesting that the new proposed system and modelling methodology is adequate and reliably and strong and promising alternative, the study has some inherent limitations which need recognition. One limitation of this work is the use of the intuitive approach to estimate part of the hot water and electrical power demand due to no data of energy usage in domestic buildings and health centres in most developing countries. In this study, the daily electrical requirement for equipment operation and the daily hot water demand is assumed to be constant throughout the year. This assumption might either overestimate or underestimate the actual load requirement. However, the used of the 3D building energy model to estimate the air conditioning load which constitute a major portion of the building reduces the error in the certainty of this study.

Another limitation, though not a primary goal of this study, is the use of simple parametric analysis based on the economic objective function to optimally size the system components. Even though this method is quick and produces satisfactory results, the global optimum size of system components based on a more advanced optimization technique may be more appropriate and could improve system reliability while also improving economic viability.

Lastly, due to heavy financial implication of implementing the actual model as proposed in this study, the study examines the performance of the proposed system only based on the numerical model developed using TRNSYS software. Even though the numerical approach does not fully

consider the problems that can appear in real situations consider the actual operation to validate robustness of the proposed model, TRNSYS software model have been reported in many studies besides this study to have good agreement with actual performance[253], [254].

5.5 Future work and recommendation

The scope of this study was limited to the development and performance assessment of the suggested OPVETC based on the developed numerical approach that could be completed within the allotted time and budget. Examining actual performance under actual load and outdoor weather conditions is necessary. In a later study, it might be useful to create an experimental setup to measure the proposed OPVETC's performance experimentally by scaling down the system's actual size.

Similarly, in this study, the novel open-loop cooling control strategy was based on the series arrangement of the PVT collector. However, what is uncertain is whether the reconfiguration of the PVT array to parallel flow control configuration based on the same proposed open-loop flow control strategy is more beneficial leading to higher system technical and economic improvement. Hence, this study could be further investigated employing the parallel arrangement of the PVT.

Furthermore, in the present study, a novel energy management and control strategy based on the Follow Total Load (FTL) control algorithm was used to coordinate the proposed energy system integrated with a grid characterised by random power failure to meet the goal of this study. Further research would be useful in testing the effectiveness of different energy management and control strategies based on a robust component sizing optimisation technique on the objective of this studies.

Integrating a heat engine with the building to supply the building's energy demand may be a cost-effective option to investigate in future studies.

It is recommended in this study that Nigeria shift its policies direction away from regular fossil fuel subsidies toward swap subsidies for solar energy technologies and infrastructure since solar energy projects are economically all part of Nigeria. As a result, many investors and individuals will quickly adopt renewable technologies. Since building energy consumption represents significant portion of Nigeria’s total energy demand, the adoption of this technology (OPVETC) in residential buildings could be a potential area for the country to target to keep to its CO_2 reduction target and make an effort to increase access to power in rural communities.

REFERENCE

[1] P. Ortega-Arriaga, O. Babacan, J. Nelson, and A. Gambhir, "Grid versus off-grid electricity access options: A review on the economic and environmental impacts," *Renew. Sustain. Energy Rev.*, vol. 143, no. March, p. 110864, 2021, doi: 10.1016/j.rser.2021.110864.

[2] IEA, IRENA, UNSD, W. Bank, and WHO, "Tracking SDG 7: The Energy Progress Report. World Bank," Washington DC., 2021. [Online]. Available: https://trackingsdg7.esmap.org/

[3] H. Adair-Rohani *et al.*, "Limited electricity access in health facilities of sub-Saharan Africa: A systematic review of data on electricity access, sources, and reliability," *Glob. Heal. Sci. Pract.*, vol. 1, no. 2, pp. 249–261, 2013, doi: 10.9745/GHSP-D-13-00037.

[4] C. G. Ozoegwu, C. A. Mgbemene, and P. A. Ozor, "The status of solar energy integration and policy in Nigeria," *Renew. Sustain. Energy Rev.*, vol. 70, no. November 2016, pp. 457–471, 2017, doi: 10.1016/j.rser.2016.11.224.

[5] O. D. Ohijeagbon, O. Ajayi, O. Waheed, M. Adekojo, E. Y. Salawu, and F. A. Oyawale, "Design of optimal hybrid renewable energy system for sustainable power supply to isolated-grid communities in North Central, Nigeria," *Procedia Manuf.*, vol. 35, no. 2016, pp. 278–284, 2019, doi: 10.1016/j.promfg.2019.05.040.

[6] U. K. Elinwa, J. E. Ogbeba, and O. P. Agboola, "Cleaner energy in Nigeria residential housing," *Results Eng.*, vol. 9, no. January 2020, p. 100103, 2021, doi: 10.1016/j.rineng.2020.100103.

[7] C. Newsom, "Renewable Energy Potential in Nigeria: A Low-carbon approaches to tackling Nigeria's energy poverty," *Int. Inst. Environ. Dev.*, vol. 1, no. 1–26, 2012,

[Online]. Available: http://ec.europa.eu/world/.

[8] H. Arbabi and M. Mayfield, “Urban and Rural—Population and Energy Consumption Dynamics in Local Authorities within England and Wales,” *Buildings*, vol. 6, no. 3, p. 34, 2016, doi: 10.3390/buildings6030034.

[9] L. O. Aghenta and M. T. Iqbal, “Design and Dynamic Modelling of a Hybrid Power System for a House in Nigeria,” *Int. J. Photoenergy*, vol. 2019, pp. 1–13, 2019, doi: 10.1155/2019/6501785.

[10] C. O. Anyaeche, T. Akappo, and A. O. Adeodu, “Optimisation of Hybrid Energy System Production Parameters for Electricity Power Generation in Nigeria,” *Energy Power Eng.*, vol. 10, pp. 198–211, 2018, doi: 10.4236/epe.2018.105014.

[11] International Finance Corporation, “Off-grid Solar Market Trends Report 2018,” Washington, D.C., 2018. doi: 10.1017/CBO9781107415324.004.

[12] E. B. Barbier and J. C. Burgess, “Sustainability and development after COVID-19,” *World Dev.*, vol. 135, p. 105082, 2020, doi: 10.1016/j.worlddev.2020.105082.

[13] E. I. Come Zebra, H. J. van der Windt, G. Nhumaio, and A. P. C. Faaij, “A review of hybrid renewable energy systems in mini-grids for off-grid electrification in developing countries,” *Renew. Sustain. Energy Rev.*, vol. 144, no. April, 2021, doi: 10.1016/j.rser.2021.111036.

[14] J. Kumar, B. V. Suryakiran, A. Verma, and T. S. Bhatti, “Analysis of techno-economic viability with demand response strategy of a grid-connected microgrid model for enhanced rural electrification in Uttar Pradesh state, India,” *Energy*, vol. 178, pp. 176–185, 2019, doi: 10.1016/j.energy.2019.04.105.

[15] A. S. Aziz, M. F. N. Tajuddin, M. R. Adzman, A. Azmi, and M. A. M. Ramli,

"Optimization and sensitivity analysis of standalone hybrid energy systems for rural electrification: A case study of Iraq," *Renew. Energy*, vol. 138, pp. 775–792, 2019, doi: 10.1016/j.renene.2019.02.004.

[16] D. Dabaro, "Factors affecting tuberculosis case detection in Kersa District, South West Ethiopia," *J. Clin. Tuberc. Other Mycobact. Dis.*, vol. 9, no. August, pp. 1–4, 2017, doi: 10.1016/j.jctube.2017.08.003.

[17] E. S. Simon, "Nigeria: Why We Completed 4 Solar Power Plants for COVID-19 Centres in 14 Days," *Daily Trust of Nigeria*, 2020. https://allafrica.com/stories/202004170647.html (accessed Feb. 04, 2022).

[18] A. Franco, M. Shaker, D. Kalubi, and S. Hostettler, "A review of sustainable energy access and technologies for healthcare facilities in the Global South," *Sustain. Energy Technol. Assessments*, vol. 22, pp. 92–105, 2017, doi: 10.1016/j.seta.2017.02.022.

[19] RTI, "Current Opportunities: Request for proposal," *RTI International*, 2022. https://www.rti.org/current-opportunities (accessed Feb. 04, 2022).

[20] A. Cheshmehzangi, "COVID-19 and household energy implications: what are the main impacts on energy use?," *Heliyon*, vol. 6, no. 10. 2020. doi: 10.1016/j.heliyon.2020.e05202.

[21] IEA, "Perspectives for the Clean Energy Transition," Paris, 2019. [Online]. Available: www.iea.org/publications/reports/PerspectivesfortheCleanEnergyTransition/

[22] N. Das, H. Wongsodihardjo, and S. Islam, "A preliminary study on conversion efficiency improvement of a multi-junction PV cell with MPPT," *Stud. Syst. Decis. Control*, vol. 57, pp. 49–73, 2016, doi: 10.1007/978-3-319-30427-4_4.

[23] EIA, "Electricity explained: Factors affecting electricity prices," 2021. [Online].

Available: https://www.eia.gov/energyexplained/electricity/prices-and-factors-affecting-prices.php

[24] D. Gielen, F. Boshell, D. Saygin, M. D. Bazilian, N. Wagner, and R. Gorini, "The role of renewable energy in the global energy transformation," *Energy Strateg. Rev.*, vol. 24, no. June 2018, pp. 38–50, 2019, doi: 10.1016/j.esr.2019.01.006.

[25] A. Gu, F. Teng, and X. Feng, "Effects of pollution control measures on carbon emission reduction in China: evidence from the 11th and 12th Five-Year Plans," *Clim. Policy*, vol. 18, no. 2, pp. 198–209, 2018, doi: 10.1080/14693062.2016.1258629.

[26] F. Martins, C. Felgueiras, and M. Smitková, "Fossil fuel energy consumption in European countries," *Energy Procedia*, vol. 153, pp. 107–111, 2018, doi: 10.1016/j.egypro.2018.10.050.

[27] C. Ghenai and M. Bettayeb, "Grid-Tied Solar PV/Fuel Cell Hybrid Power System for University Building," *Energy Procedia*, vol. 159, pp. 96–103, 2019, doi: 10.1016/j.egypro.2018.12.025.

[28] Q. Wu and H. Ren, "Design and Evaluation of a CCHP based Micro-grid for an Urban Area," *Energy Procedia*, vol. 143, pp. 798–803, 2017, doi: 10.1016/j.egypro.2017.12.765.

[29] W. Liu *et al.*, "Smart Micro-grid System with Wind/PV/Battery," *Energy Procedia*, vol. 152, pp. 1212–1217, 2018, doi: 10.1016/j.egypro.2018.09.171.

[30] A. Ibrahim, A. Fudholi, K. Sopian, M. Y. Othman, and M. H. Ruslan, "Efficiencies and improvement potential of building integrated photovoltaic thermal (BIPVT) system," *Energy Convers. Manag.*, vol. 77, pp. 527–534, 2014, doi: 10.1016/j.enconman.2013.10.033.

[31] A. Aly, M. Moner-Girona, S. Szabó, A. B. Pedersen, and S. S. Jensen, “Barriers to Large-scale Solar Power in Tanzania,” *Energy Sustain. Dev.*, vol. 48, pp. 43–58, 2019, doi: 10.1016/j.esd.2018.10.009.

[32] M. Herrando, A. Ramos, J. Freeman, I. Zabalza, and C. N. Markides, “Technoeconomic modelling and optimisation of solar combined heat and power systems based on flat-box PVT collectors for domestic applications,” *Energy Convers. Manag.*, vol. 175, no. March, pp. 67–85, 2018, doi: 10.1016/j.enconman.2018.07.045.

[33] C. O. Okoye and B. C. Oranekwu-Okoye, “Economic feasibility of solar PV system for rural electrification in Sub-Sahara Africa,” *Renew. Sustain. Energy Rev.*, vol. 82, no. July 2016, pp. 2537–2547, 2018, doi: 10.1016/j.rser.2017.09.054.

[34] O. Rodriguez-Hernandez, M. Martinez, C. Lopez-Villalobos, H. Garcia, and R. Campos-Amezcua, “Techno-economic feasibility study of small wind turbines in the Valley of Mexico metropolitan area,” *Energies*, vol. 12, no. 5, pp. 1–26, 2019, doi: 10.3390/en12050890.

[35] K. Owebor, E. O. Diemuodeke, T. A. Briggs, and M. Imran, “Power Situation and renewable energy potentials in Nigeria – A case for integrated multi-generation technology,” *Renew. Energy*, vol. 177, pp. 773–796, 2021, doi: 10.1016/j.renene.2021.06.017.

[36] S. A. Kalogirou and Y. Tripanagnostopoulos, “Industrial application of PV/T solar energy systems,” *Appl. Therm. Eng.*, vol. 27, no. 8–9, pp. 1259–1270, 2007, doi: 10.1016/j.applthermaleng.2006.11.003.

[37] O. R. O, O. A. S. O, A. T. R, A. A. Yusuff, and T. C. Mosetlhe, “An assessment of proposed grid integrated solar photovoltaic in different locations of Nigeria: Technical

and economic perspective," *Clean. Eng. Technol.*, vol. 4, p. 100149, 2021, doi: 10.1016/j.clet.2021.100149.

[38] S. Jacal, F. Brigitte, E. Olatunbosun, and G. Buchenrieder, "Energy for Sustainable Development Economic costs and environmental impacts of fossil fuel dependency in sub-Saharan Africa : A Nigerian dilemma," *Energy Sustain. Dev.*, vol. 70, pp. 45–53, 2022, doi: 10.1016/j.esd.2022.07.007.

[39] T. A. Olukan, S. Santos, A. A. Al Ghaferi, and M. Chiesa, "Development of a solar nano-grid for meeting the electricity supply shortage in developing countries (Nigeria as a case study)," *Renew. Energy*, vol. 181, pp. 640–652, 2022, doi: 10.1016/j.renene.2021.09.058.

[40] S. O. Sanni, J. Y. Oricha, T. O. Oyewole, and F. I. Bawonda, "Analysis of backup power supply for unreliable grid using hybrid solar PV/diesel/biogas system," *Energy*, vol. 227, p. 120506, 2021, doi: 10.1016/j.energy.2021.120506.

[41] P. M. Murphy, S. Twaha, and I. S. Murphy, "Analysis of the cost of reliable electricity: A new method for analyzing grid connected solar, diesel and hybrid distributed electricity systems considering an unreliable electric grid, with examples in Uganda," *Energy*, vol. 66, pp. 523–534, 2014, doi: 10.1016/j.energy.2014.01.020.

[42] W.H.O, "Access to Modern Energy Services for Health Facilities in Resource-Constrained Settings:A Review of Status, Signifi cance, Challenges and Measurement," Geneva 27, Switzerland, 2015.

[43] M. Salman, X. Long, G. Wang, and D. Zha, "Paris climate agreement and global environmental efficiency: New evidence from fuzzy regression discontinuity design," *Energy Policy*, vol. 168, no. January, p. 113128, 2022, doi:

10.1016/j.enpol.2022.113128.

[44] B. Ugwoke, O. Gershon, C. Becchio, S. P. Corgnati, and P. Leone, “A review of Nigerian energy access studies: The story told so far,” *Renew. Sustain. Energy Rev.*, vol. 120, no. June 2019, p. 109646, 2020, doi: 10.1016/j.rser.2019.109646.

[45] H. C. Lau, “Decarbonization roadmaps for ASEAN and their implications,” *Energy Reports*, vol. 8, pp. 6000–6022, 2022, doi: 10.1016/j.egyr.2022.04.047.

[46] M. Amer and T. U. Daim, “Application of technology roadmaps for renewable energy sector,” *Technol. Forecast. Soc. Change*, vol. 77, no. 8, pp. 1355–1370, 2010, doi: 10.1016/j.techfore.2010.05.002.

[47] M. Herrando, A. M. Pantaleo, K. Wang, and C. N. Markides, “Solar combined cooling, heating and power systems based on hybrid PVT, PV or solar-thermal collectors for building applications,” *Renew. Energy*, vol. 143, pp. 637–647, 2019, doi: 10.1016/j.renene.2019.05.004.

[48] S. Nikbakht Naserabad, R. Rafee, S. Saedodin, and P. Ahmadi, “Dynamic thermal analysis and 3E evaluation of a CCHP system integrated with PVT to provide dynamic loads of a typical building in a hot-dry climate,” *Sustain. Energy Technol. Assessments*, vol. 52, no. PA, p. 101970, 2022, doi: 10.1016/j.seta.2022.101970.

[49] S. Khanmohammdi, F. Musharavati, and M. Sheykhmohammadi, “Energy and exergy examinations of a PVT based hybrid system for power, heating and potable water production: Transient modeling,” *Renew. Energy*, vol. 195, pp. 540–553, 2022, doi: 10.1016/j.renene.2022.05.114.

[50] M. Herrando, C. N. Markides, and K. Hellgardt, “A UK-based assessment of hybrid PV and solar-thermal systems for domestic heating and power: System performance,” *Appl.*

Energy, vol. 122, pp. 288–309, 2014, doi: 10.1016/j.apenergy.2014.01.061.

[51] S. Aghakhani, M. Afrand, A. Karimipour, R. Kalbasi, and M. Mehdi Razzaghi, "Numerical study of the cooling effect of a PVT on its thermal and electrical efficiency using a Cu tube of different diameters and lengths," *Sustain. Energy Technol. Assessments*, vol. 52, no. PA, p. 102044, 2022, doi: 10.1016/j.seta.2022.102044.

[52] L. Wai Zhe *et al.*, "Effect of Water Cooling Temperature on Photovoltaic Panel Performance by Using Computational Fluid Dynamics (CFD)," *J. Adv. Res. Fluid Mech. Therm. Sci. J. homepage*, vol. 56, pp. 133–146, 2019, Accessed: Jun. 21, 2020. [Online]. Available: www.akademiabaru.com/arfmts.html

[53] S. A. Kalogirou, "Use of TRNSYS for modelling and simulation of a hybrid pv–thermal solar system for Cyprus," *Renew. Energy*, vol. 23, no. 2, pp. 247–260, Jun. 2001, doi: 10.1016/S0960-1481(00)00176-2.

[54] S. A. Kalogirou and Y. Tripanagnostopoulos, "Hybrid PV/T solar systems for domestic hot water and electricity production," *Energy Convers. Manag.*, vol. 47, no. 18–19, pp. 3368–3382, 2006, doi: 10.1016/j.enconman.2006.01.012.

[55] E. Wilson, "Theoretical and operational thermal performance of a 'wet' crystalline silicon PV module under Jamaican conditions," *Renew. Energy*, vol. 34, no. 6, pp. 1655–1660, Jun. 2009, doi: 10.1016/J.RENENE.2008.10.024.

[56] F. Martorana, M. Bonomolo, G. Leone, F. Monteleone, G. Zizzo, and M. Beccali, "Solar-assisted heat pumps systems for domestic hot water production in small energy communities," *Sol. Energy*, vol. 217, no. November 2020, pp. 113–133, 2021, doi: 10.1016/j.solener.2021.01.020.

[57] O. Rejeb *et al.*, "Novel solar PV/Thermal collector design for the enhancement of

thermal and electrical performances," *Renew. Energy*, vol. 146, pp. 610–627, 2020, doi: 10.1016/j.renene.2019.06.158.

[58] A. H. Besheer, M. Smyth, A. Zacharopoulos, J. Mondol, and A. Pugsley, "Review on recent approaches for hybrid PV/T solar technology," *Int. J. Energy Res.*, vol. 40, no. 15, pp. 2038–2053, Dec. 2016, doi: 10.1002/ER.3567.

[59] S. Senthilraja, R. Gangadevi, R. Marimuthu, and M. Baskaran, "Performance evaluation of water and air based PVT solar collector for hydrogen production application," *Int. J. Hydrogen Energy*, vol. 45, no. 13, pp. 7498–7507, 2020, doi: 10.1016/j.ijhydene.2019.02.223.

[60] IPCC, "An IPCC Special Report on the impacts of global warming of 1.5°C above pre-industrial levels and related global greenhouse gas emission pathways, in the context of strengthening the global response to the threat of climate change, sustainable development," Switzerland., 2018. [Online]. Available: http://www.ipcc.ch/report/sr15/

[61] European Commission, "The Road from Paris: assessing the implications of the Paris Agreement and accompanying the proposal for a Council decision on the signing, on behalf of the European Union, of the Paris agreement adopted under the United Nations Framework Convention on Cl," 2016. [Online]. Available: https://eur-lex.europa.eu/legal-content/EN/TXT/?uri=CELEX:52016DC0110%0Ahttp://eur-lex.europa.eu/legal-content/EN/TXT/PDF/?uri=CELEX:52016DC0110&from=EN

[62] X. Sun, B. Zhang, X. Tang, B. C. McLellan, and M. Höök, "Sustainable energy transitions in China: Renewable options and impacts on the electricity system," *Energies*, vol. 9, no. 12, 2016, doi: 10.3390/en9120980.

[63] M. Ghofrani, "Optimizing Hybrid Renewable Energy Systems : A Review World ' s

largest Science , Technology & Medicine Open Access book publisher," in *Sustainable Energy - Technological Issues, Applications and Case Studies*, no. February, INTECh, 2017, pp. 162–176. doi: 10.5772/65971.

[64] E. C. Kern, Jr. and M. C. Russell, "Combined photovoltaic and thermal hybrid collector systems," 1978.

[65] M. Hissouf, M. Feddaoui, M. Najim, A. Charef, and A. E. Kabeel, "Effect of optical, geometrical and operating parameters on the performances of glazed and unglazed PV/T system," *Appl. Therm. Eng.*, vol. 197, p. 117358, Oct. 2021, doi: 10.1016/J.APPLTHERMALENG.2021.117358.

[66] M. Herrando, A. Ramos, I. Zabalza, and C. N. Markides, "A comprehensive assessment of alternative absorber-exchanger designs for hybrid PVT-water collectors," *Appl. Energy*, vol. 235, pp. 1583–1602, Feb. 2019, doi: 10.1016/J.APENERGY.2018.11.024.

[67] F. Selimefendigil and C. Şirin, "Energy and exergy analysis of a hybrid photovoltaic/thermal-air collector modified with nano-enhanced latent heat thermal energy storage unit," *J. Energy Storage*, vol. 45, p. 103467, Jan. 2022, doi: 10.1016/J.EST.2021.103467.

[68] H. A. Hasan, K. Sopian, A. H. Jaaz, and A. N. Al-Shamani, "Experimental investigation of jet array nanofluids impingement in photovoltaic/thermal collector," *Sol. Energy*, vol. 144, pp. 321–334, 2017, doi: 10.1016/j.solener.2017.01.036.

[69] M. Smyth *et al.*, "Experimental performance characterisation of a Hybrid Photovoltaic/Solar Thermal Façade module compared to a flat Integrated Collector Storage Solar Water Heater module," *Renew. Energy*, pp. 1–7, 2018, doi: 10.1016/j.renene.2018.04.017.

[70] E. Erdil, M. Ilkan, and F. Egelioglu, “An experimental study on energy generation with a photovoltaic (PV)–solar thermal hybrid system,” *Energy*, vol. 33, no. 8, pp. 1241–1245, Aug. 2008, doi: 10.1016/J.ENERGY.2008.03.005.

[71] A. Kumar, P. Baredar, and U. Qureshi, “Historical and recent development of photovoltaic thermal (PVT) technologies,” *Renew. Sustain. Energy Rev.*, vol. 42, pp. 1428–1436, 2015, doi: 10.1016/j.rser.2014.11.044.

[72] J. . A. Duffie and W. A. Beckman, *Solar Engineering of Thermal Processes*, Fourth. New Jersey: y John Wiley & Sons, 2013. [Online]. Available: https://www.sku.ac.ir/Datafiles/BookLibrary/45/John A. Duffie, William A. Beckman(auth.)-Solar Engineering of Thermal Processes, Fourth Edition (2013).pdf

[73] M. Sadi, A. mohammad Behzadi, A. S. Alsagri, K. H. Chakravarty, and A. Arabkoohsar, “An innovative green multi-generation system centering around concentrating PVTs and biomass heaters, design and multi-objective optimization,” *J. Clean. Prod.*, vol. 340, no. August 2021, p. 130625, 2022, doi: 10.1016/j.jclepro.2022.130625.

[74] Y. Jia, G. Alva, and G. Fang, “Development and applications of photovoltaic–thermal systems: A review,” *Renew. Sustain. Energy Rev.*, vol. 102, no. June 2018, pp. 249–265, 2019, doi: 10.1016/j.rser.2018.12.030.

[75] F. Yazdanifard, M. Ameri, and E. Ebrahimnia-Bajestan, “Performance of nanofluid-based photovoltaic/thermal systems: A review,” *Renew. Sustain. Energy Rev.*, vol. 76, pp. 323–352, Sep. 2017, doi: 10.1016/j.rser.2017.03.025.

[76] N. Aste, G. Chiesa, and F. Verri, “Design, development and performance monitoring of a photovoltaic-thermal (PVT) air collector,” *Renew. Energy*, vol. 33, no. 5, pp. 914–927, 2008, doi: 10.1016/j.renene.2007.06.022.

[77] G. Barone, A. Buonomano, C. Forzano, A. Palombo, and O. Panagopoulos, “Photovoltaic thermal collectors: Experimental analysis and simulation model of an innovative low-cost water-based prototype,” *Energy*, vol. 179, pp. 502–516, 2019, doi: 10.1016/j.energy.2019.04.140.

[78] S. Dubey, J. N. Sarvaiya, and B. Seshadri, “Temperature dependent photovoltaic (PV) efficiency and its effect on PV production in the world - A review,” *Energy Procedia*, vol. 33, pp. 311–321, 2013, doi: 10.1016/j.egypro.2013.05.072.

[79] A. A. E. Amin and M. A. Al-Maghrabi, “The Analysis of Temperature Effect for mc-Si Photovoltaic Cells Performance,” *Silicon*, vol. 10, no. 4, pp. 1551–1555, 2018, doi: 10.1007/s12633-017-9639-5.

[80] D. Das, P. Kalita, and O. Roy, “Flat plate hybrid photovoltaic- thermal (PV/T) system: A review on design and development,” *Renew. Sustain. Energy Rev.*, vol. 84, no. January, pp. 111–130, 2018, doi: 10.1016/j.rser.2018.01.002.

[81] K. A. Moharram, M. S. Abd-Elhady, H. A. Kandil, and H. El-Sherif, “Enhancing the performance of photovoltaic panels by water cooling,” *Ain Shams Eng. J.*, vol. 4, no. 4, pp. 869–877, 2013, doi: 10.1016/j.asej.2013.03.005.

[82] S. Diwania, S. Agrawal, A. S. Siddiqui, and S. Singh, “Photovoltaic–thermal (PV/T) technology: a comprehensive review on applications and its advancement,” *Int. J. Energy Environ. Eng.*, vol. 11, no. 1, pp. 33–54, 2020, doi: 10.1007/s40095-019-00327-y.

[83] S. Vaishak and P. V. Bhale, “Photovoltaic/thermal-solar assisted heat pump system: Current status and future prospects,” *Sol. Energy*, vol. 189, no. November 2018, pp. 268–284, 2019, doi: 10.1016/j.solener.2019.07.051.

[84] S. A. Kalogirou and Y. Tripanagnostopoulos, “Hybrid PV/T solar systems for domestic hot water and electricity production,” *Energy Convers. Manag.*, vol. 47, no. 18–19, pp. 3368–3382, 2006, doi: 10.1016/j.enconman.2006.01.012.

[85] M. Barbu, M. Siroux, and G. Darie, “Numerical model and parametric analysis of a liquid based hybrid photovoltaic thermal (PVT) collector,” *Energy Reports*, Aug. 2021, doi: 10.1016/J.EGYR.2021.07.058.

[86] K. Egab, A. Okab, H. S. Dywan, and S. K. Oudah, “Enhancing a solar panel cooling system using an air heat sink with different fin configurations - IOPscience,” *3rd International Conference on Engineering Sciences*, 2020. https://iopscience.iop.org/article/10.1088/1757-899X/671/1/012133 (accessed Jun. 20, 2020).

[87] S. Nižetić, D. Čoko, A. Yadav, and F. Grubišić-Čabo, “Water spray cooling technique applied on a photovoltaic panel: The performance response,” *Energy Convers. Manag.*, vol. 108, pp. 287–296, Jan. 2016, doi: 10.1016/j.enconman.2015.10.079.

[88] L. H. Yang, J. De Liang, C. Y. Hsu, T. H. Yang, and S. L. Chen, “Enhanced efficiency of photovoltaic panels by integrating a spray cooling system with shallow geothermal energy heat exchanger,” *Renew. Energy*, vol. 134, pp. 970–981, Apr. 2019, doi: 10.1016/j.renene.2018.11.089.

[89] A. Ibrahim, A. Fudholi, K. Sopian, M. Y. Othman, and M. H. Ruslan, “Efficiencies and improvement potential of building integrated photovoltaic thermal (BIPVT) system,” *Energy Convers. Manag.*, vol. 77, pp. 527–534, Jan. 2014, doi: 10.1016/j.enconman.2013.10.033.

[90] X. Zhang, X. Zhao, S. Smith, J. Xu, and X. Yu, “Review of R&D progress and practical

application of the solar photovoltaic/thermal (PV/T) technologies," *Renew. Sustain. Energy Rev.*, vol. 16, no. 1, pp. 599–617, 2012, doi: 10.1016/j.rser.2011.08.026.

[91] W. He, T. T. Chow, J. Ji, J. Lu, G. Pei, and L. S. Chan, "Hybrid photovoltaic and thermal solar-collector designed for natural circulation of water," *Appl. Energy*, vol. 83, no. 3, pp. 199–210, Mar. 2006, doi: 10.1016/j.apenergy.2005.02.007.

[92] A. M. A. Soliman, H. Hassan, and S. Ookawara, "An experimental study of the performance of the solar cell with heat sink cooling system," in *Energy Procedia*, Apr. 2019, vol. 162, pp. 127–135. doi: 10.1016/j.egypro.2019.04.014.

[93] A. Gagliano, G. M. Tina, F. Nocera, A. D. Grasso, and S. Aneli, "Description and performance analysis of a flexible photovoltaic/thermal (PV/T) solar system," *Renew. Energy*, vol. 137, pp. 144–156, 2019, doi: 10.1016/j.renene.2018.04.057.

[94] S. A. Kalogirou, "Use of TRNSYS for modelling and simulation of a hybrid pvthermal solar system for Cyprus," *Renew. Energy*, vol. 23, pp. 247–260, 2001, doi: https://doi.org/10.1016/S0960-1481(00)00176-2.

[95] A. Akbarzadeh and T. Wadowski, "Heat pipe-based cooling systems for photovoltaic cells under concentrated solar radiation," *Appl. Therm. Eng.*, vol. 16, no. 1, pp. 81–87, Jan. 1996, doi: 10.1016/1359-4311(95)00012-3.

[96] H. Long, T. T. Chow, and J. Ji, "Building-integrated heat pipe photovoltaic/thermal system for use in Hong Kong," *Sol. Energy*, vol. 155, pp. 1084–1091, 2017, doi: 10.1016/j.solener.2017.07.055.

[97] T. T. Chow, W. He, and J. Ji, "An experimental study of façade-integrated photovoltaic/water-heating system," *Appl. Therm. Eng.*, vol. 27, no. 1, pp. 37–45, Jan. 2007, doi: 10.1016/j.applthermaleng.2006.05.015.

[98] T. T. Chow, W. He, and J. Ji, “Hybrid photovoltaic-thermosyphon water heating system for residential application,” *Sol. Energy*, vol. 80, no. 3, pp. 298–306, Mar. 2006, doi: 10.1016/j.solener.2005.02.003.

[99] H. Bahaidarah, A. Subhan, P. Gandhidasan, and S. Rehman, “Performance evaluation of a PV (photovoltaic) module by back surface water cooling for hot climatic conditions,” *Energy*, vol. 59, pp. 445–453, 2013, doi: 10.1016/j.energy.2013.07.050.

[100] S. A. Kalogirou, “Use of TRNSYS for modelling and simulation of a hybrid pv–thermal solar system for Cyprus,” *Renew. Energy*, vol. 23, no. 2, pp. 247–260, Jun. 2001, doi: 10.1016/S0960-1481(00)00176-2.

[101] H. Long, T. T. Chow, and J. Ji, “Building-integrated heat pipe photovoltaic/thermal system for use in Hong Kong,” *Sol. Energy*, vol. 155, pp. 1084–1091, 2017, doi: 10.1016/j.solener.2017.07.055.

[102] R. Braun, M. Haag, J. Stave, N. Abdelnour, and U. Eicker, “System design and feasibility of trigeneration systems with hybrid photovoltaic-thermal (PVT) collectors for zero energy office buildings in different climates,” *Sol. Energy*, vol. 196, no. September 2019, pp. 39–48, 2020, doi: 10.1016/j.solener.2019.12.005.

[103] T. You, W. Wu, H. Yang, J. Liu, and X. Li, “Hybrid photovoltaic/thermal and ground source heat pump: Review and perspective,” *Renew. Sustain. Energy Rev.*, vol. 151, no. August, p. 111569, 2021, doi: 10.1016/j.rser.2021.111569.

[104] K. Wang, M. Herrando, A. M. Pantaleo, and C. N. Markides, “Technoeconomic assessments of hybrid photovoltaic-thermal vs. conventional solar-energy systems: Case studies in heat and power provision to sports centres,” *Appl. Energy*, vol. 254, p. 113657, Nov. 2019, doi: 10.1016/j.apenergy.2019.113657.

[105] F. Calise, F. L. Cappiello, M. Dentice d'Accadia, and M. Vicidomini, "Dynamic simulation, energy and economic comparison between BIPV and BIPVT collectors coupled with micro-wind turbines," *Energy*, vol. 191, p. 116439, 2020, doi: 10.1016/j.energy.2019.116439.

[106] M. Carmona, A. Palacio Bastos, and J. D. García, "Experimental evaluation of a hybrid photovoltaic and thermal solar energy collector with integrated phase change material (PVT-PCM) in comparison with a traditional photovoltaic (PV) module," *Renew. Energy*, vol. 172, pp. 680–696, Jul. 2021, doi: 10.1016/J.RENENE.2021.03.022.

[107] M. Abbasi Kamazani and C. Aghanajafi, "Multi-objective optimization and exergoeconomic evaluation of a hybrid geothermal-PVT system integrated with PCM," *Energy*, vol. 240, p. 122806, Feb. 2022, doi: 10.1016/J.ENERGY.2021.122806.

[108] F. J. Vivas, A. De las Heras, F. Segura, and J. M. Andújar, "A review of energy management strategies for renewable hybrid energy systems with hydrogen backup," *Renew. Sustain. Energy Rev.*, vol. 82, no. April 2016, pp. 126–155, 2018, doi: 10.1016/j.rser.2017.09.014.

[109] A. F. Crossland, O. H. Anuta, and N. S. Wade, "A socio-technical approach to increasing the battery lifetime of off-grid photovoltaic systems applied to a case study in Rwanda," *Renew. Energy*, vol. 83, pp. 30–40, Nov. 2015, doi: 10.1016/J.RENENE.2015.04.020.

[110] P. García, J. P. Torreglosa, L. M. Fernández, and F. Jurado, "Optimal energy management system for stand-alone wind turbine/photovoltaic/hydrogen/battery hybrid system with supervisory control based on fuzzy logic," *Int. J. Hydrogen Energy*, vol. 38, no. 33, pp. 14146–14158, Nov. 2013, doi: 10.1016/J.IJHYDENE.2013.08.106.

[111] N. Karami, N. Moubayed, and R. Outbib, "Energy management for a PEMFC–PV

hybrid system," *Energy Convers. Manag.*, vol. 82, pp. 154–168, Jun. 2014, doi: 10.1016/J.ENCONMAN.2014.02.070.

[112] G. Bruni, S. Cordiner, M. Galeotti, V. Mulone, M. Nobile, and V. Rocco, "Control Strategy Influence on the Efficiency of a Hybrid Photovoltaic-Battery-Fuel Cell System Distributed Generation System for Domestic Applications," *Energy Procedia*, vol. 45, pp. 237–246, Jan. 2014, doi: 10.1016/J.EGYPRO.2014.01.026.

[113] T. Kamal, S. Z. Hassan, H. Li, S. Mumtaz, and L. Khan, "Energy management and control of grid-connected wind/fuel cell/battery Hybrid Renewable Energy System," *2016 Int. Conf. Intell. Syst. Eng. ICISE 2016*, pp. 161–166, 2016, doi: 10.1109/INTELSE.2016.7475114.

[114] M. S. Behzadi and M. Niasati, "Comparative performance analysis of a hybrid PV/FC/battery stand-alone system using different power management strategies and sizing approaches," *Int. J. Hydrogen Energy*, vol. 40, no. 1, pp. 538–548, Jan. 2015, doi: 10.1016/J.IJHYDENE.2014.10.097.

[115] G. Cau, D. Cocco, M. Petrollese, S. Knudsen Kær, and C. Milan, "Energy management strategy based on short-term generation scheduling for a renewable microgrid using a hydrogen storage system," *Energy Convers. Manag.*, vol. 87, pp. 820–831, Nov. 2014, doi: 10.1016/J.ENCONMAN.2014.07.078.

[116] A. Merabet, A. Al-Durra, and E. F. El-Saadany, "Energy management system for optimal cost and storage utilization of renewable hybrid energy microgrid," *Energy Convers. Manag.*, vol. 252, p. 115116, Jan. 2022, doi: 10.1016/J.ENCONMAN.2021.115116.

[117] R. Kaluthanthrige and A. D. Rajapakse, "Demand response integrated day-ahead energy

management strategy for remote off-grid hybrid renewable energy systems," *Int. J. Electr. Power Energy Syst.*, vol. 129, p. 106731, Jul. 2021, doi: 10.1016/J.IJEPES.2020.106731.

[118] S. Bhattacharjee and C. Nandi, "Design of a voting based smart energy management system of the renewable energy based hybrid energy system for a small community," *Energy*, vol. 214, p. 118977, Jan. 2021, doi: 10.1016/J.ENERGY.2020.118977.

[119] M. Jafari and Z. Malekjamshidi, "Optimal energy management of a residential-based hybrid renewable energy system using rule-based real-time control and 2D dynamic programming optimization method," *Renew. Energy*, vol. 146, pp. 254–266, Feb. 2020, doi: 10.1016/J.RENENE.2019.06.123.

[120] P. Rullo, L. Braccia, P. Luppi, D. Zumoffen, and D. Feroldi, "Integration of sizing and energy management based on economic predictive control for standalone hybrid renewable energy systems," *Renew. Energy*, vol. 140, pp. 436–451, 2019, doi: 10.1016/j.renene.2019.03.074.

[121] A. Mohamed and O. Mohammed, "Real-time energy management scheme for hybrid renewable energy systems in smart grid applications," *Electr. Power Syst. Res.*, vol. 96, pp. 133–143, Mar. 2013, doi: 10.1016/J.EPSR.2012.10.015.

[122] X. Xu, W. Hu, W. Liu, Y. Du, Q. Huang, and Z. Chen, "Robust energy management for an on-grid hybrid hydrogen refueling and battery swapping station based on renewable energy," *J. Clean. Prod.*, vol. 331, p. 129954, Jan. 2022, doi: 10.1016/J.JCLEPRO.2021.129954.

[123] Q. Ma, X. Huang, F. Wang, C. Xu, R. Babaei, and H. Ahmadian, "Optimal sizing and feasibility analysis of grid-isolated renewable hybrid microgrids: Effects of energy

management controllers," *Energy*, vol. 240, p. 122503, Feb. 2022, doi: 10.1016/J.ENERGY.2021.122503.

[124] Y. Cao *et al.*, "Development and transient performance analysis of a decentralized grid-connected smart energy system based on hybrid solar-geothermal resources; Techno-economic evaluation," *Sustain. Cities Soc.*, vol. 76, p. 103425, 2022, doi: 10.1016/j.scs.2021.103425.

[125] A. Behzadi and A. Arabkoohsar, "Comparative performance assessment of a novel cogeneration solar-driven building energy system integrating with various district heating designs," *Energy Convers. Manag.*, vol. 220, p. 113101, Sep. 2020, doi: 10.1016/J.ENCONMAN.2020.113101.

[126] H. Lin, C. Yang, and X. Xu, "A new optimization model of CCHP system based on genetic algorithm," *Sustain. Cities Soc.*, vol. 52, p. 101811, Jan. 2020, doi: 10.1016/J.SCS.2019.101811.

[127] J. Wang, S. Li, G. Zhang, and Y. Yang, "Performance investigation of a solar-assisted hybrid combined cooling, heating and power system based on energy, exergy, exergo-economic and exergo-environmental analyses," *Energy Convers. Manag.*, vol. 196, no. May, pp. 227–241, 2019, doi: 10.1016/j.enconman.2019.05.108.

[128] E. Gholamian, P. Hanafizadeh, P. Ahmadi, and L. Mazzarella, "A transient optimization and techno-economic assessment of a building integrated combined cooling, heating and power system in Tehran," *Energy Convers. Manag.*, vol. 217, p. 112962, Aug. 2020, doi: 10.1016/J.ENCONMAN.2020.112962.

[129] A. Pirmohamadi, S. M. Dastjerdi, B. M. Ziapour, P. Ahmadi, and M. A. Rosen, "Integrated solar thermal systems in smart optimized zero energy buildings: Energy,

environment and economic assessments," *Sustain. Energy Technol. Assessments*, vol. 48, p. 101580, Dec. 2021, doi: 10.1016/J.SETA.2021.101580.

[130] Y. Wang *et al.*, "Modeling and operation optimization of an integrated ground source heat pump and solar PVT system based on heat current method," *Sol. Energy*, vol. 218, pp. 492–502, Apr. 2021, doi: 10.1016/J.SOLENER.2021.03.003.

[131] E. I. Sakellariou, A. J. Wright, P. Axaopoulos, and M. A. Oyinlola, "PVT based solar assisted ground source heat pump system: Modelling approach and sensitivity analyses," *Sol. Energy*, vol. 193, pp. 37–50, Nov. 2019, doi: 10.1016/J.SOLENER.2019.09.044.

[132] M. Abu-Rumman, M. Hamdan, and O. Ayadi, "Performance enhancement of a photovoltaic thermal (PVT) and ground-source heat pump system," *Geothermics*, vol. 85, no. February, p. 101809, 2020, doi: 10.1016/j.geothermics.2020.101809.

[133] L. Xia, Z. Ma, G. Kokogiannakis, S. Wang, and X. Gong, "A model-based optimal control strategy for ground source heat pump systems with integrated solar photovoltaic thermal collectors," *Appl. Energy*, vol. 228, pp. 1399–1412, Oct. 2018, doi: 10.1016/J.APENERGY.2018.07.026.

[134] G. He, J. Lin, F. Sifuentes, X. Liu, N. Abhyankar, and A. Phadke, "Rapid cost decrease of renewables and storage accelerates the decarbonization of China's power system," *Nat. Commun.*, vol. 11, no. 1, pp. 1–9, 2020, doi: 10.1038/s41467-020-16184-x.

[135] M. Herrando, A. Ramos, J. Freeman, I. Zabalza, and C. N. Markides, "Technoeconomic modelling and optimisation of solar combined heat and power systems based on flat-box PVT collectors for domestic applications," *Energy Convers. Manag.*, vol. 175, pp. 67–85, Nov. 2018, doi: 10.1016/j.enconman.2018.07.045.

[136] A. Chakir *et al.*, "Optimal energy management for a grid connected PV-battery system,"

in *Energy Reports*, Feb. 2020, vol. 6, pp. 218–231. doi: 10.1016/j.egyr.2019.10.040.

[137] A. S. Aziz, M. F. N. Tajuddin, M. R. Adzman, M. A. M. Ramli, and S. Mekhilef, "Energy management and optimization of a PV/diesel/battery hybrid energy system using a combined dispatch strategy," *Sustain.*, vol. 11, no. 3, 2019, doi: 10.3390/su11030683.

[138] C. Li and W. Yu, "Techno-economic comparative analysis of off-grid hybrid photovoltaic/diesel/battery and photovoltaic/battery power systems for a household in Urumqi, China," *J. Clean. Prod.*, vol. 124, pp. 258–265, 2016, doi: 10.1016/j.jclepro.2016.03.002.

[139] N. H. Saad, A. A. El-Sattar, and A. E. A. M. Mansour, "A novel control strategy for grid connected hybrid renewable energy systems using improved particle swarm optimization," *Ain Shams Eng. J.*, vol. 9, no. 4, pp. 2195–2214, 2018, doi: 10.1016/j.asej.2017.03.009.

[140] A. Allouhi, "A novel grid-connected solar PV-thermal/wind integrated system for simultaneous electricity and heat generation in single family buildings," *J. Clean. Prod.*, vol. 320, no. July, p. 128518, 2021, doi: 10.1016/j.jclepro.2021.128518.

[141] A. H. Jaaz, K. Sopian, and T. S. Gaaz, "Study of the electrical and thermal performances of photovoltaic thermal collector-compound parabolic concentrated," *Results Phys.*, vol. 9, pp. 500–510, Jun. 2018, doi: 10.1016/J.RINP.2018.03.004.

[142] M. R. Elkadeem, S. Wang, S. W. Sharshir, and E. G. Atia, "Feasibility analysis and techno-economic design of grid-isolated hybrid renewable energy system for electrification of agriculture and irrigation area: A case study in Dongola, Sudan," *Energy Convers. Manag.*, vol. 196, no. August, pp. 1453–1478, 2019, doi:

10.1016/j.enconman.2019.06.085.

[143] A. Maleki, M. A. Rosen, and F. Pourfayaz, “Optimal operation of a grid-connected hybrid renewable energy system for residential applications,” *Sustain.*, vol. 9, no. 8, 2017, doi: 10.3390/su9081314.

[144] S. A. Belfedhal, E. M. Berkouk, and Y. Messlem, “Analysis of grid connected hybrid renewable energy system,” *J. Renew. Sustain. Energy*, vol. 11, no. 1, 2019, doi: 10.1063/1.5054869.

[145] J. G. García Clúa, R. J. Mantz, and H. De Battista, “Optimal sizing of a grid-assisted wind-hydrogen system,” *Energy Convers. Manag.*, vol. 166, no. April, pp. 402–408, 2018, doi: 10.1016/j.enconman.2018.04.047.

[146] P. A. Hohne, K. Kusakana, and B. P. Numbi, “Optimal energy management and economic analysis of a grid-connected hybrid solar water heating system: A case of Bloemfontein, South Africa,” *Sustain. Energy Technol. Assessments*, vol. 31, no. December 2018, pp. 273–291, 2019, doi: 10.1016/j.seta.2018.12.027.

[147] S. Gottwalt, W. Ketter, C. Block, J. Collins, and C. Weinhardt, “Demand side management—A simulation of household behavior under variable prices,” *Energy Policy*, vol. 39, no. 12, pp. 8163–8174, Dec. 2011, doi: 10.1016/J.ENPOL.2011.10.016.

[148] A. Arteconi, N. J. Hewitt, and F. Polonara, “State of the art of thermal storage for demand-side management,” *Appl. Energy*, vol. 93, pp. 371–389, May 2012, doi: 10.1016/J.APENERGY.2011.12.045.

[149] R. Zeng, X. Zhang, Y. Deng, H. Li, and G. Zhang, “Optimization and performance comparison of combined cooling, heating and power/ground source heat pump/photovoltaic/solar thermal system under different load ratio for two operation

strategies," *Energy Convers. Manag.*, vol. 208, p. 112579, Mar. 2020, doi: 10.1016/J.ENCONMAN.2020.112579.

[150] A. Behzadi, A. Arabkoohsar, and Y. Yang, "Optimization and dynamic techno-economic analysis of a novel PVT-based smart building energy system," *Appl. Therm. Eng.*, vol. 181, no. April, p. 115926, 2020, doi: 10.1016/j.applthermaleng.2020.115926.

[151] IRENA, *The Power to Change: Solar and Wind Cost Reduction Potential to 2025*, no. June. International Renewable Energy Agency, 2016. [Online]. Available: www.irena.org

[152] J. Liu, S. Cao, X. Chen, H. Yang, and J. Peng, "Energy planning of renewable applications in high-rise residential buildings integrating battery and hydrogen vehicle storage," *Appl. Energy*, vol. 281, no. June 2020, p. 116038, 2021, doi: 10.1016/j.apenergy.2020.116038.

[153] B. Surya *et al.*, "Economic Evaluation, Use of Renewable Energy, and Sustainable Urban Development Mamminasata Metropolitan, Indonesia," 2021, doi: 10.3390/su13031165.

[154] R. Braun, M. Haag, J. Stave, N. Abdelnour, and U. Eicker, "System design and feasibility of trigeneration systems with hybrid photovoltaic-thermal (PVT) collectors for zero energy office buildings in different climates," *Sol. Energy*, vol. 196, pp. 39–48, Jan. 2020, doi: 10.1016/j.solener.2019.12.005.

[155] M. Abu-Rumman, M. Hamdan, and O. Ayadi, "Performance enhancement of a photovoltaic thermal (PVT) and ground-source heat pump system," *Geothermics*, vol. 85, no. November 2019, p. 101809, 2020, doi: 10.1016/j.geothermics.2020.101809.

[156] Y. N. Dabwan, G. Pei, G. Gao, J. Feng, and J. Li, "A novel integrated solar tri-generation

system for cooling, freshwater and electricity production purpose: Energy, economic and environmental performance analysis," *Sol. Energy*, vol. 198, no. May 2019, pp. 139–150, 2020, doi: 10.1016/j.solener.2020.01.043.

[157] H. A. Kazem, T. Khatib, K. Sopian, and W. Elmenreich, "Performance and feasibility assessment of a 1.4 kW roof top grid-connected photovoltaic power system under desertic weather conditions," *Energy Build.*, vol. 82, pp. 123–129, 2014, doi: 10.1016/j.enbuild.2014.06.048.

[158] M. Herrando, A. Ramos, J. Freeman, I. Zabalza, and C. N. Markides, "Technoeconomic modelling and optimisation of solar combined heat and power systems based on flat-box PVT collectors for domestic applications," *Energy Convers. Manag.*, vol. 175, no. July, pp. 67–85, 2018, doi: 10.1016/j.enconman.2018.07.045.

[159] K. Wang *et al.*, "Spectral-splitting hybrid PV-thermal (PVT) systems for combined heat and power provision to dairy farms," *Renew. Energy*, vol. 159, pp. 1047–1065, 2020, doi: 10.1016/j.renene.2020.05.120.

[160] S. Abdul-Ganiyu, D. A. Quansah, E. W. Ramde, R. Seidu, and M. S. Adaramola, "Techno-economic analysis of solar photovoltaic (PV) and solar photovoltaic thermal (PVT) systems using exergy analysis," *Sustain. Energy Technol. Assessments*, vol. 47, no. November 2020, p. 101520, 2021, doi: 10.1016/j.seta.2021.101520.

[161] Y. Tripanagnostopoulos, "Aspects and improvements of hybrid photovoltaic/thermal solar energy systems," *Sol. Energy*, vol. 81, no. 9, pp. 1117–1131, 2007, doi: 10.1016/j.solener.2007.04.002.

[162] A. Żabnieńska-Góra, N. Khordehgah, and H. Jouhara, "Annual performance analysis of the PV/T system for the heat demand of a low-energy single-family building," *Renew.*

Energy, vol. 163, pp. 1923–1931, 2021, doi: 10.1016/j.renene.2020.10.123.

[163] K. Zelzouli, A. Guizani, R. Sebai, and C. Kerkeni, "Solar Thermal Systems Performances versus Flat Plate Solar Collectors Connected in Series," *Engineering*, vol. 04, no. 12, pp. 881–893, 2012, doi: 10.4236/eng.2012.412112.

[164] N. Karami and M. Rahimi, "Heat transfer enhancement in a hybrid microchannel-photovoltaic cell using Boehmite nanofluid," *Int. Commun. Heat Mass Transf.*, vol. 55, pp. 45–52, Jul. 2014, doi: 10.1016/J.ICHEATMASSTRANSFER.2014.04.009.

[165] F. Yazdanifard, M. Ameri, and E. Ebrahimnia-Bajestan, "Performance of nanofluid-based photovoltaic/thermal systems: A review," *Renew. Sustain. Energy Rev.*, vol. 76, no. December 2016, pp. 323–352, 2017, doi: 10.1016/j.rser.2017.03.025.

[166] S. Abdul-Ganiyu, D. A. Quansah, E. W. Ramde, R. Seidu, and M. S. Adaramola, "Investigation of solar photovoltaic-thermal (PVT) and solar photovoltaic (PV) performance: A case study in Ghana," *Energies*, vol. 13, no. 11, 2020, doi: 10.3390/en13112701.

[167] M. Chung and H. C. Park, "Comparison of building energy demand for hotels, hospitals, and offices in Korea," *Energy*, vol. 92, pp. 383–393, 2015, doi: 10.1016/j.energy.2015.04.016.

[168] F. Huide, Z. Xuxin, M. Lei, Z. Tao, W. Qixing, and S. Hongyuan, "A comparative study on three types of solar utilization technologies for buildings: Photovoltaic, solar thermal and hybrid photovoltaic/thermal systems," *Energy Convers. Manag.*, vol. 140, pp. 1–13, 2017, doi: 10.1016/j.enconman.2017.02.059.

[169] M. Jahangiri, A. Alidadi Shamsabadi, and H. Saghaei, "Comprehensive Evaluation of Using Solar Water Heater on a Household Scale in Canada," *J. Renew. Energy Environ.*,

vol. 5, no. 1, pp. 35–42, 2018, [Online]. Available: http://www.jree.ir/article_88491.html%0Ahttp://www.jree.ir/pdf_88491_51a9a7966f493d8992890ecd5bfcf104.html

[170] Meteoblue, "Simulated historical climate & weather data for Jos," *Meteoblue*, 2022. https://www.meteoblue.com/en/weather/historyclimate/climatemodelled/jos_nigeria_2335953 (accessed Mar. 12, 2022).

[171] E. Fuentes, L. Arce, and J. Salom, "A review of domestic hot water consumption profiles for application in systems and buildings energy performance analysis," *Renew. Sustain. Energy Rev.*, vol. 81, no. February, pp. 1530–1547, 2018, doi: 10.1016/j.rser.2017.05.229.

[172] T. Sikram, M. Ichinose, and R. Sasaki, "Assessment of Thermal Comfort and Building-Related Symptoms in Air-Conditioned Offices in Tropical Regions: A Case Study in Singapore and Thailand," *Front. Built Environ.*, vol. 6, no. November, pp. 1–16, 2020, doi: 10.3389/fbuil.2020.567787.

[173] H. D. Backer, "Effect of Heat on the Sterilization of Artificially Contaminated Water," *J. Travel Med.*, vol. 3, pp. 1–4, 1996, Accessed: Aug. 21, 2020. [Online]. Available: https://academic.oup.com/jtm/article/3/1/1/1804390

[174] L. Costa and P. Bracco, "Mechanisms of Crosslinking, Oxidative Degradation and Stabilization of UHMWPE," in *UHMWPE Biomaterials Handbook*, Elsevier Inc., 2009, pp. 309–323. doi: 10.1016/B978-0-12-374721-1.00021-3.

[175] P. A. Murphy, "A guide to effective care in pregnancy and childbirth. Edited by Murray Enkin, Marc J.N.C. Keirse, and Iain Chalmers. New York: Oxford University Press, 1990. 376 pages. $24.95, softcover," *Journal of Nurse-Midwifery*, vol. 38, no. 1. No

longer published by Elsevier, pp. 58–60, Jan. 01, 1993. doi: 10.1016/0091-2182(93)90137-6.

[176] T. P. Lima, J. C. C. Dutra, A. R. M. Primo, J. Rohatgi, and A. A. V. Ochoa, “Solar water heating for a hospital laundry: A case study,” *Sol. Energy*, vol. 122, pp. 737–748, 2015, doi: 10.1016/j.solener.2015.10.006.

[177] S. J. Zwalnan, G. A. Duvuna, Y. A. Abakr, and T. Banda, “Design and performance evaluation of a multi-temperature flat plate solar collector,” *Int. J. Renew. Energy Dev.*, vol. 10, no. 3, pp. 537–549, 2021, doi: 10.14710/ijred.2021.33213.

[178] A. Ramos, M. A. Chatzopoulou, I. Guarracino, J. Freeman, and C. N. Markides, “Hybrid photovoltaic-thermal solar systems for combined heating, cooling and power provision in the urban environment,” *Energy Convers. Manag.*, vol. 150, pp. 838–850, 2017, doi: 10.1016/j.enconman.2017.03.024.

[179] J. A. Duffie and W. A. Beckman, *Solar engineering of thermal processes*, 4th ed. New Jersey, 2006. doi: April 15, 2013.

[180] H. A. Kazem, T. Khatib, and K. Sopian, “Sizing of a standalone photovoltaic/battery system at minimum cost for remote housing electrification in Sohar, Oman,” *Energy Build.*, vol. 61, pp. 108–115, 2013, doi: 10.1016/j.enbuild.2013.02.011.

[181] D. Jonas, M. Lämmle, D. Theis, S. Schneider, and G. Frey, “Performance modeling of PVT collectors: Implementation, validation and parameter identification approach using TRNSYS,” *Sol. Energy*, vol. 193, no. September, pp. 51–64, 2019, doi: 10.1016/j.solener.2019.09.047.

[182] A. Zarrella, G. Emmi, J. Vivian, L. Croci, and G. Besagni, “The validation of a novel lumped parameter model for photovoltaic thermal hybrid solar collectors: a new

TRNSYS type," *Energy Convers. Manag.*, vol. 188, no. March, pp. 414–428, 2019, doi: 10.1016/j.enconman.2019.03.030.

[183] P. Eguía-Oller, S. Martínez-Mariño, E. Granada-Álvarez, and L. Febrero-Garrido, "Empirical validation of a multizone building model coupled with an air flow network under complex realistic situations," *Energy Build.*, vol. 249, p. 111197, Oct. 2021, doi: 10.1016/J.ENBUILD.2021.111197.

[184] S. A. Kalogirou, R. Agathokleous, G. Barone, A. Buonomano, C. Forzano, and A. Palombo, "Development and validation of a new TRNSYS Type for thermosiphon flat-plate solar thermal collectors: energy and economic optimization for hot water production in different climates," *Renew. Energy*, vol. 136, pp. 632–644, 2019, doi: 10.1016/j.renene.2018.12.086.

[185] N. K. C. Sint, I. A. Choudhury, H. H. Masjuki, and H. Aoyama, "Theoretical analysis to determine the efficiency of a CuO-water nanofluid based-flat plate solar collector for domestic solar water heating system in Myanmar," *Sol. Energy*, vol. 155, pp. 608–619, 2017, doi: 10.1016/j.solener.2017.06.055.

[186] M. Chinchilla, D. Santos-Martín, M. Carpintero-Rentería, and S. Lemon, "Worldwide annual optimum tilt angle model for solar collectors and photovoltaic systems in the absence of site meteorological data," *Appl. Energy*, vol. 281, no. October 2020, p. 116056, 2021, doi: 10.1016/j.apenergy.2020.116056.

[187] A. K. Yadav and S. S. Chandel, "Tilt angle optimization to maximize incident solar radiation: A review," *Renew. Sustain. Energy Rev.*, vol. 23, pp. 503–513, 2013, doi: 10.1016/j.rser.2013.02.027.

[188] "How To Charge Lithium Iron Phosphate (LiFePO4) Batteries - Power Sonic."

https://www.power-sonic.com/blog/how-to-charge-lithium-iron-phosphate-lifepo4-batteries/ (accessed Mar. 16, 2022).

[189] M. B. Sanjareh, M. H. Nazari, G. B. Gharehpetian, R. Ahmadiahangar, and A. Rosin, "Optimal scheduling of HVACs in islanded residential microgrids to reduce BESS size considering effect of discharge duration on voltage and capacity of battery cells," *Sustain. Energy, Grids Networks*, vol. 25, p. 100424, Mar. 2021, doi: 10.1016/J.SEGAN.2020.100424.

[190] D. Jie, J. Seuss, L. Suneja, and R. G. Harley, "SoC feedback control for wind and ess hybrid power system frequency regulation," *IEEE J. Emerg. Sel. Top. Power Electron.*, vol. 2, no. 1, pp. 79–86, Mar. 2014, doi: 10.1109/JESTPE.2013.2289991.

[191] Y. H. Li and W. C. Kao, "Performance analysis and economic assessment of solar thermal and heat pump combisystems for subtropical and tropical region," *Sol. Energy*, vol. 153, pp. 301–316, 2017, doi: 10.1016/j.solener.2017.05.067.

[192] O. Bany Mousa, S. Kara, and R. A. Taylor, "Comparative energy and greenhouse gas assessment of industrial rooftop-integrated PV and solar thermal collectors," *Appl. Energy*, vol. 241, pp. 113–123, May 2019, doi: 10.1016/J.APENERGY.2019.03.052.

[193] L. Romero Rodríguez, J. M. Salmerón Lissén, J. Sánchez Ramos, E. Á. Rodríguez Jara, and S. Álvarez Domínguez, "Analysis of the economic feasibility and reduction of a building's energy consumption and emissions when integrating hybrid solar thermal/PV/micro-CHP systems," *Appl. Energy*, vol. 165, pp. 828–838, Mar. 2016, doi: 10.1016/J.APENERGY.2015.12.080.

[194] N. S. Nazri *et al.*, "Energy economic analysis of photovoltaic-thermal-thermoelectric (PVT-TE) air collectors," *Renew. Sustain. Energy Rev.*, vol. 92, no. March, pp. 187–

197, 2018, doi: 10.1016/j.rser.2018.04.061.

[195] A. H. A. Al-Waeli, K. Sopian, M. T. Chaichan, H. A. Kazem, H. A. Hasan, and A. N. Al-Shamani, “An experimental investigation of SiC nanofluid as a base-fluid for a photovoltaic thermal PV/T system,” *Energy Convers. Manag.*, vol. 142, pp. 547–558, 2017, doi: 10.1016/j.enconman.2017.03.076.

[196] A. N. Al-Shamani, K. Sopian, S. Mat, H. A. Hasan, A. M. Abed, and M. H. Ruslan, “Experimental studies of rectangular tube absorber photovoltaic thermal collector with various types of nanofluids under the tropical climate conditions,” *Energy Convers. Manag.*, vol. 124, pp. 528–542, 2016, doi: 10.1016/j.enconman.2016.07.052.

[197] S. G. Sigarchian, “Small Scale Decentralized Energy Systems optimization and performance analysis,” KTH School of Industrial Engineering and Management, 2018. [Online]. Available: http://www.diva-portal.org/smash/record.jsf?pid=diva2%3A1206702&dswid=-4627

[198] F. J. Diez, L. M. Navas-Gracia, A. Martínez-Rodríguez, A. Correa-Guimaraes, and L. Chico-Santamarta, “Modelling of a flat-plate solar collector using artificial neural networks for different working fluid (water) flow rates,” *Sol. Energy*, vol. 188, pp. 1320–1331, Aug. 2019, doi: 10.1016/j.solener.2019.07.022.

[199] S. Hoseinzadeh and R. Azadi, “Simulation and optimization of a solar-assisted heating and cooling system for a house in Northern of Iran,” *J. Renew. Sustain. Energy*, vol. 9, no. 4, 2017, doi: 10.1063/1.5000288.

[200] F. A. Alturki, H. M. H. Farh, A. A. Al-Shamma’a, and K. Alsharabi, “Techno-economic optimization of small-scale hybrid energy systems using manta ray foraging optimizer,” *Electron.*, vol. 9, no. 12, pp. 1–23, 2020, doi: 10.3390/electronics9122045.

[201] H. O. Omotoso, A. M. Al-Shaalan, H. M. H. Farh, and A. A. Al-Shamma'a, "Techno-Economic Evaluation of Hybrid Energy Systems Using Artificial Ecosystem-Based Optimization with Demand Side Management," *Electron.*, vol. 11, no. 2, 2022, doi: 10.3390/electronics11020204.

[202] J. Liu, M. Wang, J. Peng, X. Chen, S. Cao, and H. Yang, "Techno-economic design optimization of hybrid renewable energy applications for high-rise residential buildings," *Energy Convers. Manag.*, vol. 213, p. 112868, Jun. 2020, doi: 10.1016/j.enconman.2020.112868.

[203] C. Sam-Amobi, O. V. Ekechukwu, and C. B. Chukwuali, "A preliminary assessment of the energy related carbon emissions associated with hotels in Enugu Metropolis Nigeria," *AFRREV STECH An Int. J. Sci. Technol.*, vol. 8, no. 2, pp. 19–30, 2019, doi: 10.4314/stech.v8i2.2.

[204] O. Krishan and S. Suhag, "Techno-economic analysis of a hybrid renewable energy system for an energy poor rural community," *J. Energy Storage*, vol. 23, no. November 2018, pp. 305–319, 2019, doi: 10.1016/j.est.2019.04.002.

[205] B. K. Das, N. Hoque, S. Mandal, T. K. Pal, and M. A. Raihan, "A techno-economic feasibility of a stand-alone hybrid power generation for remote area application in Bangladesh," *Energy*, vol. 134, pp. 775–788, Sep. 2017, doi: 10.1016/J.ENERGY.2017.06.024.

[206] A. Afzal, M. Mohibullah, and V. K. Sharma, "Optimal hybrid renewable energy systems for energy security: A comparative study," *Int. J. Sustain. Energy*, vol. 29, no. 1, pp. 48–58, Mar. 2010, doi: 10.1080/14786460903337241.

[207] S. Rahmanian and A. Hamzavi, "Effects of pump power on performance analysis of

photovoltaic thermal system using CNT nanofluid," *Sol. Energy*, vol. 201, no. February, pp. 787–797, 2020, doi: 10.1016/j.solener.2020.03.061.

[208] N. T. Mbungu, R. C. Bansal, R. M. Naidoo, M. Bettayeb, M. W. Siti, and M. Bipath, "A dynamic energy management system using smart metering," *Appl. Energy*, vol. 280, no. June, p. 115990, 2020, doi: 10.1016/j.apenergy.2020.115990.

[209] B. Lamrani, A. Draoui, and F. Kuznik, "Thermal performance and environmental assessment of a hybrid solar-electrical wood dryer integrated with Photovoltaic/Thermal air collector and heat recovery system," *Sol. Energy*, vol. 221, pp. 60–74, Jun. 2021, doi: 10.1016/J.SOLENER.2021.04.035.

[210] W. Pang, B. C. Duck, C. J. Fell, G. J. Wilson, W. Zhao, and H. Yan, "Influence of multiple factors on performance of photovoltaic-thermal modules," *Sol. Energy*, vol. 214, no. November 2020, pp. 642–654, 2021, doi: 10.1016/j.solener.2020.11.050.

[211] H. B. C. El Hocine, K. Touafek, F. Kerrour, H. Haloui, and A. Khelifa, "Model Validation of an Empirical Photovoltaic Thermal (PV/T) Collector," 2015. doi: 10.1016/j.egypro.2015.07.749.

[212] S. Bae and Y. Nam, "Comparison between experiment and simulation for the development of a Tri-generation system using photovoltaic-thermal and ground source heat pump," *Energy Build.*, vol. 231, p. 110623, 2021, doi: 10.1016/j.enbuild.2020.110623.

[213] A. Rasheed, C. S. Kwak, H. T. Kim, and H. W. Lee, "Building energy an simulation model for analyzing energy saving options of multi-span greenhouses," *Appl. Sci.*, vol. 10, no. 19, pp. 1–23, 2020, doi: 10.3390/app10196884.

[214] A. Mehmood, A. Waqas, Z. Said, S. M. A. Rahman, and M. Akram, "Performance

evaluation of solar water heating system with heat pipe evacuated tubes provided with natural gas backup," *Energy Reports*, vol. 5, pp. 1432–1444, Nov. 2019, doi: 10.1016/J.EGYR.2019.10.002.

[215] V. Sun, A. Asanakham, T. Deethayat, and T. Kiatsiriroat, "A new method for evaluating nominal operating cell temperature (NOCT) of unglazed photovoltaic thermal module," *Energy Reports*, vol. 6, pp. 1029–1042, Nov. 2020, doi: 10.1016/J.EGYR.2020.04.026.

[216] L. S. Pantic, T. M. Pavlović, D. D. Milosavljević, I. S. Radonjic, M. K. Radovic, and G. Sazhko, "The assessment of different models to predict solar module temperature, output power and efficiency for Nis, Serbia," *Energy*, vol. 109, pp. 38–48, Aug. 2016, doi: 10.1016/J.ENERGY.2016.04.090.

[217] S. A. Klein *et al.*, *TRNSYS 18: A Transient System Simulation Program, Solar Energy Laboratory*. Madison, WI 53703 – U.S.A.: University of Wisconsin, 2017.

[218] National Renewable Laboratory NREL, *A Manual for the Economic Evaluation of Energy Efficiency and Renewable Energy Technologies*. Golden, Colorado, 1995.

[219] M. A. Kamel, A. Y. Elbanhawy, and M. Abo El-Nasr, "A novel methodology to compare between side-by-side photovoltaics and thermal collectors against hybrid photovoltaic thermal collectors," *Energy Convers. Manag.*, vol. 202, no. October, p. 112196, 2019, doi: 10.1016/j.enconman.2019.112196.

[220] R. Fu *et al.*, "U . S . Solar Photovoltaic System Cost Benchmark : Q1 2020," 2020. [Online]. Available: https://www.nrel.gov/docs/fy17osti/68925.pdf

[221] S. M. Roy, R. Machavaram, S. Moulick, and C. K. Mukherjee, "Economic feasibility study of aerators in aquaculture using life cycle costing (LCC) approach," *J. Environ. Manage.*, vol. 302, p. 114037, Jan. 2022, doi: 10.1016/J.JENVMAN.2021.114037.

[222] C. Outline, *Life-Cycle Cost and Energy Productivity Analyses*. Elsevier Inc., 2018. doi: 10.1016/B978-0-12-849869-9/00005-3.

[223] A. W. Bashir and B. C. C. Leite, "Performance of aerogel as a thermal insulation material towards a sustainable design of residential buildings for tropical climates in Nigeria," *Energy Built Environ.*, vol. 3, no. 3, pp. 291–315, Jul. 2022, doi: 10.1016/J.ENBENV.2021.02.003.

[224] S. Birkha Mohd Ali, M. Hasanuzzaman, N. A. Rahim, M. A. A. Mamun, and U. H. Obaidellah, "Analysis of energy consumption and potential energy savings of an institutional building in Malaysia," *Alexandria Eng. J.*, vol. 60, no. 1, pp. 805–820, 2021, doi: 10.1016/j.aej.2020.10.010.

[225] P. Bendt, *Appropriate sizing of solar water heating system*. Springfield, VA: Solar Energy Research Institute, 1980. [Online]. Available: https://www.nrel.gov/docs/legosti/old/320.pdf

[226] S. Liu, B. Hao, X. Chen, C. Yao, and W. Zhou, "Analysis on limitation of Using Solar Fraction Ratio as Solar Hot Water System Design and Evaluation Index," *Energy Procedia*, vol. 70, pp. 353–360, 2015, doi: 10.1016/j.egypro.2015.02.134.

[227] NiMet, "Average daylight in September / Average sunshine in September Jos, Nigeria," *Weather forecast and climate Jos, Nigeria*, 2020. https://www.weather-atlas.com/en/nigeria/jos-weather-september

[228] A. Y. Abdalla, Z. S. Johnson, S. Anandan, and ..., "A Numerical Evaluation of the Effect of Building Thermal Load on the Overall Performance Characteristic of a Grid-Coupled PV/T Energy System," *J. Adv. ...*, vol. 1, no. 1, pp. 32–43, 2021, [Online]. Available: https://akademiabaru.com/submit/index.php/arnht/article/view/3798

[229] M. Cordella, C. Stramigioli, and F. Santarelli, “A Set of Coherent Indicators for the Assessment of the Energy Profitability of Energy Systems,” *J. Sustain. Bioenergy Syst.*, vol. 03, no. 01, pp. 40–47, 2013, doi: 10.4236/jsbs.2013.31005.

[230] S. . Buckles, W.E., Klein, “Analysis of solar domestic hot water heaters,” *Sol. Energy*, vol. 25, no. 5, pp. 417–424., 1980.

[231] National Renewable Laboratory NREL, “High Performance Flat Plate Solar Thermal Collector Evaluation,” 2015. [Online]. Available: https://www.nrel.gov/docs/fy16osti/66215.pdf

[232] L. M. Ayompe and A. Duffy, “Analysis of the thermal performance of a solar water heating system with flat plate collectors in a temperate climate,” *Appl. Therm. Eng.*, vol. 58, no. 1–2, pp. 447–454, Sep. 2013, doi: 10.1016/j.applthermaleng.2013.04.062.

[233] UNEP, “Emissions Gap Report 2019: Global progress report on climate action,” 2019. [Online]. Available: https://www.unep.org/interactive/emissions-gap-report/2019/index.php

[234] J. Rouleau and L. Gosselin, “Impacts of the COVID-19 lockdown on energy consumption in a Canadian social housing building,” *Appl. Energy*, vol. 287, no. February, p. 116565, 2021, doi: 10.1016/j.apenergy.2021.116565.

[235] E. Yandri, “Modeling Joule Heating Effect on Thermal Efficiency of Photovoltaic Thermal (PVT) Collectors with Operation Mode Factor (OMF),” *Appl. Sci.*, vol. 12, no. 2, 2022, doi: 10.3390/app12020742.

[236] M. Herrando, A. M. Pantaleo, K. Wang, and C. N. Markides, “Solar combined cooling, heating and power systems based on hybrid PVT, PV or solar-thermal collectors for building applications,” *Renew. Energy*, vol. 143, pp. 637–647, Dec. 2019, doi:

10.1016/j.renene.2019.05.004.

[237] B. Widyolar *et al.*, “Experimental performance of an ultra-low-cost solar photovoltaic-thermal (PVT) collector using aluminum minichannels and nonimaging optics,” *Appl. Energy*, vol. 268, no. March, p. 114894, 2020, doi: 10.1016/j.apenergy.2020.114894.

[238] Made-in-China, “Solar pump system controller,” 2021. https://mcabattery.en.made-in-china.com/product/LvRmrfouRzYg/China-High-Quality-24V-110ah-Gel-Sealed-Lead-Acid-Battery.html (accessed Mar. 05, 2021).

[239] D. C. Jordan and S. R. Kurtz, “Photovoltaic degradation rates - An Analytical Review,” *Prog. Photovoltaics Res. Appl.*, vol. 21, no. 1, pp. 12–29, 2013, doi: 10.1002/pip.1182.

[240] GlobalPetrolPrice.com, “Nigeria Diesel prices,” *GlobalPetrolPrice.com*, 2021. https://www.globalpetrolprices.com/Nigeria/diesel_prices/ (accessed Mar. 04, 2021).

[241] Jumia, “Mercury 12V, 200Ah Inverter Battery,” *Jumia Tech Week*, 2021. https://www.jumia.com.ng/mercury-12v-200ah-inverter-battery-10481917.html

[242] J. O. Oladigbolu, M. A. M. Ramli, and Y. A. Al-Turki, “Feasibility Study and Comparative Analysis of Hybrid Renewable Power System for off-Grid Rural Electrification in a Typical Remote Village Located in Nigeria,” *IEEE Access*, vol. 8, pp. 171643–171663, 2020, doi: 10.1109/access.2020.3024676.

[243] D. Annaratone, *Steam Generators Description and Design*, vol. 53. Springer, 2008.

[244] P. O. Oviroh and T. C. Jen, “The energy cost analysis of hybrid systems and diesel generators in powering selected base transceiver station locations in Nigeria,” *Energies*, vol. 11, no. 3, pp. 7–9, 2018, doi: 10.3390/en11030687.

[245] A. A. Adesanya and J. M. Pearce, “Economic viability of captive off-grid solar photovoltaic and diesel hybrid energy systems for the Nigerian private sector,” *Renew.*

Sustain. Energy Rev., vol. 114, no. August, p. 109348, 2019, doi: 10.1016/j.rser.2019.109348.

[246] P. Arévalo-Cordero, D. J. Benavides, Juan Leonardo, L. Hernández-Callejo, and F. Jurado, "Optimal energy management strategies to reduce diesel consumption for a hybrid off-grid system," *Rev. Fac. Ing. Univ. Antioquia*, no. 98, pp. 47–58, 2020, doi: 10.17533/udea.redin.20200471.

[247] V. O. Oladokun and O. C. Asemota, "Unit cost of electricity in Nigeria: A cost model for captive diesel powered generating system," *Renew. Sustain. Energy Rev.*, vol. 52, pp. 35–40, Dec. 2015, doi: 10.1016/J.RSER.2015.07.028.

[248] R. Costamagna, "Inflation and R&D investment," *J. Innov. Econ.*, vol. 17, no. 2, p. 143, 2015, doi: 10.3917/jie.017.0143.

[249] I. O. Ayodeji, "Panel logit regression analysis of the effects of corruption on inflation pattern in the Economic Community of West African states," *Heliyon*, vol. 6, no. 12, pp. 1–10, 2020, doi: 10.1016/j.heliyon.2020.e05637.

[250] T. Y. Jung, D. Kim, J. Moon, and S. K. Lim, "A scenario analysis of solar photovoltaic grid parity in the Maldives: The case of Malahini resort," *Sustain.*, vol. 10, no. 11, pp. 1–14, 2018, doi: 10.3390/su10114045.

[251] S. Jamshidi, K. Pourhossein, and M. Asadi, "Size estimation of wind/solar hybrid renewable energy systems without detailed wind and irradiation data: A feasibility study," *Energy Convers. Manag.*, vol. 234, p. 113905, Apr. 2021, doi: 10.1016/J.ENCONMAN.2021.113905.

[252] T. Brahim and A. Jemni, "Economical assessment and applications of photovoltaic/thermal hybrid solar technology: A review," *Sol. Energy*, vol. 153, pp.

540–561, 2017, doi: 10.1016/j.solener.2017.05.081.

[253] M. Soussi, M. Balghouthi, A. A. Guizani, and C. Bouden, “Model performance assessment and experimental analysis of a solar assisted cooling system,” *Sol. Energy*, vol. 143, pp. 43–62, 2017, doi: 10.1016/j.solener.2016.12.046.

[254] D. Brough, J. Ramos, B. Delpech, and H. Jouhara, “Development and validation of a TRNSYS type to simulate heat pipe heat exchangers in transient applications of waste heat recovery,” *Int. J. Thermofluids*, vol. 9, 2021, doi: 10.1016/j.ijft.2020.100056.

APPENDIX

A1: SARA equipment inventory numbering survey form

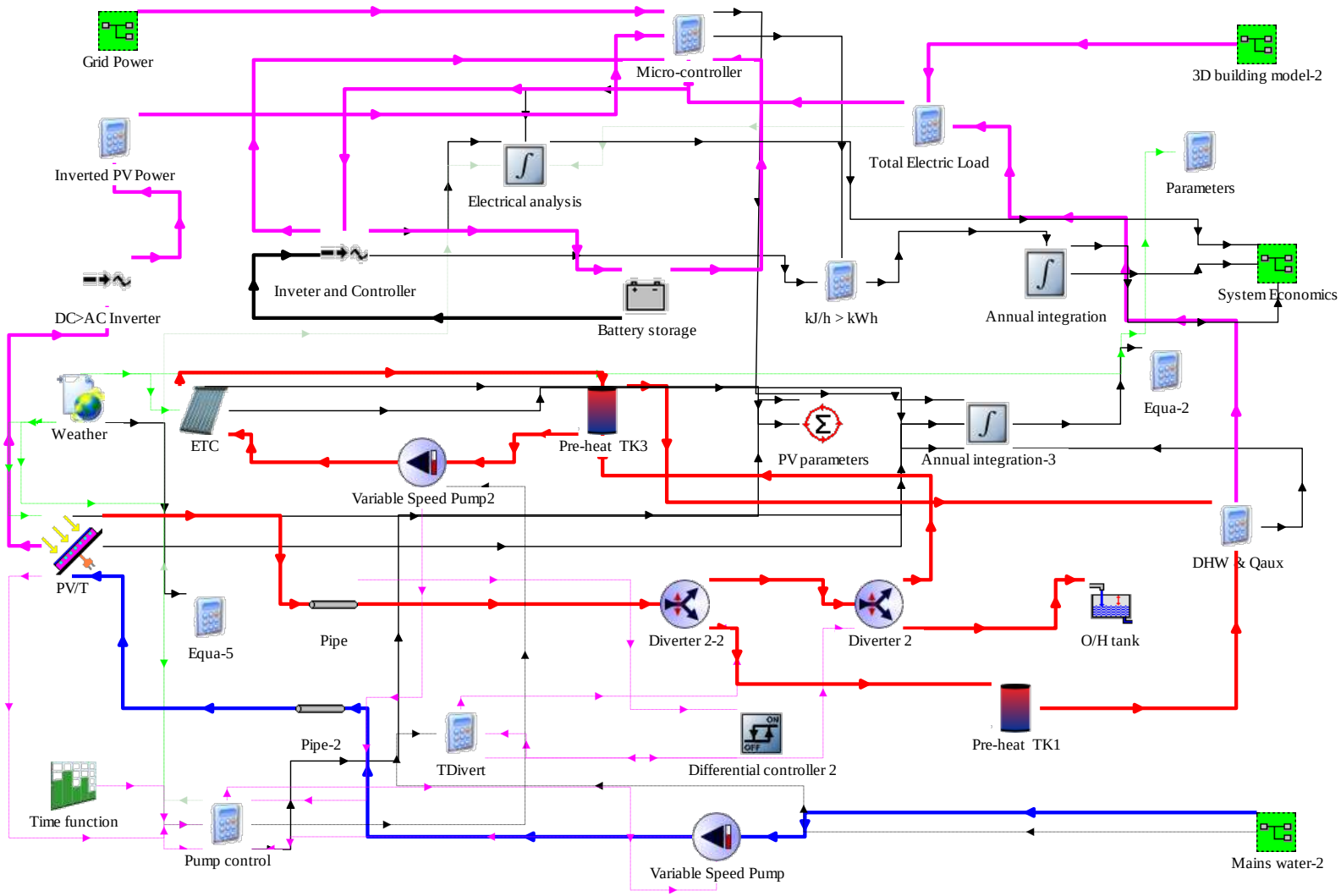
S/N	Name of equipment	S/N	Name of equipment
1	fluorescent light (T12 Krypton-filled)	10	Blood chemistry analyzer, WP 21B
2	Television (LG flatron 22”)	11	Micro haematocrit centrifuge, KHT-400
3	Desk top computer	12	Electrophoresis machine with tank,200ml
4	Printer, HP leser jet, 1020	13	microscope
5	Electric water pump	14	Hematology analyzer, BC2800
6	Haier thermocool refrigerator(190l)	15	Spectrophotometer AE-UV1609
7	Drying oven,101-1AB	16	Scanner
8	Steam sterilizer		
9	Fluorescent light (T12 Krypton-filled)		

A2: SARA health clinic electrical power profile form

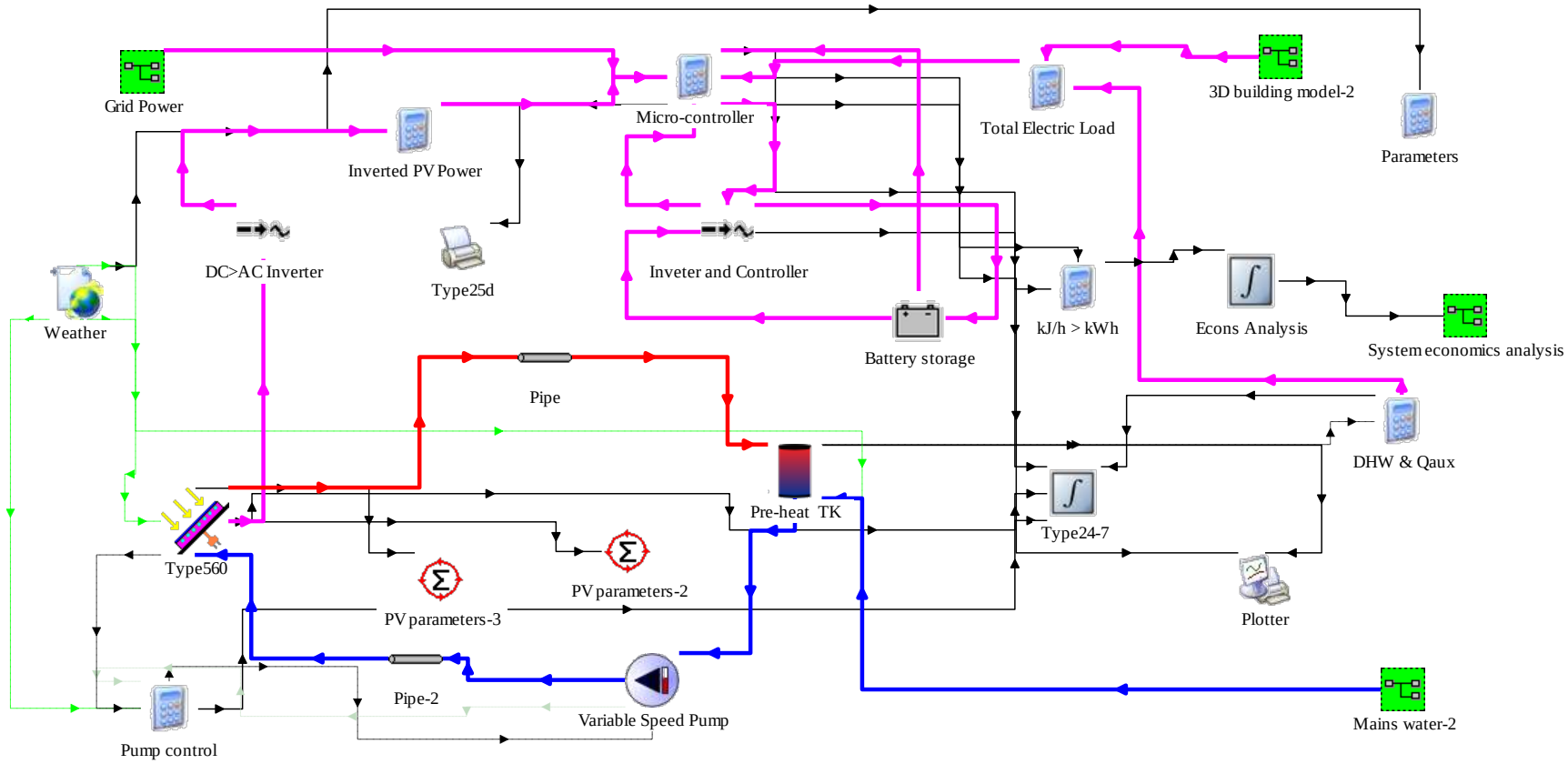
Equipment qty		16	1	1	1	1	1	1	1	1	1	1	1	1	1	1	
S/N	**Time**	**1**	**2**	**3**	**4**	**5**	**6**	**7**	**8**	**9**	**10**	**11**	**12**	**13**	**14**	**15**	
	Power rating	**20W**	**130W**	**300W**	**365W**	**375W**	**110W**	**1500W**	**2000W**	**150W**	**140W**	**60W**	**150W**	**150W**	**110W**	**160W**	**Total Energy (Wh/d)**
1	0.00-0.59	320					110				140	60					630
2	1.00-1.59	320					110				140	60					630
3	2.00-2.59	320					110				140	60					630
4	3.00-3.59	320					110				140	60					630
5	4.00-4.59	320					110				140	60					630
6	5.00-5.59	320					110				140	60					630
7	6.00-6.59	320					110				140	60					630
8	7.00-7.59	320					110										430
9	8.00-8.59		130			373	110			150	140		150		110		1163
10	9.00-9.59		130	300			110			150	140	60	150	150	110	160	1460
11	10.00-10.59		130	300			110			150	140	60	150	150	110	160	1460
12	11.00-11.59		130	300	365		110	1500		150		60	150	150	110	160	3185
13	12.00-12.59		130	300	365		110		2000	150	140		150	150		160	3655
14	13.00-13.59		130	300	365		110		2000	150	140		150	150		160	3655
15	14.00-14.59		130	300	365		110		2000	150	140		150	150		160	3655
16	15.00-1559		130				110	1500		150	140		150	150			2330
17	16.00-16.59		130				110	1500		150	140		150	150			2330
18	17.00-17.59	320	130				110	1500		150	140		150	150			2650
19	18.00-18.59	320	130				110	1500		150	140		150	150			2650
20	19.00-19.59	320					110										430

21	20.00-20.59	320					110										430
22	21.00-21.59	320					110										430
23	22.00-22.59	320					110										430
24	23.00-23.59	320					110										430
	Total	4800	1430	1800	1460	373	2640	7500	6000	1650	2380	600	1650	1500	440	960	35183

Appendix B: TRNSYS model of the OPVETC



Appendix C: TRNSYS model of the Basic hybrid PVT



Appendix D: Building's measured indoor temperature for zone 2

No.	Time	Measured zone temperature (°C)	Simulated zone temperature (°C)
1	09-01-2020 09:36:49	19.9	17.43
2	09-01-2020 09:51:59	20	17.56
3	09-01-2020 10:07:09	20.1	17.71
4	09-01-2020 10:22:19	20.2	18.26
5	09-01-2020 10:37:29	20.3	18.78
6	09-01-2020 10:52:39	20.5	18.90
7	09-01-2020 11:07:49	20.6	19.03
8	09-01-2020 11:22:59	20.7	19.60
9	09-01-2020 11:38:09	20.9	20.11
10	09-01-2020 11:53:19	21.0	20.11
11	09-01-2020 12:08:29	21.1	20.16
12	09-01-2020 12:23:39	21.3	20.75
13	09-01-2020 12:38:49	21.4	21.31
14	09-01-2020 12:53:59	21.5	21.32
15	09-01-2020 13:09:09	21.7	21.36
16	09-01-2020 13:24:19	21.8	21.90
17	09-01-2020 13:39:29	21.9	22.38
18	09-01-2020 13:54:39	22.1	22.31
19	09-01-2020 14:09:49	22.2	22.31
20	09-01-2020 14:24:59	22.3	22.85
21	09-01-2020 14:40:09	22.4	23.37
22	09-01-2020 14:55:19	22.4	23.38
23	09-01-2020 15:10:29	22.5	23.38
24	09-01-2020 15:25:39	23.3	23.77
25	09-01-2020 15:40:49	23.1	24.07
26	09-01-2020 15:55:59	23.1	23.91
27	09-01-2020 16:11:09	23.1	23.81
28	09-01-2020 16:26:19	23.2	24.10
29	09-01-2020 16:41:29	23.2	24.37
30	09-01-2020 16:56:39	23.2	24.28
31	09-01-2020 17:11:49	23.1	24.17
32	09-01-2020 17:26:59	23.0	24.23
33	09-01-2020 17:42:09	22.9	24.23
34	09-01-2020 17:57:19	22.8	24.08
35	09-01-2020 18:12:29	22.7	23.90
36	09-01-2020 18:27:39	22.7	23.50
37	09-01-2020 18:42:49	22.6	23.13
38	09-01-2020 18:57:59	22.5	22.98
39	09-01-2020 19:13:09	22.4	22.98
40	09-01-2020 19:28:19	22.3	22.80
41	09-01-2020 19:43:29	22.2	22.61
42	09-01-2020 19:58:39	22.2	22.60
43	09-01-2020 20:13:49	22.2	22.58
44	09-01-2020 20:28:59	22.1	22.42
45	09-01-2020 20:44:09	22.1	22.26
46	09-01-2020 20:59:19	22.0	22.25
47	09-01-2020 21:14:29	21.9	22.23

48	09-01-2020 21:29:39	21.9	22.08
49	09-01-2020 21:44:49	21.8	21.93
50	09-01-2020 21:59:59	21.7	21.91
51	09-01-2020 22:15:09	21.7	21.90
52	09-01-2020 22:30:19	21.6	21.74
53	09-01-2020 22:45:29	21.5	21.58
54	09-01-2020 23:00:39	21.5	21.58
55	09-01-2020 23:15:49	21.4	21.56
56	09-01-2020 23:30:59	21.3	21.39
57	09-01-2020 23:46:09	21.2	21.24
58	10-01-2020 00:01:19	21.1	21.23
59	10-01-2020 00:16:29	21.0	21.21
60	10-01-2020 00:31:39	21.0	21.04
61	10-01-2020 00:46:49	20.9	20.87
62	10-01-2020 01:01:59	20.9	20.87
63	10-01-2020 01:17:09	20.9	20.86
64	10-01-2020 01:32:19	20.8	20.68
65	10-01-2020 01:47:29	20.7	20.52
66	10-01-2020 02:02:39	20.7	20.51
67	10-01-2020 02:17:49	20.7	20.48
68	10-01-2020 02:32:59	20.6	20.29
69	10-01-2020 02:48:09	20.6	20.12
70	10-01-2020 03:03:19	20.5	20.12
71	10-01-2020 03:18:29	20.4	20.11
72	10-01-2020 03:33:39	20.4	19.94
73	10-01-2020 03:48:49	20.3	19.78
74	10-01-2020 04:03:59	20.3	19.78
75	10-01-2020 04:19:09	20.3	19.77
76	10-01-2020 04:34:19	20.2	19.59
77	10-01-2020 04:49:29	20.2	19.42
78	10-01-2020 05:04:39	20.1	19.43
79	10-01-2020 05:19:49	20.1	19.41
80	10-01-2020 05:34:59	20.0	19.23
81	10-01-2020 05:50:09	20.0	19.06
82	10-01-2020 06:05:19	19.9	19.06
83	10-01-2020 06:20:29	19.9	19.04
84	10-01-2020 06:35:39	19.8	18.85
85	10-01-2020 06:50:49	19.8	18.68
86	10-01-2020 07:05:59	19.8	18.68
87	10-01-2020 07:21:09	19.8	18.67
88	10-01-2020 07:36:19	19.8	18.49
89	10-01-2020 07:51:29	19.8	18.36
90	10-01-2020 08:06:39	19.8	18.49
91	10-01-2020 08:21:49	19.9	18.65
92	10-01-2020 08:36:59	20.0	18.68
93	10-01-2020 08:52:09	20.1	18.90
94	10-01-2020 09:07:19	20.2	19.47
95	10-01-2020 09:22:29	20.3	19.89
96	10-01-2020 09:37:39	20.4	20.15
97	10-01-2020 09:52:49	20.5	20.30
98	10-01-2020 10:07:59	20.7	20.42
99	10-01-2020 10:23:09	20.9	20.56
100	10-01-2020 10:38:19	21.0	20.98

101	10-01-2020 10:53:29	21.2	21.38
102	10-01-2020 11:08:39	21.4	21.48
103	10-01-2020 11:23:49	21.5	21.60
104	10-01-2020 11:38:59	21.7	22.07
105	10-01-2020 11:54:09	21.9	22.52
106	10-01-2020 12:09:19	22.1	22.63
107	10-01-2020 12:24:29	22.3	22.73
108	10-01-2020 12:39:39	22.4	23.22
109	10-01-2020 12:54:49	22.6	23.65
110	10-01-2020 13:09:59	22.8	23.62
111	10-01-2020 13:25:09	22.9	23.65
112	10-01-2020 13:40:19	23.0	24.19
113	10-01-2020 13:55:29	23.2	24.72
114	10-01-2020 14:10:39	23.3	24.83
115	10-01-2020 14:25:49	23.5	24.90
116	10-01-2020 14:40:59	23.5	25.29
117	10-01-2020 14:56:09	23.6	25.59
118	10-01-2020 15:11:19	23.7	25.47
119	10-01-2020 15:26:29	23.8	25.40
120	10-01-2020 15:41:39	23.8	25.67
121	10-01-2020 15:56:49	23.9	25.89
122	10-01-2020 16:11:59	23.9	25.75
123	10-01-2020 16:27:09	23.9	25.63
124	10-01-2020 16:42:19	25.9	25.67
125	10-01-2020 16:57:29	25.2	25.64
126	10-01-2020 17:12:39	25.2	25.35
127	10-01-2020 17:27:49	25.0	25.14
128	10-01-2020 17:42:59	24.7	25.08
129	10-01-2020 17:58:09	24.2	24.99
130	10-01-2020 18:13:19	24.0	24.83
131	10-01-2020 18:28:29	23.9	24.68
132	10-01-2020 18:43:39	23.8	24.38
133	10-01-2020 18:58:49	23.7	24.11
134	10-01-2020 19:13:59	23.7	24.04
135	10-01-2020 19:29:09	23.6	24.04
136	10-01-2020 19:44:19	23.6	23.86
137	10-01-2020 19:59:29	23.5	23.69
138	10-01-2020 20:14:39	23.4	23.68
139	10-01-2020 20:29:49	23.3	23.66
140	10-01-2020 20:44:59	23.3	23.49
141	10-01-2020 21:00:09	23.2	23.33
142	10-01-2020 21:15:19	23.2	23.33
143	10-01-2020 21:30:29	23.2	23.33
144	10-01-2020 21:45:39	23.1	23.17
145	10-01-2020 22:00:49	23.2	23.02
146	10-01-2020 22:15:59	23.1	23.02
147	10-01-2020 22:31:09	23.0	23.02
148	10-01-2020 22:46:19	23.0	22.85
149	10-01-2020 23:01:29	22.9	22.70
150	10-01-2020 23:16:39	22.8	22.69
151	10-01-2020 23:31:49	22.8	22.67
152	10-01-2020 23:46:59	22.7	22.49
153	11-01-2020 00:02:09	22.6	22.32

154	11-01-2020 00:17:19	22.6	22.30
155	11-01-2020 00:32:29	22.5	22.28
156	11-01-2020 00:47:39	22.4	22.08
157	11-01-2020 01:02:49	22.3	21.90
158	11-01-2020 01:17:59	22.2	21.90
159	11-01-2020 01:33:09	22.2	21.88
160	11-01-2020 01:48:19	22.1	21.69
161	11-01-2020 02:03:29	22.0	21.51
162	11-01-2020 02:18:39	21.9	21.51
163	11-01-2020 02:33:49	21.9	21.49
164	11-01-2020 02:48:59	21.8	21.29
165	11-01-2020 03:04:09	21.7	21.10
166	11-01-2020 03:19:19	21.6	21.09
167	11-01-2020 03:34:29	21.5	21.06
168	11-01-2020 03:49:39	21.5	20.84
169	11-01-2020 04:04:49	21.5	20.64
170	11-01-2020 04:19:59	21.4	20.64
171	11-01-2020 04:35:09	21.4	20.63
172	11-01-2020 04:50:19	21.3	20.42
173	11-01-2020 05:05:29	21.2	20.23
174	11-01-2020 05:20:39	21.2	20.23
175	11-01-2020 05:35:49	21.1	20.21
176	11-01-2020 05:50:59	21.0	20.00
177	11-01-2020 06:06:09	21.0	19.79
178	11-01-2020 06:21:19	20.9	19.78
179	11-01-2020 06:36:29	20.9	19.75
180	11-01-2020 06:51:39	20.9	19.51
181	11-01-2020 07:06:49	20.8	19.30
182	11-01-2020 07:21:59	20.8	19.30
183	11-01-2020 07:37:09	20.8	19.28
184	11-01-2020 07:52:19	20.9	19.06
185	11-01-2020 08:07:29	21.2	18.97
186	11-01-2020 08:22:39	21.5	19.34
187	11-01-2020 08:37:49	21.6	19.82
188	11-01-2020 08:52:59	21.7	20.22
189	11-01-2020 09:08:09	21.8	20.50
190	11-01-2020 09:23:19	22.0	20.49
191	11-01-2020 09:38:29	22.1	20.41
192	11-01-2020 09:53:39	22.2	20.81
193	11-01-2020 10:08:49	22.3	21.29
194	11-01-2020 10:23:59	22.4	21.53
195	11-01-2020 10:39:09	22.5	21.74
196	11-01-2020 10:54:19	22.6	22.18
197	11-01-2020 11:09:29	22.7	22.59
198	11-01-2020 11:24:39	22.8	22.72
199	11-01-2020 11:39:49	22.9	22.86
200	11-01-2020 11:54:59	23.0	23.39
201	11-01-2020 12:10:09	23.2	23.87
202	11-01-2020 12:25:19	23.2	23.93
203	11-01-2020 12:40:29	23.5	24.00
204	11-01-2020 12:55:39	23.5	24.53
205	11-01-2020 13:10:49	23.7	25.02
206	11-01-2020 13:25:59	23.8	25.02

207	11-01-2020 13:41:09	24.0	25.05
208	11-01-2020 13:56:19	24.3	25.55
209	11-01-2020 14:11:29	24.5	26.01
210	11-01-2020 14:26:39	24.7	25.99
211	11-01-2020 14:41:49	24.9	25.99
212	11-01-2020 14:56:59	25.2	26.40
213	11-01-2020 15:12:09	25.4	26.76
214	11-01-2020 15:27:19	25.6	26.68
215	11-01-2020 15:42:29	25.5	26.63
216	11-01-2020 15:57:39	25.5	26.94
217	11-01-2020 16:12:49	25.5	27.19
218	11-01-2020 16:27:59	25.5	27.07
219	11-01-2020 16:43:09	25.5	26.98
220	11-01-2020 16:58:19	25.4	27.18
221	11-01-2020 17:13:29	25.4	27.37
222	11-01-2020 17:28:39	25.3	27.32
223	11-01-2020 17:43:49	25.0	27.22
224	11-01-2020 17:58:59	24.8	27.11
225	11-01-2020 18:14:09	24.7	26.89
226	11-01-2020 18:29:19	24.6	26.55
227	11-01-2020 18:44:29	24.5	26.27
228	11-01-2020 18:59:39	24.5	25.89
229	11-01-2020 19:14:49	24.4	25.57
230	11-01-2020 19:29:59	24.3	25.47
231	11-01-2020 19:45:09	24.2	25.46
232	11-01-2020 20:00:19	24.2	25.20
233	11-01-2020 20:15:29	24.1	24.96
234	11-01-2020 20:30:39	24.1	24.95
235	11-01-2020 20:45:49	24.1	24.94
236	11-01-2020 21:00:59	24.1	24.71
237	11-01-2020 21:16:09	24.1	24.49
238	11-01-2020 21:31:19	24.0	24.48
239	11-01-2020 21:46:29	24.0	24.46
240	11-01-2020 22:01:39	23.9	24.23
241	11-01-2020 22:16:49	23.8	24.02
242	11-01-2020 22:31:59	23.7	24.01
243	11-01-2020 22:47:09	23.6	23.98
244	11-01-2020 23:02:19	23.5	23.75
245	11-01-2020 23:17:29	23.5	23.53
246	11-01-2020 23:32:39	23.3	23.52
247	11-01-2020 23:47:49	23.2	23.49
248	12-01-2020 00:02:59	23.1	23.25
249	12-01-2020 00:18:09	23.1	23.02
250	12-01-2020 00:33:19	22.9	23.00
251	12-01-2020 00:48:29	22.9	22.96
252	12-01-2020 01:03:39	22.9	22.70
253	12-01-2020 01:18:49	22.8	22.46
254	12-01-2020 01:33:59	22.7	22.44
255	12-01-2020 01:49:09	22.6	22.39
256	12-01-2020 02:04:19	22.5	22.11
257	12-01-2020 02:19:29	22.4	21.86
258	12-01-2020 02:34:39	22.2	21.86
259	12-01-2020 02:49:49	22.2	21.85

260	12-01-2020 03:04:59	22.2	21.60
261	12-01-2020 03:20:09	22.0	21.37
262	12-01-2020 03:35:19	22.0	21.38
263	12-01-2020 03:50:29	21.8	21.37
264	12-01-2020 04:05:39	21.8	21.12
265	12-01-2020 04:20:49	21.7	20.89
266	12-01-2020 04:35:59	21.6	20.90
267	12-01-2020 04:51:09	21.6	20.89
268	12-01-2020 05:06:19	21.5	20.64
269	12-01-2020 05:21:29	21.4	20.41
270	12-01-2020 05:36:39	21.4	20.42
271	12-01-2020 05:51:49	21.3	20.41
272	12-01-2020 06:06:59	21.2	20.15
273	12-01-2020 06:22:09	21.2	19.91
274	12-01-2020 06:37:19	21.0	19.91
275	12-01-2020 06:52:29	20.9	19.88
276	12-01-2020 07:07:39	21.0	19.61
277	12-01-2020 07:22:49	20.9	19.36
278	12-01-2020 07:37:59	21.0	19.35
279	12-01-2020 07:53:09	21.2	19.32
280	12-01-2020 08:08:19	21.3	19.03
281	12-01-2020 08:23:29	21.5	18.84
282	12-01-2020 08:38:39	21.6	19.07
283	12-01-2020 08:53:49	21.8	19.36
284	12-01-2020 09:08:59	22.0	19.46
285	12-01-2020 09:24:09	22.1	19.62
286	12-01-2020 09:39:19	22.2	19.91
287	12-01-2020 09:54:29	22.3	20.08
288	12-01-2020 10:09:39	22.6	20.28
289	12-01-2020 10:24:49	22.8	20.49
290	12-01-2020 10:39:59	22.6	20.65
291	12-01-2020 10:55:09	22.9	20.79
292	12-01-2020 11:10:19	22.9	21.06
293	12-01-2020 11:25:29	23.0	21.30
294	12-01-2020 11:40:39	23.2	21.32
295	12-01-2020 11:55:49	23.3	21.37
296	12-01-2020 12:10:59	23.3	21.78
297	12-01-2020 12:26:09	23.6	22.22
298	12-01-2020 12:41:19	23.6	22.40
299	12-01-2020 12:56:29	23.7	22.53
300	12-01-2020 13:11:39	23.9	22.94
301	12-01-2020 13:26:49	23.9	23.28
302	12-01-2020 13:41:59	24.1	23.27
303	12-01-2020 13:57:09	24.5	23.30
304	12-01-2020 14:12:19	24.7	23.73
305	12-01-2020 14:27:29	24.9	24.15
306	12-01-2020 14:42:39	25.2	24.17
307	12-01-2020 14:57:49	25.5	24.20
308	12-01-2020 15:12:59	25.5	24.59
309	12-01-2020 15:28:09	25.6	24.96
310	12-01-2020 15:43:19	25.8	24.97
311	12-01-2020 15:58:29	25.7	24.95
312	12-01-2020 16:13:39	25.7	25.22

313	12-01-2020 16:28:49	25.5	25.44
314	12-01-2020 16:43:59	25.6	25.31
315	12-01-2020 16:59:09	26.0	25.21
316	12-01-2020 17:14:19	26.1	25.35
317	12-01-2020 17:29:29	26.1	25.45
318	12-01-2020 17:44:39	25.7	25.32
319	12-01-2020 17:59:49	25.3	25.19
320	12-01-2020 18:14:59	25.0	25.10
321	12-01-2020 18:30:09	24.8	24.94
322	12-01-2020 18:45:19	24.7	24.72
323	12-01-2020 19:00:29	24.6	24.52
324	12-01-2020 19:15:39	24.5	24.12
325	12-01-2020 19:30:49	24.4	23.77
326	12-01-2020 19:45:59	24.3	23.66
327	12-01-2020 20:01:09	24.2	23.65
328	12-01-2020 20:16:19	24.3	23.39
329	12-01-2020 20:31:29	24.3	23.15
330	12-01-2020 20:46:39	24.3	23.16
331	12-01-2020 21:01:49	24.2	23.16
332	12-01-2020 21:16:59	24.2	22.96
333	12-01-2020 21:32:09	24.1	22.75
334	12-01-2020 21:47:19	24.0	22.75
335	12-01-2020 22:02:29	24.0	22.74
336	12-01-2020 22:17:39	23.9	22.52
337	12-01-2020 22:32:49	23.8	22.31
338	12-01-2020 22:47:59	23.7	22.31
339	12-01-2020 23:03:09	23.6	22.30
340	12-01-2020 23:18:19	23.5	22.09
341	12-01-2020 23:33:29	23.5	21.89
342	12-01-2020 23:48:39	23.4	21.89

E1: MATLAB code OPVTEC economics

```
clear all
clc
close all
UCGrid=0.070%[USD/kWh] cost of kWh from grid in Nigeria
UCdiesel=0.48 %[USD/L] cost of Diesel fuel per litre in Nigeria
UCGenOM=0.050%[USD/kWh] generator maintenance cost
kWh_diesel=945.7 % [kWh of load met from diesel generator]
LDiesel=kWh_diesel/5% liter of diesel consummed
GridPurchased=3528.7%[kWh] power from grid source
LCOE_gen = 0.2465%[USD/kWh] Benchmark Cost of power from diesel generator
kWhRen=22744.9% load met by renewable
kWhLoad1=28567.08
Dp_rate=0.5/100% annaul percentage of power degradation from system
N_tank = 2% number of tanks
N_diverter = 2% number of diverters
N_pump = 2% number of pumps
N_controller = 2% number of controllers
N_inv = 8%kW_rating of invereter
N_ETC = 2% number of evacuated tube collector
N_PVT = 33% number of PVT collector
N_batt=15% number of batteries
NGen=1
% FINDING TOTAL INITIAL INVESTMENT
%PVT collector
UC_PVT_watt_DC = 380% [USD/unit] USD/unit of PVT collector from 2021 Q1 US
Benchmark
PVT_cost = UC_PVT_watt_DC*N_PVT% total cost of purchasing PVT
%ET Collector
UC_ETC = 295% USD/unit of ETC from market survey in Alibaba.com
ETC_cost = UC_ETC*N_ETC% Total cost of ETC collector
TCC=PVT_cost+ETC_cost
%Pump and controller
UCpump=12
UCcontroller=210
ControllerCost=N_controller*UCcontroller
PumpCost=N_pump*UCpump
%Inveter
UC_Inverter = 120%[USD/kW] USD/unit of INVERTER from 2021 Q1
Inverter_cost = UC_Inverter*N_inv% Total cost of inverter
% Battery
UC_Batt = 380%[USD/kWh] Unit cost of battery
Batt_cost = UC_Batt*N_batt% total cost of battery
%Gen set
Genset_cost=1580*NGen%[USD/unit] cost of 20kW diesel generator set
% Hydronic
Dcontroller=N_controller*210
Hydronic_cost = N_tank*380+N_diverter*11.8+N_pump*12+N_controller*210% grouping
some costs are hydronic cost
% Installation
Instal_Cost = 0.1*PVT_cost%[USD]Installation cost taken as 10% of the cost of
component
BOS_elec = 0.1*PVT_cost%[USD]Balance of structure electrical (this includes things
like wires, etc)
```

```
BOS_struct = 0.1*PVT_cost%[USD]Balance of structure mechanical (this includes
things like frames support etc, etc)
%Total PVETC
T_PVETC_cost =
PVT_cost+ETC_cost+Batt_cost+Inverter_cost+BOS_elec+BOS_struct+Instal_Cost+Hydronic
_cost+Genset_cost% [USD] overal cost for the installation of the PVT collector

T_IC = T_PVETC_cost% Total capital investment at year zero.

%%%%REPLACEMENT COST%%%%%%%%%%
i=0.14%yearly inflation rate [fraction]
r=0.06%Discount rate yearly

n=[0:1:25]'
IF=(1+i).^n
PVIF=1./((1+r).^n)
PVIF_IF=((1+i).^n)./((1+r).^n)% Present worth factor
PVIF_25=PVIF(26,1)

nzero=[1 0 0 0 0 0 0 0 0 0 0 0 0 0 0 0 0 0 0 0 0 0 0 0 0 0 ]'% initial investement
time operator
oAp=[0 1 1 1 1 1 1 1 1 1 1 1 1 1 1 1 1 1 1 1 1 1 1 1 1 1 ]'% Annual time operator
obatr=[0 0 0 0 0 1 0 0 0 0 1 0 0 0 0 1 0 0 0 0 1 0 0 0 0 0 ]'% Battery replacement
and scrap value time operator
obats=[0 0 0 0 0 1 0 0 0 0 1 0 0 0 0 1 0 0 0 0 1 0 0 0 0 0 ]'%  scrap value time
operator
opvts=[0 0 0 0 0 0 0 0 0 0 0 0 0 0 0 0 0 0 0 0 0 0 0 0 0 1 ]'% PVT scrap value
time operator
oInvr=[0 0 0 0 0 0 0 0 0 0 1 0 0 0 0 0 0 0 0 0 1 0 0 0 0 0 ]'% Inverter
replacement and scrap value time operator
oInvs=[0 0 0 0 0 0 0 0 0 0 1 0 0 0 0 0 0 0 0 0 1 0 0 0 0 0 ]'% Inverter  scrap
value time operator
ogenr=[0 0 0 0 0 0 0 0 0 0 0 0 0 0 0 1 0 0 0 0 0 0 0 0 0 0 ]'% Generator No
replacement  time operator
ogens=[0 0 0 0 0 0 0 0 0 0 0 0 0 0 0 1 0 0 0 0 0 0 0 0 0 0 ]'% Generator No scrap
value  time operator

opumpr=[0 1 1 1 1 1 1 1 1 1 1 1 1 1 1 1 1 1 1 1 1 1 1 1 1 1 ]'% Pump  replacement
time operator
ocontrollerr=[0 0 0 0 0 1 0 0 0 0 1 0 0 0 0 1 0 0 0 0 1 0 0 0 0 0  ]'% Controller
replacement  time operator

TICzero=T_IC*nzero%investment at year zero
RC_battery=Batt_cost.*PVIF_IF.*obatr% Periodic replacement cost for battery
RC_battery_sum=sum(RC_battery,'all')% Total replacement cost for battery
RC_Inverter=Inverter_cost.*PVIF_IF.*oInvr% Periodic replacement cost for inverter
RC_Inverter_sum=sum(RC_Inverter,'all')%Total replacement cost for battery
RC_Gen=Genset_cost.*PVIF_IF.*ogenr*0%% Periodic replacement cost for generator
RC_Gen_sum=sum(RC_Gen,'all')% Tot al replacement cost for generator
RC_Pump=PumpCost.*PVIF_IF.*opumpr% Periodic replacement cost for pump
RC_Pump_sum=sum(RC_Pump,'all')% Total replacement cost for pump
RC_Controller=ControllerCost.*PVIF_IF.*ocontrollerr% Periodic replacement cost for
controller
RC_Controller_sum=sum(RC_Controller,'all')% Total replacement cost for pump
TRC=RC_battery+RC_Inverter+RC_Gen+RC_Pump+RC_Controller% Project total yearly
replacement cost
TRC4=RC_battery+RC_Inverter+RC_Gen%+RC_Controller% Project total yearly
replacement cost
```

```
TRCm2=RC_Pump+RC_Controller% Project total yearly replacement cost
TRC_sum=sum(TRC,'all')% Project total yearly replacement cost
%%%%%%%%%%%%Scrapt value%%%%%%%%%%%%%%%%
%%%%%%%%%%%%%%Salvage/Scrap Value of project%%%%%%%%%%%%%%%%
SalvageBatt=0.1*Batt_cost.*PVIF_IF.*obats% Battery scrap value
Bsum=sum(SalvageBatt,'all')
SalvageInverter=0.1*Inverter_cost.*PVIF_IF.*oInvs% Invereter scrap value
Invsum=sum(SalvageInverter,'all')
SalvageGen=0.1*Genset_cost.*PVIF_IF.*ogens% Generator scrap value
Gensum=sum(SalvageGen,'all')
SalvagePVT=0.1*(PVT_cost+ETC_cost).*opvts.*PVIF_IF% PVT scrap value
PVTsum=sum(SalvagePVT,'all')
Tsalvage=SalvageBatt+SalvageInverter+SalvageGen+SalvagePVT% Total yearly scrap
value
Tsalvage_sum=sum(Tsalvage,'all')% Life time project scrap vale
TRCb=[0.00
0.00
0.00
0.00
0.00
8201.06
0.00
0.00
0.00
0.00
13786.82
0.00
0.00
0.00
0.00
21682.84
0.00
0.00
0.00
0.00
28540.00
0.00
0.00
0.00
0.00
0.00
]

%%%%%%%%OPERATION AND MAINTENANCE COST (O&M)%%%%%%%%%%%%%%%
ie=r
PVIF_IFe=((1+ie).^n)./((1+r).^n)

GenMCost=kWh_diesel.*UCGenOM.*PVIF_IFe.*oAp% cost of maintenance of generator
GenMCost_sum=sum(GenMCost,'all')
DieselfuelCost=LDiesel.*UCdiesel.*PVIF_IFe.*oAp% cost of power from diesel genset
DieselCost_sum=sum(DieselfuelCost,'all')
GridCost=GridPurchased.*UCGrid.*PVIF_IFe.*oAp% total cost of energy met from Grid
source
GridCost_sum=sum(GridCost,'all')
T_O_and_M=GenMCost+DieselfuelCost+GridCost
TOpM_sum=sum(T_O_and_M,'all')
T_Cash_outflow=TICzero+TRC+ T_O_and_M% yearly cash out flow discounted
TLCCyearly=T_Cash_outflow
```

```
TLCC=sum(T_Cash_outflow,'all')%Total life cycle cost of project
%%%%%%%%%%%%%%Salvage/Scrap Value of project%%%%%%%%%%%%%%%%
C_analysis=[T_IC GenMCost_sum DieselCost_sum GridCost_sum TRC_sum  TLCC]'
% Base case comparison system (Diesel engine)

D_rate=1./(1+Dp_rate).^n% annaul power degradation factor
Esavings=kWhRen.*D_rate.*LCOE_gen.*PVIF_IFe.*oAp
Esaving_sum1=sum(Esavings,'all')
Tcashinflow=Esavings+Tsalvage
Tcashinflow_sum=sum(Tcashinflow,'all')
Cashflowp=(Tcashinflow-T_Cash_outflow)
Cashflowb=[-26342.0
4526.9
4499.6
4472.4
4445.2
-3567.1
4391.0
4364.0
4336.9
4309.9
-8994.7
4255.9
4228.9
4201.8
4174.7
-16618.0
4120.3
4093.0
4065.6
4038.1
-23475.4
3982.7
3954.7
3926.5
3898.1
12069.7
]
CumNet1=cumsum(Cashflowp)
CumTLCC=cumsum(T_Cash_outflow)
CumNet2=cumsum(Cashflowb)
CC1=[CumNet1 CumNet2]

NPV_sum=sum(Cashflowp,'all')
yROI=(CumNet1./CumTLCC)*100
ROI=(NPV_sum/TLCC)*100% [%] Project Return on investment (Rule: accept project if
ROI>0 other reject
LCOE = TLCC./(25*kWhLoad1)

%%%%%%%%%%%%%%END%%%%%%%%%%%%%%
figure(1)
CB=[ Cashflowp Cashflowb]
CCF=[CumNet1 CumNet2]
h6=bar(n,CB,0.8)
set(h6,'EdgeColor', 'white')
legend('OPVETC','Basic PVT')
xlabel('Period of analysis [years]')
ylabel('Project cashflow [$/yr]')
```

```
figure(2)
h6=bar(n,CCF,1)
set(h6,'EdgeColor', 'white')
legend('OPVETC','Basic PVT')
xlabel('Period of analysis [years]')
ylabel('Project cashflow [$/yr]')

figure(3)
h7=bar(n,CumNet1,0.4)
set(h7,'EdgeColor', 'white')
legend('OPVETC')
xlabel('Period of analysis [years]')
ylabel('Cumulative cashflow [$]')

figure(4)
h8=bar(n ,CumNet1,0.8)
set(h8,'EdgeColor', 'white')
xlabel('Period of analysis [years]')
ylabel('Cumulative cashflow [$]')

g=0
```

E2: MATLAB code basic hybrid economics

```
clear all
clc
close all
UCGrid=0.10%[USD/kWh]cost of kWh from grid in Nigeria
UCdiesel=0.48 %[USD/L]cost of Diesel fuel per litre in Nigeria
UCGenOM=0.050%[USD/kWh] generator maintenance cost
kWh_diesel=1873.32% [kWh of load met from diesel generator]
LDiesel=kWh_diesel/5% liter of diesel consummed
GridPurchased=4723.96%[kWh] power from grid source
LCOE_gen = 0.2465%[USD/kWh] Benchmark Cost of power from diesel generator
kWhRen=21550.07
kWhLoad2=29715.10 % annual system load
% load met by renewable
Dp_rate=0.5/100% annaul percentage of power degradation from system
N_tank = 1% number of tanks
N_diverter =0% number of diverter
N_pump = 1% number of pumps
N_controller = 2% number of controllers
N_inv = 8%kW_rating of invereter
N_ETC = 0% number of evacuated tube collector
N_PVT = 35% number of PVT collector
N_batt=15% number of batteries
% FINDING TOTAL INITIAL INVESTMENT
%PVT collector
UC_PVT_watt_DC = 380% [USD/unit] USD/unit of PVT collector from 2021 Q1 US
Benchmark
PVT_cost = UC_PVT_watt_DC*N_PVT% total cost of purchasing PVT
%ET Collector
UC_ETC = 295%  USD/unit of ETC from market survey in Alibaba.com
ETC_cost = UC_ETC*N_ETC%  Total cost of ETC collector
%Pump and controller
TCC=PVT_cost+ETC_cost
UCpump=12
UCcontroller=210
ControllerCost=N_controller*UCcontroller
PumpCost=N_pump*UCpump
%Inveter
UC_Inverter = 120%[USD/kW] USD/unit of INVERTER from 2021 Q1
Inverter_cost = UC_Inverter*N_inv% Total cost of inverter
% Battery
UC_Batt = 380%[USD/kWh] Unit cost of battery
Batt_cost = UC_Batt*N_batt% total cost of battery
%Gen set
Genset_cost=1580%[USD/unit] cost of 20kW diesel generator set
% Hydronic
Hydronic_cost = N_tank*380+N_diverter*11.8+N_pump*UCpump+N_controller*210%
grouping some costs are hydronic cost
% Installation
Instal_Cost = 0.1*PVT_cost%[USD]Installation cost taken as 10% of the cost of
component
BOS_elec = 0.1*PVT_cost%[USD]Balance of structure electrical (this includes things
like wires, etc)
BOS_struct = 0.1*PVT_cost%[USD]Balance of structure mechanical (this includes,
things like frames support etc,  etc)
```

```
%Total PVETC
T_PVETC_cost =
PVT_cost+ETC_cost+Batt_cost+Inverter_cost+BOS_elec+BOS_struct+Instal_Cost+Hydronic
_cost+Genset_cost% [USD] overal cost for the installation of the PVT collector
T_IC = T_PVETC_cost% Total capital investment at year zero.

%%%%REPLACEMENT COST%%%%%%%%%%
i=0.14%yearly inflation rate [fraction]
r=0.06%Discount rate yearly


n=[0:1:25]'
IF=(1+i).^n
PVIF=1./((1+r).^n)
PVIF_IF=((1+i).^n)./((1+r).^n)% Present worth factor

nzero=[1 0 0 0 0 0 0 0 0 0 0 0 0 0 0 0 0 0 0 0 0 0 0 0 0 0 ]'% initial investement
time operator
oAp=[0 1 1 1 1 1 1 1 1 1 1 1 1 1 1 1 1 1 1 1 1 1 1 1 1 1 ]'% Annual time operator
obatr=[0 0 0 0 0 1 0 0 0 0 1 0 0 0 0 1 0 0 0 0 1 0 0 0 0 0 ]'% Battery replacement
and scrap value time operator
obats=[0 0 0 0 0 1 0 0 0 0 1 0 0 0 0 1 0 0 0 0 1 0 0 0 0 0 ]'%  scrap value time
operator
opvts=[0 0 0 0 0 0 0 0 0 0 0 0 0 0 0 0 0 0 0 0 0 0 0 0 0 1 ]'% PVT scrap value
time operator
oInvr=[0 0 0 0 0 0 0 0 0 0 1 0 0 0 0 0 0 0 0 1 0 0 0 0 0 ]'% Inverter
replacement and scrap value time operator
oInvs=[0 0 0 0 0 0 0 0 0 0 1 0 0 0 0 0 0 0 0 1 0 0 0 0 0 ]'% Inverter  scrap
value time operator
ogenr=[0 0 0 0 0 0 0 0 0 0 0 0 0 0 0 1 0 0 0 0 0 0 0 0 0 0 ]'% Generator No
replacement  time operator
ogens=[0 0 0 0 0 0 0 0 0 0 0 0 0 0 0 1 0 0 0 0 0 0 0 0 0 0 ]'% Generator No scrap
value  time operator

opumpr=[0 1 1 1 1 1 1 1 1 1 1 1 1 1 1 1 1 1 1 1 1 1 1 1 1 1 ]'% Pump  replacement
time operator
ocontrollerr=[0 0 0 0 0 1 0 0 0 0 1 0 0 0 0 1 0 0 0 0 1 0 0 0 0 0  ]'% Controller
replacement  time operator

TICzero=T_IC*nzero%investment at year zero
RC_battery=Batt_cost.*PVIF_IF.*obatr% Periodic replacement cost for battery
RC_battery_sum=sum(RC_battery,'all')% Total replacement cost for battery
RC_Inverter=Inverter_cost.*PVIF_IF.*oInvr% Periodic replacement cost for inverter
RC_Inverter_sum=sum(RC_Inverter,'all')%Total replacement cost for battery
RC_Gen=Genset_cost.*PVIF_IF.*ogenr%% Periodic replacement cost for generator
RC_Gen_sum=sum(RC_Gen,'all')% Tot al replacement cost for generator
RC_Pump=PumpCost.*PVIF_IF.*opumpr% Periodic replacement cost for pump
RC_Pump_sum=sum(RC_Pump,'all')% Total replacement cost for pump
RC_Controller=ControllerCost.*PVIF_IF.*ocontrollerr% Periodic replacement cost for
controller
RC_Controller_sum=sum(RC_Controller,'all')% Total replacement cost for pump
TRC=RC_battery+RC_Inverter+RC_Gen+RC_Pump+RC_Controller% Project total yearly
replacement cost
TRC4=RC_battery+RC_Inverter+RC_Gen%+RC_Controller% Project total yearly
replacement cost
TRCm2=RC_Pump+RC_Controller% Project total yearly replacement cost
TRC_sum=sum(TRC,'all')% Project total yearly replacement cost
%%%%%%%%%%%%%Scrapt value%%%%%%%%%%%%%%%%%
```

```
%%%%%%%%%%%%%Salvage/Scrap Value of project%%%%%%%%%%%%%%%%
SalvageBatt=0.1*Batt_cost.*PVIF_IF.*obats% Battery scrap value
SalvageInverter=0.1*Inverter_cost.*PVIF_IF.*oInvs% Invereter scrap value
SalvageGen=0.1*Genset_cost.*PVIF_IF.*ogens% Generator scrap value
SalvagePVT=0.1*PVT_cost.*opvts.*PVIF_IF% PVT scrap value
Tsalvage=SalvageBatt+SalvageGen+SalvageInverter+SalvagePVT% Total yearly scrap
value
Tsalvage_sum=sum(Tsalvage,'all')% Life time project scrap vale
%%%%%%%%%OPERATION AND MAINTENANCE COST (O&M)%%%%%%%%%%%%%%%
ie=r
PVIF_IFe=((1+ie).^n)./((1+r).^n)

GenMCost=kWh_diesel.*UCGenOM.*PVIF_IFe.*oAp% cost of mantenance of generator
GenMCost_sum=sum(GenMCost,'all')
DieselfuelCost=LDiesel.*UCdiesel.*PVIF_IFe.*oAp% cost of power from diesel genset
DieselCost_sum=sum(DieselfuelCost,'all')
GridCost=GridPurchased.*UCGrid.*PVIF_IFe.*oAp% total cost of energy met from Grid
source
GridCost_sum=sum(GridCost,'all')
T_O_and_M=GenMCost+DieselfuelCost+GridCost
TOpM_sum=sum(T_O_and_M,'all')
T_Cash_outflow=TICzero+TRC+ T_O_and_M% yearly cash out flow discounted
CumTLCC1=cumsum(T_Cash_outflow)
TLCC=sum(T_Cash_outflow,'all')%Total life cycle cost of project
%%%%%%%%%%%%%Salvage/Scrap Value of project%%%%%%%%%%%%%%%%
C_analysisb=[T_IC GenMCost_sum DieselCost_sum GridCost_sum TRC_sum TLCC]'
C_analysisb1=[T_IC GenMCost_sum DieselCost_sum GridCost_sum TRC_sum ]'
C_analysisp=[26359.60
1213.53
2329.97
9112.63
73795.94
112811.65
]

% Base case comparison system (Diesel engine)

D_rate=1./(1+Dp_rate).^n% annaul power degradation factor
Esavings=kWhRen.*D_rate.*LCOE_gen.*PVIF_IFe.*oAp
Esaving_sum1=sum(Esavings,'all')
Tcashinflow=Esavings+Tsalvage
Tcashinflow_sum=sum(Tcashinflow,'all')
NPV=(Tcashinflow-T_Cash_outflow)
CumNet1=cumsum(NPV)
NPV_sum=sum(NPV,'all')

NPV_sum=sum(NPV,'all')
yROI1=(CumNet1./CumTLCC1)*100
ROI=(NPV_sum/TLCC)*100% [%] Project Return on investment (Rule: accept project if
ROI>0 other reject
LCOE = TLCC/(25*kWhLoad2)
%%%%%%%%%%%%%END%%%%%%%%%%%%%%


figure(1)
h7=bar(n,CumNet1,0.4)
set(h7,'EdgeColor', 'white')
legend('Basic PVT')
```

```
xlabel('Period of analysis [years]')
ylabel('Cumulative cashflow [$]')
figure(2)
h8=bar(C_analysisb,0.6)
set(h8,'EdgeColor', 'white')

set(gca,'xtick',1:6,...
 'xticklabel',{'Investment','O&M','Fuel ','Grid power ','Repl. cost','TLCC'})
ylabel('Cost [$]')
hold on
h9=bar(C_analysisp,0.4)
set(h9,'EdgeColor', 'white')
legend('basic PVT','OPVETC')

ylabel('Cost [$]')
legend('basic PVT','OPVETC')
figure(3)
h8=bar(C_analysisb1,0.6)
set(h8,'EdgeColor', 'white')

set(gca,'xtick',1:6,...
 'xticklabel',{'Investment','O&M','Fuel ','Grid power ','Repl. cost'})
ylabel('Cost [$]')
hold on
h9=bar(C_analysisp,0.4)
set(h9,'EdgeColor', 'white')
legend('basic PVT','OPVETC')

ylabel('Cost [$]')
legend('basic PVT','OPVETC')
figure(4)
h10=bar(n,CumNet1,0.4)
set(h10,'EdgeColor', 'white')
g=0
```

F1: The basic hybrid system economic analysis result

		Payback time	**7.7 years**	
year	Outflow ($/yr)	Inflow ($/yr)	Net Cashflow ($/yr)	Cumulative cash flow ($/yr)
0.0	26342.00	0.0	-26342.0	-26342.0
1.0	758.81	5285.7	4526.9	-21815.1
2.0	759.78	5259.4	4499.6	-17315.6
3.0	760.83	5233.2	4472.4	-12843.2
4.0	761.95	5207.2	4445.2	-8398.0
5.0	9568.51	6001.4	-3567.1	-11965.1
6.0	764.47	5155.5	4391.0	-7574.1
7.0	765.87	5129.8	4364.0	-3210.1
8.0	767.38	5104.3	4336.9	1126.8
9.0	769.00	5078.9	4309.9	5436.7
10.0	15427.00	6432.3	-8994.7	-3558.0
11.0	772.62	5028.5	4255.9	697.9
12.0	774.63	5003.5	4228.9	4926.8
13.0	776.80	4978.6	4201.8	9128.6
14.0	779.13	4953.8	4174.7	13303.3
15.0	23715.42	7097.5	-16618.0	-3314.7
16.0	784.34	4904.7	4120.3	805.6
17.0	787.24	4880.3	4093.0	4898.6
18.0	790.36	4856.0	4065.6	8964.3
19.0	793.72	4831.8	4038.1	13002.4
20.0	31137.14	7661.8	-23475.4	-10473.0
21.0	801.21	4783.9	3982.7	-6490.3
22.0	805.38	4760.1	3954.7	-2535.7
23.0	809.87	4736.4	3926.5	1390.8
24.0	814.70	4712.8	3898.1	5289.0
25.0	**819.89**	**12889.6**	**12069.7**	**17358.7**

F2: The proposed OPVETC hybrid system economic analysis result

PBP=6.75 year

year	Outflow ($/yr)	Inflow ($/yr)	Net Cashflow ($/yr)	Cumulative cash flow ($/yr)
0.0	26359.6	0.0	-26359.6	-26359.6
1.0	410.9	5578.7	5167.8	-21191.8
2.0	412.8	5551.0	5138.1	-16053.6
3.0	414.9	5523.4	5108.4	-10945.2
4.0	417.2	5495.9	5078.7	-5866.5
5.0	9225.0	6288.6	-2936.3	-8802.9
6.0	422.2	5441.3	5019.1	-3783.8
7.0	425.0	5414.3	4989.2	1205.5
8.0	428.0	5387.3	4959.3	6164.8
9.0	431.3	5360.5	4929.2	11094.0
10.0	15091.0	6712.5	-8378.5	2715.5
11.0	438.5	5307.3	4868.8	7584.3
12.0	442.5	5280.9	4838.4	12422.7
13.0	446.9	5254.6	4807.7	17230.4
14.0	451.5	5228.5	4776.9	22007.3
15.0	18684.4	7370.8	-11313.7	10693.7
16.0	462.0	5176.6	4714.6	15408.3
17.0	467.8	5150.8	4683.1	20091.4
18.0	474.0	5125.2	4651.2	24742.6
19.0	480.7	5099.7	4619.0	29361.6
20.0	30827.7	7928.3	-22899.4	6462.2
21.0	495.7	5049.1	4553.4	11015.6
22.0	504.0	5024.0	4519.9	15535.5
23.0	513.0	4999.0	4486.0	20021.5
24.0	522.7	4974.1	4451.4	24472.9
25.0	533.1	13044.8	12511.7	36984.7

G. Data sheet of the commercial TEZEUS PVT collector

Specifications of TESZEUS® PV-T Photovoltaic Thermal Module

Polycrystalline PV-T Hybrid Collector

TESZEUS 240P	
External Dimensions (mm)	1650 x 992 x 50
Thermal Absorber material	Copper/Aluminum
Peak power (pm)	240W
Open Circuit (Voc)	37.00V
Short Circuit (Isc)	8.54A
Maximum Power Voltage (Vmp)	30.20V
Maximum Power Current (Imp)	7.95A
Cell efficiency	16.75%
Panel efficiency	14.60%
Loss Factor Pmax [%/K]	0.40%
Working Temperature	-40°C TO +85°C
Tolerance	±3%

TESZEUS 280P	
External Dimensions (mm)	1956 x 992 x 50
Thermal Absorber material	Copper/Aluminum
Peak power (pm)	280W
Open Circuit (Voc)	44.30V
Short Circuit (Isc)	8.40A
Maximum Power Voltage (Vmp)	36.10V
Maximum Power Current (Imp)	7.76A
Cell efficiency	16.00%
Panel efficiency	14.46%
Loss Factor Pmax [%/K]	0.40%
Working Temperature	-40°C TO +85°C
Tolerance	±3%

Monocrystalline PV-T Hybrid Collector

TESZEUS 250M	
External Dimensions (mm)	1650 x 992 x 50
Thermal Absorber material	Copper/Aluminum
Peak power (pm)	250W
Open Circuit (Voc)	36.50V
Short Circuit (Isc)	9.51A
Maximum Power Voltage (Vmp)	29.80V
Maximum Power Current (Imp)	8.39A
Cell efficiency	17.36%
Panel efficiency	16.83%
Loss Factor Pmax [%/K]	0.40%
Working Temperature	-40°C TO +85°C
Tolerance	±3%

TESZEUS 300M	
External Dimensions (mm)	1956 x 992 x 50
Thermal Absorber material	Copper/Aluminum
Peak power (pm)	300W
Open Circuit (Voc)	44.53V
Short Circuit (Isc)	8.90A
Maximum Power Voltage (Vmp)	37.10V
Maximum Power Current (Imp)	8.09A
Cell efficiency	17.35%
Panel efficiency	15.54%
Loss Factor Pmax [%/K]	0.40%
Working Temperature	-40°C TO +85°C
Tolerance	±3%

TESZEUS PV-T Thermal Power Output

Peak Power output for G = 1000 W /m² and u = 0 m/s = 651 W Power output per m²

Tm – Ta = 2K	Net irradiance G		
	G = 400 W / m²	G = 700 W / m²	G = 1000 W / m²
u = 0.0 m/s	248	448	651
u = 1.0 m/s	245	438	644
u = 1.5 m/s	244	441	641
u = 2.0 m/s	242	438	637
u = 2.5 m/s	241	436	634
u = 3.0 m/s	240	429	630
u = 3.5 m/s	238	432	627

Certifications: CE, ROHS, IEC 61215:2005, EN 61000-6-1:2007, EN61000-6-3:2007, IEC61730





Photos of installation of one PV-T panel for electrical production and daily

H. Data sheet of the commercial AP evacuated tube collector

Main Component Specifications



Component	Materials & Specifications
Evacuated Tubes	**Material:** Borosilicate 3.3 **Tube style:** Twin wall all glass **Dimensions:** ø58mm / 2.28" outer tube; ø47mm / 1.85" inner tube; 1.8m / 71" length, 1.8mm / 0.07" outer tube wall thickness
Solar Absorber Coating	**Material:** Graded AL/N on AL **Absorptance:** >92% (AM1.5); **Emittance:** <8% (80°C / 176°F) **Vacuum:** P<5x10^{-3}Pa; **Heat loss:** <0.6W/(m^2·°C) / 0.14Btu/hr/ft^2/°F
Heat Pipes	**Material:** High purity "oxygen free" copper (ASTM: C10200; DIN: OF-Cu) **Heat transfer fluid:** distilled water **Maximum heat transfer capacity:** 220W / 750Btu **Operating angle:** 20-80° **Startup temperature:** -30°C / 86°F
Copper Header Pipe	**Material:** Copper (ASTM: C1100, DIN: ECu-58); Potable water rated. **Brazing rod material:** BAg15CuZn **Maximum pressure:** 800kPa **Connection options:** 3/4" (¾" OD) US copper; 19.1mm OD copper with DN20 flared nut (Australia); 22mm OD copper (Europe)
Heat Transfer Fins	**Material:** High purity aluminium
Rubber Components	**Material:** HTV Silicone Rubber (UV stabilized)
Mounting Frame	**Material:** 439 Stainless Steel or 6005-T5 Aluminium Alloy
Tube Clips	**Material:** 301 Stainless Steel
Fasteners	**Material:** 304 Stainless Steel
Manifold Casing	**Material:** 3A21 Aluminium with Anodized or Powder Coated Finish
Manifold Insulation	**Material:** Glass Wool (K = 0.043W/mK) **Thickness:** Average >50mm / 2"

Instantaneous Efficiency

The instantaneous efficiency level depends on the surface area used for the calculation. It is important to us same area (absorber, aperture or gross) when comparing collectors. Aperture is the standard area measure for presenting efficiency values.

AP Collector Performance Variables for Different Surface Areas

Variable	Absorber	Aperture	Gross Area
AP-30 Area *	2.4 m^2 / 25.8 ft^2	2.83 m^2 / 30.46ft^2	4.4 m^2 / 47.4ft^2
Eta0 (η0)	0.81	0.687	0.442
a1	1.77	1.505	0.968
a2	0.0130	0.0111	0.0071

* Surface area values differ slightly from Europe to North America due to difference in measuring methods.

The following is the AP solar collector performance curve based on the aperture area.

